



If you have discovered material in AURA which is unlawful e.g. breaches copyright, (either yours or that of a third party) or any other law, including but not limited to those relating to patent, trademark, confidentiality, data protection, obscenity, defamation, libel, then please read our [Takedown Policy](#) and [contact the service](#) immediately

Synthetic Analogues of Protein-Lipid Complexes

Patchara Punyamoonwongsa

Doctor of Philosophy

Aston University

September 2007

This copy of the thesis has been supplied on condition that anyone who consults it is understood to recognize that its copyright rests with its author and that no quotation from the thesis and no information derived from it may be published without proper acknowledgement

Aston University

Synthetic Analogues of Protein-Lipid Complexes

Patchara Punyamoongsa

Submitted for the Degree of Doctor of Philosophy

September 2007

Summary

Hypercoiling poly(styrene-*alt*-maleic anhydride) (PSMA) is known to undergo conformational transition in response to environmental stimuli. This responsive behaviour makes it possible to mimic structural aspects of native apoproteins. The association of PSMA with lipid 2-dilauryl-*sn*-glycero-3-phosphocholine (DLPC) produces polymer-lipid complex analogues to lipoprotein assemblies found in lung surfactant. These complexes represent a new bio-mimetic delivery vehicle with applications in the cosmetic and pharmaceutical industries.

The primary aim of this study was to develop a better understanding of PSMA-DLPC association by using physical and spectroscopic techniques. Ternary phase diagrams were constructed to examine the effects of various factors, such as molecular weight, pH and temperature on PSMA-DLPC association. ³¹P-NMR spectroscopy was used to investigate the polymorphic changes of DLPC upon associating with PSMA. The Langmuir Trough technique and surface tension measurement were used to explore the association behaviour of PSMA both at the interface and in the bulk of solution, as well as its interaction with DLPC membranes.

The ultimate aim of this study was to investigate the potential use of PSMA-DLPC complexes to improve the bioavailability and therapeutic efficacy of a range of drugs. Typical compounds of ophthalmic interest range from new drugs such as Pirenzepine, which has attracted clinical interest for the control of myopia progression, to the well-established family of non-steroidal anti-inflammatory drugs. These drugs have widely differing structures, sizes, solubility profiles and pH-sensitivities. In order to understand the ways in which these characteristics influence incorporation and release behaviour, the marker molecules Rhodamine B and Oil red O were chosen. PSMA-DLPC complexes, incorporated with marker molecules and Pirenzepine, were encapsulated in hydrogels of the types used for soft contact lenses. Release studies were conducted to examine if this smart drug delivery system can retain such compounds and deliver them at a slow rate over a prolonged period of time.

Keywords: Hypercoiling, polymer-lipid complexes, Langmuir Trough, surface tension, hydrogel drug delivery systems

There are a few people

in my life. The first person

whose love and support have shaped me

is my mother. I wish to thank Dr. [Name]

and deeply grateful to Dr. [Name]

for his guidance, inspiration and his unwavering support

throughout my Ph.D. journey.

Dr. [Name], from the School of

his insightful comments and suggestions

has helped me write for his [Name]

To my family

would also like to thank

for his [Name]

to all members of the [Name]

and [Name]

and their warm [Name]

and in particular

to [Name]

and [Name]

for [Name]

and [Name]

to my [Name]

for [Name]

and [Name]

to [Name]

and [Name]

ACKNOWLEDGEMENTS

There are a number of people whose help with this project has been invaluable. The first person is my supervisor, Professor Brian Tighe, whose vast knowledge and kind support have carried me through the challenges of researching and writing this thesis. Next, I wish to thank Dr. Steve Tonge, whose work this thesis has been based on. I am also deeply grateful to Dr. Robert and Dr. Nipapan Molloy for opening my eyes to the world of science and inspiring me to do research, for their continuous support and valuable advice throughout my PhD studies.

Thanks are due to the generous Dr. YongFeng Wang, from the School of Life and Health Sciences at Aston University, for his insightful comments and access to the freeze drying equipment, as well as Dr. Dave Walton for his warm help and generous access to the FTIR spectroscopy equipment. I would also like to thank Dr. Mike Perry, who took time to help me with my NMR spectroscopy experiments.

Thank you, to all members of the Biomaterials Research Unit at Aston University, and especially to Muriel and Raminder, for their support from the day I arrived in Birmingham, the nights out and their warm friendship. My gratitude to the Thai society in Birmingham, both past and present, and in particular to Adisak Pattiya for countless hours spent keeping my computer running. To La-ongdao Hamer for her support, good humor and making me feel at home. Special thanks are due to Jan Duracz for reviewing the work, and in particular, for helping with the conceptual work on the stoichiometric model.

I thank my dear parents for all the support and love, without which I would surely not have been able to complete this thesis. To my kind brother, for enthusiastically motivating me, and to my lovely sister for sending me Thai care packages that brightened up the long dark hours spent working in front of the computer.

Finally, thanks are due to Mae Fah Luang University as well as the Royal Thai Government, for their financial support during my PhD studies in the UK.

LIST OF CONTENTS

	Page
Title page	1
Summary	2
Dedication	3
Acknowledgments	4
List of Contents	5
List of Figures	11
List of Tables	16
List of Symbols and Abbreviations	17
CHAPTER 1 INTRODUCTION	20
1.1 Responsive Hydrophobically Associating Polymer: Analogies to Protein Structure	21
1.2 Factors Influencing Polymer Conformation in Solution	23
1.2.1 The Hydrophobic Effect	23
1.2.2 Effect of pH	24
1.2.3 Effect of Dissolved Salt	25
1.2.4 Effect of Organic Components	26
1.3 Cationic Hypercoiling Polymers	26
1.3.1 Poly(4-vinylpyridine)	26
1.3.2 Poly(vinylimidazole)-Containing Copolymers	27
1.3.3 Poly(tertiary amines)	28
1.4 Anionic Hypercoiling Polymers	29
1.4.1 Copolymers of Acrylic Acid and Ethyl Acrylate	29
1.4.2 Copolymers of Maleic Anhydride and Alkyl Vinyl Ethers	30
1.4.3 Copolymers of Maleic Anhydride and Styrene	32
1.5 Surface Properties of Hypercoiling Polymers	33
1.5.1 Background Consideration Relating to Polymeric Surface Activity	33
1.5.2 Surface Activity of Polyelectrolyte Solution	34
1.5.3 Solubilizing Ability of Polyelectrolytes	35

1.6	Potential Medical Applications of Anionic Hypercoiling Polymers	37
1.6.1	Interaction of Anionic Hypercoiling Polymers with Phospholipid Bilayers	37
1.6.2	Enhanced Endosomal Escape of Biomolecules	39
1.6.3	Synthetic Protein-Lipid Complexes as Vesicle for Poorly Water Soluble Active Compounds	41
1.6.3.1	General Background of Lipoprotein	41
1.6.3.2	Application of Lipoprotein in Drug Delivery System	44
1.6.3.3	Polymer-Lipid Complexes	46
1.7	Aims and Scope of Research	52
CHAPTER 2	MATERIALS AND METHOD	54
2.1	Introduction	55
2.2	Synthesis of Polymer-Lipid Complexes	55
2.2.1	Materials	55
2.2.2	Methods	56
2.3	Freeze-Drying of Loaded Polymer-Lipid Complexes	57
2.4	Synthesis of Hydrogel Membranes	58
2.4.1	Materials	58
2.4.2	Thermal Free-Radical Polymerization	59
2.4.3	UV-Polymerization (Photopolymerization)	60
2.4.3.1	Photopolymerizable Materials	61
2.4.3.2	Photoinitiators	62
2.4.3.3	Poly(vinyl alcohol) (PVA)	63
2.4.3.4	Photopolymerization of PVA	66
2.5	Experimental Techniques	67
2.5.1	Langmuir-Blodgett Trough Technique	68
2.5.2	Surface Tension Measurement	72
2.5.3	³¹ P-NMR Spectroscopy Study	72
2.5.4	UV-Vis Spectroscopy	73

CHAPTER 3	SYNTHESIS AND PHASE BEHAVIOUR OF POLYMER-LIPID COMPLEXES	74
3.1	Theories of Polymer-Lipid Formation	75
3.2	Aims	76
3.3	Experimental	76
3.3.1	Materials	76
3.3.2	Synthesis of PSMA-DLPC Complexes	77
3.3.3	Phase Behaviour of PSMA-DLPC Complexes	77
3.4	Results and Discussion	78
3.4.1	Ternary Phase Diagrams of PSMA-DLPC-Water System: Low Molecular Weight PSMA Type	78
3.4.2	Ternary Phase Diagrams of PSMA-DLPC-Water System: Medium-High Molecular Weight Type	80
3.5	Conclusions	81
CHAPTER 4	THE STUDY OF POLYMER-LIPID INTERACTION: LANGMUIR BLODGETT STUDY	82
4.1	Polymer-Lipid Interaction	83
4.1.1	Polymer-Lipid Interaction at Neutral pH	83
4.1.2	pH-Dependent Polymer-Lipid Complexation	84
4.2	Scope of Polymer-Lipid Interaction Studies	85
4.3	Langmuir-Blodgett Trough Technique	86
4.3.1	Introduction	86
4.3.2	Aims	87
4.3.3	Experimental	87
4.3.3.1	Surface Pressure (π)-Area (A) Isotherms of Pure DLPC Monolayers	87
4.3.3.2	Surface Pressure (π)-Area (A) Isotherms of Pure PSMA Monolayers	88
4.3.3.3	Effect of PSMA Complexation on DLPC Monolayer	88

4.3.4	Results and Discussion	89
4.3.4.1	Surface Pressure (π)-Area (A) Isotherms of Pure DLPC Monolayers	89
4.3.4.2	Surface Pressure (π)-Area (A) Isotherms of Pure PSMA Monolayers	92
4.3.4.3	Effect of PSMA Complexation on DLPC Monolayer	95
4.3.5	Conclusions	105
CHAPTER 5	THE STUDY OF POLYMER-LIPID INTERACTION: SURFACE TENSION STUDY	106
5.1	Introduction	107
5.2	Aims	108
5.3	Experimental	109
5.3.1	Surface Tension Behaviour of PSMA	109
5.3.2	Effect of DLPC on Surface Tension Behaviour of PSMA	110
5.4	Results and Discussion	111
5.4.1	Surface Tension Behaviour of PSMA	111
5.4.2	Effect of DLPC on Surface Tension Behaviour of PSMA	118
5.5	Conclusions	122
CHAPTER 6	THE STUDY OF POLYMER-LIPID INTERACTION: ³¹P-NMR SPECTROSCOPY STUDY	124
6.1	Introduction	125
6.2	Aims	126
6.3	Experimental	126
6.4	Results and Discussion	127
6.5	Conclusions	137

CHAPTER 7	FABRICATION AND CHARACTERIZATION OF NOVEL DRUG DELIVERY CONTACT LENSES	138
7.1	Introduction	139
7.2	Aims	141
7.3	Experimental	143
7.3.1	Materials	143
7.3.2	Synthesis Methods	144
7.3.2.1	Synthesis of PSMA-DLPC Complexes	144
7.3.2.2	Encapsulation of Active Compounds into PSMA-DLPC Complexes	144
7.3.2.3	Freeze-Drying of Loaded PSMA-DLPC Complexes	144
7.3.2.4	Synthesis of Vesicle-Loaded Hydrogel Membranes	145
7.3.2.5	Loading of Dye of Drug into the Hydrogels	147
7.3.3	Shape and Morphology of PSMA-DLPC Complexes	147
7.3.4	Hydrogel Characterization Studies	148
7.3.5	<i>In Vitro</i> Release Studies	148
7.4	Results and Discussion	149
7.4.1	Shape and Morphology Study of PSMA-DLPC Complexes	149
7.4.2	Hydrogel Characterization Studies	155
7.4.2.1	Transparency of Loaded Hydrogels	155
7.4.2.2	Microstructure of Vesicle-Loaded Hydrogels	156
7.4.3	<i>In Vitro</i> Release Studies	160
7.4.3.1	Dye Loading and Release Studies	160
7.4.3.2	Drug Loading and Release Studies	169
7.5	Conclusions	179

CHAPTER 8	SUMMARY AND DISCUSSION: SUGGESTION FOR FURTHER WORK	180
8.1	Summary and Discussion	181
8.1.1	The Study of Polymer-Lipid Interaction	181
8.1.2	The Polymer-Lipid End-State Complexes: A Stoichiometric Model	184
8.1.3	Drug Delivery Application of Polymer-Lipid Complexes	194
8.2	Suggestions for Further Work	197
8.2.1	Purification and Characterization of Polymer-Lipid Complexes	197
8.2.2	Study of Drug Release from Polymer-Lipid Complexes	201
8.2.3	Study of Drug Release from Vesicle-Loaded Hydrogels	203
	References	206

LIST OF FIGURES

Title	Page
Fig.1.1 Quaternized poly(4-vinylpyridine)	27
Fig.1.2 Poly(vinylimidazole)	28
Fig.1.3 Poly(thio-1- <i>N,N</i> -diethylaminoethylethylene)	28
Fig.1.4 Random copolymers of acrylic acid and ethyl acrylate	30
Fig.1.5 Poly(maleic anhydride- <i>alt</i> -alkyl vinyl ether)	31
Fig.1.6 Poly(styrene- <i>alt</i> -maleic anhydride)	32
Fig.1.7 Structure and disposition of pulmonary surfactant protein SP-B	41
Fig.1.8 Negative-stained electron micrographs of lipoproteins from human CSF and rat astrocyte-conditioned media	42
Fig.1.9 Amphipathic coil showing hydrophobic (dark grey) and hydrophilic facets (light grey) facets	46
Fig.1.10 Polymer-lipid nanostructure with amphipathic polymer arrange around lipid bilayer	47
Fig.1.11 Cryo-TEM electron micrographs of PSMA-DLPC vesicles showing axial (left) and lateral (right) views of nanostructures formed	47
Fig.1.12 Microstructures of (a) β -lactoglobulin-phospholipid (DLPC) vesicles (x10,000 magnification) and (b) poly(styrene- <i>alt</i> -maleic anhydride)-phospholipid (DLPC) micelles (x50,000 magnification)	47
Fig.1.13 Surface activity of the PSMA-DLPC complexes (1.25/0.5%) measured by pulsating bubble surfactometry at 5 min of pulsing	50
Fig.1.14 Concept map of research and thesis structure	53
Fig.2.1 Chemical structures of (a) Rhodamine B, (b) Oil red O and (c) Pirenzepine dihydrochloride	56
Fig.2.2 Chemical structures of chemicals used to prepare hydrogel in this study	59
Fig.2.3 Injection mould used to prepare hydrogel membrane	59
Fig.2.4 Chemical structures of materials that can be photopolymerized to create crosslinked hydrogel network	61

Fig.2.5	Photoinitiators that promote radical photopolymerization by photocleavage mechanism (e.g., Irgacure 2959)	62
Fig.2.6	Photoinitiators that promote radical photopolymerization by hydrogen abstraction mechanism	63
Fig.2.7	Modification of poly(vinyl alcohol)	64
Fig.2.8	Modification of Irgacure® 2959 photoinitiator	66
Fig.2.9	A schematic illustration showing the components of phospholipid (left) and the orientation of phospholipid adopted at an air-water interface (right)	68
Fig.2.10	Schematic illustration of a Langmuir film balance with a Wilhelmy plate, measuring the surface pressure and the barriers for reducing the available surface area	70
Fig.2.11	Typical π -Area isotherm of phospholipids	70
Fig.2.12	(a) Langmuir-Blodgett Trough and (b) chemical structure of 2-dilauryl- <i>sn</i> -glycero-3-phosphocholine (DLPC) used in this study	71
Fig.3.1	Ternary phase diagrams of PSMA-DLPC-water systems at room temperature without heat treatment; (a) at pH 4, (b) at pH 7 and with heat treatment; (c) at pH 4, (d) at pH 7 (using PSMA with MW=1,600)	78
Fig.3.2	Ternary phase diagrams of PSMA-DLPC-water systems at room temperature at (a) pH 4 and (b) pH 7 (using PSMA sodium salt with MW=120,000)	80
Fig.4.1	Pressure-area isotherms at room temperature of DLPC monolayer on deionized water and phthalate buffer of pH 4 subphases	90
Fig.4.2	Pressure-area isotherms at room temperature of DLPC monolayer on deionized water with using different barrier speeds	90
Fig.4.3	Pressure-area isotherms at room temperature of the three PSMA types; PSMA-partial methyl ester (MW 350,000), PSMA-sodium salt (MW 120,000) and PSMA (MW 1,600) on subphases of (a) deionized water and (b) phthalate buffer of pH 4	93
Fig.4.4	Schematic representation of the association of PSMA molecules in solution by a zipper mechanism	93

Fig.4.5	Changes of the pressure-area isotherms as a function of time for DLPC monolayers in the presence of (a) PSMA (MW 1,600), (b) PSMA-sodium salt (MW 120,000) and (c) PSMA-partial methyl ester (MW 350,000). The PSMA was introduced beneath the water subphase at t=0 min when barrier is completely opened and stationary	96
Fig.4.6	Changes of the pressure-area isotherms as a function of time for DLPC monolayers in the presence of (a) PSMA (MW 1,600), (b) PSMA-sodium salt (MW 120,000) and (c) PSMA-partial methyl ester (MW 350,000). The PSMA was introduced beneath the phthalate buffer pH 4 subphase at t=0 min when barrier is opened and stationary	99
Fig.4.7	Changes in surface areas of DLPC monolayers at 20 mN/m induced by addition of 10 μ L of PSMA (1 mg/ml) as a function of time on phthalate buffer of pH 4	100
Fig.4.8	Relative area increase ($\Delta A/A$) of DLPC monolayers as a function of surface pressure at pH 4 buffer measured at 30 min after PSMA addition	101
Fig.4.9	Overlay plots of surface pressure-area isotherms on phthalate buffer of pH 4 for the pure DLPC, pure PSMA and mixed DLPC-PSMA monolayers	102
Fig.4.10	Schematic representation of a possible molecular arrangement at the interface for the mixed monolayer of DLPC and PSMA	103
Fig.5.1	Idealized surface tension of a weakly interacting polymer/surfactant mixture which also interacts at the interface	108
Fig.5.2	Molecular structures of poly(styrene- <i>alt</i> -maleic anhydride) hydrolyzed to different degrees of ionization	109
Fig.5.3	Schematic representation of the changes in hypercoiling behaviour of PSMA with decreasing degrees of ionization	110
Fig.5.4	Effect of the molecular weights on the surface tension-concentration dependence of PSMA at (a) pH 12, (b) pH 6 and (c) pH 4 (after 20 min)	112
Fig.5.5	Effect of pH on the surface tension-concentration dependence of PSMA; (a) MW 1,600, (b) MW 120,000 and (c) MW 350,000	114

Fig.5.6	Surface tension as a function of logarithmic concentration for PSMA in acidic aqueous solution (pH 4)	116
Fig.5.7	Schematic representation of the equilibrium linking the partition of PSMA molecules in solution and at the air-water interface	117
Fig.5.8	Variation in surface tension at pH 4 with DLPC concentration in the presence of 0.20 wt% PSMA with different molecular weights; (a) MW 1,600, (b) MW 120,000 and (c) MW 350,000	118
Fig.6.1	Proton-dipolar decoupled 109 MHz ³¹ P-NMR spectra of palmitoyllysophosphatidylcholine in 23 wt% aqueous polyethylene-glycol	125
Fig.6.2	Proton-decoupled ³¹ P-NMR spectra of aqueous DLPC-PSMA mixtures at room temperature and (a) pH 10, (b) pH 6, (c) pH 5 and (c) pH 4. The ³¹ P-NMR spectra of pure DLPC (5 mg/ml) and pure PSMA (30 mg/ml) at pH 4 were also shown for comparison along with their chemical structures in (e) and (f), respectively	128
Fig.6.3	Effect of PEG concentration on the lamellar phase	133
Fig.6.4	Freeze-fracture electron microscopy images of sample at 50°C (at 1 g/L lipids)	134
Fig.6.5	Negative stain (2% phosphotungstic acid) electron micrograph of DOPC/PEAA (1:1 mixture) at pH 6.1	134
Fig.6.6	Schematic illustration of the parameters defining the critical packing parameter (P_c)	135
Fig.6.7	Schematic illustration of association structures formed in surfactant systems and the packing of surfactant molecules in different association structures	136
Fig.7.1	Schematic representation of the ocular disposition of topically applied formulations	139
Fig.7.2	Schematic illustration of vesicle-laden lens inserted in the eye	142
Fig.7.3	Representative cartoons corresponding to the structures proposed for the sequential states of lipid-surfactant interaction during vesicle to micelle transformation	150
Fig.7.4	Optical micrograph at pH 4 of PSMA-DLPC complexes loaded with Rhodamine B dye at 40x magnification. Concentration of PSMA, and dye used were 3.0, 0.5 and 0.5% w/v, respectively	152

Fig.7.5	Optical micrograph at pH 4 of PSMA-DLPC complexes loaded with Oil red O dye at 40x magnification	152
Fig.7.6	Photograph showing optical transparencies of PSMA-DLPC samples	153
Fig.7.7	Optical micrograph of particles observed in aqueous dispersion of PSMA-DLPC complexes after 4 days of incubation	153
Fig.7.8	SEM micrographs showing interior morphology of Rhodamine-loaded PSMA-DLPC mixed micelles	154
Fig.7.9	Optical micrographs of Rhodamine-loaded PVA hydrogel at (a) 10x and (b) 40x magnifications. The optical micrographs of PVA hydrogel containing Rhodamine-loaded DLPC-PSMA vesicles at magnification of 40x are also shown in (c)-(d)	157
Fig.7.10	Optical micrographs of Rhodamine-loaded poly(HEMA- <i>co</i> -MAA) hydrogel and poly(HEMA- <i>co</i> -MAA) hydrogel loaded with Rhodamine-incorporated DLPC-PSMA vesicles	158
Fig.7.11	Molecular (ionic) structures of Rhodamine B equilibrium species	160
Fig.7.12	Binding of Rhodamine B to PSMA-DLPC vesicles	161
Fig.7.13	Rhodamine-release data from PVA hydrogels with dye (denoted as PVA1) and PSMA-DLPC vesicle (denoted as PVA2) incorporation	164
Fig.7.14	Rhodamine-release data from poly(HEMA- <i>co</i> -MAA) hydrogels with dye (denoted as pHEMA-MAA1) and PSMA-DLPC vesicle (denoted as pHEMA-MAA2) incorporation	166
Fig.7.15	Chemical structure and Pirenzepine dihydrochloride drug (left) and ultraviolet spectrum of the drug in acidic solution (right)	170
Fig.7.16	Pirenzepine-release data from PVA hydrogels with drug (denoted as PVA3) and PSMA-DLPC vesicle (denoted as PVA4) incorporation	173
Fig.7.17	Pirenzepine-release data from poly(HEMA- <i>co</i> -MAA) hydrogels with drug (denoted as pHEMA-MAA3) and PSMA-DLPC vesicle (denoted as pHEMA-MAA4) incorporation	175
Fig.8.1	Schematic illustration for the parameters	188
Fig.8.2	Illustration of setup for <i>in vitro</i> release from microspheres using the Float-a-Lyzer	202

LIST OF TABLES

Title	Page
Table 2.1 Chemicals used to prepare unloaded and loaded PSMA-DLPC complexes	55
Table 2.2 Characteristics of Rhodamine B, Oil red O and Pirenzepine drug	57
Table 2.3 Chemicals used to prepare unloaded- and loaded hydrogel membranes	58
Table 2.4 Characteristics of resultant PVA hydrogels synthesized by photopolymerization of functionalized PVA macromer using Lightstream Technology™ process	67
Table 2.5 Molecular weights and suppliers of PSMA copolymers, DLPC and other chemicals used in this study	71
Table 3.1 Molecular weights and suppliers of the anionic PSMA copolymers used	76
Table 7.1 Chemicals used in this study	143
Table 7.2 Feed compositions of smart hydrogel membrane	145
Table 7.3 Characteristics of resultant PVA hydrogels synthesized by photopolymerization of functionalized PVA macromer using Lightstream Technology™ process	146
Table 7.4 Transmittance values of the PVA and poly(HEMA- <i>co</i> -MAA) hydrogels with and without dye (or drug)-loaded PSMA-DLPC vesicle incorporation	155
Table 7.5 Comparison of percent loading efficiencies of Rhodamine dye in PVA and poly(HEMA- <i>co</i> -MAA) hydrogels after polymerization	162
Table 7.6 Some quantification of Pirenzepine drug	170
Table 7.7 Comparison of percent loading efficiencies of Pirenzepine drug in PVA and poly(HEMA- <i>co</i> -MAA) hydrogels after polymerization	172
Table 8.1 Evaluation of stoichiometric model by comparison with ternary phase diagram data of water-DLPC-PSMA (MW 1,600) system	192
Table 8.2 Evaluation of stoichiometric model by comparison with ternary phase diagram data of water-DLPC-PSMA (MW 120,000) system	193

LIST OF SYMBOLS AND ABBREVIATIONS

EA	ethyl acrylate
AA	acrylic acid
S	styrene
MA	maleic anhydride
MAA	methacrylic acid
HEMA	2-hydroxyethyl methacrylate
EGDMA	ethyleneglycol dimethacrylate
AIBN	azobisisobutyronitrile
SDS	sodium dodecyl sulphate
PBS	phosphate buffered saline
PC	phosphatidylcholine
DLPC	dilauroylphosphatidylcholine
DPPC	dipalmitoylphosphatidylcholine
DMPC	dimyristoylphosphatidylcholine
DOPC	dioleoylphosphatidylcholine
DSPC	distearoylphosphatidylcholine
CF	carboxyfluorescein
RBC	red blood cell
LDL	low density lipoprotein
VLDL	very low density lipoprotein
HDL	high density lipoprotein
apo-A	apoprotein A
apo-B	apoprotein B
apo-C	apoprotein C
apo-E	apoprotein E
PAA	poly(acrylic acid)
PEAA	poly(2-ethacrylic acid)
PHEMA	poly(2-hydroxyethyl methacrylate)
Poly(HEMA-co-MAA)	poly(2-hydroxyethyl methacrylate-co-methacrylic acid)
PSMA	poly(styrene- <i>alt</i> -maleic anhydride)
PVA	poly(vinyl alcohol)

Acr-PVA	acrylate-modified poly(vinyl alcohol)
PEG	poly(ethylene glycol)
PLGA	poly(lactic acid- <i>co</i> -glycolic acid)
DDS	drug delivery system
RDS	respiratory distress syndrome
CSA	chemical shift anisotropy
CMC	critical micelle concentration
CAC	critical aggregation concentration
LE-LC	liquid expanded-liquid condensed phase transition
UV	ultraviolet
Vis	visible
NMR	nuclear magnetic resonance
³¹P	phosphorus atom
SEM	scanning electron microscopy
FFEM	freeze-fracture electron microscopy
DSC	differential scanning calorimetry
SAXS	small angle X-ray scattering
α	degree of dissociation
γ	surface tension
π	surface pressure
ϕ	surface coverage
δ	chemical shift
T_m	melting transition temperature
P_c	critical packing parameter
pK_a	acid dissociation constant
pK_b	base dissociation constant
C_{sat}	saturation concentration
Pt-Ir	platinum-iridium
A	area
MW	molecular weight
M_n	number average molecular weight
M_w	weight average molecular weight
MWCOs	molecular weight exclusion cutoffs

M	molar concentration
mM	millimolar concentration
mol/mol	mole per mole ratio
L	liter
mL	milliliter
μL	microliter
g	gram
mg/mL	milligram per milliliter
mg/ 100 mL	milligram per a hundred milliliter
μg/L	microgram per liter
%wt	percent by weight
%w/v	percent weight by volume
s	second
min	minute
hr	hour
°C	degree Celsius
Hz	hertz
MHz	megahertz
mm	millimeter
μm	micrometer
nm	nanometer
Å	angstrom
Pa	pascal
MPa	megapascal
kJ/mol	kilojoule per mole
g/mol	gram per mole
mW/cm²	milliwatt per square centimeter
mN/m	millinewton per meter
cm²/min	square centimeter per minute
Å²/molecule	square angstrom per molecule

CHAPTER 1

INTRODUCTION

1.1 RESPONSIVE HYDROPHOBICALLY ASSOCIATING POLYMERS : Analogies to protein structure [1, 2]

Living systems are composed of a variety of macromolecules that can change their conformation and function in response to environmental stimuli. Such dynamic behaviour can be partly reproduced by charged, synthetic macromolecules.

The ability of certain polymers to hypercoil or to associate hydrophobically to form excessively compact molecules offers one possible mechanism by which macromolecules could be made to change their conformation, and therefore, their function, in response to local stimuli. Polymers with weakly charged pendant groups form an extended structure as a result of mutual repulsion between the charged groups. If the polymer also bears alkyl pendant groups, then the latter will be subject to hydrophobic interactions which will tend to restrict the alkyl side chains to minimal volume within an aqueous environment, thereby, allowing maximal hydrogen bonding to occur between the water molecules.

Polymers bearing weakly ionizable pendant groups that form weak bases, such as pyridine or imidazole, are substantially charged below their pK_b values. The resulting ionic repulsion overcomes hydrophobic interactions between alkyl side chains within such polymers and leads to uncoiling of the polymer chain. Conversely, as the pH is raised the proportion of charged pendant groups falls and hydrophobic interactions between the alkyl side chains become the predominant factor, causing the polymer chain to progressively collapse into distinct hydrophobic microdomains. This effect is known as hydrophobic association and is occasionally referred to as hypercoiling, a process that ultimately results in the formation of a compact, insoluble, which precipitates from aqueous solution. Conversely, polymers possessing pendant alkyl chains and weakly charged negative pendant groups (e.g. carboxylic acids) exhibit an extended chain conformation above their pK_a and progressively collapse as the pH are lowered.

A progressive and possibly non-uniform loss of charge occurs during the hypercoiling process and leads to the formation of an amphipathic molecule. Such molecules are usually surface active, leading to the possibility that surface activity and related functional properties could be 'switched on or off' in response to changes in the pH. Hence, by substituting either weakly cationic or anionic pendant group onto a polymer backbone, the polymer can respond to either increases or decreases in pH. However, it should be noted that protein molecules do not hypercoil but are subject to hydrophobic associative forces. Proteins do, indeed, make use of hydrophobic effect, not as a result of changes in the degree of ionization of their side chains induced by variation of pH, but in response to a variation of the surrounding hydrophobic environment, for example by responding to changes in fluidity of the bilayer lipid annulus which surrounds membrane proteins. The latter appears to consist of a tightly bound boundary layer, such as that identified around acetylcholine receptors. Variation of the hydrophobic environment is energetically a far more efficient method of inducing conformational change in macromolecules than that elicited by changing the degree of macromolecular ionization and this may offer a teleological explanation for conformation changes observed in nature.

Hypercoiling or hydrophobically associating switchable polymers have two essential features that may be applied to biological systems to confer upon the latter an ability to change their structure, and hence, their function [3];

- 1) To act as a simple switch either in an 'on' or 'off' state. Such molecular switches may be considered analogous to the digital switching mechanism found within integrated circuits and may when arranged in multiple arrays, enable complex tasks to be performed.
- 2) To function as the trigger for a cascade mechanism, where uncoiling of the molecule will result in co-operative effects that facilitate further changes of molecular shape, and hence, lead to greatly altered function.

Both of the above characteristics are fundamental in determining the dynamic aspects of living systems.

In summary, hypercoiling polymers can be said to mimic the behaviour of some of the functions which account for the essential living processes, and may therefore, be suited for application to living systems and in particular to human medicine. They also have considerable potential for use in drug delivery systems and as synthetic apoproteins.

1.2 FACTORS INFLUENCING POLYMER CONFORMATION IN SOLUTION [2, 3]

The conformation of a solvated macromolecule can be considered to result from a balance between the following forces acting both within the molecule and between the molecule and surrounding solution:

- 1) Electrostatic repulsion between charged subgroups.
- 2) Van der Waals cohesion of uncharged side groups.
- 3) Hydrogen bonds.
- 4) Interaction with the solvent.

The solvent-polymer interaction can be regarded as the most important factor in determining the conformation of solubilized polymer in general, and hypercoiling or hydrophobically associating polymers in particular, since the latter tend to undergo extensive conformational changes in solution.

1.2.1 The Hydrophobic Effect

The hydrophobic effect can be considered as a restriction of non-aqueous components into the smallest possible area, in order to minimize disorder within the aqueous phase. This property was first recognized by Traube in 1891, who described the ability of water to push out, or to the surface of a solution, components which disrupt bonding between the water molecules. It was realized that the attraction of water for itself is energetically the overriding influence in aqueous systems and experimental studies led to the introduction of Traube's Rule, which relates dissolution

to molecular size and states that for each additional methyl group in an alkyl chain the surface to bulk ratio rises by a factor of three. Hence, within a body of water, even quite short aliphatic chains will produce a large hydrophobic cavity. Longer aliphatic chains will induce a proportionate increase in the hydrophobic force, thereby limiting their incursion into the hydrophilic environment. The term 'hydrophobic effect' is somewhat of a misnomer for this phenomenon which in reality is an anti-hydrophilic rather than a pro-hydrophobic effect.

Application of Traube's Rule to polymers allows predicting that the presence of sizeable aliphatic components within polymer will result in exclusion of the polymer from the aqueous environment and cause the polymer to collapse or hypercoil into hydrophobic domains. To observe the magnitude of these changes, one needs to compare the free energy of interaction of a hydrophobic group with both water and a hydrophobic solvent. The difference between the free energy of interaction with the two solutions is found to be directly dependent upon the number of carbon atoms in the hydrophobic chain, that is, proportional to the surface area of the hydrophobic cavity. The presence of a double bond will reduce the size of this cavity, as will an aromatic grouping. Therefore, the relative efficacy of pendant groups in forming a hydrophobic centre is as follows: saturated aliphatic chain > unsaturated chain > aromatic group respectively.

1.2.2 Effect of pH

Changes in hydrogen ion equilibria usually induce the most profound conformational transitions within hypercoiling polymers and can easily be monitored by potentiometric titration. Hypercoiling polymers exhibit a deviation from the normal curve of pH changes vs. degree of dissociation (α) or ionization. For example, in a simple polyelectrolyte, e.g. poly(acrylic acid) (PAA), the degree of ionization is directly proportional to the pH of the solution. However, in a hypercoiling polymer, a discontinuity in the pK_a is apparent as the polymer changes from a compact to an extended chain conformation. As the polymer backbone uncoils, ionizable groups become progressively more accessible and hence, are more readily able to gain or lose

protons, resulting in a changed dissociation constant, as the polymer effectively becomes a stronger acid.

In the case of anionic hypercoilers, addition of alkali causes the weak acid pendant groups to become ionized and repel one another, leading to an uncoiling of the polymer backbone. This process acts to expose further uncharged pendant groups, which in turn, neutralize more alkali, and as a result additional alkali causes only a small change in pH, leading to the presence of an inflection in the titration curve.

When expressed as log pH vs. degree of dissociation, the conventional titration curve is linear, such that the dissociation constant can be deduced directly from the gradient. If data obtained from the titration of a hypercoiling polymer are expressed in this manner, a change in slope is observed as the polymer molecules uncoil from a compact conformation to form an extended chain. This method can be used to identify the presence of hypercoiling behaviour. In addition to potentiometric titration, viscometry and colorimetry, several spectroscopic techniques such as ultraviolet (UV), Raman, Fourier transformed infrared (FTIR) and nuclear magnetic resonance (NMR) spectroscopy, have been used to characterize conformational transition of hypercoiling polymers [1].

1.2.3 Effect of Dissolved Salts

Changes in the tonicity of solutions containing a hypercoiling polymer, by the addition of salts, lead to a reduction of intrachain electrostatic repulsion within the polymer by a process known as charge shielding. The presence of long chain counterions is capable of binding to ionized pendant groups within such polymer will, themselves, result in hydrophobic association and this will tend to overcome any ionic repulsive effects and so act to stabilize polymers in their compact conformation.

1.2.4 Effect of Organic Components

If water is replaced by an organic solvent or urea, then hydrophobic interactions between side chains will be diminished or destroyed. This results in a reduction or complete disappearance of the compact form of the molecule. In organic media (such as an acetone/water mixture), a monotonic increase in both pH and viscosity is observed upon ionization and this behaviour is indicative of a conventional polyelectrolyte. Similarly, the presence of urea causes a rise in solution viscosity by interfering with water structuring, thereby, minimizing the hydrophobic effect which would normally act to collapse the polymer chain. In 8 M urea solutions, discontinuities in viscosity vs. titration curves completely disappear.

The opposite effect is caused by increasing the number of hydrophobic side chains associated with polyelectrolyte, e.g. by the addition of lipid soluble dyes. In this case, the conformational changes observed within the polymer occur at higher values of ionization as the concentration of dye is increased. This can be explained by the ability of the dye to stabilize the compact conformation.

1.3 CATIONIC HYPERCOILING POLYMERS [2]

1.3.1 Poly(4-vinylpyridine)

Hypercoiling polymers synthesized by free radical polymerization were first described by Fuoss [4] in a series of studies aimed at elucidating the behaviour of polyelectrolytes in aqueous solution. The term hypercoiling was not adopted at this stage. Fuoss studied the effects of quaternizing poly(4-vinylpyridine) (PVpy) with alkyl halides (e.g. butyl bromide) to form cationic alkylpyridinium pendant groups. The resultant structure is illustrated in Fig.1.1. The combination of hydrophobic side chains and charged pyridinium groups conferred amphipathic properties upon the polymers and as a result, these polymers were described as polysoap. By progressively increasing the proportion of hydrophobic side chains, a transition from polyelectrolyte to polysoap was observed and monitored by potentiometric titration.

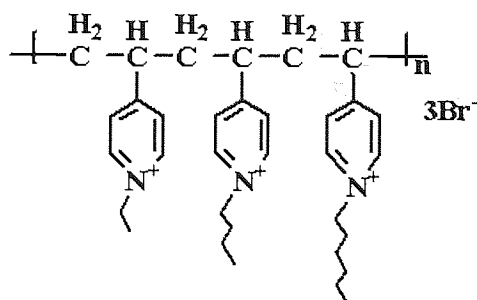


Fig.1.1 Quaternized poly(4-vinylpyridine).

Substituted PVpy can not be considered to be a typical hypercoiling polymer, in that the molecules do not collapse as a result of deionization arising from variation of solution pH, but from an increase in hydrophobicity that occurs upon substituting alkyl side chains.

1.3.2 Poly(vinylimidazole)-Containing Copolymers

Poly(vinylimidazole), as shown in Fig.1.2, substituted with alkyl side chains, has been reported to hypercoil and copolymers of *N*-vinyl imidazole and styrene have also been found to exhibit an amphipathic nature.

A sharp conformational change is observed in poly(styrene-*co*-imidazole) copolymers upon protonation of the imidazole moiety and is manifest as a transition from a 'supercoiled' polymer, existing as an emulsion, to a water soluble extended chain. In non-polar environments the copolymer occupies a smaller hydrodynamic volume, due to the aggregation of the styrene side chains. Whereas, in aqueous solution, styrene pendant groups form a water insoluble core and water soluble imidazole groups become arranged at the surface. This segmental reorientation is made possible by a high degree of flexibility within the backbone. In acidic media, the polymer coil is extended due to electrostatic repulsion between the protonated imidazole groups, although above pH 4, micelles begin to form and above pH 7, complete deprotonation of the imidazole groups leads to precipitation of the polymer from aqueous solution. Fluorescent probes, in which emission is quenched in aqueous environments, e.g. pyrene, has also been used to study conformational changes in these polymers [5].

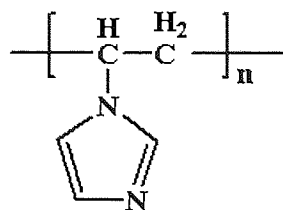


Fig.1.2 Poly(vinylimidazole).

1.3.3 Poly(tertiary amines)

Polymers with tertiary amine pendant groups have also been reported to uncoil and hypercoil upon either *N*-protonation or *N*-alkylation of the amine side chains respectively. One such example is poly(thio-1-*N,N*-diethylaminoethylethylene), the structure of which is shown in Fig.1.3. This is a polybase containing a thioether backbone and tertiary amine pendant groups, which may be methylated to form quaternary derivatives. Deprotonation of this polymer results in the formation of distinct hydrophobic microdomains that are found to be readily destabilized or unfolded by the addition of protonating agents such as a strong acid. Structural changes were observed as discontinuities in potentiometric, viscometric and photometric measurements, e.g. laser light scattering and optical rotatory dispersion. These changes were found to be completely reversible and therefore this molecule would appear to represent an ideal polymer in which to entrap water insoluble molecules for release at specified pH.

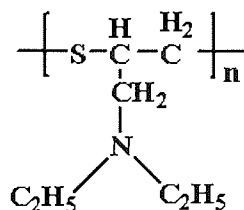


Fig.1.3 Poly(thio-1-*N,N*-diethylaminoethylethylene).

Unlike the tertiary amine polymers, which become insoluble in aqueous solution upon deprotonation, partially methylated tertiary amines (quaternary amines) remain in solution. The formation of microdomains also occurs as the pH is raised between 6 and 7.5, making these polymers of potential interest for application to biological systems.

1.4 ANIONIC HYPERCOILING POLYMERS [2]

1.4.1 Copolymers of Acrylic Acid and Ethyl Acrylate

Copolymers of acrylic acid and ethyl acrylate, shown in Fig.1.4, offer an alternative means of forming a hypercoiling polymer, where the ethyl ester group provides the hydrophobic nucleus. Dynamic light scattering studies using a 3:1 random copolymer of ethyl acrylate and acrylic acid [6] demonstrate that this copolymer behaves as a simple polyelectrolyte in solutions at low ionic concentration and possesses a high radius of gyration, while at concentrations of sodium chloride higher than 1.2 M, the polymer coil adopts a compact conformation. The particularly interesting finding of these studies is the sudden break in curves of radius of gyration vs. ionic strength, which clearly indicate a collapse in polymeric dimensions above a specific sodium chloride concentration.

The fluorescent probe, toluidinyl naphthalene-6-sulphonate, has also been used to investigate the hydrophobic environment formed in the presence of added counterions [6]. The studies show that a change in the relative fluorescence intensity occurs with ionic strength and is most pronounced in the region of 0.3-0.5 M sodium chloride, with the coil reaching a minimum size in 0.7 M sodium chloride. By applying Flory and Mark-Houwink equations to data obtained in several organic and aqueous media at varying salt concentrations, the average mean-square end-to-end distance of the polymer could be calculated and was found to be some 1.3 times greater in organic media than in aqueous media. Light scattering studies confirm these observations and indicate a similar difference in magnitude (1.4 times greater) again indicating a collapsed state in aqueous conditions [6].

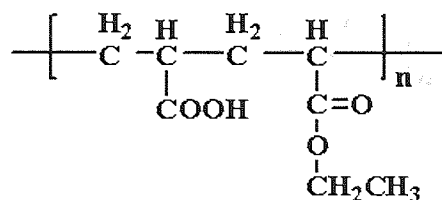


Fig.1.4 Random copolymers of acrylic acid and ethyl acrylate.

1.4.2 Copolymers of Maleic Anhydride and Alkyl Vinyl Ethers

Alternating copolymers of maleic anhydride (hydrolysed to maleic acid) and *n*-alkyl vinyl ethers, shown in Fig.1.5, exhibit hypercoiling behaviour in aqueous solution and undergo a transition from a compact polysoap to an expanded polyelectrolyte in response to changes in charge density. This property was first reported by Dubin and Strauss [7] in copolymers where alkyl group contained more than 12 carbon atoms. Such polymers form polysoaps and are resistant to pH-induced conformational change, such as that encountered by conventional polyelectrolytes.

Intrinsic viscosity measurement of copolymers of maleic anhydride and ethyl vinyl ether indicate that copolymers with short side chains behave as typical extended chain, polyelectrolytes, i.e. they exhibit a rise of intrinsic viscosity upon dilution. Methyl vinyl ether maleic anhydride for example, does not show any conformational change upon ionization beyond that expected of a conventional polyelectrolyte, presumably because there is an insufficient ratio of hydrophobic units per repeat unit. However, similar measurements of butyl and hexyl copolymers indicate an abnormal compact state at low degree of dissociation. The dimensions increase rapidly between 35 and 65% ionization, indicating destruction of the compact state and formation of an extended chain, while at high charge densities these copolymers exhibit intrinsic viscosities typical of expanded polyelectrolytes. In comparison, octyl and decyl vinyl ether copolymers remain hypercoiled even at high charge density as a result of intense hydrophobic association between the pendant groups.

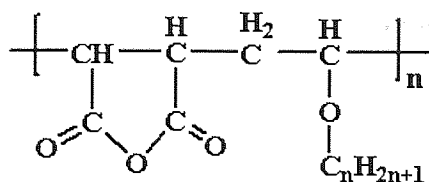


Fig.1.5 Poly(maleic anhydride-*alt*-alkyl vinyl ether).

Potentiometric titration of the ethyl vinyl ether copolymer conducted in sodium chloride solution at various concentrations [8] indicates that conformational change can be largely prevented by the presence of 0.1 M sodium chloride. The presence of ions causes charge shielding which in turn inhibits intrachain repulsion. Consequently, a greater degree of ionization is needed in the presence of high salt concentrations to uncoil the polymer chain. In contrast, the butyl copolymers was found to be less susceptible to added salt and undergoes a conformational change, even at high salt concentrations, due to the predominance of hydrophobic effects.

Spectrophotometric techniques have been used to study the nature of the hydrophobic environment within copolymers of maleic acid and alkyl vinyl ethers and confirm the results obtained by potentiometric and viscometric studies [2]. In the former studies, absorption conjugates are formed between the test polymer and optical probes that fluoresce in hydrophobic environments, e.g. the dansyl group. These studies demonstrate that the dansyl group is embedded in a nonpolar hydrophobic environment at low degrees of polymer ionization and this gradually changes to a polar environment as the degree of ionization of the polymer increases. In the butyl copolymer, fluorescence was found to fall markedly as the degree of ionization increased and this effect was found to be reduced in the presence of 0.2 and 0.5 M sodium chloride, where the transition occurred only at higher degree of ionization. Once again, this illustrates the importance of charge shielding in determining polymer conformation.

Proton-NMR (100 MHz) techniques have been applied to study conformational change in polyelectrolytes. The line width of proton resonances from the side chains of maleic acid *n*-butyl vinyl ether were found to exhibit a sharp decrease upon conformational transition of the polymer, an effect not observed with methyl vinyl ether maleic acid. This result demonstrates the importance of alkyl chain length,

showing that the butyl derivative adopts a compact conformation at low ionization, which restricts free rotation of its pendant side chains.

1.4.3 Copolymers of Maleic Anhydride and Styrene

Styrene pendant groups also provide a hydrophobic moiety and combine with maleic anhydride (hydrolyzed to maleic acid) to form a pseudo alternating hypercoiling copolymer, as shown in Fig.1.6. Indeed, the term hypercoiling was first used by Dannhauser [9] to describe the behaviour of a styrene/maleic acid copolymer (PSMA).

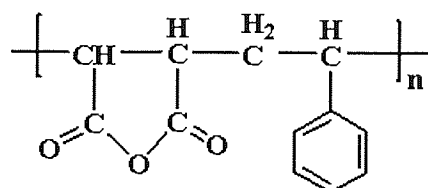


Fig.1.6 Poly(styrene-*alt*-maleic anhydride).

Investigations by potentiometric titration and dilatometry indicate a pH-induced conformational transition, characteristic of a hypercoiling polymer. At 30% ionization, a change in pK_a becomes apparent as assessed by titration. Potentiometric titration of copolymers of maleic anhydride and styrene [2] conducted in the presence of increasing concentrations of sodium chloride also provide confirmatory evidence of hypercoiling behaviour. In these studies, the curves of pH vs. ionization (α) show a progressive decline with increases in sodium chloride concentration as the polymer adopts a more compact conformation with increase in the degree of charge shielding.

By conducting titration measurements at various temperatures [10], the standard enthalpy change of the transition from random to collapsed coil could be calculated and was found to be similar in magnitude to that observed for the heat of transfer of benzene from a hydrophobic to an aqueous medium, i.e. 1.5 kJ/mol. The energy changes involved in conformational transitions, in the presence of sodium chloride, are of such magnitude that the titration curves observed are not influenced by

temperature variations in the range of 15-40°C. Hence, the gain in free energy favors the formation of a compact structure stabilized by hydrophobic interactions between phenyl pendant groups, and in this case, the change in free energy of the system from hypercoil to expanded coil at zero energy is high, of the order of 1.3-4.6 kJ/mol.

Additionally, spectroscopic studies conducted by incorporating an optical probe (acridine orange) into a maleic acid/styrene copolymer, have been found to exhibit many isoderivative points indicating of two conformational states where the compact form demonstrates a hydrophobicity equivalent to that of a 40-50% solution of aqueous ethanol [2].

1.5 SURFACE PROPERTIES OF HYPERCOILING POLYMERS

1.5.1 Background Consideration Relating to Polymeric Surface Activity [3]

Monomeric surfactants form micelles above their critical micellar concentration (CMC) and this phenomenon is characterized by a fall in surface tension, and hence, a rise in surface activity. However, the micelles themselves are not expected to be surface active, since they expose only their hydrophilic segments to the aqueous phase. This contention can not be tested using the conventional surfactants, because the micelles formed under these conditions are in dynamic equilibrium with highly surface active unassociated surfactant molecules which readily associate with the surface and lower the surface tension, so masking any changes. Whereas, in polysoaps, no 'free' surfactant molecules are available and so the surface activity of micelles can be measured directly. Indeed, these polymers exhibit no wetting, foaming or detergent properties and it is probably correct to assume that they do not orientate themselves at the aqueous air-water interface. They do usually, possess an ability to solubilize non-polar materials and adsorb onto the interface which is somewhat paradoxical for non-surface active molecules.

1.5.2 Surface Activity of Polyelectrolyte Solutions [3]

The influence of polymer structure on surface activity and use of surface activity as a means of monitoring polymeric conformation has received scant attention in the published literatures. Studies on the conformation of polysoaps, by Jorgensen [11], observed that dilute (0.0025-0.75%) aqueous solutions of poly(4-vinylpyridine) partially quaternized with *n*-dodecyl and ethyl bromide, differed little in their surface tension from water, except in the presence of KBr, where charge shielding and chain collapse become important. Even in this instance, the surface tension did not fall below 62 mN/m. The addition product of poly(2-vinylpyridine) and bromopropylbenzene depressed surface tension to ~45 mN/m. It is clearly important to note that in neither case was surface tension monitored whilst changing pH, which may have a limited effect on polysoap conformation and a much greater effect on non-polysoap hypercoiling polymers.

Pop [12] and Boiko [13] investigated the effects of pH (percentage ionization) and polymer concentration upon the surface tension of polyelectrolytes in solution. These authors focused principally on the ammonium and potassium salts of a styrene maleic acid copolymer and reported that a reduction in ionization led to a sharp fall in surface tension. The studies of Pop reported a fall in reduced viscosity and this suggested the formation of a more compact molecular form.

Increasing the concentration of the predominantly charged polymer (>50% ionized) was found to cause a progressive fall in surface tension in a concentration-dependent manner [12]. At this level of ionization the molecules were assumed to be in their fully extended state exposing their hydrophobic groups and were therefore assumed to pack at the air-water interface and reduce the surface tension in direct proportion to the concentration of polymer present, until a critical concentration was reached at very high polymer concentrations. At this point, conventional intermolecular micelles were formed and a further reduction in surface tension occurred. Closer inspection of this data reveals a reversal of this trend as the charge is reduced, i.e. at 50% ionization, the values of surface tension were generally higher than those observed with the 100% ionized polymer [12]. The surface tension vs. neutralization

curves reported by Boiko also reveal that at high polymer concentrations, the fully charged polymer exhibited a lower surface tension than the values observed at 75% ionization [13]. Boiko accounted for this change by assuming that high degrees of charge shielding occur upon neutralization and this leads to a collapse in the polymer chain. An alternative explanation of the rise in surface tension noted upon acidification may be provided thus; as the molecule transforms from an extended chain to a dumb-bell shape it adopts an intramolecular micellar structure, which is not, itself, surface active and hence, the rise in surface tension. Both sets of data would tend to support this theory.

In contrast, in the predominantly uncharged polymer (<25% ionized), a sharper reduction in surface tension occurred in response to increases in polymer concentration and this occurred at lower concentrations than was observed in the fully charged polymer. In this case, there is insufficient charge on the molecule to extend the chain, resulting in partial collapse and formation of distinct hydrophobic domains. Boiko ascribed the overall fall in surface tension on raising the polymer concentration to polyelectrolyte unfolding.

1.5.3 Solubilizing Ability of Polyelectrolytes

The early studies by Strauss [2] showed that the polysoap poly(2-vinylpyridine) partially quaternized with *n*-dodecyl bromide was able to solubilize normally water insoluble hydrocarbons and it was not found to be necessary to achieve a critical micelle concentration before solubilization occurred. The solubilization was found to be proportional to the polysoap concentration, suggesting that the micelles were intramolecular in nature. The concept of intramolecular micelles as proposed by Strauss, in which micelles are not surface active but can solubilize hydrophilic agents within their hydrophobic domains, is consistent with the surface tension finding of Pop [12] and Boiko [13].

Solubilization of isooctane and *n*-octane [14] was observed to result in a fall in reduced viscosity, supporting the concept of polymer collapse around a hydrophobic core. In contrast, solubilization of benzene in an aqueous polysoap solution [2] resulted in a reduction of reduced viscosity at low polymer concentrations and a raised viscosity as the concentration of polysoap was increased. This difference was said to arise from the ability of aliphatic groups to become solubilized within a micellar core and so reduce the molecular dimensions, compared to benzene, which was considered to span hydrophobic regions of neighboring micelles and lead to aggregation, resulting in an apparent rise of molecular volume.

It is considered that intramolecular micelles do not exist as independent units, unlike micelles within conventional monomeric surfactant systems, and as a result, their molecular dimensions can not be determined by conventional light scattering or hydrodynamic methods [3]. Consequently, luminescence quenching has been employed as an alternative method of assessing micellar size, by incorporating both luminescent probe and quencher molecules into the polymer chain [3]. In the presence of excess micelles, the chance of both molecules being present in any one micelle is inversely proportional to the number of micelles and the degree of quenching observed reflects this relationship. Such studies demonstrated that micellar size is independent of polymer concentration and this, once again, suggested intramolecular micellization.

The studies of surface tension and solubilization, when viewed together, demonstrate that the surface and interfacial tension measurements offer a simple method of monitoring conformational change within macromolecules. As a result, the hydrophobically associating polymer, poly(styrene-*alt*-maleic anhydride), described in the later chapter of this thesis, will be investigated using these techniques.

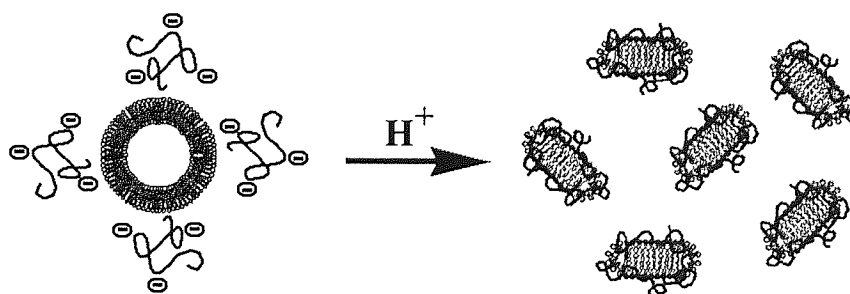
1.6 POTENTIAL MEDICAL APPLICATIONS OF ANIONIC HYPERCOILING POLYMERS

1.6.1 Interaction of Anionic Hypercoiling Polymers with Phospholipid Bilayers

Among all synthetic polyelectrolytes, polyanions have been investigated for various applications in the medical field. They have been found to inhibit adjuvant arthritis and modulate phagocytic activity [1]. Recently, polyanions have been evaluated as part of drug delivery systems, either as complexes/conjugates with biomolecules or in the preparation of pH-responsive liposomal formulation [1]. The application of anionic hypercoiling polymers to medicine was first suggested by Seki and Tirrell [2]. This work sprang from a need to synthesize phospholipid vesicles or liposomes that could be made to respond to their environment and used, for example, to selectively release drugs. Such liposomes were complexed with various poly(acrylic acid) derivatives to render the vesicle membrane sensitive to pH, whereby, a variation of pH acted as a 'trigger' mechanism to change polymer structure and alter the properties of the liposomal membrane.

Poly(2-ethacrylic acid) (PEAA) (0.1%) [15] was found to adsorb onto the surface of dipalmitoylphosphatidylcholine (DPPC) liposome (0.1%) suspended in aqueous solution at pH 7.4, that is, above the pK_a value of the polymer. Such behaviour was explained in terms of hydrogen bonding between the charged carboxylic acid pendant groups within the polymer and the phosphodiester head groups of the phospholipid. Lowering of the pH to 6.5 (towards the pK_a of the polymer) caused a loss of charge within the polymer, at which point hydrophobic interactions between ethyl pendant groups then predominated and led to a collapse of the polymer chain. The resultant hydrophobic domains acted to disrupt the liposomal membrane and caused a release of its contents, e.g. the marker compound carboxyfluorescein [15]. Concomitant differential scanning calorimetry studies showed a sudden broadening of the melting endotherms as the pH of the system was lowered, indicating a reorganization of vesicle structure [15, 16].

The presence of hydrophobic domains within PEAA molecules also resulted in an association of the polymer with the aliphatic side chains of the phospholipid, causing the lipid and polymer components to form discoidal polymer-lipid assemblies, analogous to those found in lipoprotein [2]. Electron microscopy provided a further insight into these pH-induced structural changes, and showed the presence of small (125-400 Å) diameter micellar particles, similar to those observed in high density lipoprotein [2]. The pH-dependent reorganization of phospholipid vesicle membranes by PEAA can be illustrated in Scheme 1. Such pH-induced macromolecular reorganization resulted in the formation of optically clear, aqueous suspensions [15]. The pH at which conformational transition in polymer-liposome structure was found to occur depended, not only on the chemical structure of the polymer, but also upon its tacticity. Incorporation of the photophysical probe pyrene, into PEAA, enabled the presence of hydrophobic environments to be identified. Studies using this technique [17] revealed that a large increment in fluorescence occurred as the pH was raised above 6.2 and this was concomitant with a conformational transition of the polymer. Binding of DPPC to PEAA was also found to result in a shift in the pK_a value of the polymer causing a decrease in its apparent acidity [17], i.e. behaved as a weaker polyacid. This shift of pK_a value was believed to attribute to hydrogen-bonding interactions between PEAA and the membrane surface.



Scheme 1 pH-Dependent reorganization of phospholipid vesicle by PEAA [18].

1.6.2 Enhanced Endosomal Escape of Biomolecules [1]

The efficient intracellular delivery of endocytosed active biomolecules generally requires a membrane-disrupting agent, which would facilitate release of the drug from the endosomes (e.g. pH-sensitive liposomes) and/or eventually destabilize the endosomal membrane to promote drug escape in the cytoplasm. Since endosomes have a slightly acidic pH, anionic carboxylated polymers are potentially useful for this purpose because they can destabilize membrane bilayers by a pH-triggered conformational change.

To assess whether improved cytoplasmic delivery of drugs could be achieved with these polymers, their ability to disrupt eukaryotic cell membranes has been investigated using red blood cell (RBC) as endosomal membrane models [1]. In this model, the extent of membrane disruption is determined by measuring hemoglobin leakage. PEAA as well as random copolymers of ethyl acrylate and acrylic acid or methacrylic acid (50/50 mol/mol) showed similar hemolytic activity at pH 5.5 and below. Study of the structure-activity relationship of a set of different MAA copolymers demonstrated that the presence of EA greatly increased the ability of the polymer to destabilize the membrane bilayer [19]. It was further shown that, for efficient destabilization at acidic pH, the copolymers should exhibit sharp conformational transition. Murthy et al. [20] also found that increasing the alkyl chain length of monomer units enhanced membrane lytic activity. Compared to PEAA, the more hydrophobic polymer, poly(propylacrylic acid) and poly(butylacrylic acid), exhibited greater hemolytic activity and achieved complete RBC lysis at higher pH values (pH 6.1 and 7.4, respectively). However, excessive polymer hydrophobicity was not associated with membrane destabilization and resulted in high macrophage cytotoxicity at neutral pH [19]. This is probably due to the globule configuration adopted by the polymer in solution, which renders it more susceptible to phagocytosis. Thus, pH-sensitive synthetic polymers can be molecularly engineered to efficiently disrupt eukaryotic membranes within a defined pH range by adjusting their hydrophilic-hydrophobic balance.

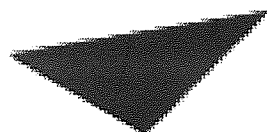
The therapeutic uses of the membrane reorganization process, shown in Scheme 1, will require that the polyelectrolyte, e.g. PEAA, remains irreversibly bound to the bilayer and that the average systemic concentration of free polyelectrolyte remains small. In principle, this can be achieved by either surface conjugation or surface attachment of the polyelectrolyte. The procedure for the latter can be simply accomplished by incubation of the polymer with vesicles [18]. The sensitivity of such vesicle preparations to small changes in pH was demonstrated by an experiment in which the fluorescent dye, calcein, was entrapped in the vesicle interior at pH 7.0. Since loading at a dye concentration of 200 mM would lead to quenching of the calcein fluorescence, so the release of vesicle contents can be detected by an increase in emission as the quenching condition is relieved. Experimental results by Tirrell [18] showed that at room temperature and pH 7.0, the fluorescence intensity remained constant over a period of 10 min. However, the acidification of the suspension to pH 6.5 then caused a rapid increase in emission intensity, as the contents of the vesicles were released quantitatively.

Sensitivity to pH in a range of 7.4 to 6.5 is potentially useful in several areas of drug delivery, as a result of the fact that conditions of abnormal acidity may arise in inflamed or infected areas, in certain tumor tissues, or in ischemia. Papahadjopoulos and coworkers [18] also suggested that pH-sensitization may be generally useful in vesicular delivery systems, in that it provides a mechanism for rapid release into the cytoplasm of drugs entrapped in liposomes that have been taken up by cells via endocytosis. Such liposomes undergo acidification after intake, but highly charged or high molecular weight species gain access to the cytoplasm only very slowly. A pH trigger would promote rapid release to the cytoplasm after endocytic uptake. The precise pH response of PEAA-modified vesicles can be optimized for a particular application through variations in polymer molecular weight, composition and stereochemistry [18].

1.6.3 Synthetic Protein-Lipid Complexes as Vehicle for Poorly Water Soluble Active Compounds

1.6.3.1 General Background of Lipoprotein [3]

Serum lipoproteins are somewhat analogous to the apoprotein-lipid recombinants found in lung surfactant. Their apoproteins are structurally similar to those of surfactant protein, but are distinct from SP-C, in that, they do not contain regions of an exclusively hydrophobic nature, but are more like the proposed structure for SP-B, possessing hydrophilic and hydrophobic facets within the same area of the polypeptide chain. The hypothetical model of SP-B folded structure and its proposed mode of interaction with a phospholipid bilayer are illustrated in Fig.1.7.

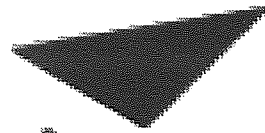


Aston University

Illustration removed for copyright restrictions

Fig.1.7 Structure and disposition of pulmonary surfactant protein SP-B. (a) Model of the structure of dimeric surfactant protein SP-B according to the saposin-like folding. (b) Probable disposition of SP-B associated with surfactant bilayers and monolayers. (Pictures modified from [21].)

The serum apoproteins can be divided into four categories, apoprotein A, B, C and E. The basic function of these molecules is to transport lipids within the bloodstream and interstitial spaces. The apoprotein-lipid complexes that form are organized into four distinct structures, namely; chylomicrons, low density lipoprotein (LDL)-mainly apo-B, very low density lipoprotein (VLDL) or high density lipoprotein (HDL)-mainly apo-A. Depending on apoprotein composition, lipoproteins can be assembled into different supramolecular shapes such as, spherical HDL-like particles and discoidal particles [22] (see Fig.1.8).



Aston University

Illustration removed for copyright restrictions

Fig.1.8 Negative-stained electron micrographs of lipoproteins from human CSF and rat astrocyte-conditioned media. Size bar is 25 nm. Arrows indicate a large spherical particle from human CSF (A). A small spherical particle from human CSF (B) and a stack of discoidal particles from rat astrocyte-conditioned media (C) [22].

Segrest [3] attempted to explain the mechanism by which these macromolecular lipoprotein assemblies carry lipid components in aqueous media. He observed a change in measurements of circular dichroism as apoproteins bound phospholipids, indicating an increase in the α -helical content of the protein. Specific amino acid sequences were identified which formed helical structures and exhibited an amphipathic character. This led to the suggestion that apoproteins form a series of α -helices, each arranging their amino acid side chains such that hydrophobic groups are exposed on one facet, perpendicular to the axis of the helix, while hydrophilic groups are arranged at the opposite facet, so forming an amphipathic helix. A number of such helices then surround a bilayer of lipid, in a 'doughnut' arrangement, which prevents contact between the hydrophobic portions of the lipids and surrounding water molecules.

Removal of lipid from an aqueous environment gives a far greater gain in free energy to the overall system than that lost by the removal of the hydrophilic head groups. Such changes minimize the free energy of the system, by maximizing hydrogen bonding between the water molecules within the surrounding solution, and are biological examples of the hydrophobic effect. Consequently, the binding of lipoproteins to lipid is primarily dependent upon hydrophobic interactions, hydrophilic head-groups specificity does not appear to be important, although the presence of charged groups in the amino acid side chains of lipoproteins does not make their conformation sensitive to change in pH.

The cooperative behaviour of apoproteins on binding lipid suggests that they are quite dynamic structures and that lipid binding induces a conformational change within apoproteins which facilitates further lipid binding and results in an increase in the overall size of the lipoprotein complex. As a result of the reversible conformational changes undergone by some apoproteins (Apo-A), these proteins are often referred to as exchangeable apoprotein. Their conformation changes in response to both association with lipid and in response to the solvent environment, e.g. Apo-E unfolds as the pH is changed from 7.4 to 4.8.

To assess the structure of lipoprotein assemblies, artificial produced recombinants of DPPC and partially purified apoprotein A-1 have been produced [3]. These appear as optically clear solutions and when examined by SEM, these assemblies can be seen to be made up of discoidal phospholipid bilayer. Differential scanning calorimetry studies indicated a decrease in enthalpy of the phospholipid gel-liquid crystalline transition which is a feature associated with the presence of co-operative lipoprotein complex [3]

Recombinant DNA-technology has recently been used to synthesize amphipathic α -helical peptide analogous to those found in apolipoproteins and proposed to undergo reversible hydrophobic interactions. Peptides containing 11 amino acid tandem repeats have been formed, in which leucine residues constitute a hydrophobic face along the longitudinal axis of the helix [3].

1.6.3.2 Application of Lipoprotein in Drug Delivery System [23]

Human plasma low density lipoproteins (LDL) are water-soluble nanoparticles which may be regarded as natural counterparts of liposomes. Physiologically, LDL serves as the primary transport vehicle of cholesterol and water-insoluble natural compound, such as vitamins and hormones to various cell types. The obvious idea to exploit the lipophilic properties of this carrier in the aqueous environment of blood for the purpose of drug delivery has been early recognized [23, 24], but so far the successful application for therapeutic purposes is still lacking. The apolar core of LDL, which attains a fluid, oily consistence at physiological temperature, is best qualified to act as an efficient lipophilic solubilizing medium. The second site for drug intercalation is the phospholipid surface monolayer, however, close to the surface the drugs are less well protected from hydrolysis [25] and drugs may undergo spontaneous exchange (redistribution) with other lipoprotein subspecies in plasma [26].

An enormous advantage of LDL as compared with liposomal formulations lays in the fact that LDL as natural component of blood induces no immune response. The key notion, however, is the recognized fact that tumour cells in general possess a higher level of LDL receptor activity than normal cells, which facilitates specific binding and internalization of LDL by cancer cells [23]. Another important aspect concerns the prolonged life-time of LDL in circulation as LDL is biodegradable and not recognized by the reticulo-endothelial system. However, one of the main requirements for the successful use of LDL as drug delivery system is that drug-loading does not alter structural properties of LDL. Little is known about the impact of drug incorporation on the structural integrity of the particle, which is an important factor in controlling rates of metabolic processes, as receptor binding or enzyme activity. Therefore, a physico-chemical characterization, i.e. determination of different parameters like phospholipid-shell and cholesterylester-core morphology, conformation of apoprotein and aggregation tendency, essentially need to explore to assess the applicability of the LDL-drug complex as a delivery system.

The uses of different analytical techniques to exploit such important characteristics of LDL-drug complex were recently established by Hammel et al. [23]. In their studies, LDL particles were loaded with two thymidine derivatives of distinct lipophilicity, i.e. monooleoyl (MOT)- and dioleoyl (DOT)- thymidine esters using reconstitution procedure. Such procedure involves the lyophilisation of LDL in the presence of protective agent. The drug in organic solution was mixed with the dry extract of LDL, followed by organic solvent evaporation and LDL reconstitution in aqueous buffer. Their results revealed that this method of drug incorporation does not alter the chemical composition of LDL, suggesting that the lipid from the dry LDL extract prepared in the presence of sucrose has not been permanently removed by the organic solvent. For MOT, an incorporation efficiency of 80% of the initial amount of drug with about ~150 MOT molecules per LDL particle was achieved by this method, whereas DOT, only negligible amounts of drug were successfully incorporated. The low incorporation efficiency for DOT could be based on the low water solubility of DOT, resulting in an extremely low concentration of DOT monomers in the water phase. Besides, they proposed that DOT may be susceptible to hydrolysis. Structural changes upon drug loading were monitored by differential scanning calorimetry (DSC) and small angle X-ray scattering (SAXS). The results showed that the influence of MOT and DOT were predominantly confined to the surface monolayer of LDL seen as a destabilization of the protein moiety and a small increase in particle diameter. The core lipid region of the LDL-drug complexes remains essentially unaffected, as verified by undisturbed core lipid arrangement and core lipid melting behaviour.

It seems likely that the choice of the lipophilic anchor of drug is of important issues for successful application of LDL. The lipophilicity of drug may be a rough guideline for drug encapsulation efficiency, i.e. the lesser hydrophobicity of the pyrimidine analogue products, the greater amounts of drug conjugated with LDL vesicle. It may be as well that this characteristic would determine the drug location in LDL vesicle [23].

1.6.3.3 Polymer-Lipid Complexes

(a) Analogies to Lipoprotein Assemblies

As mentioned earlier in Section 1.1, responsive hydrophobically associating polymers are widely known to undergo conformational transition in response to environmental stimuli. In aqueous media, at least over a particular pH range, the associating polymer will generally adopt a helical coil configuration with the hydrophobic side chain groups presented along one facet and the anionic hydrophilic groups presented along the opposite facet. This smart behaviour can mimic that of native apoproteins that arrange their hydrophobic and hydrophilic groups at opposite facets of α -helical coil to form an amphipathic structure such as that shown in Fig.1.9 [2, 3, 27].



Fig.1.9 Amphipathic coil showing hydrophobic (dark grey) and hydrophilic (light grey) facets.

When hypercoiling polymers are combined with film-forming lipids, they associate to produce lipid-polymer nanostructures analogous to lipoprotein assemblies such as HDL present in the blood plasma and responsible for transporting the fatty materials around the body. As such, they represent a new biomimetic delivery vehicle for fatty or water insoluble substances for both pharmaceutical and cosmetic industries [27]. It has been found by Tonge et al. [2, 3, 27] that these synthetic nanostructures, at least when freshly prepared, have a maximum diameter or cross-sectional dimension of less than 50 nm under physiological conditions. Sizes of the discoidal micellar assemblies appear to be in the range of 10-40 nm in diameter, typically 20 nm, and 5-7 thick. This is similar to the dimensions of lipoprotein micellar assemblies found in nature, such as the well characterized system between apolipoprotein III and dimyristoyl phosphatidylcholine (DMPC) that has been identified in insects [28].

In the case of an alternating copolymer of maleic acid and styrene, the amphipathic segments surround a phospholipid bilayer in a ‘doughnut’ arrangement (see Fig.1.10) [2, 27]. The synthetic nanostructures produced are subliposomal in dimension illustrated in the micrographs, shown in Fig.1.11 and Fig.1.12b. The poly(styrene-*alt*-maleic anhydride) used has previously been employed as part of a carrier system for an injectable anticancer medication and is therefore, approved for human use [29].

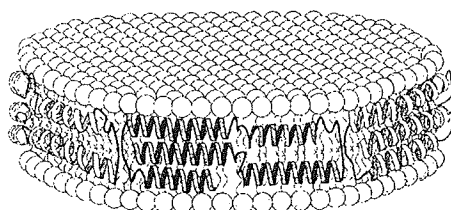


Fig.1.10 Polymer-lipid nanostructure with amphipathic polymer arrange around lipid bilayer [2].

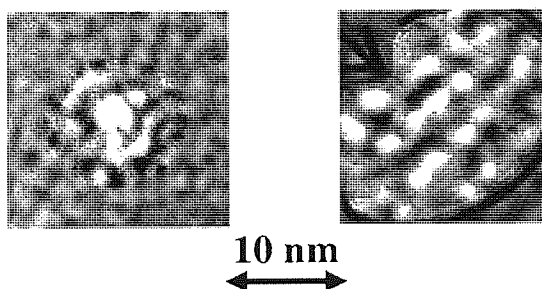


Fig.1.11 Cryo-TEM electron micrographs of PSMA-DLPC vesicles showing axial (left) and lateral (right) views of nanostructures formed (magnification x120,000) [3].

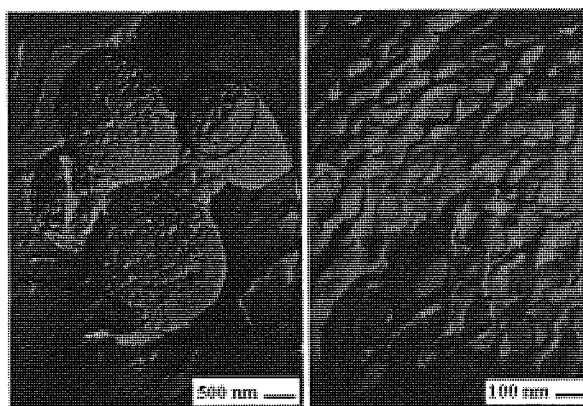


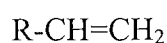
Fig.1.12 Microstructures of (a) β -lactoglobulin-phospholipid (DLPC) vesicles (x10,000 magnification) and (b) poly(styrene-*alt*-maleic anhydride)-phospholipid (DLPC) micelles (x50,000 magnification) [27].

(b) **Design of Polymer-Lipid Complexes [27]**

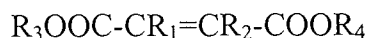
A formulation to fabricate such polymer-lipid nanostructure is generally based on membrane forming polar lipid together with a synthetic amphipathic polymer containing both anionic hydrophilic groups and hydrophobic groups.

The polar lipids are usually phospholipids based on glycerol in the form of phosphatidic acid derivatives in which the non-polar acyl ester groups contain between 8 and 25 carbon atoms. The acyl ester groups, however, are preferably selected from lauryl, palmitoyl and myristoyl and the polar head of molecule is typically provided by the phosphate group with a choline substituent, i.e. the lipid with a phosphatidylcholine. Nevertheless, it is also possible to use other polar lipids, especially phospholipids, based on different structures for example, sphingosine or ceramide.

The selected synthetic amphipathic polymer is generally a linear alternating vinyl copolymer formed by free-radical addition polymerization of an unsaturated dicarboxylic acid, or an anhydride or monoester of dicarboxylic acid, with a monoenoic vinyl monomer or monomer in alternating relationship. The second monomer type (i.e. monoenoic vinyl monomer) is generally selected from compound with a formula of;



where R is hydrogen, C1-C8 alkyl, alkoxy, phenyl or benzyl, which may be optionally substituted with an alkyl or other hydrophobic group. The first monomer type (i.e. dicarboxylic acid) is generally a compound with formula of;



where R_1 and R_2 are each independently hydrogen or C1-C9 alkyl. At least one of the R_3 and R_4 is hydrogen and the other is hydrogen or C2-C9 alkyl.

The copolymer structure should be such that the second monomer units alternate with dicarboxylic acid (or ester unit), providing a regular arrangement of alternate pendant anionic hydrophilic side groups and hydrophobic side groups along a linear backbone.

With regards to the criterion mentioned above, if, in case of monoenoic vinyl monomer, R is hydrogen or is methoxy or ethoxy (C₁ or C₂ alkoxy), R₃ and R₄ should not then be both hydrogen. Usually, in preferred embodiments, R₁ and R₂ should be both hydrogen. It is important to note that, the copolymers derived from alkyl vinyl ether monomer with alkyl groups longer than seven carbon atoms may not be suitable for this invention because of their poor aqueous solubility. The number of carbon atoms in the hydrophobic side groups of the polymer or copolymer should usually be equal to or greater than the number of carbon atoms in the backbone of the polymer and when polymer is ionized, the average charge ratio per backbone carbon should be less than or equal to unity.

Suitable polymers may be formed as alternating copolymers of maleic acid (or maleic anhydride) with styrene, indene or a C1-C4 alkyl. It is important that the selected polymer must have physiologically or pharmaceutically acceptable non-toxic properties. Also, the molecular weight or relative mass of polymer should be within the range of 2,000 to 20,000 daltons. Furthermore, the polymer must not be in the form of a block copolymer.

The method to form the polymer-lipid nanostructure comprises the steps of mixing a membrane-forming lipid with synthetic amphipathic polymer, at a pH above a critical solubilizing value in order to form a cloudy or turbid aqueous dispersion. Then the mixture was treated with an acidifying agent to lower the pH below critical solubilizing value whilst the temperature is above a phase transition temperature of the lipid.

(c) **Dynamic Surface Activity of Polymer-Lipid Complexes [27]**

One of the most important properties of the polymer-phospholipid complexes with regard to their applications such as, solubilizing agent and artificial lung surfactant, is the manner in which surface tension varies with repetitive changes in surface area. One test method used to obtain such profile is a pulsating bubble technique using a pulsating bubble surfactometer consisting of a sample chamber, pulsator unit and pressure-recording device. The pulsating bubble technique simulates to some extent the contraction and expansion of the alveolar sacks in the lungs and allows the surface tension to be assessed at minimum and maximum bubble volumes. This technique also allows the effect of repeated expansion and compression cycles upon the adsorption of surface active components to be observed and quantified. The technique has been used as a model *in vitro* system for testing the efficacy of synthetic lung surfactants.

Tonge et al. revealed [2, 3, 27] that the nanostructure, consisting of poly(styrene-*alt*-maleic anhydride) (PSMA) and dilauroylphosphatidylcholine (DLPC), when tested under dynamic surface compression exhibit remarkably high surface activity and approach the values observed with commercially available lung surfactant, see Fig.1.13. This finding indicates a high suitability of using these complexes as artificial lung surfactants and as solubilizing agent.

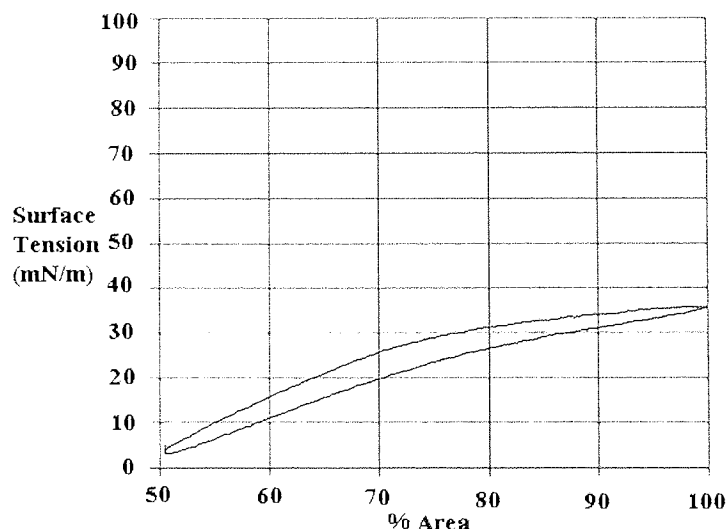


Fig.1.13 Surface activity of the PSMA-DLPC complexes (1.25/0.5%) measured by pulsating bubble surfactometry at 5 min of pulsing [27].

(d) Applications of Polymer-Lipid Complexes

The polymer-lipid complexes are believed to be ideally suited to transport and delivery of drug substances into the body, especially oily materials, by either topical (skin or eye) or systemic (via lung) routes or directly into the blood circulation. It may also be possible to target specific cells and parts of cell within the body by incorporating targeting proteins or lectins into the structure.

The most immediate use of this nanostructure lies in its application to the skin, where the nanostructure offers an aqueous alternative to liposomal, niosomal and ceramide based systems and present a completely novel delivery concept for both pharmaceuticals and active botanical products for dermatological, cosmeceutical and cosmetic applications. The polymer-lecithin mixture is optimally formulated around skin pH.

The polymer-lipid complexes may offer an entirely novel platform technology to treat disease processes that arise from deficiencies in lubrication, such as the degenerative joint diseases so apparent in osteoarthritis and the dry eye condition prevalent in rheumatic patients. The likely presence within the lung and the eye of natural nanostructures formed from interactions between apoproteins and lipids suggests that synthetic mimics would offer an effective means of rendering these bio-surfaces lubricious and wettable.

The nanostructures formed may act as powerful surfactants and these properties could be utilized to provide a surface coating of delicate tissues such as those of the lung, e.g. in the treatment of neonatal respiratory distress syndrome (RDS). RDS is a potentially fatal condition that is currently most effectively treated with artificial surfactants which often contain animal derived proteins. The polymer-lipid complexes reduce the surface tension in an *in vitro* test system dramatically in a manner comparable to that of the best of the currently available artificial lung surfactants and superior to some of the marketed products.

For the ocular applications, the nanostructure formulation offer both a vehicle for ocular drug delivery and a treatment for the common eye condition known as dry eye disease. This formulation has the great advantage over existing products in that it enables oil soluble active agents to be incorporated into a clear and colourless aqueous composition that is most acceptable to the eye and avoids the use of ointments and emulsion. The aqueous gel formulation of the nanostructures is perhaps the most acceptable and long lasting presentation for ophthalmic application from the viewpoint of both patient and practitioner.

1.7 AIMS AND SCOPE OF RESEARCH

The polymer-lipid complexes prepared from hydrophobically associating polymers and natural phospholipids were first introduced by the group at Aston University. The motivation for this innovation was drawn from the fact that PSMA is capable of interacting with phospholipids to form nanostructures of analogous size to those of high density lipoproteins, possessing the ability to solubilize poorly water soluble compounds into their lipoidal core to render them aqueous soluble. The nanostructure produced is highly surface active and therefore, be suited for applications in biomedicine [27].

The primary aim of this research was to examine the potential of using these polymer-lipid complexes in conjunction with hydrogels as new vehicles for ophthalmic drug delivery. The principle has been studied by examining the encapsulation of active compounds (e.g. Rhodamine B dye, Oil red O dye and Pirenzepine drug) in a new type of nanoparticle. The incorporated nanovesicles are then encapsulated in a hydrogel matrix of the type used for soft contact lenses. The release studies of active compounds from nanoparticle containing hydrogels are also observed to examine whether such smart hydrogels can retain compounds and deliver them at a slow rate for a prolonged period of time.

The thesis has been divided into 8 Chapters. Chapter 1 provides general background concerning hydrophobically associating polymers and their potential medical applications. In particular it focuses on the ability of such polymers to mimic the behaviour of natural proteins, which makes it possible to use them for drug delivery applications. Chapter 2 covers in detail the materials, synthesis methods and some characterization techniques used in this research. Chapter 3 provides details concerning the phase behaviour as well as the theory behind the formation of polymer-lipid complexes.

The investigation of polymer-lipid interaction was carried out through various experimental techniques, such as Langmuir-Blodgett, Surface tension measurements and ^{31}P -NMR spectroscopy. Details of these studies are described in Chapters 4-6. Techniques for encapsulating active compounds into polymer-lipid nanostructures and for incorporating nanoparticles into hydrogel matrices are presented in Chapter 7. Morphology studies of encapsulated nanoparticles both in the aqueous solution and within hydrogel matrices as well as the release studies of compounds delivered from hydrogel are also described in Chapter 7. Finally, Chapter 8 provides a summary of the research presented in Chapters 3-7, followed by suggestions for further work. The following chart diagram displays a concept map of the research and thesis structure.

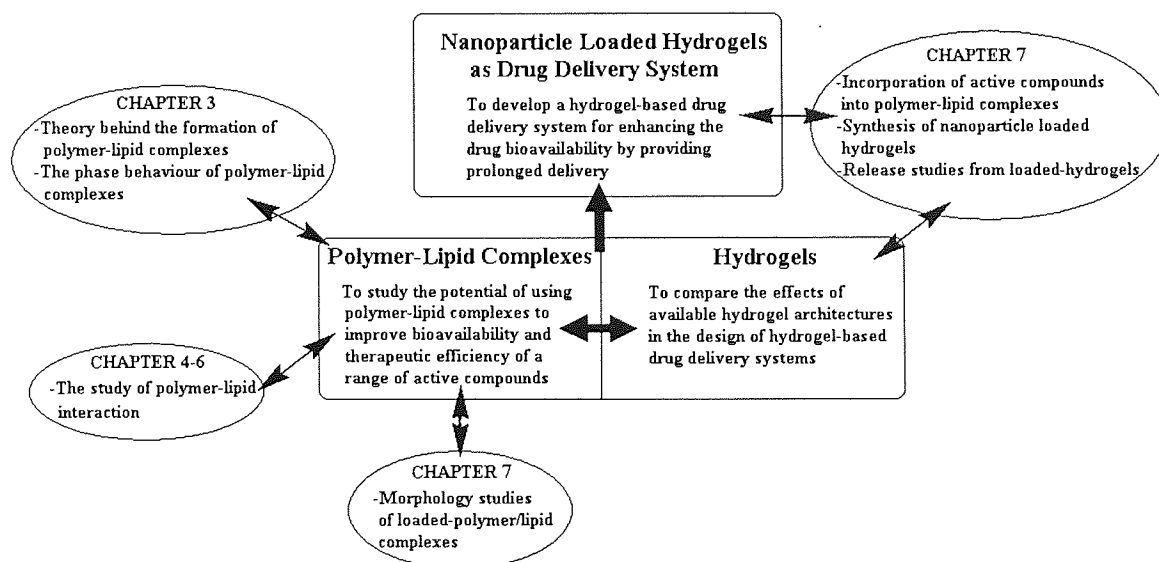


Fig.1.14 Concept map of research and thesis structure.

CHAPTER 2
MATERIALS AND METHODS

2.1 INTRODUCTION

In this chapter, the preparation method for anionic hypercoiling polymer-phospholipid (PSMA-DLPC) complexes, the technique for encapsulation of active compounds (e.g., Rhodamine B and Oil red O and Pirenzepine drug) within these complexes and the freeze drying technique for the obtained loaded complexes will be described. The methodology for polymer membrane synthesis via thermal free-radical and UV polymerization, the technique for encapsulating loaded PSMA-DLPC complexes within these membranes and the method of obtaining release profiles will be described. Last but not least, various analytical techniques used to study PSMA-DLPC complexes, for example; Langmuir-Blodgett Trough, surface tension measurements and ^{31}P -NMR spectroscopy will also be discussed in this Chapter.

2.2 SYNTHESIS OF PSMA-DLPC COMPLEXES

2.2.1 Materials

Chemicals used to prepare unloaded and loaded PSMA-DLPC complexes were obtained from commercial sources listed in Table 2.1.

Table 2.1 Chemicals used to prepare unloaded and loaded PSMA-DLPC complexes.

Chemicals	Molecular Formula	MW	Suppliers
1. Poly(styrene- <i>alt</i> -maleic anhydride) (PSMA)	$-(\text{C}_{12}\text{H}_{10}\text{O}_3)_n-$	1,600.0 (M_n)	Scientific polymer product
2. 2-Dilauryl- <i>sn</i> -glycero-3-phosphocholine (DLPC)	$\text{C}_{32}\text{H}_{64}\text{NO}_8\text{P}$	621.8	Genzyme
3. Rhodamine B	$\text{C}_{28}\text{H}_{31}\text{ClN}_2\text{O}_3$	479.0	Sigma-Aldrich
4. Oil red O	$\text{C}_{26}\text{H}_{24}\text{N}_4\text{O}$	408.5	Sigma-Aldrich
5. Pirenzepine dihydrochloride	$\text{C}_{19}\text{H}_{21}\text{N}_5\text{O}_2 \cdot 2\text{HCl}$	424.3	Sigma-Aldrich
6. Deionized water	H_2O	18.0	Produced in house

2.2.2 Methods

In order to prepare polymer-phospholipid complexes from 2-dilauryl-*sn*-glycero-3-phosphocholine (DLPC) and PSMA copolymers (listed in Table 2.1), the appropriate amount of hydrogenated DLPC and polymer were mixed together. The complexes were obtained by slowly lowering the pH of the resultant cloudy mixture to pH 4.0. Whilst lowering the pH, a white water-insoluble substance was precipitated out and was then rapidly solubilized to form a clear solution. This phenomenon shows the formation and the incorporation of the hypercoiling polymers into the bilayer of DLPC to produce nanostructural polymer-phospholipid complexes. The formation of these complexes could be observed by an increase of the viscosity and transparency of the mixture. After the optically clear viscous solution was obtained, the pH of the mixture was gradually increased to pH 7.4.

The model compounds (Rhodamine B, Oil red O and Pirenzepine) were used in order to determine a potential of using PSMA-DLPC complexes to encapsulate drug and to understand the interaction between drug and the complexes. The physical entrapment of the model drugs (listed in Table 2.1) into PSMA-DLPC complexes was carried out in a similar way to that of the preparation of pure PSMA-DLPC complexes except that appropriate amount of active compound was added together with DLPC and PSMA before lowering the pH of the solution to pH 4. The final concentrations of Rhodamine, Oil red O and Pirenzepine in such complexes were 0.5, 0.1 and 0.5% w/v, respectively. Chemical structures and some characteristics of the three active compounds are illustrated in Fig.2.1 and Table 2.2, respectively.

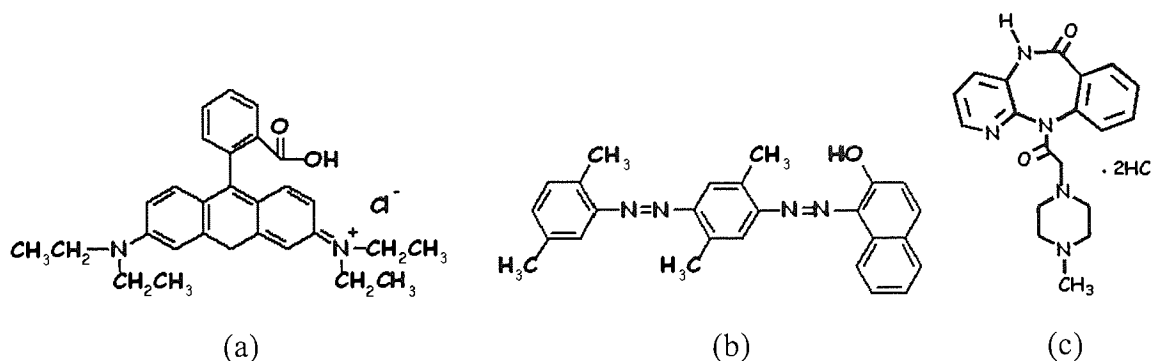


Fig.2.1 Chemical structures of (a) Rhodamine B, (b) Oil red O and (c) Pirenzepine dihydrochloride.

Table 2.2 Characteristics of Rhodamine B, Oil red O and Pirenzepine drug.

Properties	Rhodamine B	Oil red O	Pirenzepine dihydrochloride
Molecular Formula (MW)	C ₂₈ H ₃₁ ClN ₂ O ₃ (479.0 g/mol)	C ₂₆ H ₂₄ N ₄ O (408.49 g/mol)	C ₁₉ H ₂₁ N ₅ O ₂ • 2HCl (424.30 g/mol)
Log P(octanol/water)*	+1.85	+9.81	-0.22
Absorbance wavelength (nm)	550	515 (in ethanol)	280
Solubility	Soluble in water	Insoluble in water, moderate soluble in ethanol	Soluble in water

* Calculated using estimation software (available online at <http://www.esc.syrres.com/interkow>)

2.3 Freeze-Drying of Loaded PSMA-DLPC Complexes

In the preparation of pharmaceutical formulations, drying is usually the final stage of processing and is designed to yield a stable homogeneous product which is easy to manipulate in subsequent operations of packing or formulating. The removal of water vapour from a frozen solution by sublimation forms the basis of freeze-drying [30]. The process of drying from the frozen state is carried out by subjecting the material to be dried to low absolute pressure (high vacuum) after it has been frozen at temperature below -4°C. Under these conditions, the frozen water will be sublimated. The water vapour is removed from the system by condensation in a cold trap maintained at a lower temperature than the frozen material. In general, moisture levels of freeze dried products are designed to be less than 3%.

In this work, freshly prepared encapsulated PSMA-DLPC complexes, as obtained from Section 2.2.2, were freeze-dried without a cryoprotectant. Firstly, sample was dispensed in glass vials and frozen at -40°C for 20 min. After that the frozen sample was immediately placed on the freeze-dryer plate with a temperature of -60°C. Sublimation lasted 48 hours at a vacuum pressure of 10-13 Pa and without heating,

being maintained at the condenser surface temperature of -60°C . Finally, the glass vial was sealed under anhydrous conditions and stored at 4°C until being re-hydrated by using the same initial volume of deionized water.

2.4 SYNTHESIS OF HYDROGEL MEMBRANES

2.4.1 Materials

Chemicals used to prepare unloaded and loaded-hydrogel membranes were obtained from commercial sources listed in Table 2.3. The chemical structures of chemicals used to prepare hydrogel membranes are presented in Fig.2.2.

Table 2.3 Chemicals used to prepare unloaded and loaded-hydrogel membranes.

Chemicals	Molecular Formula	MW	Suppliers
1. 2-Hydroxyethyl methacrylate (HEMA)	$\text{C}_6\text{H}_{10}\text{O}_3$	130.1	Cornelius
2. Methacrylic acid (MAA)	$\text{C}_4\text{H}_6\text{O}_2$	86.1	Acros Organics
3. Ethylene glycol dimethacrylate (EGDMA)	$\text{C}_{10}\text{H}_{14}\text{O}_4$	198.2	Acros Organics
4. Azobisisobutyronitrile (AIBN)	$\text{C}_8\text{H}_{12}\text{N}_4$	164.2	Aldrich
5. Modified-PVA Macromers	N/a	N/a	Ciba Vision
6. Deionized water	H_2O	18.0	Produced in-house

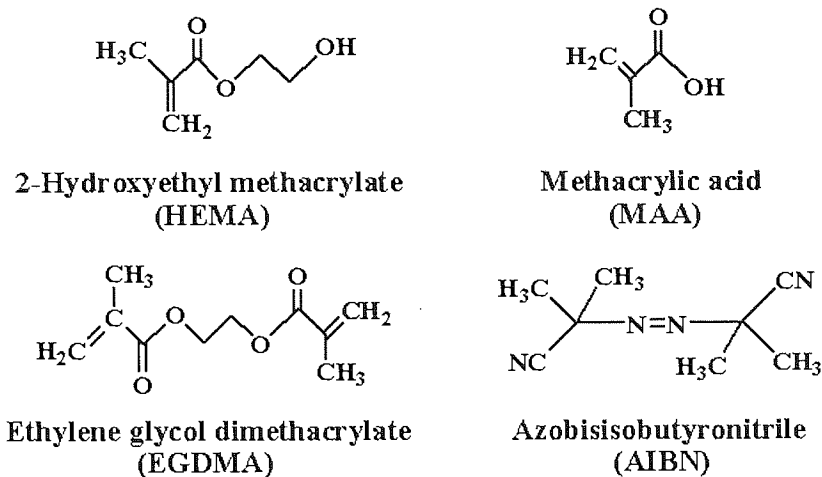


Fig.2.2 Chemical structures of chemicals used to prepare hydrogel in this study.

2.4.2 Thermal Free-Radical Polymerization

The technique of preparing hydrogel membranes by thermal polymerization is as follows. The hydrogel membrane was synthesized in the bulk of a mixture of monomers and a thermal free radical initiator within a suitable mould. A glass mould used in this work consists of two glass plates (about 4" x 4"), each coated with a layer of melinex (polyethylene terephthalate film) by using a spray-on adhesive. The glass plates were separated first by a polyethylene gasket and then with a syringe needle, inserted at the apex of the glass plates. A whole glass mould was finally clamped tightly with spring clips, as shown in Fig.2.3.

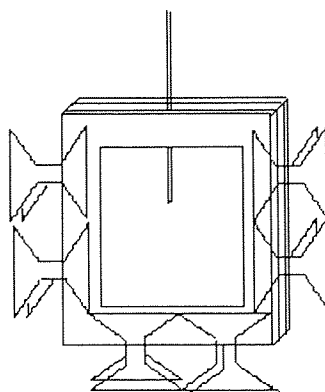


Fig.2.3 Injection mould used to prepare hydrogel membrane.

A monomer mixture, containing HEMA and MAA, a free radical initiator (AIBN) and a cross-linking agent (EGDMA) (listed in Table 2.3), was made ensuring that a homogeneous solution was obtained. The monomer mixture was degassed prior to injection to the moulds. The injected mould was left for three days in the oven, being maintained at 60°C and then was post-cured at 90°C for three hours in order to complete a reaction. Finally, the obtained hydrogel membrane was removed from a mould.

In order to prepare a laden-hydrogel membrane, an appropriate amount of active compound (e.g. loaded PSMA-DLPC complexes, drug or dye) was mixed together with monomers mixture prior to polymerization.

2.4.3 UV-Polymerization (Photopolymerization)

Photopolymerization reactions are driven by chemicals that produce free radicals when exposed to specific wavelengths of light. A variety of *photoinitiators*, each with its unique spectrum, are available and more are continually being developed. A photon from a light source excites or dissociates the photoinitiator into a high-energy radical state. This radical then induces the polymerization of a macromer solution.

In general, the process is benign and the polymers can be fabricated at temperatures and pH values near physiological ranges and even in presence of biologically active materials. The process also proceeds very rapidly at these conditions for most monomers and conventional initiators. In addition, the ability to direct the exposure of UV light and time of incidence to achieve temporal control is particularly advantageous for the formation of complex devices [31].

2.4.3.1 Photopolymerizable Materials

Polymerization of monomers using visible or UV irradiation has been thoroughly investigated. While such systems work well for many applications, they generally can not be utilized in biomedical application because most monomers are cytotoxic. As a result, photopolymerizable hydrogels for biomedical applications have generally been formed from macromolecular hydrogel precursors. These are water-soluble polymers with two or more reactive groups. Examples of photopolymerizable macromers include poly (ethylene glycol) acrylate derivatives, poly (ethylene glycol) methacrylate derivatives and poly (vinyl alcohol) (PVA) derivatives. Chemical structures of some of the macromers that can be used to form photopolymerizable hydrogels are shown in Fig.2.4.

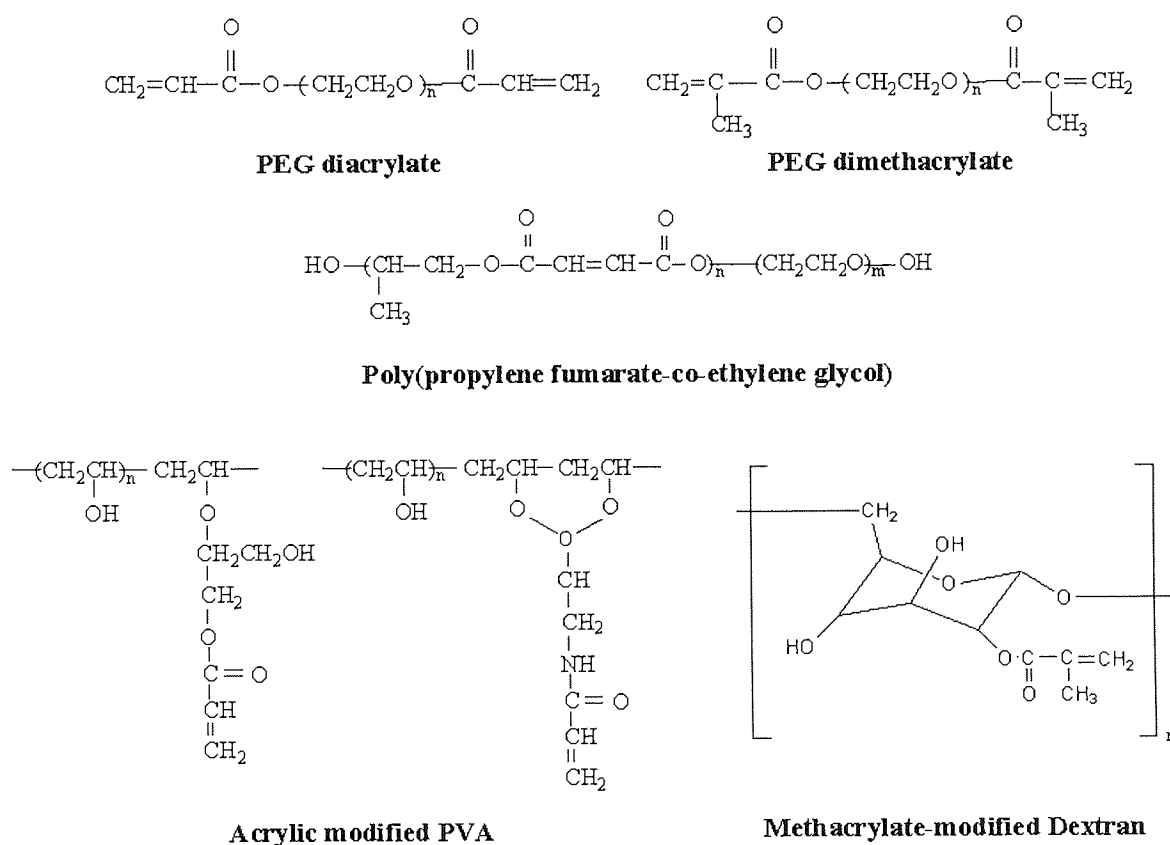


Fig.2.4 Chemical structures of materials that can be photopolymerized to create crosslinked hydrogel networks.

2.4.3.2 Photoinitiators

Photopolymerization schemes generally use a photoinitiator that has high absorption at a specific wavelength of light to produce radical initiating species. Other factors that should be considered in selecting the photoinitiator include its biocompatibility, solubility in water, stability and cytotoxicity. Over the last decade, various photoinitiators have been investigated to achieve better photopolymerization. Three major classes of photoinitiation, depending on the mechanism involved in photolysis, include radical polymerization through photocleavage, hydrogen abstraction and cationic photopolymerization. Cationic photoinitiators are generally not utilized in biomedical applications because they generate protonic acids.

(a) Radical photopolymerization by photocleavage

The photoinitiators undergo cleavage at C-C, C-Cl, C-O, or C-S bonds to form radicals when exposure to light as shown in Fig.2.5. These photoinitiators include aromatic carbonyl compounds such as benzoic derivatives, benziketals, acetophenone derivatives and hydroxyalkylphenones.

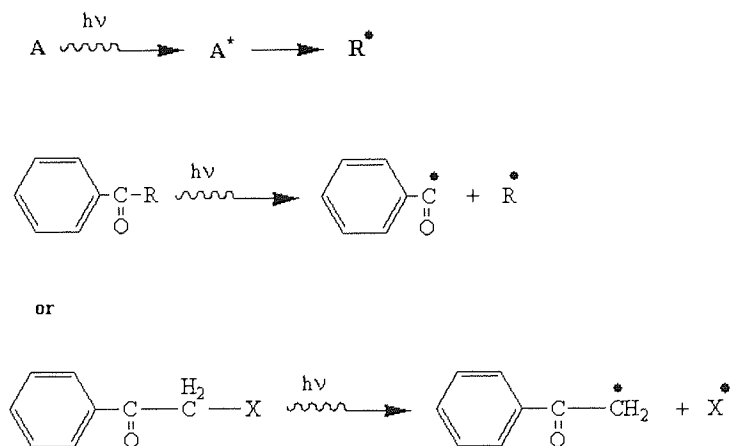


Fig.2.5 Photoinitiators that promote radical photopolymerization by photocleavage mechanism (e.g., Irgacure 2959).

(b) *Radical photopolymerization by hydrogen abstraction*

Upon UV irradiation, photoinitiators such as aromatic ketone undergo hydrogen abstraction from an H-donor molecule to generate a ketyl radical and a donor radical as shown in Fig.2.6. The initiation of photopolymerization usually occurs through the H-donor radical while the ketyl radical undergoes radical coupling with the growing macromolecular chains.

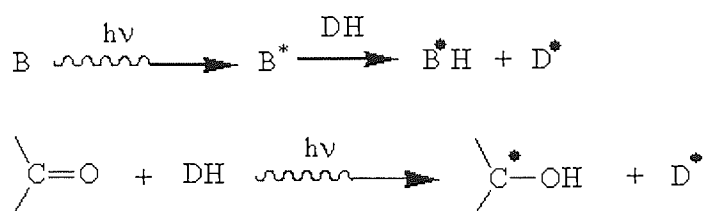


Fig.2.6 Photoinitiators that promote radical photopolymerization by hydrogen abstraction mechanism.

2.4.3.3 Poly (vinyl alcohol) (PVA)

In this study, *Poly (vinyl alcohol)*; PVA, has been chosen as secondary drug carrier. This is because it has been employed in several biomedical applications including contact lenses, e.g., ‘nelfilcon A’ daily contact lenses. PVA hydrogels have been reported to be biocompatible and have been shown to resist protein adsorption and cell adhesion. Also, PVA hydrogels can form by physical crosslinking using freeze-thaw processes, chemical crosslinking with aldehydes, or even radiation [32].

(a) *Photocrosslinkable PVA*

The functional group of PVA is the secondary alcohol, repetitive as polyol in 1,3-position. This 1,3-polyol-structure is ideally suited for the formation of cyclic acetal (Fig.2.7). This reaction is of great importance in some industrial applications. For example, Vinylon fibers are made from acetal-modified PVA. Also, PVA-acetals like polyvinyl formal and polyvinyl butyral are used in paint additives and foams. Normally, acetals are formed under acidic conditions in water-free media and

are cleaved under aqueous acidic conditions. But PVA can be modified by cyclic-acetal formation in aqueous solution at room temperature nearly quantitative. The reason for this high conversion is the outstanding stability of the (cyclic) acetal. With a crosslinker, consisting of both aldehyde and polymerizable functional groups, crosslinked PVA macromers can be prepared and can then be photo-polymerized upon UV irradiation. In general, crosslinker was attached to the PVA backbone by cyclic-acetal formation, using the well-established polymer analogue reaction, thus creating the desired photo-polymerizable macromer with a well-controlled number of reactive groups per macromer chain.

There are three reactions going on simultaneously during the modification of partially acetylated PVA in aqueous acidic (Fig.2.7). The acetal structure of the crosslinker is hydrolyzed to the corresponding aldehyde, the aldehyde reacts with PVA to form the stable cyclic acetal function, and the acetate of the PVA is partially hydrolyzed to form additional OH groups. The reactions are acid-catalyzed and can be stopped by neutralization at any time. The cyclic acetals of the modified PVA are stable under neutral condition even at autoclaving temperatures [33].

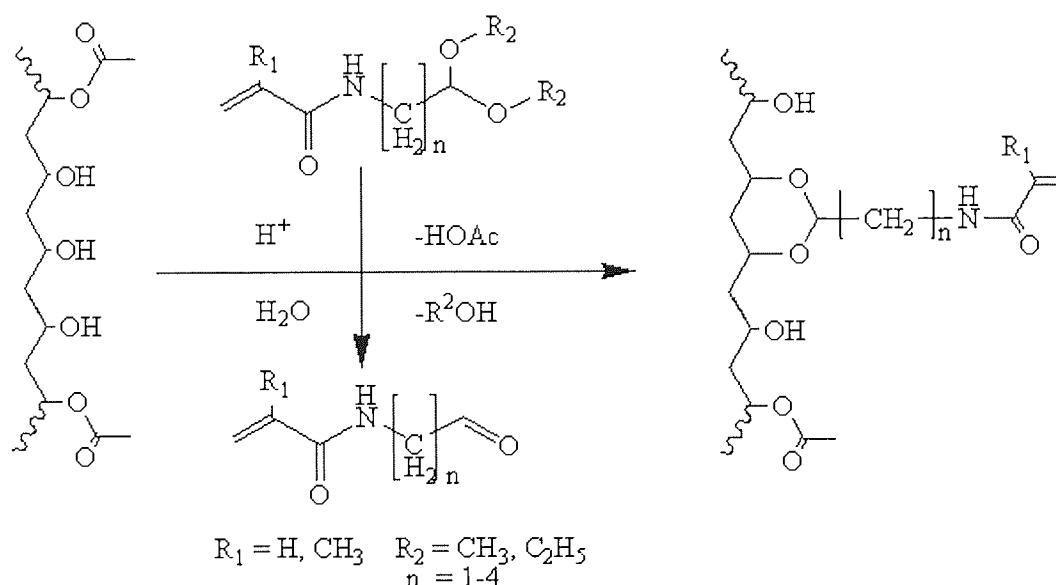


Fig.2.7 Modification of Poly (vinyl alcohol).

(b) *Design of the Crosslinker*

The acetalization of PVA is accomplished under aqueous acidic conditions, and therefore, the crosslinking groups have to be designed in a way that they are stable under these conditions. Amides are much more stable than the corresponding esters and in methacryl- or acrylamide, the double bond additionally stabilizes the amide function against hydrolysis. Another big advantage of the amide is the higher reactivity in polymerization. In this study a protected aliphatic amino aldehyde in form of the dialkylacetal has been used as crosslinker. Such compounds can be easily synthesized by reacting the protected amino aldehyde with the acid chloride. They can be purified by extraction and, depending on the molecular size, either by distillation or crystallization.

(c) *Photoinitiator*

The photo-polymer requires a photoinitiator to crosslink. In order to have no extractable in the lens and not even traces of unreacted photoinitiator, the initiator should be linked to the polymer backbone. This can be achieved in a simultaneous reaction with the linking of the photocrosslinkable moieties, using the same type of acetalization chemistry (Fig.2.8)

The primary OH group of Irgacure ® 2959, a commercially available photoinitiator, is activated by mesylate and then reacted with the protected amino aldehyde. It can be further transformed into a compound which contains three functions; the aldehyde, the initiator and the acrylamide function.

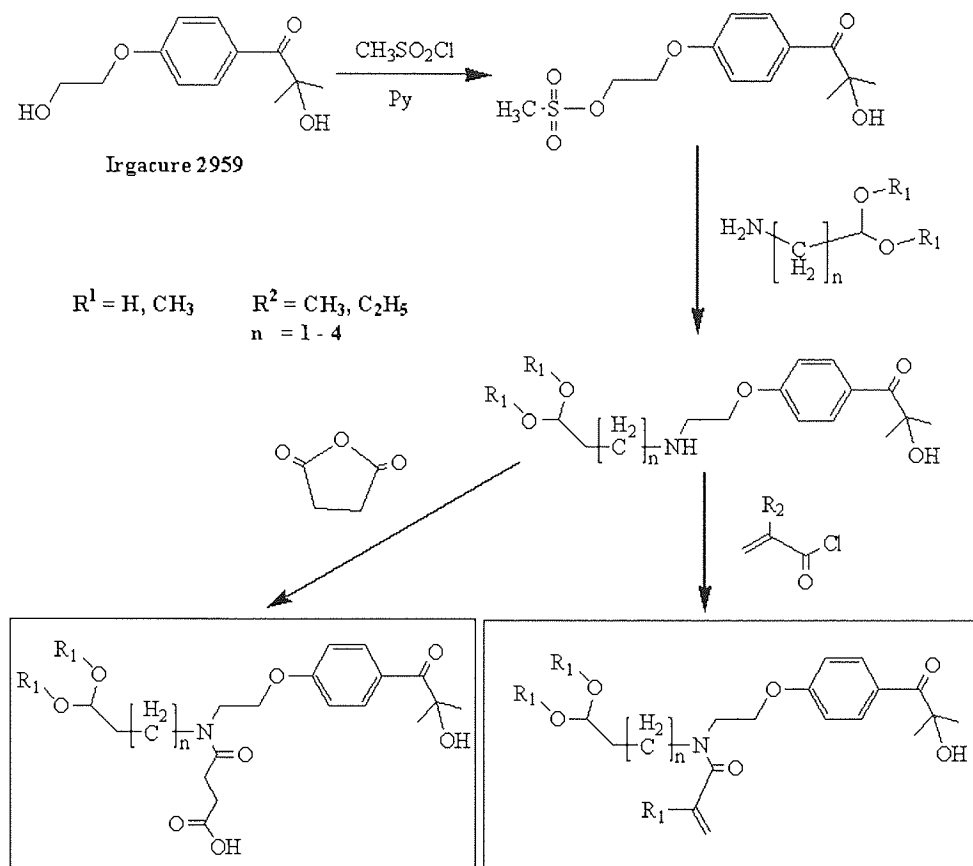


Fig.2.8 Modification of Irgacure ® 2959 photoinitiator.

2.4.3.4 Photopolymerization of PVA

In this study, aqueous solution of functionalized PVA macromer was present from Ciba Vision. The photoinitiator ‘Irgacure® 2959’ was already added to the macromer solution as received. Macromer was a water soluble polymer of poly(vinyl alcohol) modified by the addition of *N*-acryloylaminoacetaldehyde-dimethylacetal [34]. The acrylic side chain is photocrosslinked to form a stable hydrogel. The network is formed by photocrosslinking using Lightstream Technology™ process. This fast, light-curing process has been extensively documented in both the patent and scientific literature [34, 35]. The resultant material characters are listed in Table 2.4 and the idealized structure of modified PVA macromer is also shown in Fig.2.7.

Table 2.4 Characteristics of resultant PVA hydrogels synthesized by photopolymerization of functionalized PVA macromer using Lightstream Technology™ process [34].

Parameter	Measured value
Light transmission	≥99% (380-780 nm)
Refractive index	1.38 @ 589.3 nm
Water content	69 ± 2%; determined gravimetrically
Oxygen permeability (Dk)	26 barriers @ 35°C
Elastic modulus (Young's)	0.91 MPa

To synthesize the loaded PVA hydrogel membrane, active compound (e.g. loaded PSMA-DLPC complexes, dye or drug) was thoroughly mixed with appropriate amount of functionalized PVA macromer prior to photopolymerization. The obtained mixture containing active compound was then poured onto the glass sheet mould, shown in Fig.2.3, and exposed to the long wavelength UV light (365 nm, 10 mW/cm²) for 20 min.

2.5 EXPERIMENTAL TECHNIQUES

Experimental techniques such as Langmuir-Blodgett Trough, surface tension measurements and ³¹P-NMR spectroscopy were used in order to explore the association behaviour of PSMA both at the air-water interface and in the bulk of solution, as well as its interaction with DLPC membranes. The UV-Vis spectrophotometer was used to obtain release profiles of dyes and Pirenzepine drug from hydrogels.

2.5.1 Langmuir-Blodgett Trough Technique

Surface active agent (surfactant) is a larger class of molecules which have a significant technological and biological importance. Generally, these molecules consist of a hydrophilic (water soluble) and a hydrophobic (water insoluble) part. This amphiphilic nature of surfactants is responsible for their association behaviour in solution (micelles, bilayers, vesicles, etc.) and their accumulation at the interfaces (air-water or oil-water), see Fig.2.9. The hydrophobic part usually consists of hydrocarbon or fluorocarbon chains while the hydrophilic part consists of a polar group.

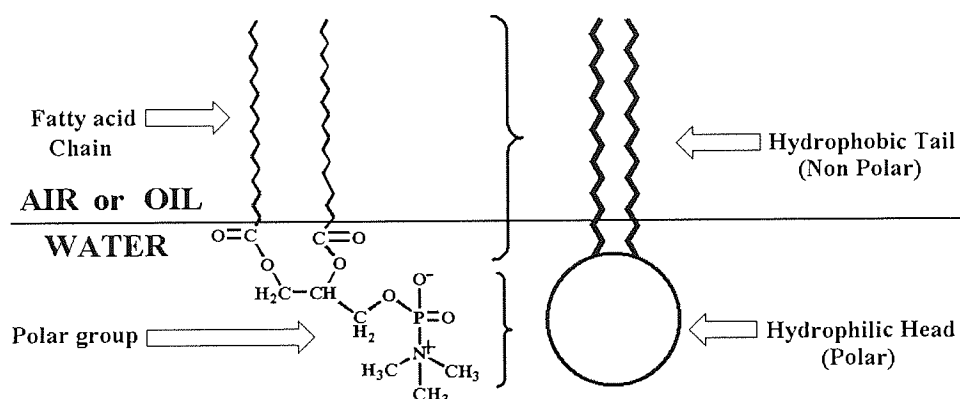


Fig.2.9 A schematic illustration showing the components of phospholipid (left) and the orientation of phospholipid adopted at an air-water interface (right).

The association behaviour of surfactants in solution and their affinity for interfaces is determined by the physical and chemical properties of the hydrophobic and hydrophilic groups, respectively. The size and shape of the hydrocarbon moiety and the size, charge and hydration of the hydrophilic head group are of utmost importance in this respect. Depending on the balance between these properties a wide variety of self-assembled structures, both at interfaces and in bulk, have been observed. The driving force behind the association is the reduction of the free energy of the system. Therefore, when a surfactant comes in contact with water it accumulates at the air-water interface causing a *decrease* in the surface tension of water.

Many of these amphiphilic substances are insoluble in water. However, with using of a volatile and water insoluble solvent, they can be easily spread on a water surface to form an insoluble monolayer at the air-water interface. These monolayers, also called *Langmuir* monolayer. The amphiphilic nature of the surfactants dictates the orientation of the molecules at the interface (air-water or oil-water) in such a way that the polar head group is immersed in the water and that the long hydrocarbon chain is pointing towards air or oil, see Fig.2.9. When a solution of an amphiphile in a water insoluble solvent is deposited on a water surface, the solution spreads rapidly to cover the available area. As the solvent evaporates, a monolayer is formed. When the available area for the monolayer is large the distance between adjacent molecules is large and their interactions are weak. The monolayer can then be regarded as a two-dimensional gas. Under these conditions the monolayer has little effect on the surface tension of water. If the available surface area of the monolayer is reduced by a barrier system (see Fig.2.10), the molecules start to exert a repulsive effect on each other. This two-dimensional analogue of a pressure is called the *surface pressure* (π) and is given by the following relationship:

$$\pi = \gamma - \gamma_0$$

where γ is the surface tension in absence of a monolayer and γ_0 the surface tension in the present of a monolayer.

As shown in equation above, the surface pressure is, therefore, a reduction of the surface tension. The plot at a constant temperature of surface pressure versus the area of water surface available to each molecule is known as a ‘pressure-area isotherm (π -A isotherm)’. The shape of the isotherms is characteristic of the molecules making up the film and hence provides a two-dimensional fingerprint. Usually an isotherm is recorded by compressing the film (reducing the area with the barriers) at a constant rate while continuously monitoring the surface pressure. Depending on the material being studied, repeated compressions and expansions may be necessary to achieve a reproducible trace.

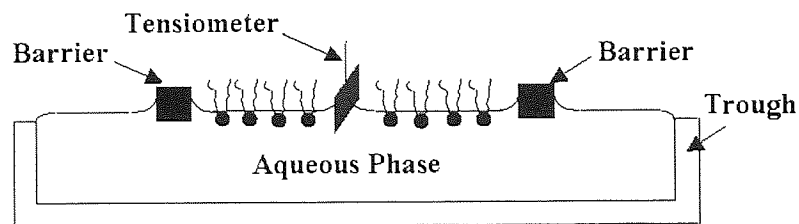


Fig.2.10 Schematic illustration of a Langmuir film balance with a Wilhelmy plate, measuring the surface pressure, and the barriers for reducing the available surface area.

A schematic π -A isotherm of typical phospholipid is shown in Fig.2.11. The isotherm can be seen to consist of three distinct regions. After initial deposition of amphiphile molecules onto subphase, the monolayer is formed. When no external pressure is applied to the monolayer the molecules in this state behave as *gas*. This means that the area on the water subphase available for each monolayer is rather large and the surface pressure is low. As the surface area is compressed the monolayers are closer packed and form a *liquid expanded state (LE)*. Consequently, the surface pressure is starting to increase. As the barrier is move even further the onset of *liquid condensed state (LC)* can be noted by an even steeper rise in the surface pressure.

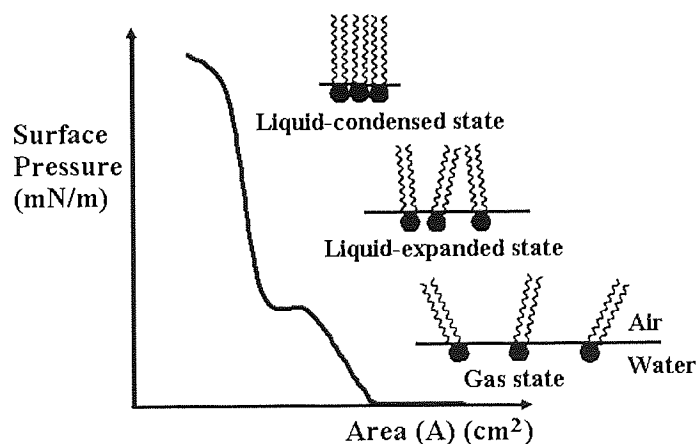


Fig.2.11 Typical π -Area isotherm of phospholipids.

The Langmuir-Blodgett Trough Model 601M (Nima Technology Ltd., Coventry, England), as seen in Fig.2.12a, was used to investigate the Langmuir monolayer of DLPC (chemical structure shown in Fig.2.12b) at the air-water interface in the absence and presence of PSMA. The Langmuir Trough machine used in this study includes a 105 cm² trough with two mechanically coupled barriers, a surface pressure sensor, a dipper mechanism (25 mm stroke), an IU4 computer interface unit and operating software version 5.16. The method used to form the monolayers at the aqueous-air interface will be described in detail in Chapter 4. The three different PSMA types (MW 1,600, 120,000 and 350,000), DLPC and other chemicals used in this work were obtained from commercial sources listed in Table 2.5.

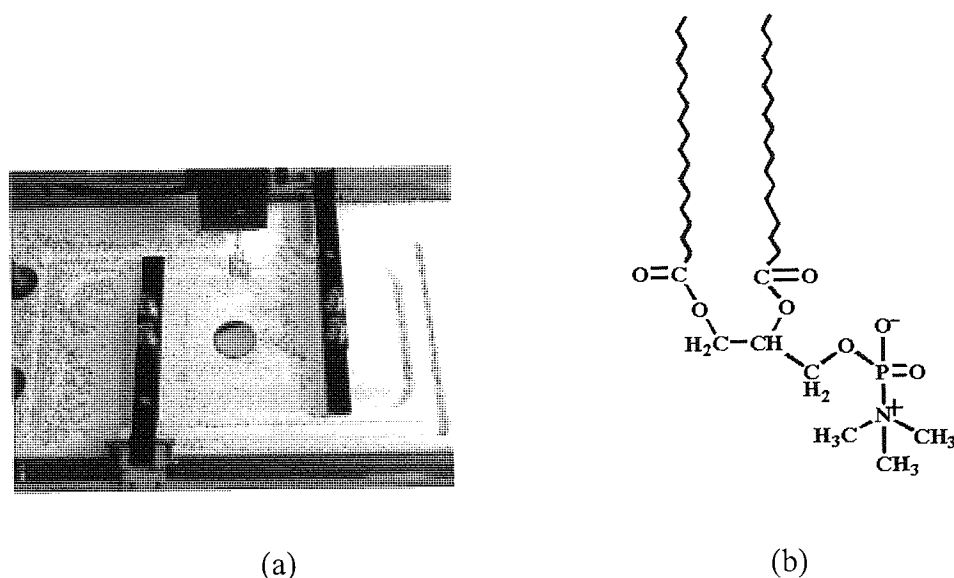


Fig.2.12 (a) Langmuir-Blodgett Trough and (b) chemical structure of 2-dilauryl-*sn*-glycero-3-phosphocholine (DLPC) used in this study.

Table 2.5 Molecular weights and suppliers of PSMA copolymers, DLPC and other chemical used in this study.

Anionic Polymer	MW	Supplier
PSMA ^a	1,600.0 (M _n)	Scientific Polymer Products
PSMA sodium salt ^b	120,000.0 (M _w)	Sigma
PSMA partial methyl ester ^c	350,000.0 (M _w)	Sigma-Aldrich
DLPC	424.3	Genzyme
Phthalate buffer pH 4	N/a	Fisher Scientific
Deionized water	18.0	Produced-in house

PSMA = poly(styrene-*alt*-maleic anhydride)

^a classified as the low molecular weight PSMA type

^b classified as the medium high molecular weight PSMA type

^c classified as the high molecular weight PSMA type

2.5.2 Surface Tension Measurement

In this study, the association behaviour of PSMA (MW 1,600, 120,000 and 350,000) in aqueous solutions (pH 4, 6 and 12) and at the air-aqueous interface as well as their interaction with DLPC bilayer were studied by measuring surface tension at room temperature. The du-Noüy tensiometer, using a Pt-Ir ring by the ring detachment technique, was used. The du-Noüy ring method utilizes the interaction of a platinum ring with the liquid interface being tested. The ring is submerged below the interface and subsequently raised upwards. As the ring moves upwards it raises a meniscus of the liquid. This meniscus eventually tears from the ring and returns to its original position. Prior to this event, the volume of the meniscus, and thus the force exerted, passes through a maximum value and begins to diminish prior to the actual tearing event. The calculation of surface or interfacial tension by this technique is based on the measurement of this maximum force. The three different PSMA types and DLPC used in this study are listed in Table 2.5.

The samples were prepared under different conditions (see Chapter 5 in more details). After that, sample was transferred from the storage vials to the surface tension measurement dish, thoroughly cleaned and rinsed with deionized water. The sample was allowed to rest 20 min before measurement. Between each experiment, the Pt-Ir ring of the tensiometer was cleaned in a flame to avoid contamination.

2.5.3 ³¹P-NMR Spectroscopy Study

In this study, the ³¹P-NMR spectroscopy was used to examine the polymorphic behaviour of aqueous DLPC dispersions in the presence and absence of PSMA. The PSMA used in this study was the low molecular weight type. The pH-dependent ability of this polymer to destabilize the DLPC vesicles was investigated at pH 4, 5, 6 and 10. The pH of solution was adjusted to the required value by using NaOH or HCl solution. The PSMA (MW 1,600) and DLPC were obtained from commercial sources listed in Table 2.5.

In this investigation, the ^{31}P -NMR spectra were acquired at 121.5 MHz on Bruker Avance 300 Spectrometer. XWIN NMR Version 3.5 software was used to process the spectra. The spectrometer field was locked during acquisition by using D_2O . The proton-decoupled spectra were obtained using a relaxation delay of 4 s, spectral width of 18,248 Hz and acquisition time of 1.8 s. The numbers of acquisitions were 160 scans. All spectra were recorded at room temperature and the chemical shifts were measured relative to H_3PO_4 (85%) as an external reference. The ^{31}P -NMR spectrum for aqueous DLPC dispersion was recorded at lipid concentration of 5 mg/mL, while for aqueous PSMA solution, a 30 mg/mL polymer concentration was used to obtain the NMR spectrum. For all DLPC-PSMA mixtures, the NMR spectra were recorded at lipid and polymer concentrations of 5 and 30 mg/mL, respectively. The water used throughout the experiment was deionized water.

2.5.4 UV-Vis Spectroscopy

The UV-Vis spectrophotometer (Hitachi Model U2000) was used to obtain release profiles of dyes and Pirenzepine drug from hydrogels. The release studies were conducted by immersing loaded hydrogels (as obtained from Section 2.4.2 and Section 2.4.3.4) in glass vials filled with 5 mL of phosphate buffered saline solution (purchased from Sigma-Aldrich) of pH 7.4 with gentle agitation at room temperature. At a predetermined period of time, samples were taken out from solution and placed into the new vial containing 5 mL fresh PBS solution. The concentration of dye or drug, delivered from hydrogel, was determined spectrophotometrically using UV-Vis spectrophotometer at wavelengths as shown in Table 2.2. All experiments were run in triplicate.

CHAPTER 3
SYNTHESIS AND PHASE BEHAVIOUR OF
POLYMER-LIPID COMPLEXES

3.1 THEORIES OF POLYMER-LIPID FORMATION

Poly(styrene-*alt*-maleic anhydride) (PSMA) has been used in many fields due to its superior properties. Hydrolyzed PSMA is soluble in water but sufficiently amphiphilic to be adsorbed by surfaces and interfaces. This polymer has also been reported to uncoil and hypercoil upon protonation of carboxylic acid pendant groups. The hypercoiling process of PSMA has been suggested to be a pH-dependent phenomenon [2, 36]. At pH above its pK_a value, the PSMA is substantially charged. The resulting ionic repulsion overcomes hydrophobic interactions between phenyl side chains within the polymer and leads to uncoiling of the polymer chain. Conversely, as the pH is lowered, the proportion of charged pendant groups falls and hydrophobic interactions become the dominant factor, causing the polymer to collapse into distinct hydrophobic microdomains. This effect is known as hydrophobic association.

The application of synthetic hypercoiling polymers to medicine was first inspired by a need to synthesize phospholipid vesicles or liposomes that could be prepared to respond to their environment and used, for example, to selectively release a drug [37]. Such liposomes were complexed with various poly(acrylic acid) derivatives to render the vesicle membrane sensitive to pH. The membrane reorganization of 0.1% dipalmitoylphosphatidylcholine (DPPC) vesicles upon adsorbing poly(2-ethylacrylic acid) (0.1%) was extremely sensitive to the conformational transition of the polymer [15]. Lowering the pH of the polymer to 6.5, toward its pK_a , caused a loss of charge within the polymer, at which point hydrophobic interactions between ethyl pendant groups then became dominant and led to a collapse of the polymer chain. The resultant hydrophobic domains did not only disrupt the liposomal membrane but also induced the polymer to associate with phospholipids, forming discoidal polymer-lipid assemblies analogous to those found in lipoproteins [38].

The polymer-lipid assemblies prepared from PSMA and DLPC were first introduced by the group at Aston [2]. The original idea was to develop a novel pharmaceutical approved drug delivery system produced from the hypercoiling polymers. The inspiration for this innovation was drawn from the fact that PSMA is capable to interact with phospholipids to form nanostructures of analogous size to those of high density lipoproteins, possessing the ability to solubilize poorly water soluble

drugs into their lipoidal core to render them aqueous soluble. From previous studies [2], this amphipathic polymer surrounds the phospholipid bilayer in a ‘doughnut arrangement’ (Fig.1.10), giving a nanostructure in sub-liposomal dimension, as illustrated in the micrographs, shown in Fig.1.11. The nanostructure produced is highly surface active when tested under conditions of dynamic surface compression and may therefore be suited for application to biomedicine.

3.2 AIMS

The primary aim of this study was to synthesize and to investigate the phase behaviour of mixture prepared from anionic PSMA copolymers and DLPC. The work also aimed to explore the effect of different experimental parameters, such as pH, temperature, counterions and copolymer architecture, on the phase behaviour of the system.

3.3 EXPERIMENTAL

3.3.1 Materials

In this work, a synthesis protocol used to prepare the PSMA-DLPC complexes has followed the Patent owed by Tighe and Tonge [27]. A range of sources and samples of DLPC and PSMA copolymers were examined. For the experiments described here, the following components were used. DLPC was purchased from Genzyme. All of the polymers were obtained from commercial sources listed in Table 3.1 and were hydrolysed prior to use

Table 3.1 Molecular weights and suppliers of the anionic PSMA copolymers used.

Anionic Polymer	MW	Supplier
PSMA ^a	1,600 (M_n)	Scientific Polymer Products
PSMA sodium salt ^b	120,000 (M_w)	Sigma

PSMA = poly(styrene-*alt*-maleic anhydride)

^a classified as the low molecular weight PSMA type

^b classified as the medium high molecular weight PSMA type

3.3.2 Synthesis of PSMA-DLPC Complexes

In order to prepare the polymer-lipid complexes from DLPC and PSMA, the appropriate amount of hydrogenated DLPC and aqueous solution of hydrolyzed PSMA were firstly mixed together. The complexes were obtained by slowly lowering the pH of the resultant cloudy mixture to 4.0. Whilst lowering the pH, a white water-insoluble substance was precipitated out and was then rapidly solubilized to form a clear solution. This phenomenon shows the formation and the incorporation of the hypercoiling polymers into the bilayer of DLPC to produce nanostructural polymer-phospholipid complexes. The formation of these complexes could be observed by an increase in the viscosity and transparency of the mixture. After the optically clear viscous solution was obtained, the pH of the mixture was gradually increased to 7.4.

3.3.3 Phase Behaviour of PSMA-DLPC Complexes

The relationship between the phase behaviour of a mixture and its composition can be captured with the use of a phase diagram. The phase behaviour of the system, consisting of PSMA, DLPC and water can be studied with the aid of a ternary phase diagram in which each corner represents 100% of that particular component. In this study, the phase diagrams of the PSMA-DLPC-water systems prepared at room temperature with and without heat treatment program were obtained by mixing an appropriate amount of water with the DLPC and PSMA solutions. The pH of the mixture was slowly lowered to 4 and then left for agitation at room temperature. After that, the pH was readjusted back to 7 and the phase diagrams were determined by measuring the %transmittance (%T) of formulations at 600 nm using a UV-Vis spectrophotometer.

For those samples that were subjected to the heat treatment program, the mixtures, whose pH had already been adjusted to 4, were placed in an autoclave machine. The autoclave cycle was at 121°C and 100 MPa for 20 minutes. After the autoclaving was completed, the samples were allowed to cool down at room temperature. The %T of these samples was measured first at pH 4. After that the pH of the samples was readjusted back to 7. The phase diagrams at both pH values of samples subjected to the heat treatment program were obtained by using the same methods as described for the untreated samples.

3.4 RESULTS AND DISCUSSION

3.4.1 Ternary Phase Diagrams of PSMA-DLPC-Water System: Low Molecular Weight PSMA Type

Fig.3.1a-d shows the high water content ternary phase diagrams of the DLPC-PSMA (MW 1,600)-water systems. The compositions of PSMA and DLPC range from 0-5.0 wt% and 0-1.0 wt%, respectively. The shaded areas in the phase diagrams correspond to a transparent single phase and the tie lines represent a constant ratio of PSMA and DLPC.

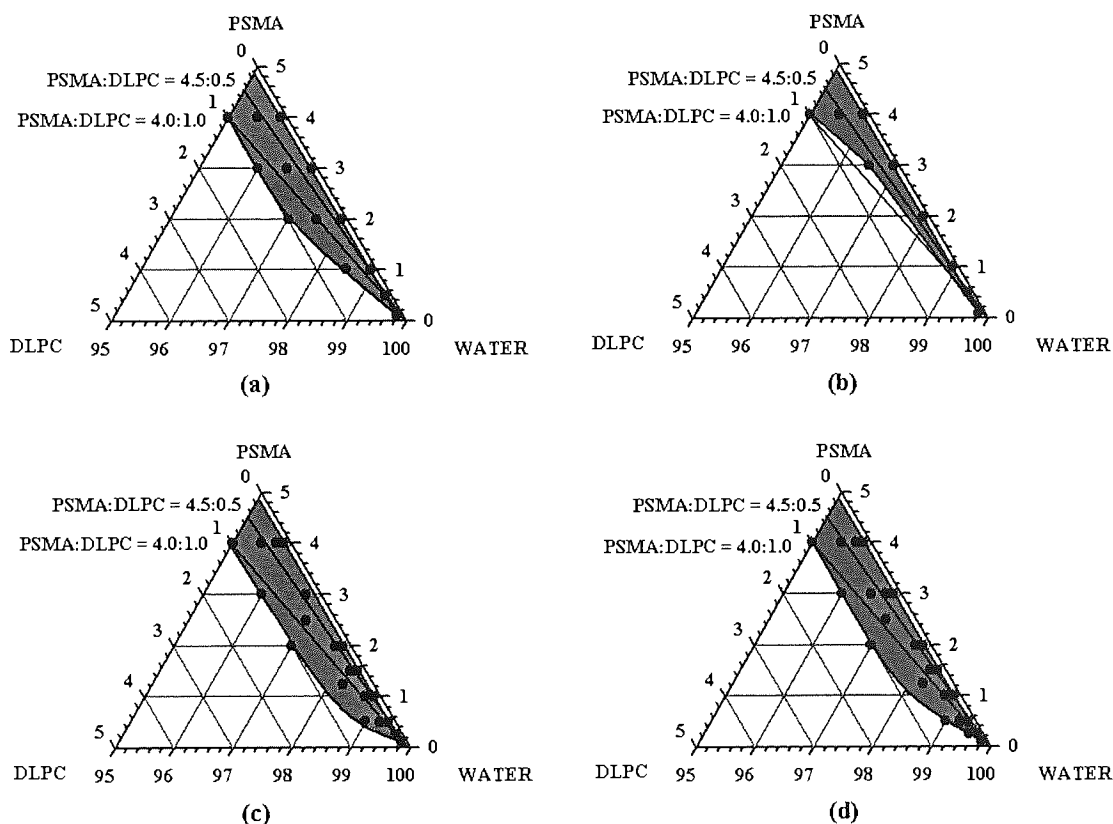


Fig.3.1 Ternary phase diagrams of PSMA-DLPC-water systems at room temperature without heat treatment; (a) at pH 4, (b) at pH 7 and with heat treatment; (c) at pH 4, (d) at pH 7 (using PSMA with MW=1,600). The Shaded area corresponds to a single transparent phase and the tie line represents a constant ratio of PSMA and DLPC.

The formulations that fall within the shaded area show a successful complexation between PSMA and DLPC. This assumption is based on the fact that the complexation of PSMA and DLPC causes both components to reorganize and form mixed complexes that do not scatter the light, and as a consequence, produce a homogeneously clear formulation.

The tie lines shown in Fig.3.1a-d correspond to constant ratios of PSMA and DLPC = 4.5:0.5 and 4.0:1.0. The effect of dilution on the complexation, when keeping the PSMA/DLPC ratio constant, may be seen as moving down along these tie lines toward 100% water. Fig.3.1a-b show ternary phase diagrams at room temperature for both pH 4 and pH 7 without heat treatment. Fig.3.1a indicates that the complexes with these ratios and at pH 4 are not affected by dilution, showing that they are dependent on the PSMA/DLPC ratio and not their concentrations. In contrast to the results found in Fig.3.1b, the formation of the nanostructure at pH 7 is somehow dependent on their concentrations. The maximum water contents for the complexes with the ratios PSMA/DLPC = 4.0/1.0 at neutral pH are $\leq 95.0\%$. Beyond these critical limits, the polymer-lipid complexes are not successfully formed. The greater success of the complex formation at pH 4, as compared to that at pH 7, can be explained in terms of the stronger hydrophobic interaction between the hydrophobic microdomains of PSMA and the aliphatic side chains of phospholipids.

The effect of temperature on the formation of polymer-lipid complexes can also be seen in Fig.3.1c-d. It is found that an increase in temperature enlarges the shaded areas, particularly at pH 7, indicating a wider range of PSMA-DLPC ratios for successful complex formation. This may be explained in term of energy input. The energy input (either sonication or heating) applied during preparation is believed to enhance the penetration of molecules such as PSMA into the phospholipid bilayer. This finding is consistent with the research done by Kyung [39] showing that the dispersion size of mixed pluronic block copolymers decreases as the temperature during preparation is increased.

3.4.2 Ternary Phase Diagrams of PSMA-DLPC-Water System: Medium-high Molecular Weight PSMA Type

Fig.3.2a-b show high water content ternary phase diagrams at room temperature of the PSMA-DLPC-water system using PSMA sodium salt with molecular weight of 120,000.

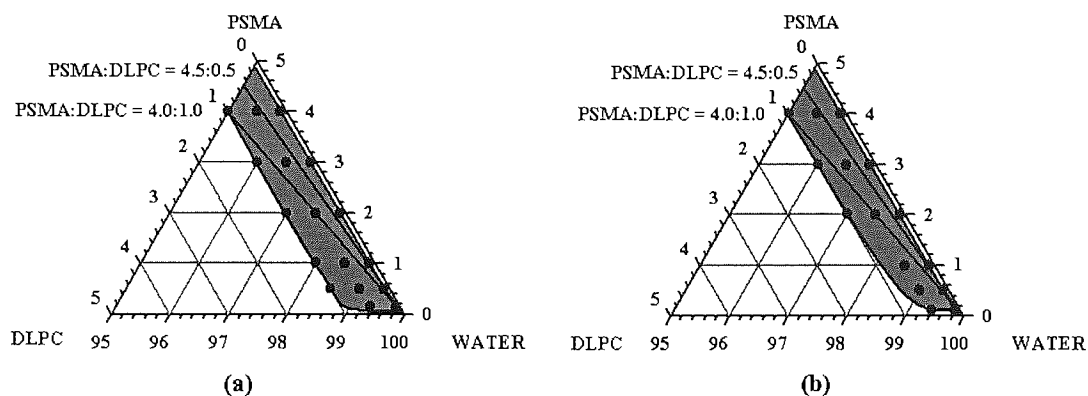


Fig.3.2 Ternary phase diagrams of PSMA-DLPC-water systems at room temperature at; (a) pH 4 and (b) pH 7 (using PSMA sodium salt with MW=120,000). The shaded area corresponds to a single transparent phase and the tie line represents a constant ratio of PSMA and DLPC.

As expected, the complexation produced from the PSMA (MW 120,000), are more probable to form at pH 4 than that at pH 7. This finding is also explained in terms of a more pronounced hypercoiling association between PSMA and phospholipids at lower pH. When comparing Fig.3.1a with Fig.3.2a, the effect of polymer molecular weight on the lipid-polymer formation can be observed. The larger shaded area found in Fig.3.2a, suggests that higher molecular weight PSMA is more capable to integrate with the phospholipid assembly than the lower molecular weight one. This observation indicates a stronger hydrophobic interaction between the longer chain PSMA and the aliphatic side chains of phospholipids.

There are some important parameters for the solubilization of a polymer within a lipid bilayer that need to be considered; the hydrophobic association between polymer and the lipid, the polymer molecular weight (radius of gyration) and the bilayer separation at maximum swelling. Demé and his colleagues [40] reported that the confinement of a polymer coil in a thin slit with a dimension smaller than the gyration

radius of the polymer results in an entropy loss. If the entropy loss is not counterbalanced by the adsorption energy of the hydrophobic group in the bilayers, the solubility may be strongly reduced and may result in a phase separation. In some cases, the polymer may be completely excluded from the lamellar phase. However, if this condition is satisfied, the polymer chains may be kept in the bilayer and stabilization at large dilutions may be observed.

Thus, there has to be a limit to the size of polymer molecules that a given phospholipid can enclose. This limit is considered to be proportional to the size of the enclosed polymer.

3.5 CONCLUSIONS

Therefore, it is logical to conclude from the above discussion that the formation of PSMA-DLPC complexes is dependent on:

1. The pH value and the temperature used for synthesis.
2. The optimal ratio between PSMA and the phospholipid.
3. The % water content used in the formulation; i.e., dilution of PSMA and DLPC.
4. The hydrophobic association between the hypercoiled PSMA and the long chain hydrocarbon of the phospholipid.
5. The molecular weight of the polymer, which is a function of the radius of gyration, relative to the bilayer separation (bilayer thickness) at maximum swelling.
6. The charge shielding effect obtained from the added salt and the presence of the counterions.

CHAPTER 4
THE STUDY OF POLYMER-LIPID
INTERACTION:
LANGMUIR-BLODGETT TROUGH STUDY

4.1 POLYMER-LIPID INTERACTION

Surface active polymers can sensitize phospholipid bilayer membranes to a variety of external stimuli. This feature has been exploited to create vesicles that readily release their contents in response to changes in temperature, glucose concentration, light intensity and pH [1]. In the preparation of a pH-sensitive delivery system, designed to exhibit maximal activity under acidic conditions, minimal membrane perturbation is generally expected to occur at neutral pH. Thus, it is important to study the interaction of polyelectrolyte with membrane bilayers at acidic as well as at neutral pH.

4.1.1 Polymer-Lipid Interaction at Neutral pH

It is commonly known that water-soluble polyelectrolytes, bearing a sufficient proportion of hydrophobic groups, can undergo intramolecular self-association in aqueous solution. However, when lipid membranes are mixed with such polymers, incorporation of hydrophobic groups into the bilayer often prevails over this association. This was demonstrated for an *N*-isopropylacrylamide copolymer bearing pH-sensitive glycine carboxyl groups and hydrophobically-modified with pyrenyl-octadecyl moieties (PNIPAM-Py-Gly). In aqueous solution, this polymer adopted a micellar structure with a hydrophobic core composed of pyrene and octadecyl groups. Addition of the copolymer to a suspension of cationic liposomes induced micelle disruption, as the hydrophobic groups penetrated into the bilayer [41]. In this case, binding of the polymer to the phospholipid was shown to be primarily driven by electrostatic interactions between cationic lipids and glycine residues, as well as by hydrophobic forces. Addition of PNIPAM-Py-Gly to a suspension of neutral liposomes, however, did not modify polymeric micellar structure. This was due to the absence of electrostatic interactions.

Ladavière et al. published that when hydrophobic forces are sufficiently important, binding of anionic polymers to neutral and even to negatively charged lipid bilayers becomes possible [42]. Conversely if interactions between hydrophobic groups are too strong, intramolecular association may prevail over insertion into the bilayers

[1]. Depending on the proportion of hydrophobic side group within the polymer backbone, the charge density and polymer concentration, the association can either stabilize the vesicles by adsorption or induce structural changes (leakage, membrane disruption, phase transformations to micelles or lamellar gel) [1, 42, 43]. For example, the studies involving hydrophobically modified poly(acrylic acid) (PAA) of varying hydrophobicity showed that at pH 7, polymers bearing a few pendant octadecyl chains along the backbone adsorbed to vesicles and induced their stabilization. However, more hydrophobic polymers bearing >25 mol% octyl groups completely destabilized small unilamellar vesicles by forming smaller, mixed structures and triggered dextran leakage from giant unilamellar vesicles [42].

Overall, studies of anionic polymer-lipid interactions at neutral pH showed that anionic polyelectrolytes are capable of inducing domain formation in oppositely charged lipid bilayers by means of electrostatic attractions. In the absence of attractive forces, interactions between polyelectrolytes and phospholipid bilayers are driven by hydrophobic forces [1, 41-43].

4.1.2 pH-Dependent Polymer-Lipid Complexation

Seki and Tirrell [16] demonstrated that some poly(alkylacrylic acid) could associate to phosphatidylcholine membranes and modify their phase transition behaviour in a pH-dependent manner. Upon acidification, PAA and poly(methacrylic acid) (PMAA) induced vesicle aggregation and increased the bilayer permeability to small molecules [44]. In contrast to PAA and PMAA, which showed no ability to solubilize phospholipid membranes at any pH, poly(ethacrylic acid) (PEAA) was found to cause complete membrane reorganization under acidic conditions [16]. PEAA alone underwent pH-dependent conformational transition at pH 6.1-6.2, whereas the pH of transition was shifted to 6.5 in the presence of dipalmitoylphosphatidylcholine (DPPC) vesicles. This shift was attributed to hydrogen bonding between the unionized carboxyl groups of PEAA and the phosphodiester functions of the lipid surface[1].

Studies showed that the pH at which membrane reorganization occurs can be modulated by varying the polymer molecular weight [45] and copolymerizing methacrylic acid with a more hydrophilic or hydrophobic monomer [1]. Polymers with a greater molecular weight collapse at higher pH values and form mixed micelles that exclude water more effectively. The addition of increasing amounts of hydrophilic MAA units in the polymeric structure leads to a progressive reduction in the pH at which vesicle solubilization occurs.

The mechanism of polymer-induced membrane reorganization is essentially conjectural, although some parallels may be drawn. Whether a change in polymer conformation is required for membrane solubilization is still open. Thomas and Tirrell hypothesized that a change in polymer conformation may not be required for membrane solubilization [1]. As carboxylic groups are protonated, PEAA becomes more hydrophobic and adsorbs to the outer leaflet of the bilayer. This may cause membrane expansion, which increases lateral compression of the bilayer and leads to membrane disruption.

4.2 SCOPE OF POLYMER-LIPID INTERACTION STUDIES

The interactions of anionic polyelectrolytes with membranes have been extensively studied as a means to develop new responsive delivery systems. Over the last decades, studies of membrane interactions with these polymers have been focused on copolymers of *N*-isopropylacrylamide, acrylic and methacrylic acid. However, there are very few studies on poly(styrene-*alt*-maleic anhydride).

This work will focus on the pH-dependent membrane binding behaviour of PSMA. Under acidic conditions, binding of PSMA onto phospholipid membranes is expected to induce the formation of mixed PSMA-phospholipid complexes. This complexation may be useful in pharmaceutical formulations requiring targeted or controlled release. In this study, techniques such as Langmuir Blodgett, surface tension measurements and phosphorus nuclear magnetic resonance (^{31}P -NMR) were used in order to explore the association behaviour of PSMA both at the air-water interface and in solution, as well as its interaction with phospholipid membranes. The Langmuir

technique was successfully proven to be useful to study the pH-dependent monolayer formation of PSMA. Furthermore, valuable details concerning PSMA-induced membrane disruption were also obtained using this technique. The occurrence of critical phenomena in solution, such as micelle formation and mixed-micelle formation, was explored using surface tension measurements. ^{31}P -NMR was used as a means to elucidate the structure of polymer-phospholipid complexes.

A discussion of polymer-lipid association data obtained by the Langmuir Blodgett technique will be presented later in this Chapter. Association data obtained by surface tension measurements will be addressed in Chapter 5 and ^{31}P -NMR spectroscopy data will be discussed in Chapter 6.

4.3 LANGMUIR-BLODGETT TROUGH TECHNIQUE

4.3.1 Introduction

The interaction between polyanions, such as PAA, PEAA and PSMA, and lipid vesicles has long been investigated by many researchers using different approaches (e.g., fluorescence spectroscopy, differential scanning calorimetry and monolayer techniques). Among those currently available techniques, the Langmuir Trough technique has been proved to be very useful in characterizing the lipid monolayer at the air-water interface in the absence and presence of polyanions. The advantage of using this technique is that the measurement of the surface pressure as a function of surface area (π -A isotherms) can be conveniently carried out and analyzed in various environmental conditions such as pH, type of subphase, deposition condition and temperature. This makes it possible to provide information regarding various important molecular phenomena; such as the pH-dependent membrane rupture, the kinetics of membrane micellization by the polyanions and the conformational transitions of phospholipid at the air-water interface, that play a crucial part in the development of vesicular drug delivery and biomimetic systems.

4.3.2 Aims

The aim of this work was to gain a better understanding of the pH-dependent complexation of PSMA with DLPC membrane at the air-water interface. As a means to achieve that, observation of DLPC monolayers were conducted in the absence and presence of PSMA at different pH.

4.3.3 Experimental

4.3.3.1 Surface Pressure (π)-Area (A) Isotherms of Pure DLPC Monolayers

The Langmuir-Blodgett Trough Model 601M (Nima Technology Ltd., Coventry, England), seen in Fig.2.12, was used to investigate the Langmuir monolayer of DLPC at the air-water interface. The Langmuir Trough machine includes a 105 cm² trough with two mechanically coupled barriers, a surface pressure sensor, a dipper mechanism (25 mm stroke), an IU4 computer interface unit and operating software version 5.16. The method used to form the pure DLPC monolayers at the aqueous-air interface is described briefly as follows. The appropriate amount of DLPC was dissolved in chloroform and was spread on the water subphase using a Hamilton syringe. Fifteen minutes were allowed for solvent evaporation and monolayer equilibration before each experiment was started. After allowing for the solvent to evaporate, the monolayer was continuously compressed and then expanded, at a constant rate, to obtain the isotherms. Each cycle was repeated at least twice to obtain reproducible results. The water subphase was replaced by a phthalate buffer of pH 4 as a means to examine the influence of pH on the lipid monolayer at the interface. The effect of barrier speed (varying from 25 to 200 cm²/min) on the monolayer structure of DLPC was also investigated in this study.

4.3.3.2 Surface Pressure (π)-Area (A) Isotherms of Pure PSMA Monolayers

The association behaviour of hydrolyzed PSMA in aqueous solution and at the air-water interface was observed in this work using the Langmuir-Blodgett Trough machine (as seen in Fig.2.12). The PSMA monolayer was formed at the interface by spreading 10 μ L of the hydrolyzed PSMA (4.59 mM) onto the water subphase using a Hamilton microsyringe. The PSMA film was compressed after the standby period and the isotherm for the PSMA alone was obtained by continuously recording the surface pressure during the barrier displacement. As well as pure water, phthalate buffer of pH 4 was also used as a subphase to understand the pH-dependent self-association of this polymer.

4.3.3.3 Effect of PSMA Complexation on DLPC Monolayers

The experiment examining the effect of PSMA on the molecular packing of DLPC monolayer was conducted by injecting 10 μ L of the PSMA solution (4.59 mM) beneath the pre-forming DLPC monolayer, as previously described in section 4.3.3.1. The isotherm of the mixed PSMA-DLPC monolayer was then recorded under the same conditions as for the DLPC alone. The time-dependent changes in the isotherms of the DLPC monolayer in the presence of PSMA were recorded 5, 15 and 30 min after injection of the polymer. The phthalate buffer of pH 4 was also used as a subphase to understand the pH-dependent complexation of PSMA with DLPC monolayer.

4.3.4 Results and Discussion

4.3.4.1 Surface Pressure (π)-Area (A) Isotherms of Pure DLPC Monolayers

Before each experiment was carried out, the cleanliness of the water subphase needed to be checked by investigating the pressure reading increase as the barriers were compressed to a minimum area. If any contaminant was present, then an increase of pressure would have been observed. Fig.4.1 shows the π -A isotherms for two subphases; water (pH \sim 5) and phthalate buffer of pH 4. It is clearly seen that, over the entire range of compression, there is no remarkable pressure reading increase in the pressure-area isotherms for these two subphases. This result shows the absence of contaminants on the subphases.

The pressure-area isotherms at room temperature of pure DLPC monolayer on water and phthalate buffer pH 4 subphases are also presented in Fig.4.1. It is found that, in the low surface pressure region ($\pi < 30$ mN/m), the phthalate buffer pH 4 subphase causes the isotherm to shift towards larger molecular area. This expansion may be due to the association between the buffer components ($\text{H}_2\text{C}_8\text{H}_4\text{O}_4$, Na^+ , K^+ and Cl^-) and the DLPC at the interface. It is inferred that the association with buffer possibly reorganizes the molecular arrangement of the DLPC at the interface. As a result of this phenomenon, a more expanded monolayer is obtained. It is worth to note that the enlarged molecular area of DLPC observed at pH 4 may not be a consequence of increased charge repulsion between the lipid molecules at the interface. This is due to the polar head group of DLPC maintaining its zero net charge both on subphases of pH 4 and 5. Consequently, one expects a comparable repulsive force between the lipid molecules for DLPC monolayers on pH 4 buffer and on water subphases

As the DLPC monolayer is compressed to the high surface pressure region, its isotherm coincides with that of the pure water isotherm at surface pressure 30 mN/m (Fig.4.1). This implies that the phthalate molecules are possibly expelled from the interface as the pressure is increased. Surprisingly, for surface pressures higher than 35 mN/m, the observed surface pressure of DLPC in pH 4 buffer is lower than that in

the water subphase, suggesting a decrease in the repulsive interaction between lipid molecules. It is likely to be due to the charge shielding effect by the monovalent salt. An alternative explanation of this finding is that the lipid molecules, which are strongly adsorbed to the phthalate molecules, are being desorbed from the interface.

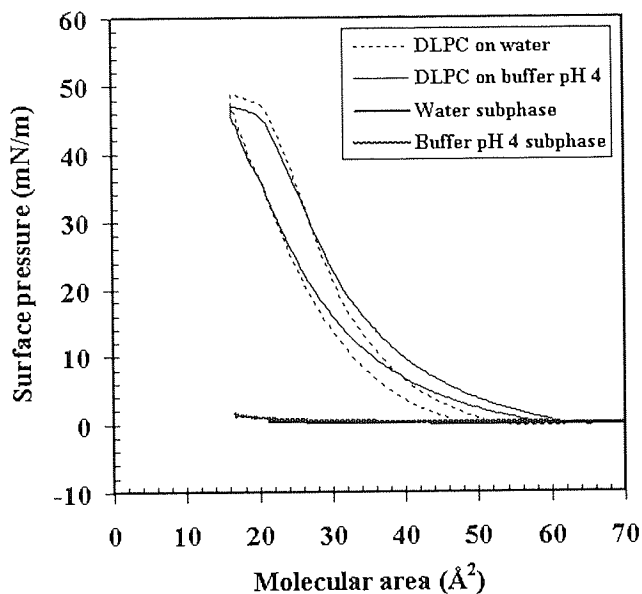


Fig.4.1 Pressure-area isotherms at room temperature of DLPC monolayer on deionized water and phthalate buffer of pH 4 subphases (barrier speed 25 cm²/min). In comparison with the pressure-area isotherms of water and phthalate buffer pH 4.

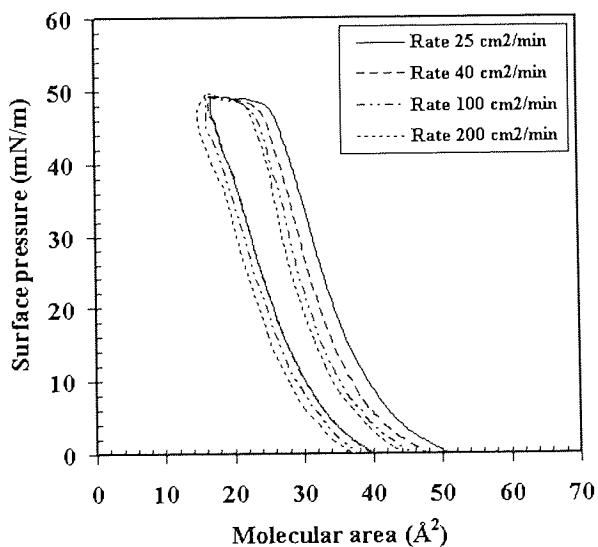


Fig.4.2 Pressure-area isotherms at room temperature of DLPC monolayer on deionized water with using different barrier.

In this study, the effect of different compression rates (ranging from 25 to 200 cm²/min) on the π -A isotherms of DLPC monolayers was investigated. Typical results, shown in Fig.4.2, indicate that the apparent collapse pressures do not vary significantly with barrier speed. The collapse pressures for DLPC monolayers at the air-water interface obtained in this study were all \approx 49 mN/m, which is consistent with previous work [46, 47]. As the barrier speed is increased, two observations can be made. The first is that, at a given surface pressure, the isotherms are shifted towards a smaller area region, and the second is that the isotherm loops become thinner. The minimum area seems to decrease slightly from 28 to 22 Å²/molecule when the barrier speed is increased from 25 to 200 cm²/min. These observations may be attributed to turbulence, due to excessive barrier speeds. The turbulence perhaps increases the lipid leakage and the lipid desorption from the interface, resulting in the reduced surface coverage and eventually, destabilization of the lipid monolayer at the interface.

The absence of a phase transition between liquid-expanded (LE) and liquid-condensed (LC) states, as illustrated in Fig.4.2 confirms that the DLPC monolayers exist in the LE state. This preference may be explained by the acyl chain length of DLPC (C₁₂) not being long enough to generate a strong hydrophobic interaction, as is required in the liquid-condensed state.

4.3.4.2 Surface Pressure (π)-Area (A) Isotherms of Pure PSMA Monolayers

In this study, the Langmuir Trough technique was used, for the first time, to understand the association behavior of PSMA in aqueous solution and at the air-water interface. The monolayer behavior of the two different conformational forms of PSMA; an extended and a compact hypercoiled forms, was also examined in this study. In all experiments, the PSMA monolayer was performed at the air-water interface by spreading hydrolyzed PSMA onto the aqueous subphase. The surface-area isotherms for PSMA monolayers spread on pure water subphase (pH 5) and on buffer subphase (pH 4) are shown in Fig.4.3a, and Fig.4.3b, respectively.

To interpret the effect of pH subphase on the interfacial properties of PSMA monolayers, it is necessary to remember that the hydrolyzed PSMA molecule is an amphiphilic molecule. When spread on aqueous subphase, PSMA molecules orient themselves with their apolar moieties (phenyl groups) toward the air phase and their polar moieties (carboxyl groups) immersed in the subphase. The ability of PSMA to form insoluble monolayer at the interface is actually dependent on the interaction between polymer and water subphase. The water-polymer interaction is more pronounced when the PSMA molecules are mostly ionized. This ionization of PSMA leads the polymer molecules to dissolve into subphase and not to maintain at the air-water interface. However, when the polymer-water interaction is less favorable, for example when the PSMA molecules are partially ionized or exist in nonionized form, the polymer molecules may repel from the water subphase, thus forming an insoluble monolayer at the air-water interface.

The π -A isotherms in Fig.4.3a show that in the water subphase (pH 5), the three types of PSMA do not have a detectable surface pressure, suggesting that they are not capable of forming the insoluble monolayer on the water subphase. This is perhaps related to the fact that all PSMA types are mostly ionized in the pure water (pH 5) and thus are likely to dissolve in the bulk of subphase than to spread on the air-water interface.

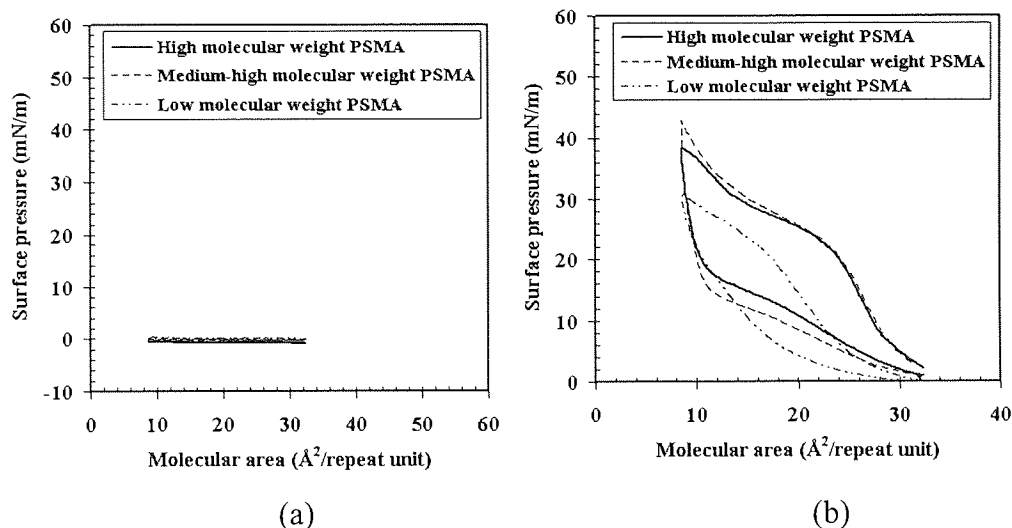


Fig.4.3 Pressure-area isotherms at room temperature of the three PSMA types; PSMA-partial methyl ester (MW 350,000), PSMA-sodium salt (MW 120,000) and PSMA (MW 1,600) on subphases of (a) deionized water and (b) phthalate buffer of pH 4. Monolayers compressed at 25 cm²/min rate.

A possible association of PSMA molecules in solution was postulated by Garnier and coworkers [48], who proposed a zipper-like association mechanism. The polymer molecules can link via hydrophobic interactions between the phenyl groups, producing long effective chains (Fig.4.4). Association dimerization is favoured when the chains are stretched by charging them, because of less loss in conformational entropy upon association. However, if the chains are too highly charged, the electrostatic repulsion between the chains disfavours the association [48].

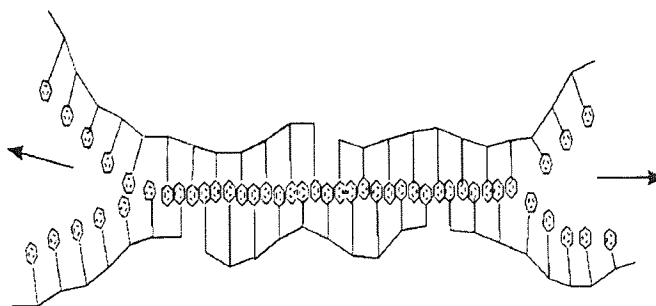


Fig.4.4 Schematic representation of the association of PSMA molecules in solution by a zipper mechanism [48].

Interestingly, when the acidic buffer was used as a subphase, all three types of PSMA monolayers show the compression isotherms, as illustrated in Fig.4.3b. As mentioned before, when the subphase becomes acidic, the ionization of PSMA is reduced. This phenomenon increases the hydrophobicity of the PSMA, which is then leading the polymer to form insoluble monolayer at the interface. As illustrated in Fig.4.3b, the three types of PSMA show a plateau region. There are several factors that may cause the appearance of a plateau region in the pressure isotherms, for example; the coexistence of monolayer phases (liquid-expanded and liquid-condensed), the collapse of the monolayer film into multilayer film, molecular orientational changes upon film compression, a combination of both the orientational changes and the monolayer collapse and the dissolution of monolayer material in the water subphase upon film compression [49].

By comparing the isotherms of PSMA (MW 1,600) with that of the other two PSMA types (MW 120,000 and 350,000), in Fig.4.3b, two observations can be made. Firstly, the isotherms for the high molecular weight PSMA types (MW 120,000 and 350,000) shift towards higher surface pressure over the whole range of molecular areas. This finding reflects that both inter- and intramolecular repulsive interactions of the polymer are more pronounced with increased chain length. Secondly, at the low surface pressure region, the area expansion of the high molecular weight PSMA types is greater than that of the lower molecular weight type, as observed in Fig.4.3b, suggesting that the conformational configuration of PSMA at the interface is dependent on the molecular weight. Interestingly, the limiting area corresponding to the maximum surface pressure, obtained from Fig.4.3b for the three PSMA types, is of the same value ($\sim 10 \text{ \AA}^2/\text{repeat unit}$). One may assume that, at higher surface pressures, the conformational configuration of PSMA at the interface may not depend on the molecular weight of polymer anymore.

In general, the repulsive interaction of the polymer molecules should increase with increased molecular weight. This should manifest as a shift in the isotherms towards higher surface pressure for higher molecular weight. If this postulation faithfully describes this phenomenon, one would expect the shift to increase with increasing molecular weight. This is true in the case of PSMA (MW 1,600) when compared to the other two PSMA types, as describe above. However, this assumption

does not suffice to explain the relationship between the two high molecular weight types. It seems that the isotherm shift is a consequence of combined factors, one of which obviously is the molecular weight.

In the large molecular area region ($>20 \text{ \AA}^2/\text{repeat unit}$), the two isotherms overlap, as seen in Fig.4.3b, suggesting that the two PSMA types (MW 120,000 and 350,000), both reach the maximum surface coverage. It is also found that in the small area region ($<20 \text{ \AA}^2/\text{repeat unit}$), in Fig.4.3b, the isotherm of the PSMA (MW 350,000) lies slightly below the isotherm of PSMA (MW 120,000), indicating lesser repulsive interaction between the polymer molecules. This observation points out that the chemical structure of the repeat unit may contribute to the isotherm shift. The slight difference in repeat unit between PSMA (MW 120,000) and PSMA (MW 350,000), is the presence of the hydrophobic ester ($-\text{COOCH}_3$) moieties in PSMA (MW 350,000). The incorporation of ester moiety (10-15%) in PSMA (350,000) possibly increases the short-range hydrophobic attraction (methyl-methyl attraction) and, hence, reduces the interfacial repulsive interaction between the polymer chains. The isotherm of PSMA (MW 350,000) lies below the isotherm of PSMA (MW 120,000), as seen in Fig.4.3b, is, therefore, a consequent of this effect.

4.3.4.3 Effect of PSMA Complexation on DLPC Monolayers

(a) Pressure-Area Isotherms on Water Subphase

The changes of the π -A isotherms as a function of time (0, 5, 15 and 30 min) for DLPC monolayers in the presence of PSMA on water subphase are shown in Fig.4.5a-c. The amount of DLPC and PSMA used to obtain the isotherms in Fig.4.5 was the same as that used to obtain the isotherms in Fig.4.2, Fig.4.3. The barrier was compressed at a constant rate of $25 \text{ cm}^2/\text{min}$ and was static between runs.

The isotherms recorded at time=0 min (solid line isotherms in Fig.4.5a-c) correspond to the isotherms of pure DLPC monolayer prior to injection of PSMA. The isotherms at t=5, 15 and 30 min (the dashed, dashed-dotted and dotted line isotherms in Fig.4.5a-c, respectively) correspond to the isotherms of mixed DLPC-PSMA monolayers after 5, 15 and 30 min upon addition of PSMA. The isotherms for the three PSMA types on water subphase were also shown for comparison, in Fig.4.5d.

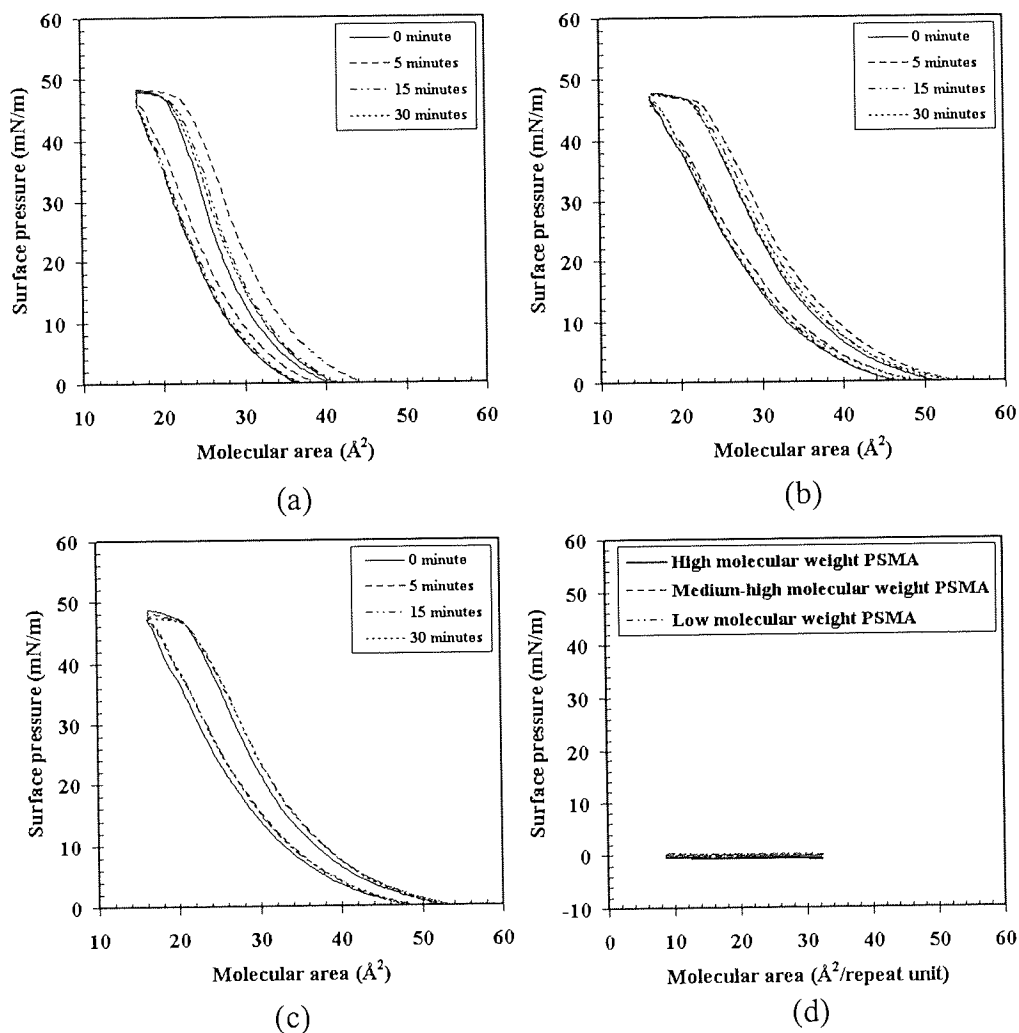


Fig.4.5 Changes of the pressure-area isotherms as a function of time for DLPC monolayers in the presence of (a) PSMA (Mw 1,600), (b) PSMA-sodium salt (Mw 120,000) and (c) PSMA-partial methyl ester (MW 350,000). The PSMA solution was introduced beneath the water subphase (pH 5) at t=0 min when barrier is completely opened and stationary. Monolayers were compressed using barrier rate of 25 cm²/min. The isotherms of the three PSMA types on water subphase were shown in (d) for comparison.

It is seen from Fig.4.5a-c that, at a constant surface pressure of 20 mN/m, the surface-area isotherm changes of DLPC upon addition of PSMA to the water subphase undergoes two stages. The first stage is characterized by an instantaneous shift of isotherm towards larger molecular areas within 5 minutes after addition of PSMA, as observed in Fig.4.5a-c (dashed line isotherms). The second stage is illustrated by the contraction of the pressure-area isotherm back towards small areas after 5 min upon addition of PSMA, as observed in Fig.4.5a-c (dashed-dotted and dotted line isotherms). The first stage is corresponding to the first penetration of the PSMA molecules into the DLPC monolayer, leading to the monolayer enlargement and then, the isotherm expansion, in Fig.4.5a-c. In the second stage, the molecular arrangement at the air-water interface possibly reaches equilibrium state. The ionized (or partially ionized) PSMA at the interface may desorb back to the bulk of water subphase, resulting in the contraction of monolayer at the interface and then the shift of isotherm back towards smaller areas, in Fig.4.5a-c.

The fact that the addition of PSMA to the water subphase does not cause a major change in the shape of the DLPC isotherms suggests the lesser favourable adsorption of the PSMA into the monolayer at the pH of pure water subphase.

(b) Pressure-Area Isotherms on Buffer pH 4

Fig.4.6a-c show the time-dependent changes in the pressure-area isotherms of DLPC monolayers on buffer pH 4 subphase upon injection of PSMA beneath the expanded lipid film. The amount of DLPC and PSMA used to obtain the isotherms in Fig.4.6 was the same for Fig.4.2, Fig.4.3 and Fig.4.5. The barrier was compressed at a constant rate of $25 \text{ cm}^2/\text{min}$ and was static between runs.

The isotherms recorded at time=0 min (solid line isotherms in Fig.4.6a-c) correspond to the isotherms of pure DLPC monolayer prior to injection of PSMA. The isotherms at time=5, 15 and 30 min (the dashed, dashed-dotted and dotted line isotherms in Fig.4.6a-c, respectively) correspond to the isotherms of mixed DLPC-PSMA monolayers 5, 15 and 30 min after addition of PSMA. The isotherms for the three PSMA types on phthalate buffer of pH 4 were also shown for comparison, in Fig.4.6d.

Interesting results are obtained when comparing Fig.4.5a-c with Fig.4.6a-c. It is found that the area expansion of the lipid monolayer is greater in Fig.4.6, suggesting that the incorporation of PSMA into DLPC monolayer is more pronounced on pH 4 buffer than on pure water subphase. This effect may be explained as follows. At low pH subphase, the anionic character of PSMA decreases, and its hydrophobic character increases due to the protonation of the carboxyl groups. This resultant phenomenon leads the PSMA to complex with DLPC through hydrogen-bonding and the hydrophobic interaction [44]. In agreement with previous studies [2, 15, 37, 38, 44, 50], the results obtained herein demonstrate a pH-dependent association of PSMA and phosphatidylcholine.

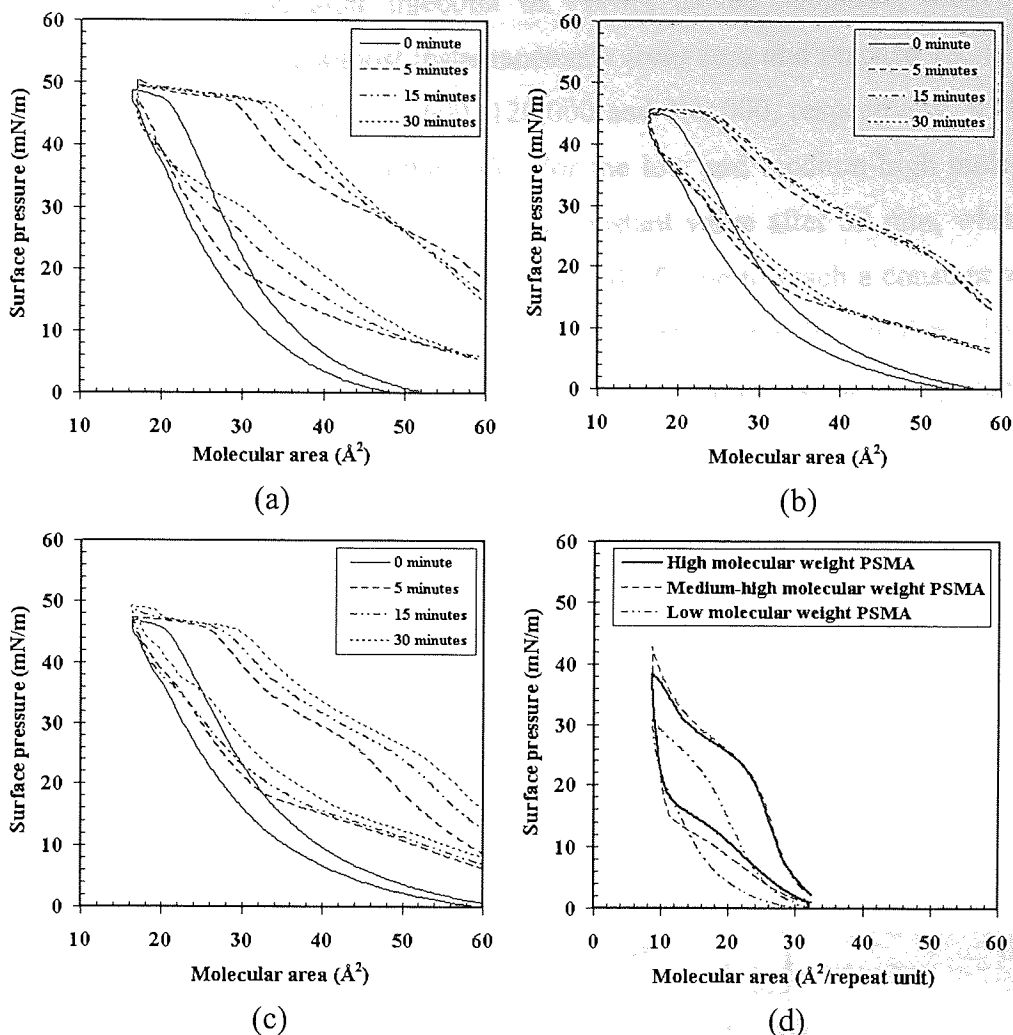


Fig.4.6 Changes of the pressure-area isotherms as a function of time for DLPC monolayer in the presence of (a) PSMA (MW 1,600), (b) PSMA sodium salt (MW 120,000) and (c) PSMA partial methyl ester (MW 350,000). The PSMA was introduced beneath the phthalate buffer pH 4 subphase at $t = 0$ min when barrier is completely opened and stationary. Monolayers were compressed using barrier rate of $25 \text{ cm}^2/\text{min}$. The isotherms of the three PSMA types on phthalate buffer pH 4 were shown in (d) for comparison.

It should be noted that the adsorption of the PSMA to the DLPC monolayer at the interface is a time-dependent process. Fig.4.6a-c show the changes with time in the surface pressure of the DLPC monolayers upon injection of PSMA. The lipids were spread on a high surface area at 62 Å^2 ; i.e., when barrier is completely opened and stationary, resulting in a zero surface pressure. The lipid film was compressed and the isotherm for the lipid alone was obtained (solid line isotherms in Fig.4.6a-c).

Interestingly, after injection of PSMA to the subphase, the surface pressure readings start to rise almost instantaneously from zero and reached 18, 14, and 10 mN/m, for PSMA with MW of 1,600, 120,000 and 350,000, respectively, within 5 minutes, Fig.4.6a-c (dashed line isotherms). For the low and medium-high molecular weight PSMA, the surface pressures reached a constant value after 30 min, while the high molecular one possibly requires a longer period of time to reach a constant value, see Fig.4.6a-c (dotted line isotherms) and Fig.4.7. These results confirm that the adsorption of PSMA at the interface is diffusion controlled process and is dependent on molecular weight of PSMA.

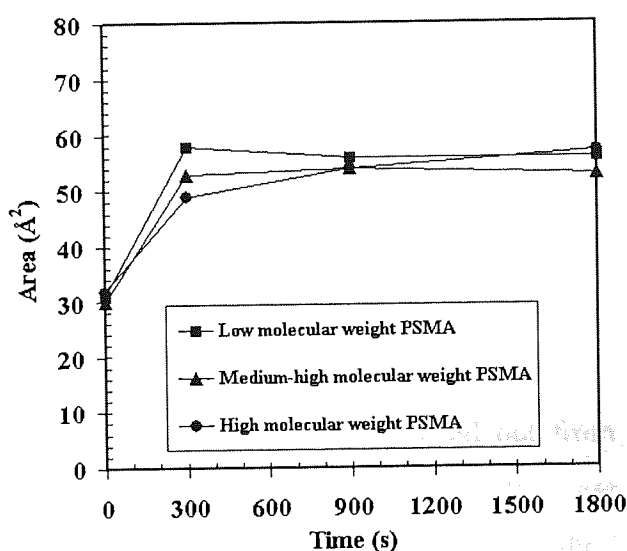


Fig.4.7 Changes in surface areas of DLPC monolayers at 20 mN/m induced by addition of 10 μ L of PSMA (1 mg/ml) as a function of time on phthalate buffer of pH 4.

The monolayer expansion caused by the penetration of polymer into phospholipid monolayer decreases with increasing packing density of the lipid molecules. The relative area increase ($\Delta A/A$), which is a ratio between the change in surface area (ΔA) of monolayer induced by the penetration of polymer and the surface area (A) of pure monolayer prior to the injection of polymer solution, is also surface pressure dependent [44]. By plotting the graph of the relative area ($\Delta A/A$) as a function of surface pressure, the limiting surface pressure, which is a measurement of the polymer's ability to penetrate into the membrane, can be obtained by extrapolating the graph to the x-axis intercept [44].

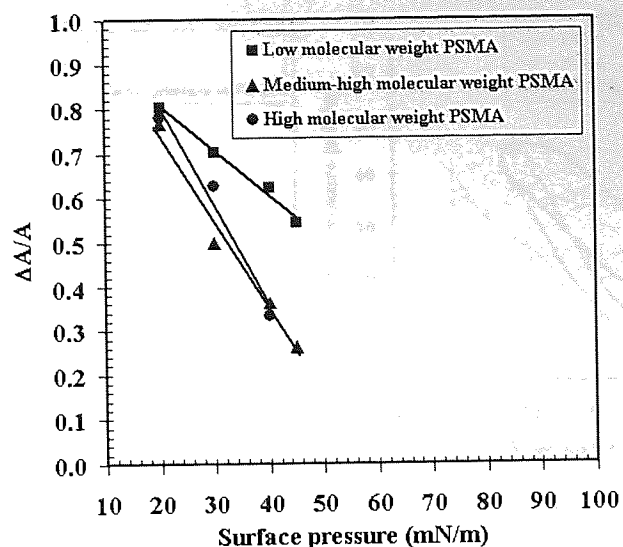


Fig.4.8 Relative area increase ($\Delta A/A$) of DLPC monolayers as a function of surface pressure at pH 4 buffer measured at 30 min after PSMA addition.

As shown in Fig.4.8, the limiting surface pressures for medium-high and high molecular weights PSMA, determined from the extrapolation of the graphs to the x-axis, have the same value (~ 52 mN/m), indicating that these two PSMA types can no longer incorporate into the DLPC monolayer above a surface pressure of 48 mN/m. It may be because the polymer molecules are squeezed out from the interface at this collapse pressure. Interesting results are obtained in the case of the PSMA with molecular weight of 1,600. Among the three PSMA types, the low molecular weight PSMA shows the highest value of limiting surface pressure (~ 82 mN/m). This value is so much higher than a typical collapse pressure of DLPC monolayer (49-52 mN/m), suggesting that the incorporation of this PSMA types raises the intermolecular interaction at the interface.

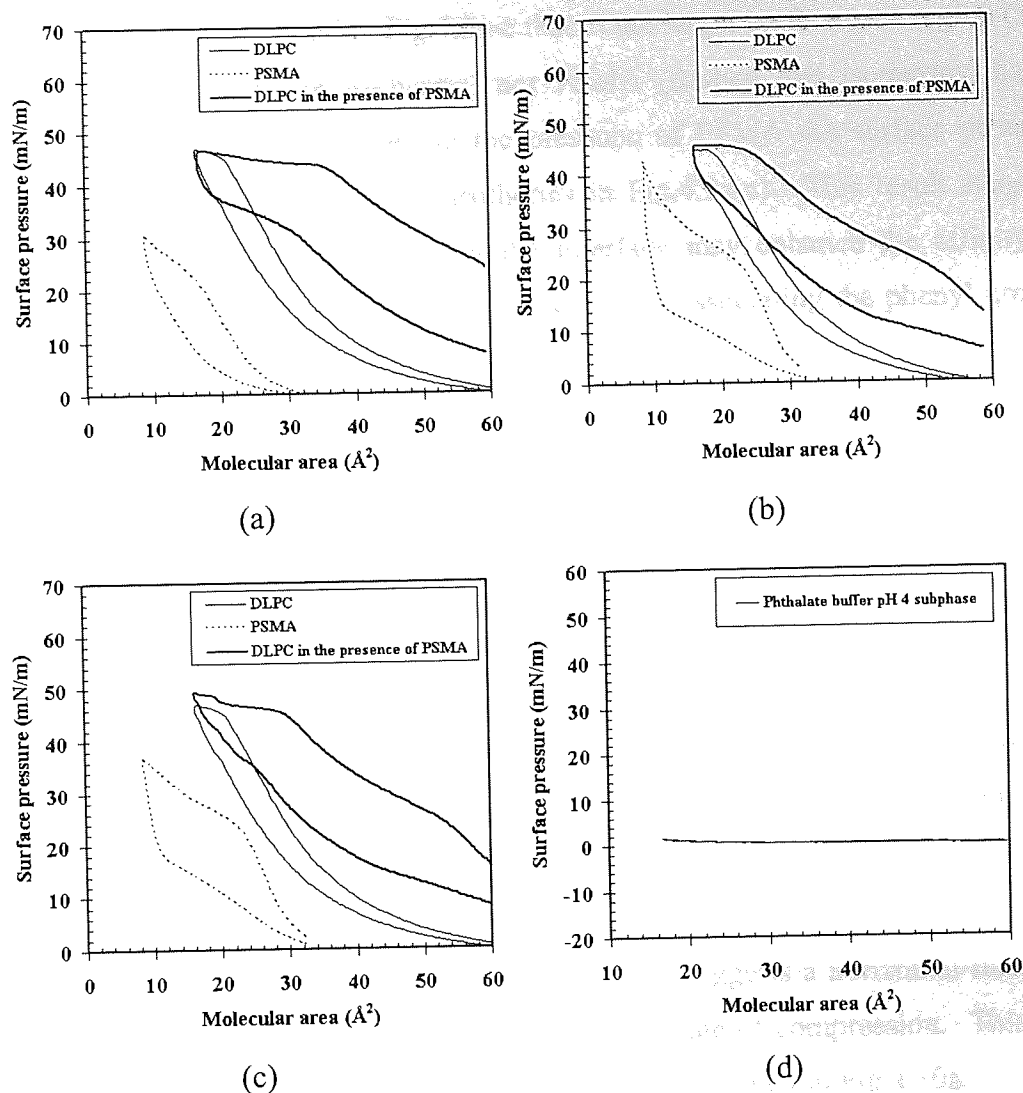


Fig.4.9 Overlay plots of surface pressure-area isotherms on phthalate buffer of pH 4 for the pure DLPC, pure PSMA and mixed DLPC-PSMA monolayers. The molecular weights used for PSMA were (a) 1,600, (b) 120,000 and (c) 350,000. The isotherm of phthalate buffer pH4 subphase was shown in (d) for comparison.

Fig.4.9a-c show the overlay of isotherms on pH 4 buffer subphase for the monolayers of pure DLPC (solid lines), pure PSMA (dashed lines) and DLPC in the presence of PSMA (bold solid lines). The molecular weights of the three PSMA types used to obtain the isotherms in Fig.4.9a, b and c were 1,600, 120,000 and 350,000, respectively. As a control, the isotherm of pH 4 buffer subphase was also recorded. The result obtained shows no dependence of surface pressure on area, indicating an inability of pH 4 buffer to form a stable monolayer at the interface, Fig.4.9d.

It has been found in Fig.4.9a-c that at the larger surface area region ($>60 \text{ \AA}^2$), neither DLPC (solid line isotherms) nor PSMA (dashed line isotherms) has a detectable surface pressure, however, in the presence of PSMA the surface pressure increase is remarkable (bold solid line isotherms in Fig.4.9a-c). This result suggests that the presence of DLPC monolayer at the interface may enhance the affinity of PSMA molecules to adsorb at the interface, possibly by associating the phenyl groups with their hydrophobic tails.

Some things are worth noting when comparing the isotherms of DLPC in the presence of low molecular weight PSMA (MW 1,600), in Fig.4.9b, with that in the presence of higher molecular weight PSMA (MW 120,000 and 350,000), in Fig.4.9b-c. It is found that, the collapse surface pressure values of lipid monolayer in the presence of PSMA (MW 120,000 and 350,000) are similar to that of lower molecular weight PSMA. However, their limiting areas are significantly different. The limiting area for the lipid monolayers in the presence of PSMA (MW 1,600) is around 36 \AA^2 , while that of the PSMA (MW 350,000) and PSMA (120,000) are 30 and 24 \AA^2 , respectively. The fact that the monolayer with PSMA (MW 1,600) shows the largest limiting area and shows the absence of a plateau phase transition region, suggests a horizontal flat-lying polymer arrangement at the interface over the whole range of compression. This flat-lying arrangement of PSMA in the mixed monolayer is illustrated in Fig.4.10a.

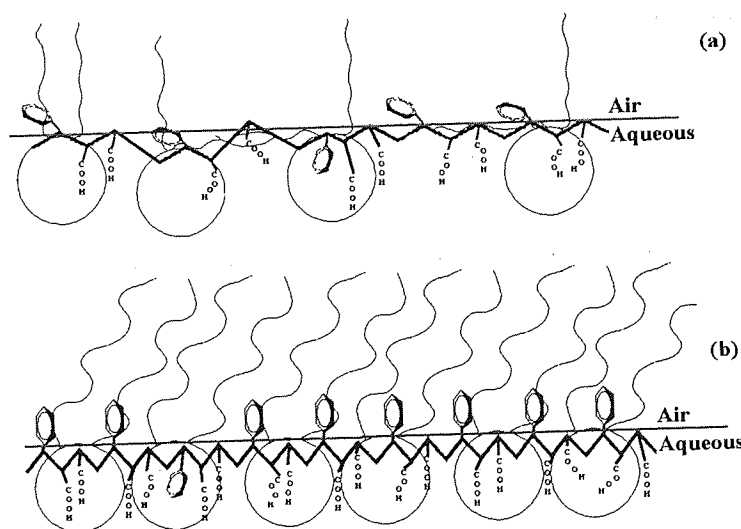


Fig.4.10 Schematic representation of a possible molecular arrangement at the interface for the mixed monolayer of DLPC and PSMA; (a) flat-lying arrangement, and (b) vertically oriented arrangement.

The flat-lying arrangement may be explained in terms of the PSMA (MW 1,600) having a certain degree of interaction with the water. The hydrogen-bonding between the water molecules and the un-ionized (or partially ionized) carboxyl group of the PSMA is possibly involved in this polymer-solvent interaction. It can also be that the phenyl ring is in some way able to interact through π -electrons with water molecules [51]. Moreover, irregularity of the polymer sequence distribution is another explanation for this arrangement. For example, if the alternating pattern of the copolymer sequence is broken, say by two styrene units coming in sequence, it is then possible that the repulsive interaction between the phenyl groups will drive one or both styrene units into the water.

The polymer-lipid arrangements at the air-water interface for the other two PSMA types (MW 120,000 and MW 350,000) are more complicated. Since the isotherms in Fig.4.9b-c (bold solid line isotherms), show plateau regions at the same molecular area of $54\text{-}40 \text{ \AA}^2$, one should propose two possible molecular arrangements at the interface for these two PSMA types.

At the very large molecular area region ($>53 \text{ \AA}^2$), the two high molecular weight PSMA types may adsorb at the interface and rearrange themselves in a flat-lying position (LE state), see Fig.4.10a. As the mixed monolayers of DLPC and PSMA (MW 120,000 and 350,000) are compressed to a plateau region, $40 \text{ \AA}^2 < \text{Area} < 53 \text{ \AA}^2$, the monolayers coexist in the LE and LC state. Since the pure DLPC monolayer does not possess any LE-LC phase transition (solid line isotherms in Fig.4.9b-c), therefore, the phase transition as observed in Fig.4.9b-c (bold solid line isotherms) may correspond to a transition of the polymer from a flat-lying position to a more vertically oriented position at the interface, see Fig.4.10b. This is reasonable because, the higher molecular weight the PSMA has, the more hydrophobic it becomes and thus, it is less likely to be in the flat-lying position. As the mixed monolayers are continuously compressed, the onset of LC state can be noted by a steeper rise of the surface pressure. A further compression of monolayers will eventually lead them to collapse, a situation where molecules at the interface are forced out of the interface.

4.3.5 Conclusions

The pH-dependent complexation of DLPC with the three poly(styrene-*alt*-maleic anhydride) (PSMA) types, differing in their molecular weights (MW 1,600, 120,000 and 350,000) was characterized by the Langmuir Trough technique. The ability of the PSMA to interact with the monolayer increased with decreasing the pH. The structural reorganization of the phospholipid monolayer is also sensitive to the molecular weight of the polymer. The two PSMA (MW 120,000 and 350,000) types, having high molecular weights, behave nearly identically, in that each induces a LE-LC phase transition of the mixed monolayer. This suggests a phase transform of the PSMA monolayer from a horizontal to a more oriented vertical arrangement at the interface. However, the mixed monolayer with PSMA (MW 1,600) does not show a LE-LC phase transition, suggesting a horizontal flat-lying arrangement (LE) of the polymer in the mixed monolayer over a whole range of compression.

CHAPTER 5
THE STUDY OF POLYMER-LIPID
INTERACTION:
SURFACE TENSION STUDY

5.1 INTRODUCTION

Surface methods, especially surface tension measurements, have long been used in the study of interactions between polymers and surfactants. Other surface methods, including neutron reflection, surface rheology, X-ray reflectivity and fluorescence probes, have provided an important complement to this traditional technique. One of the major advantages of using surface tension measurements to study adsorption behaviour of surfactants is that the interesting information is readily accessible. This offers an opportunity to make a systematic pilot exploration of the adsorption behaviour of polymers both on their own and in mixtures with surfactants.

There have been numerous publications where this technique was used to investigate polymer-surfactant association. In Taylor [52], an idealized plot of surface tension variation with the surfactant concentration for a weakly interacting aqueous polymer/surfactant mixture was proposed. This plot is illustrated schematically in Fig.5.1 and the changes in the surface tension profiles are as follows.

In the absence of polymers, the surface tension of surfactant solution shows a monotonous decrease with increasing surfactant concentration, until the CMC (critical micelle concentration), where the surface tension abruptly levels off and becomes essentially constant. On addition of polymer, on the other hand, a completely different behaviour is observed. At low surfactant concentrations, the surface tension decreases in a similar way as in the absence of polymer, although for moderately surface active polymers the absolute value of the surface tension in the presence of the polymer is often lower than in the absence of polymer due to the adsorption of the polymer at the air-water interface. At a particular surfactant concentration, however, the surface tension dependence of the surfactant concentration levels off, and only at higher surfactant concentrations does it decrease again to a second break point.

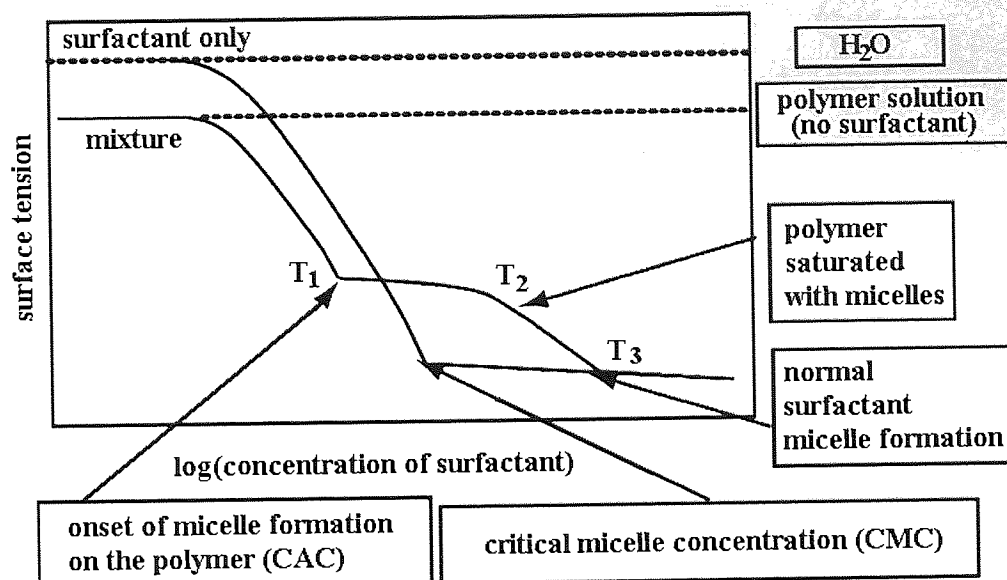


Fig.5.1 Idealized surface tension of a weakly interacting polymer/surfactant mixture which also interacts at the surface. The surface tension for the surfactant on its own is also shown [52].

As shown in Fig.5.1, there are three points in the surface tension of the mixture, designated as T_1 , T_2 and T_3 . The first break (T_1), at the low surfactant concentration is the critical aggregation concentration (CAC) for the system. This is the concentration at which the surfactant starts to form micelle on the polymer. The T_3 break point corresponds to the formation of another plateau in the surface tension at high surfactant concentration and is the critical micelle concentration (CMC) for the formation of the free surfactant micelles in the bulk. The T_2 break point is the point where the bulk polymer is saturated with the surfactant micelles and this point is generally less well defined than T_1 and T_3 .

5.2 AIMS

In this study, the association in solution and adsorption behaviour at the air–water interface of PSMA as well as its interaction with DLPC was investigated for the first time using surface tension measurements. It was expected that by using this technique, some aspects of the fundamental behaviour of the PSMA-DLPC complexes, such as surface adsorption and bulk behaviour, would be revealed.

5.3 EXPERIMENTAL

5.3.1 Surface Tension Behaviour of PSMA

In this study, the association behaviour of PSMA as well as its interaction with DLPC bilayer was studied by measuring surface tension at room temperature.

The three different molecular weights of PSMA (MW 1,600, 120,000 and 350,000) were hydrolyzed in aqueous solution under alkaline conditions. PSMA samples with different degree of ionization, see Fig.5.2, were obtained by controlling the molar ratio of alkali/polymer. The schematic representation of changes in hypercoiling behaviour of PSMA with decreasing degree of ionization is also illustrated in Fig.5.3. The PSMA samples at pH 12 were obtained by adding the polymer to a 0.1 M NaOH solution. The PSMA samples at pH 6 were prepared by adding the polymer to a solution containing the stoichiometric amount of NaOH. The PSMA samples at pH 4 were prepared similarly to those at pH 6, by dissolving the polymer with the appropriate amount of base.

Before each sample was analyzed, the surface tension of deionized water was determined (approximately 72 N/m) to ensure that the apparatus was clean. The polymer samples were transferred from the storage vials to the surface tension measurement dishes, thoroughly cleaned and rinsed with deionized water. The samples were allowed to rest 20 min before measurement. Between each experiment, the Pt-Ir ring of the tensiometer was cleaned in a flame to avoid contamination.

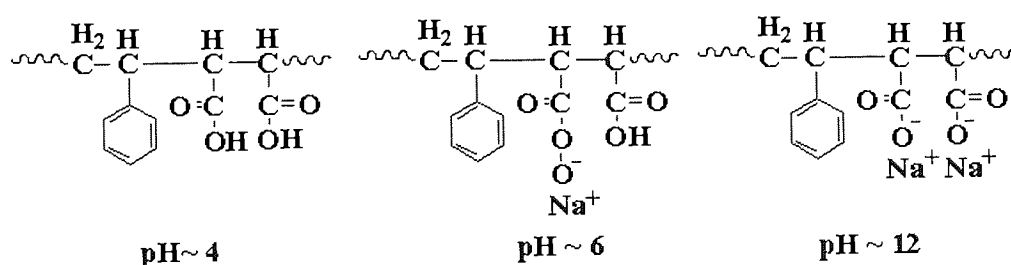


Fig.5.2 Molecular structures of poly(styrene-*alt*-maleic anhydride) hydrolyzed to different degrees of ionization.

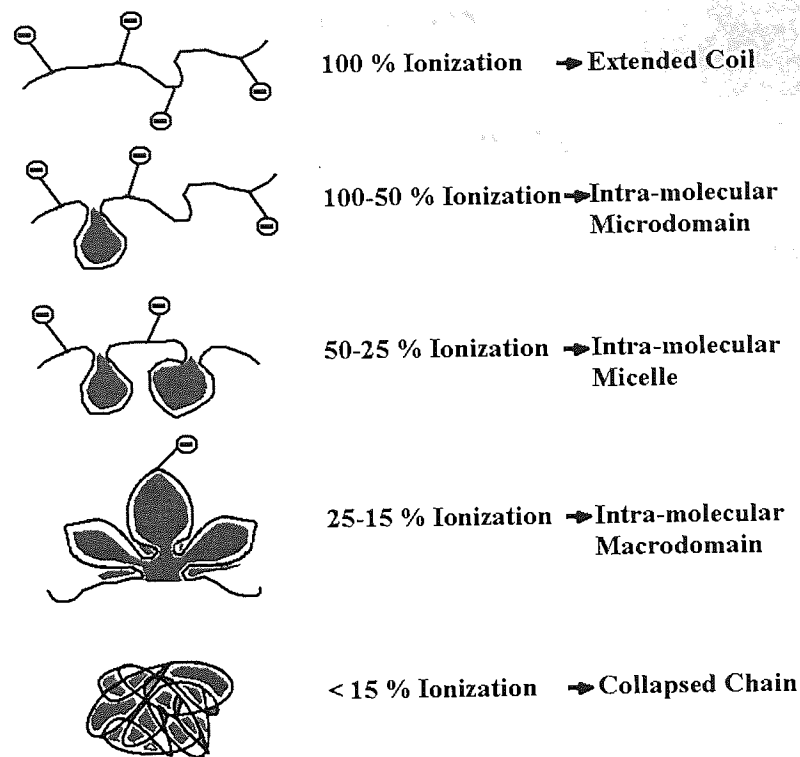


Fig.5.3 Schematic representation of the changes in hypercoiling behaviour of PSMA with decreasing degree of ionization.

5.3.2 Effect of DLPC on Surface Tension Behaviour of PSMA

The du-Nouÿ tensiometer, using Pt-Ir ring by the ring detachment technique, was utilized. The surface tension for a PSMA-DLPC mixture is measured as a function of the DLPC concentration (ranging from 10^{-7} -1.2 wt%) at a constant polymer concentration of 0.2 wt%. From earlier experiments, the surface activity of PSMA is greatly enhanced at pH 4. Based on this observation, the pH 4 was used to evaluate the effect of DLPC surfactant on the surface activity of PSMA. In general, the pH solution was adjusted toward pH 4 by the addition of NaOH or HCl. All measurement was performed at room temperature. The mixtures were transferred from the storage vials to the surface tension measurement dishes thoroughly cleaned and rinsed with deionized water. The mixtures were allowed to rest 20 min before measurement. Between each experiment, the Pt-Ir ring of the tensiometer was cleaned in a flame to avoid contamination.

5.4 RESULTS AND DISCUSSION

5.4.1 Surface Tension Behaviour of PSMA

The surface tension-concentration dependencies of PSMA (MW 1,600, 120,000 and 350,000) both in pH 12 and 6 are shown in Fig.5.4a and b, respectively. For all cases, a sharp decrease in surface tension at polymer concentration 0.2 wt% is followed by a plateau region. The decrease in surface tension at very low PSMA concentration demonstrates the surface activity of PSMA in both solutions. By comparing Fig.5.4a with Fig.5.4b, it is found that the polymer surface activity at pH 12 is quite weak and independent of molecular weight. This behaviour contrasts with that found at pH 6, where the surface activity for PSMA is found to be slightly affected by polymer molecular weight.

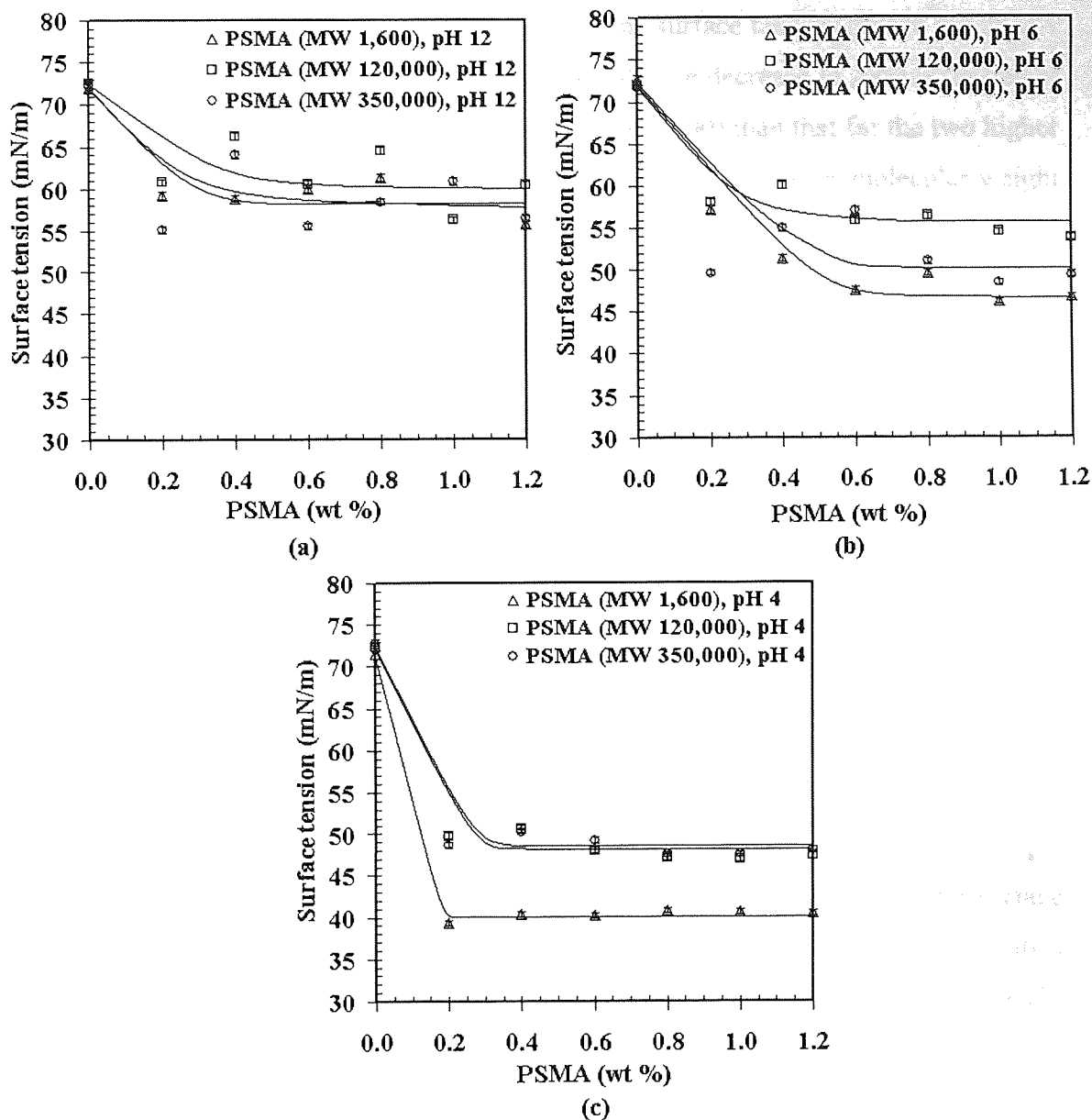


Fig.5.4 Effect of the molecular weights on the surface tension-concentration dependence of PSMA at (a) pH 12, (b) pH 6 and (c) pH 4 (after 20 min).

The surface tension-concentration dependencies of the three PSMA types (MW 1,600, 120,000 and 350,000) at pH 4 are illustrated in Fig.5.4c. All PSMA types show an initial abrupt decrease in surface tension at 0.2 wt% PSMA, owing to the adsorption of PSMA at the interface. This change is followed by a surface tension plateau at polymer concentrations above ~ 0.2 wt%. The breaking points at around 0.2 wt% may be the points at which the polymers begin to saturate the interface. The fact that all three PSMA types have the same saturation concentration values (C_{sat}) suggests that surface coverage for this polymer may be independent of molecular weight. A further discussion of this independence will be presented later.

The effect of molecular weight on the surface tension profile for PSMA at pH 4 may also be observed in Fig.5.4c. At this pH, the decrease in surface tension at 0.2 wt% PSMA is more pronounced for PSMA (MW 1,600) than that for the two higher molecular weight types. This leads to the conclusion that, the lower molecular weight PSMA possesses the strongest surface activity.

It is worth noting, from Fig.5.4c, that a smooth plateau region after the breaking point is observed for all PSMA types. This observation suggests that in pH 4 solution, the surface equilibrium is perhaps achieved quickly. Similar conclusions were drawn by Garnier and coworkers [48] who studied the association of PSMA both in the solution and at the interface. They established that at pH 3, the surface equilibrium of PSMA was accomplished within seconds, while, at pH 12 and at pH 6, the equilibriums were reached within minutes and after 24 hours, respectively.

The effect of pH on the surface tension profiles for PSMA with molecular weights 1,600, 120,000 and 350,000 is compared in panel (a), (b) and (c), of Fig.5.5, respectively. Two observations are worth noting. Firstly, in all cases the pH strongly affects the surface activity of the PSMA. For each PSMA type, the surface activity increases with decreased pH, giving a series of pH dependent surface activities for PSMA: at pH 4 > at pH 6 > at pH 12. Secondly, the polymer molecular weight affects the shape of the curves but not the relative pH-dependence.

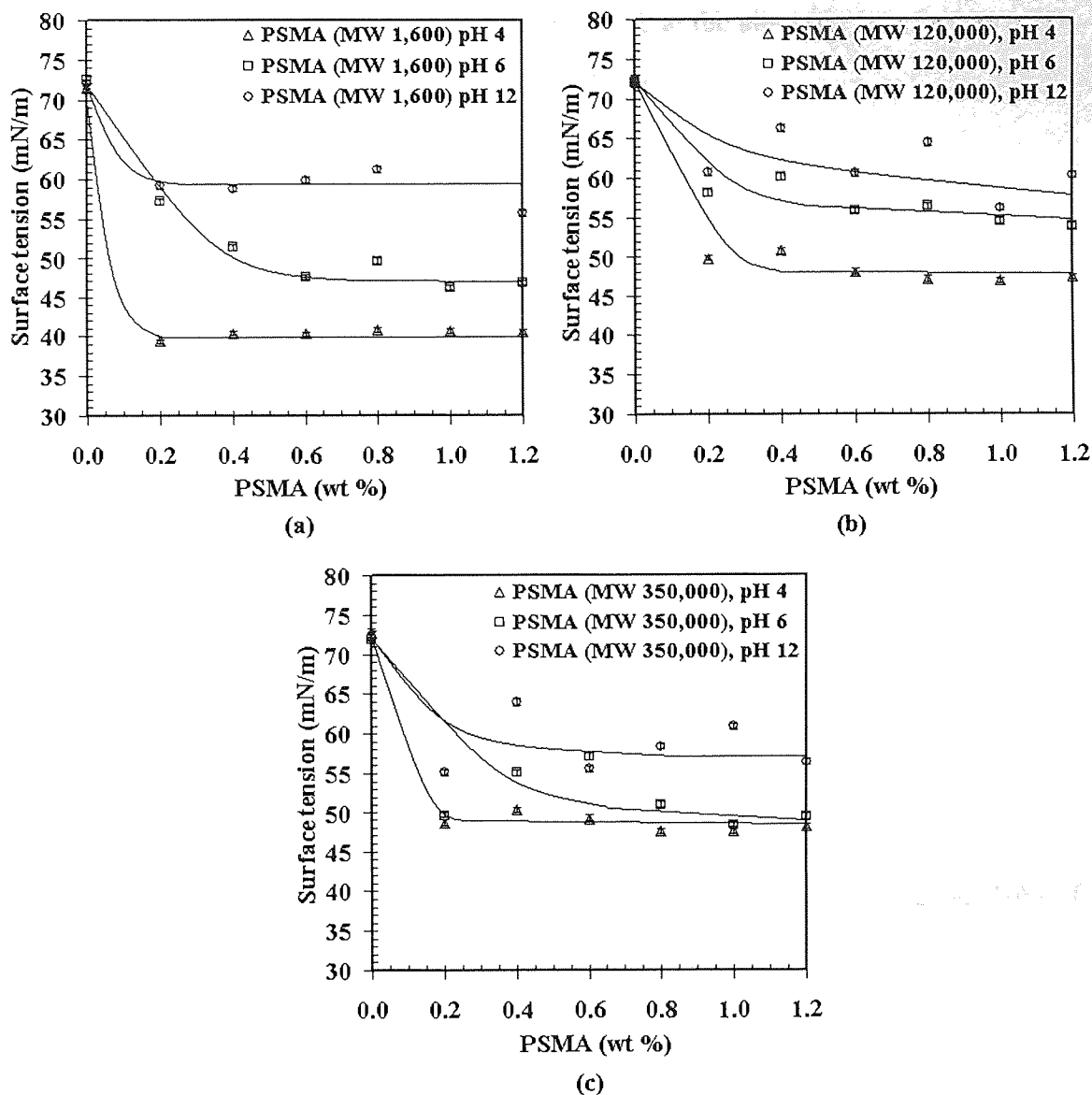


Fig.5.5 Effect of pH on the surface tension-concentration dependence of PSMA; (a) MW=1,600, (b) MW 120,000 and (c) MW 350,000 (after 20 min).

Overall, the results obtained in the surface tension study show that the adsorption of PSMA at the interface is strongly dependent on the pH and slightly dependent on the polymer molecular weight. This molecular weight-independence of polymer adsorption at the interface corroborates with the earlier works [48, 51, 53]. Following the discussion in Garnier et al. [48], the molecular weight-adsorption independence can be demonstrated as below;

By assuming PSMA molecules adsorb at the air-water interface as a 2D-coil, the surface coverage (ϕ) can be approximated by;

$$\phi \approx \frac{Nbd}{\pi r^2}$$

Where N is the number of monomer units per polymer chain and b and d are the length and diameter of the PSMA monomer, respectively.

The end-to-end distance r of a random coil in a condition θ is described by;

$$r^2 = CNb^2$$

Here C is the characteristic ratio, which typically ranges from 5 to 20 (for a very flexible to a very rigid molecule).

Combining the equations above yields:

$$\phi \approx \frac{Nbd}{\pi CNb^2} = \frac{d}{\pi b C}$$

The final equation states that the surface coverage is independent of the polymer molecular weight. By assuming flexible molecules at the interface and $d \approx b$, one may approximate $\phi \approx 0.1$, which means that PSMA molecules cover about 10% of the air-water interface. This may be one of the reasons explaining why the surface coverage of PSMA at pH 12 and pH 6, as shown in Fig.5.4a-b, only has a slight dependence on molecular weight.

Led by the results obtained from Fig.5.4c, additional surface tension measurements were performed for very low polymer concentrations as a mean to clarify the adsorption behaviour of PSMA at pH 4. This can be done by carrying out surface tension measurements for a series of dilute polymer concentrations ranging from 10^{-7} to 1.2 wt% using the du-Noüy tensiometer. All measurements were performed at room temperature. The plot of surface tensions at pH 4 against logarithmic concentrations of PSMA; MW 1,600, 120,000 and 350,000 at very low polymer concentrations is presented in Fig.5.6.

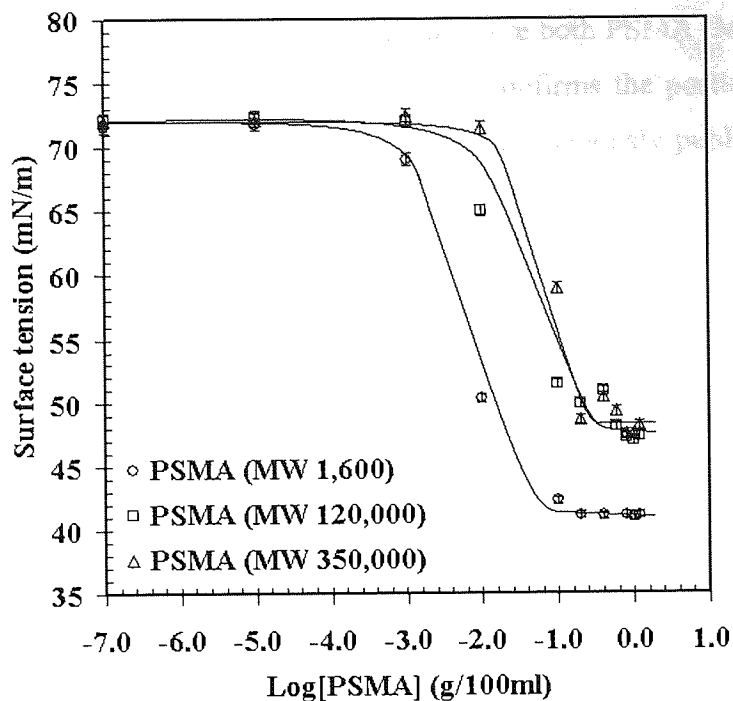


Fig.5.6 Surface tension as a function of logarithmic concentration for PSMA in acidic aqueous solution (pH 4). Measurements were performed at room temperature.

In the case of PSMA (MW 1,600), the surface tension begins to decrease at polymer concentration of 10^{-5} wt% and remains constant at concentrations above 0.06 wt%, see Fig.5.6. This finding demonstrates that the polymer starts to adsorb and saturates the interface at concentrations of 10^{-5} and 0.06 wt%, respectively. The surface tension profiles of PSMA (MW 120,000 and 350,000), observed in Fig.5.6, share some common features. One is that they begin to decrease at the same polymer concentration, firstly, around 10^{-3} wt%, suggesting that these PSMA types may start adsorbing at this concentration. Moreover, their surface tension profiles show plateau regions at concentrations above 0.25 wt%.

The concentration C_{sat} at which PSMA starts to saturate the interface may be estimated from the surface tension-concentration curve, shown in Fig.5.6. The value C_{sat} is the concentration at which the surface tension becomes constant since further additional polymer chain can no longer occupy the interface. Fig.5.6 shows that the estimated C_{sat} values for PSMA (MW 1,600) is ~ 0.06 wt%, which is less than that of the higher molecular weight PSMA types (0.25 wt%). This finding suggests the greater affinity to the surface of the former and the preference of the latter to undergo self-

association in the bulk of solution. The situation where both PSMA (MW 120,000) and PSMA (350,000) possess the same C_{sat} value also confirms the postulation of surface coverage-molecular weight independency, which was previously published by Garnier et al. [48].

The association mechanism for PSMA in solution was proposed by Garnier et al. Based on light scattering results, they discovered that even at a very low concentration (0.05 wt%), PSMA tends to aggregate in solution. Only high molecular weight molecules at high pH and low concentrations preferentially remain as individual random coils. The aggregation size of PSMA was found to be pH-dependent and the largest size was obtained at pH 6.5. They explained that aggregation size is correlated with the time required to reach equilibrium at the interface. The schematic representation of the equilibrium, linking the partition of PSMA molecules between the bulk solution and the interface, is demonstrated in Fig.5.7. The longer time the polymer has to aggregate in solution, the larger aggregation size will be obtained.

Garnier et al. [48] also proposed that PSMA adsorbs at the interface as a 2-D random coil and that its surface coverage is inversely proportional to the aggregation size in solution. The saturation concentration at the interface is not always correlated to the critical association concentration in solution, since the self-association of PSMA in solution is energetically favoured over adsorption at the interface. This behaviour contrasts with that of surfactants.

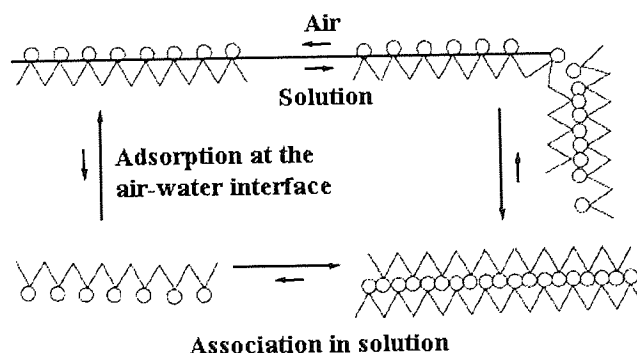


Fig.5.7 Schematic representation of the equilibrium linking the partition of PSMA molecules in solution and at the air-water interface [48].

5.4.2 Effect of DLPC on Surface Tension Behaviour PSMA

The surface behavior of aqueous DLPC solution at pH 4 as a function of its concentration is shown in Fig.5.8 (filled circle profiles). From Fig.5.8, the estimated critical micelle concentration (CMC) at pH 4 for DLPC is around 0.04 wt%.

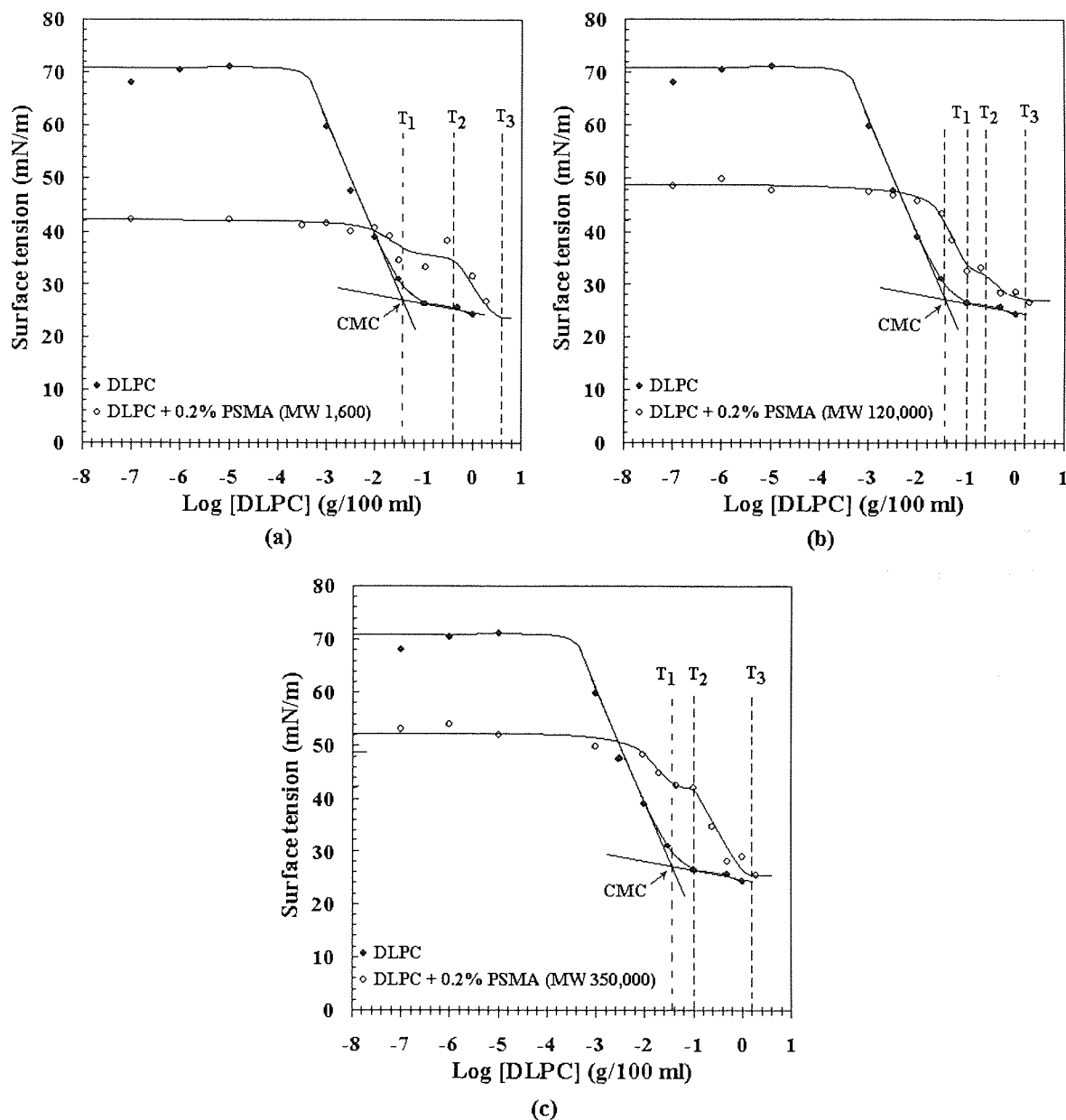


Fig.5.8 Variations in surface tension at pH 4 with DLPC concentration in the presence of 0.20 wt% PSMA with different molecular weights; (a) MW 1,600, (b) MW 120,000 and (c) MW 350,000 (The line through the data points are a guide to the eye only). The surface tension profile for DLPC on its own is also presented in each of panels.

The effect of DLPC on surface tension behaviour at pH 4 of PSMA (MW 1,600) may also be observed in Fig.5.8a. As illustrated in Fig.5.8a, the initial surface tension plateau is observed at a very low DLPC concentration region (10^{-7} -0.01 wt%), suggesting that within this region the additional DLPC molecules do not significantly adsorb at the interface. The polymer molecules, instead, strongly adsorb at the interface and hence, display significant surface activity. At DLPC concentration of 0.01 wt%, the surface tension begins to drop. The T_1 and T_3 values for the DLPC-PSMA (MW 1,600) mixture, estimated from Fig.5.8a, are 0.04 and 4.00 wt% DLPC, respectively. The interpretation of this finding is as follows.

At concentrations well above 0.01 wt% but below T_1 ($0.01 < C < 0.04$ wt%), the additional DLPC bind onto polymer chains, resulting in a formation of surface-active polymer-surfactant complexes at the interface. This complex is generally formed by cooperative binding of DLPC monomers onto the polymer backbone. A further addition of DLPC (at T_1 , in Fig.5.8a) results in a formation of nonsurface-active polymer-micelle aggregates, where DLPC molecules cooperatively adsorb to the polymer backbone in the form of micelles [52, 54]. The nonsurface-active complexes occur at relatively high surfactant concentrations, but do not correspond to any significant change in the surface tension profile. The subsequent decrease in surface tension at high surfactant concentrations ($0.40 < C < 4.00$ wt%) suggests an increased DLPC adsorption as the lipid monomer concentration in solution increases, in Fig.5.8a. Any further lipid added to the solution at 0.40 wt% is not bound to the polymer and therefore lowers the surface tension down to 26 mN/m. The breaking point T_2 for low molecular weight PSMA-DLPC system is less defined. Therefore, the interpretation of this point is limited.

The break point T_3 for PSMA (MW 1,600), in Fig.5.8a, is assumed to be at a concentration ~ 4.00 wt% since at this concentration, the surface tension for PSMA-DLPC mixture is similar to that for the pure DLPC at the same lipid concentration. At first glance, the point T_3 would appear to be the CMC in the weakly interacting systems, shown in Fig.5.1. However, for a system where there is an adsorption of surfactant as some sort of micelle on the polymer chain, this identification of T_3 may need to be assessed carefully because the properties of the layer may still be changing substantially with increasing surfactant concentration [52].

Fig.5.8b and Fig.5.8c illustrate the variation of surface tension as a function of logarithm of DLPC concentration, at a fixed polymer concentration (0.20 wt%) for PSMA with molecular weights 120,000 and 350,000, respectively.

As seen in Fig.5.8b-c, both high molecular weight PSMA types show a sharp decrease in surface tension with increased lipid concentrations, up to a point where the surface tension remains constant (T_1). This initial decrease in surface tension may result from a formation of a surface-active polymer/surfactant complex at the interface. When comparing Fig.5.8b and Fig.5.8c, it is found that the lowering of surface tension at a low lipid concentration region ($0.01 < C < T_1$) is more pronounced in the case of PSMA (MW 120,000) than for PSMA (MW 350,000), suggesting that the cooperative binding of DLPC monomers onto specific active sites of PSMA (MW 120,000), may produce stronger surface-active polymer/surfactant complexes.

At the breaking point, T_1 in Fig.5.8b-c, another type of polymer-surfactant complex starts to form. This complex differs from the first one in that it occurs at higher lipid concentration and it is generally formed by the micellization of the lipid, not by cooperative binding of lipid monomers, onto polymer backbone. Since the polymer-micelle aggregate is nonsurface-active in nature, therefore, the formation of this complex would not significantly change the surface tension profile. This may explain the existence of a plateau region at low concentration ($T_1 < C < T_2$), as observed in Fig.5.8b-c.

In case of PSMA (MW 120,000), the plateau region ends at concentration of 0.25 wt%, while that for PSMA (MW 350,000), the constant region ends at 0.10 wt% (Fig.5.8b-c). These estimated endpoints are the points where the bulk polymers are saturated with surfactant micelles and are denoted as T_2 . Any further DLPC added to the solutions after T_2 is not bound to the polymers and therefore, lowers the surface tension as T_3 is approached. The observed decrease in surface tension above T_2 , shown in Fig.5.8b-c, may indicate that the monomer (DLPC) equilibrium is shifted to the water-air interface [55]. This pathway is only interrupted when surfactant concentration reaches the T_3 point.

The morphology of aggregates developing after point T_2 is an open question. In some strongly interacting systems, for example in the bovine serum albumin (BSA)/sodium dodecyl sulphate (SDS) system, the binding of SDS causes the globular protein to transform from a native compact shape to a more open structure. This may be possible since large amounts of absorbed ionic surfactants can be expected both to break the inter-chain hydrophobic bonding and provide an electrostatic repulsion favouring an extended structure [55]. Whether or not DLPC can cause such effects to PSMA is still uncertain since surface tension measurement by itself does not provide any clear-cut information on morphological features. However, combining surface tension measurements with other surface sensitive techniques such as, ellipsometry, neutron and X-ray reflectivity and interfacial rheology, may yield complementary information about conformational changes in PSMA/DLPC complexes.

As already known, the main driving force of PSMA-DLPC association in an acidic aqueous solution (pH 4) is hydrophobic interaction between the phenyl groups along polymer backbones and the hydrocarbon long tails of the lipid. The stronger the hydrophobic interaction is, the easier the polymer-lipid aggregates would form and hence, a smaller CAC will be obtained. By comparing CAC values for the three different molecular weight PSMA types (or in other words, comparing T_1 values estimated from Fig.5.8a-c) it is found that PSMA (MW 120,000) shows the highest value of 0.10 wt%. The other two PSMA types show a similar CAC value of around 0.04 wt%. From this observation, one may assume that the hydrophobic association between hypercoiling PSMA and DLPC is more pronounced in the cases of PSMA (MW 1,600 and 350,000) than that of PSMA (MW 120,000). This finding also implies the ease of PSMA-DLPC association relative to polymer molecular weight as follows; $MW\ 1,600 \approx MW\ 350,000 > MW\ 120,000$.

Apart from the number of hydrophobic moieties in the polymer backbone, one should also remember that the polymer chain architecture (e.g. presence of methyl ester moieties), polymer chain flexibility and the presence of counterion, are all important parameters influencing the association of polymer and surfactant [54]. There is also experimental evidence for the predicted increase in CAC with increasing charge density in the case of hydrophobic polyelectrolytes. The explanation for this behaviour is that the hydrophobic polyelectrolytes are generally distributed closer to the hydrophobic core of the bound micelles than for hydrophilic polyelectrolytes where the association is mainly an electrostatic interaction with the micellar head groups. A lower charge density, therefore, makes it possible for the polymer to associate more with the surfactant tail region [52].

5.5 CONCLUSIONS

In this study, the association in bulk solution and adsorption at the air-water interface of poly(styrene-*alt*-maleic anhydride) (PSMA) as well as its interaction with the zwitterionic surfactant (DLPC) in aqueous solution was investigated for the first time using surface tension measurements. All three PSMA types (MW 1,600, 120,000 and 350,000) show surface activity in aqueous pH 12, 6 and 4 solutions. The surface activity for all PSMA types increased with decreasing pH, giving a series of pH-dependent surface activities for PSMA: at pH 4 > pH 6 > pH 12. The effect of molecular weight on surface activity could only be observed in pH 4 solution. At this pH, PSMA (MW 1,600) showed the strongest surface activity. PSMA molecules preferentially aggregate in solution up to a certain concentration before adsorbing onto the interface. This behaviour differs from that of surfactants whose molecules first saturate the interface before forming micelles in solution. The adsorption of PSMA at the air-water interface is strongly dependent on pH solution but slightly dependent on the chain length. Equilibrium is believed to control the partition of PSMA molecules between the bulk solution and air-water interface.

In this study, the association behaviour at pH 4 of PSMA (MW 1,600, 120,000 and 350,000) with DLPC was also investigated using a surface tension technique. Three breaking points were observed in the surface tension curves for all of the PSMA-DLPC mixtures, denoted as T_1 , T_2 and T_3 . At very low surfactant concentrations, polymer strongly adsorbed at the interface, hence displayed significant surface activity. For surfactant concentrations between 0.01 and T_1 wt%, DLPC monomers bound to the PSMA chains, resulting in a surface-active polymer/surfactant complex. At T_1 , a further addition of the lipid resulted in the formation of non-surface-active polymer/surfactant complex. This complex differs from the first one in that it occurs at higher surfactant concentration and it is formed by the micellization of the phospholipid onto polymer chains. At T_2 , the polymer was saturated with surfactant. Above the saturation concentration, surfactant was not bound to the polymer and therefore lowered the surface tension as T_3 was approached. Above T_3 , coexistence of pure DLPC micelles and mixed micelles of PSMA and DLPC was observed.

It was found that the hydrophobic association between DLPC and PSMA was more pronounced in the case of PSMA (MW 1,600 and 350,000) than that of PSMA (MW 120,000), implying that the affinity for polymer-surfactant association relative to polymer molecular weight is as follows; $MW\ 1,600 \approx 350,000 > 120,000$. Apart from the number of hydrophobic moieties in the polymer backbone, one should also remember that the polymer chain architecture, chain flexibility, polymer charge density and the presence of counterions, are all important factors influencing polymer/surfactant association.

The surface tension technique provides fundamental information about the interfacial behaviour of the polymer/surfactant complex. However, other crucial information, such as the composition, the structure and the thickness of the mixed polymer-surfactant layer at the air-water interface, is inaccessible to this traditional technique. Therefore, there is a need for further investigation using other surface-sensitive methods that, when combined with the surface tension data, might shed light on these important properties of the PSMA-DLPC system.

CHAPTER 6
THE STUDY OF POLYMER-LIPID
INTERACTION:
³¹P-NMR SPECTROSCOPY STUDY

6.1 INTRODUCTION

^{31}P -NMR spectroscopy is particularly well suited for the study of polymorphic phase behaviour of hydrated phospholipids since the naturally abundant ^{31}P atom provides a sensitive indicator for the structure and dynamics of the phospholipid headgroup. The technique senses the behaviour and environment of the phosphorus atom in the phospholipid headgroup and reports on the conformation and structural dynamics of the phosphate group. It reveals the phospholipid membrane structure without labeling and without perturbing the membrane assembly [56].

In general, there are two main ways to obtain information about phospholipid aggregates through ^{31}P -NMR. One involves measurements of the spin-lattice (T_1) and spin-spin (T_2) relaxation times which give the amplitudes and time scale (between 10^{-11} and 10^{-12} s) of different motions present in the system. The other requires an analysis of the spectral line shape, which characterizes the topology of each aggregate [57].

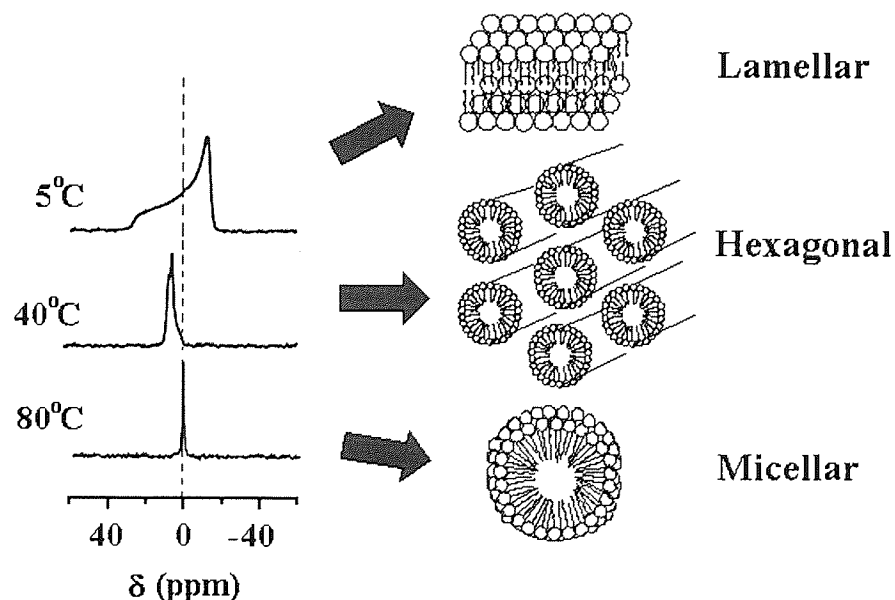


Fig.6.1 Proton-dipolar decoupled 121.5 MHz ^{31}P -NMR spectra of palmitoyllysophosphatidylcholine in 23 wt% aqueous polyethylene glycol. Spectra are recorded at temperature as indicated. Representation of the lipid phases are given on the left of the Figure (picture modified from [58]).

The use of ^{31}P -NMR for lipid phase identification is illustrated in Fig.6.1, which demonstrates the polymorphism of lysophosphatidylcholine dispersed in polyethylene glycol solution. The powder patterns of the ^{31}P -NMR spectra directly reflect the symmetry of the corresponding lipid phases. In the lamellar phase, the spectrum corresponds to axial symmetry and has negative chemical shift anisotropy (CSA). In the hexagonal phase, the spectrum also indicates axial symmetry but has a CSA which is opposite sign and less than half the size of that for the lamellar phase. In the micellar phase, the spectral anisotropy is completely averaged, a single isotropic NMR spectrum should thus be observed. The observed isotropic peak arises from the rapid rotation of the small micelles, giving rise to a conventional high resolution spectrum [58].

6.2 AIMS

In this study, ^{31}P -NMR was used to examine the polymorphic behaviour of aqueous DLPC dispersions in the presence and absence of poly(styrene-*alt*-maleic anhydride) (PSMA). The PSMA used in this study is a low molecular weight PSMA type (MW 1,600). The pH-dependent ability of this copolymer to destabilize the DLPC vesicles was also investigated at pH 4, 5, 6 and 10. Since the observed ^{31}P -NMR spectra are characteristic of different lipid phases [56-65], therefore it should be possible to investigate the phase transitions of phospholipid membranes upon binding with PSMA by analyzing the ^{31}P -NMR spectral line shapes.

6.3 EXPERIMENTAL

In this investigation, the ^{31}P -NMR spectra were acquired at 121.5 MHz on Bruker Avance 300 Spectrometer. XWIN NMR Version 3.5 software was used to process the spectra. The spectrometer field was locked during acquisition by using D_2O . The proton-decoupled spectra were obtained using a relaxation delay of 4 s, spectral width of 18,248 Hz and acquisition time of 1.8 s. The numbers of acquisitions were 160 scans. All spectra were recorded at room temperature and the chemical shifts were measured relative to H_3PO_4 (85%) as an external reference.

The ^{31}P -NMR spectrum for aqueous DLPC dispersion was recorded at lipid concentration of 5 mg/mL, while for aqueous PSMA solution, a 30 mg/mL polymer concentration was used to obtain the NMR spectrum. For all DLPC-PSMA mixtures, the NMR spectra were recorded at lipid and polymer concentrations of 5 and 30 mg/mL, respectively. The water used throughout the experiment was deionized water. The pH of solution was adjusted to the required value by using NaOH or HCl solution.

6.4 RESULTS AND DISCUSSION

Fig.6.2a-d show proton-decoupled ^{31}P -NMR spectra of aqueous DLPC-PSMA mixtures at room temperature and pH 10, 6, 5 and 4, respectively. The ^{31}P -NMR spectra of pure DLPC and pure PSMA at pH 4 are also shown for comparison in Fig.6.2e and f, respectively.

As may be noticed in Fig.6.2a, a mixture of DLPC and PSMA at pH 10 shows two spectral peaks, one at chemical shift (δ) around -10 ppm and another at zero chemical shift. This suggests that there are two distinct populations of lipid experiencing different motional environments. These populations may be in slow exchange with one another on the time scale of the ^{31}P -NMR. The NMR spectral line shape at $\delta=-10$ ppm, Fig.6.2a, indicates a bilayer lamellar organization for the DLPC at pH 10 in the presence of PSMA. This lamellar type spectrum is typically characteristic for phosphatidylcholine in excess water [57, 61, 62, 65].

The narrow symmetrical NMR spectrum at $\delta=0$ ppm, observed in Fig.6.2a, also suggests the presence of another isotropic phase (e.g., micellar). This isotropic phase is a phase where phosphate heads undergo rapid isotropic averaging motion, which produces a narrow symmetrical ^{31}P -NMR spectrum. Narrow signals at isotropic shift value have been observed in phospholipid systems by many authors and under various conditions [57-59, 65]. The coexistence of two phases (lamellar and isotropic phase) indicates that under alkaline conditions, the polymer is capable of partial binding with the phospholipid. This cooperation is visible by the detection of the isotropic lipid spectral line shape, as observed in Fig.6.2a. However, this cooperation

may compete with other possible lipid self-associations such as bilayer, as is evidenced by the existence of a lamellar peak, see Fig.6.2a.

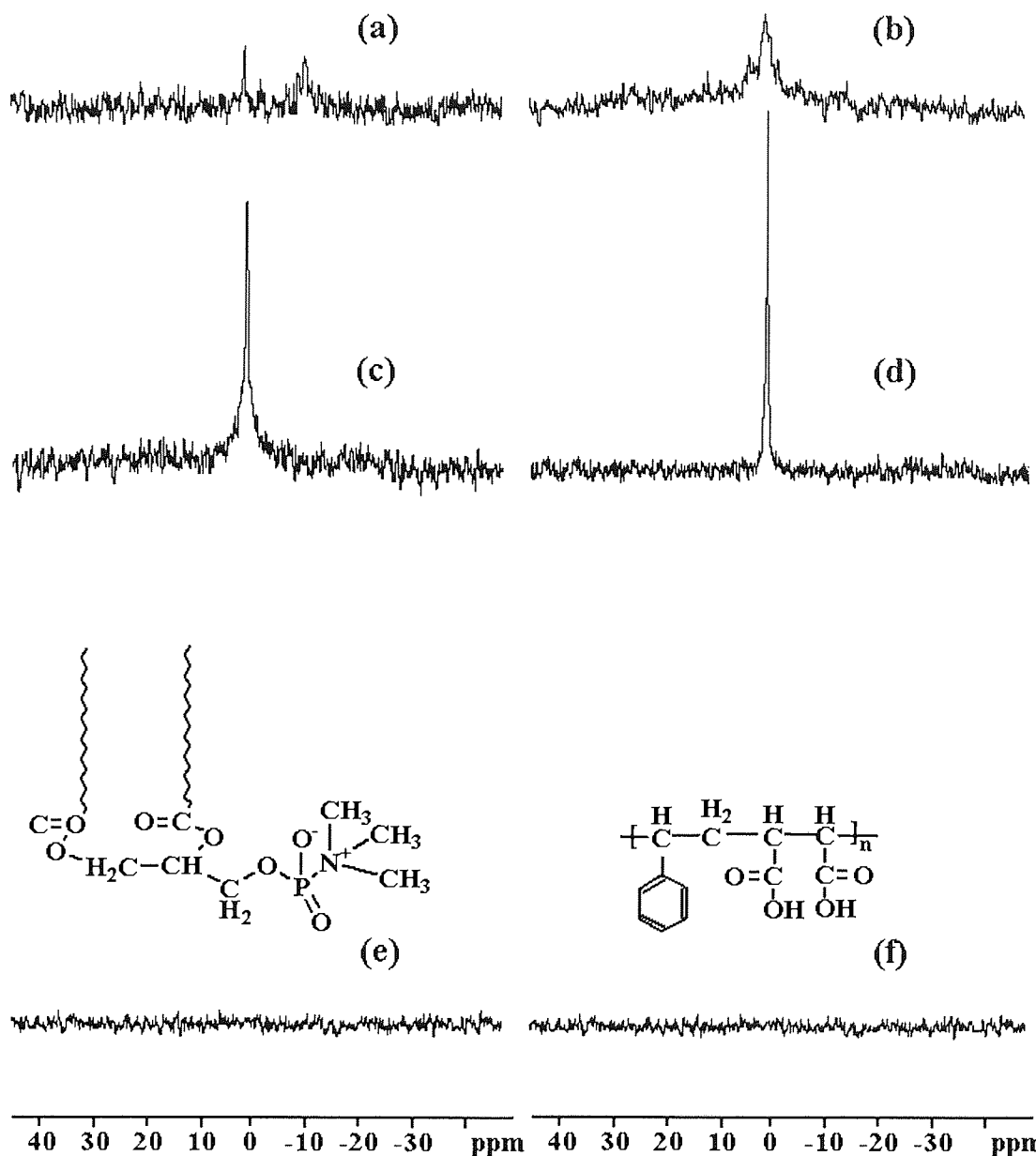


Fig.6.2 Proton-decoupled ^{31}P -NMR spectra of aqueous DLPC-PSMA mixtures at room temperature and (a) pH 10, (b) pH 6, (c) pH 5 and (d) pH 4. The ^{31}P -NMR spectra of pure DLPC (5 mg/mL) and pure PSMA (30 mg/mL) at pH 4 were also shown for comparison along with their chemical structures in (e) and (f), respectively. All spectra were recorded at lipid and polymer concentrations of 5 and 30 mg/ml, respectively. The low molecular weight PSMA type (MW 1,600) was used in this study.

As the pH of the DLPC-PSMA mixture decreases from 10 to 6, a broad ^{31}P -NMR peak appears at chemical shifts between +10 and -10 ppm, see Fig.6.2b. The peak observed at pH 6 is believed to be a result of the superposition of individual peaks; one corresponding to isotropic lipid phase and another corresponding to hexagonal lipid phase. It is useful to note that the peak that corresponds to the hexagonal phase differs from the lamellar peak in that it exhibits a spectral line shape with a low field peak and a high field shoulder [56]. The isotropic phase coexists once again with another anisotropic phase. However, this time the isotropic phase possibly coexists with a hexagonal phase instead of a lamellar bilayer phase. The disappearance of the lamellar peak, as observed in Fig.6.2b, indicates that the polymer completely destabilizes the bilayer assemblies and then associates with the phospholipid. This association is believed to induce the formation of both hexagonal and isotropic phases, which explains the coexistence of distinct lipid phases. This is evidenced by the superimposed peaks as observed in Fig.6.2b. The fact that the proportion of the hexagonal spectral component is half the size of that for the isotropic component indicates that the lipid molecules favour existence in isotropic phases rather than hexagonal phase. It is important to note that apart from the micellar structure, other isotropic structures that give rise to a narrow isotropic peak include the sonicated vesicles, cubic, rhombic and inverted micellar structures [56, 60, 65].

Further decreasing the pH of the DLPC-PSMA mixture toward 5 causes the hexagonal peak to disappear and only the isotropic peak at $\delta = 0$ ppm remains, see Fig.6.2c. As the pH of the solution is decreased to 4, these changes are even more pronounced, as illustrated by a sharper isotropic resonance with higher peak intensity, see Fig.6.2d. The fact that the ^{31}P -NMR spectra for DLPC-PSMA at pH 4 and 5 show only narrow signals at isotropic shift value, as observed in Fig.6.2c-d, demonstrates that at these pH values, the phospholipid-polymer complexes favor forming micelles, small vesicles or other isotropic structures. The anisotropic phases may no longer exist under these conditions.

The ^{31}P -NMR spectra of unsonicated DLPC dispersion (5 mg/mL) and pure PSMA solution (30 mg/mL) at pH 4 are presented in Fig.6.2e and d, respectively. One may notice that neither sample shows any detectable NMR resonance. The obvious explanation for the PSMA sample is that it does not have any phosphorus nuclei to give rise to a ^{31}P -NMR spectrum. The case of the DLPC sample may be explained by the molecular packing constraint of the lipid. When phospholipid molecules are dispersed in water, they tend to assemble into the lipid bilayers. This self-association is an example of the so-called hydrophobic effect, which has a large entropic contribution arising from the configurational entropy of the hydrogen bond networks within the water [66]. Because of this effect, the lipid bilayers arrange themselves in such a way that they have no edges and thus form multilayer supramolecular structures, which constrain the molecular freedom of the phospholipid head groups.

Earlier researchers reported that these supramolecular structures do not give rise to high resolution NMR spectra. Maddy and colleagues [67] obtained that high resolution NMR spectra of phospholipid are not observed until the large aggregates are broken up by ultrasonication. The fact that one observes a high resolution NMR spectrum only after sonication raises the question whether some phase change has occurred. Most authors [67] suggest that ultrasonication merely breaks up the large lamellar aggregates into smaller fragments and these fragments maintain a bilayer organization. The lipid molecules within these small fragments generally tumble with greater molecular freedom (e.g., translational freedom). The increased degree of molecular motion would result in decreased chemical shift anisotropy in the lipid phase and so give rise to a high resolution NMR spectrum.

In agreement with Maddy and coworkers, the unsonicated-DLPC sample (Fig.6.2e) does not show any ^{31}P -NMR spectrum. This observation suggests that under these conditions, the DLPC may self-assemble into multilayer supramolecular structures and that the phospholipid molecules within these structures may be strictly immobilized. This molecular packing constraint may explain the absence of ^{31}P -NMR signal shown in Fig.6.2e.

The change in molecular shape is considered the main driving force behind the anisotropic-isotropic phase transformation [56]. PSMA possibly modifies the shape of the lipid assembly through hydrogen bonding, electrostatic and hydrophobic interactions. At pH 10, the obtained spectral line shape (Fig.6.2a) indicates that half of the phospholipid remains in a typical bilayer organization, while the other half complexes with the polymer, giving isotropic structures. Under these basic conditions, one may assume that the binding strength of the polymer is not sufficient to induce all of the phospholipid to undergo the bilayer-nonbilayer transformation.

At pH 6, there is little or no evidence of bilayer spectral component at $\delta = -10$ ppm, see Fig.6.2b, suggesting that now the binding strength of the PSMA is strong enough to completely destabilize the lipid bilayer and induce all of the lipid to undergo bilayer-nonbilayer phase transformation. The binding of PSMA to phospholipid is believed to occur through a combination of hydrogen bonding and hydrophobic interactions, with electrostatic interactions being secondary. The two possible nonbilayer lipid organizations at pH 6 proposed here are the hexagonal and micellar structure. The PSMA molecules are believed to modify the shape of the phospholipids by surrounding the polar heads. An interface curvature is possibly induced by the PSMA molecules preferentially inserting themselves between the phospholipids at the level of the polar head groups. As a result, the phospholipid-PSMA complexes adopt a more conical shape and so form a hexagonal structure. It is possible that several head groups are completely solvated by the PSMA which would favor the formation of micelles or small vesicles that produce an isotropic-type signal because of their greater mobility [56].

As may be observed in Fig.6.2c, lowering of the mixture pH to 5 causes the hexagonal phase spectrum to completely disappear and only a peak at the isotropic chemical shift is present. This indicates that all the phospholipids interact with PSMA to form an isotropic phase, in which the motions are sufficiently fast to completely average the chemical shift anisotropy. Further decrease of pH to 4 produces an increase of the isotropic signal and a reduction of spectral width, see Fig.6.2d. This finding also once again suggests the formation of a lipid-polymer complex favouring isotropic structures. An interesting result is found when comparing the isotropic peaks

of DLPC-PSMA mixture obtained at pH 5 with that at pH 4, see Fig.6.2c-d. The spectrum at pH 4 shows a narrower peak with only half the size of that at pH 5, indicating a greater motional freedom of phospholipid head groups in the mixed lipid complexes performed at pH 4.

Overall results show that upon lowering the pH of PSMA-DLPC mixtures, the phospholipid undergoes phase transformations from bilayer lamellar to hexagonal, and finally, to isotropic (e.g., micellar, cubic and rhombic). The question of whether this observed phase transformation is reversible (via raising the pH of the mixture) is still open. Additional experiments will be required to answer this question.

The pH-dependent membrane disruptive activity of PSMA is believed to be associated with the conformational transition of the polymer. The protonation of the free carboxylic groups of PSMA is known to trigger this transition from an expanded conformation at high pH to a relatively hydrophobic globular coil in acidic solution [1, 50]. The collapsed polymer chain provides an increased number of hydrophobic sites which enhance polymer adsorption to the phospholipid and so the ability of PSMA to disrupt the DLPC membrane.

Whether or not increasing the molecular weight affects the pH-dependent membrane disruptive activity of the PSMA is of particular interest. Increasing the molecular weight (e.g., from MW 1,600 to 120,000 and to 350,000) is expected to enhance the effect of the phenyl group on the hydrophobicity of the polymer at lower pH, and as a consequence, a greater binding efficacy of the polymer to the membrane. This is possible as the longer chains collapse in a higher cooperative fashion and are more effective in excluding water from the coiled domain at higher pH [50, 63]. Introduction of different ratios of esterified alkyl chains of various lengths to PSMA back bone would probably be another way to enhance the membrane binding efficacy of the polymer.

The conversion from a lamellar to a mixed vesicular phase has been observed earlier in many different systems [42, 43, 68]. Recently, Maldonado et al. [68] observed the effect of adding polyethylene glycol (PEG) on the lamellar phase of a zwitterionic surfactant system (tetradecyldimethylaminoxide (C_{14} DMAO)-hexanol-

water). The results of freeze-fracture electron microscopy, as seen in Fig.6.3a-c, allowed them to draw the conclusion that the addition of PEG induces the spontaneous formation of highly monodispersed multilayered vesicles above a threshold polymer concentration.

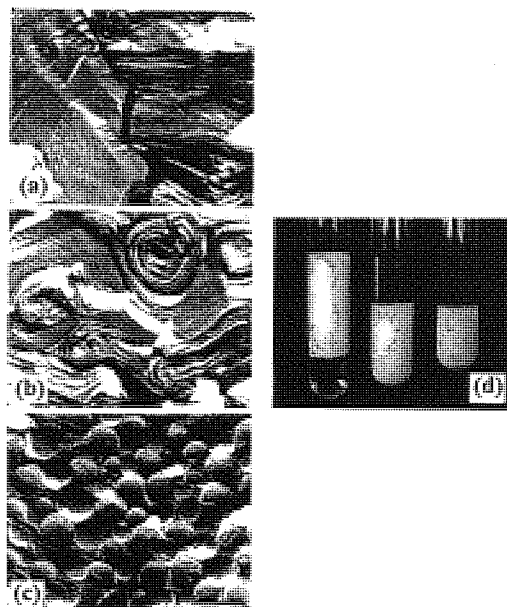


Fig.6.3 Effect of PEG concentration on the lamellar phase. (a) Polymer-free lamellar phase. (b) Lamellar phase where the PEG concentration is 1 g/L. (c) multilayered vesicles obtained with PEG concentration of 5 g/L. In all cases, the bilayer volume fraction is 0.2. The bar in (c) represents 1 μ m. The observed vesicular phase is shown for comparison in (d). From left to right, the surfactant volume fractions are 0.1, 0.2 and 0.3. The PEG concentration is 2 g/L in each sample. (Reproduced from [68].)

The slow reorganization of small phosphatidylcholine vesicles upon adsorption of hydrophobic modified polymer was studied by Ladavière et al. [42] using light scattering measurements and freeze-fracture electron microscopy (FFEM). The FFEM images, showed in Fig.6.4a-c, indicate that at the temperatures well above the melting transition T_m of dipalmitoylphosphatidylcholine (DPPC), the modified poly(acrylic acid) can induce lipid reorganization, progressing from large unilamellar vesicles to smaller vesicles and finally, to small compact globules. In the final state the large vesicles completely vanish and only small final species are observed, see Fig.6.4c. The smaller vesicles, shown in Fig.6.4b, were proposed by Ladavière and co-workers to be the intermediate species and they can only be observed at the temperatures well above the T_m of DPPC.

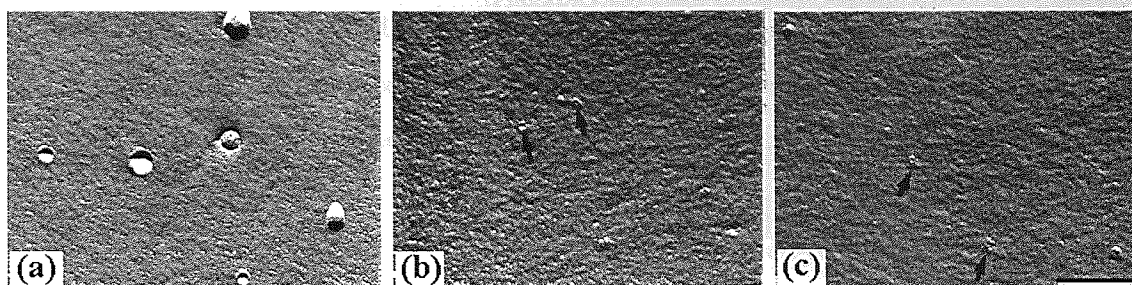


Fig.6.4 Freeze-fracture electron microscopy images of samples at 50°C (at 1 g/L lipids). (a) Spherical vesicles before the addition of modified poly(acrylic acid); (b) small vesicles (arrows) at time 3 min after the addition of polymer (polymer/lipid ratio = 0.42 mol/mol); (c) aggregated globules (arrows) and free globules at time 5 hr after the addition of the polymer. The scale bar in (c) represents 250 nm; all the photographs are at the same scale. (Reproduced from [42].)

Similar membrane reorganization has been observed for the dioleoyl phosphatidylcholine (DOPC). Thomas and Tirrell [43] established that poly(2-ethacrylic acid) (PEAA) binds to DOPC in a pH-dependent manner, forming mixed polymer-lipid micelles. Evidence for these mixed micelles can be seen in the negative stain electron microscopy image, as shown in Fig.6.5. The photograph illustrates that the DOPC membrane has been converted by the PEAA into small, disc-shaped micelles.

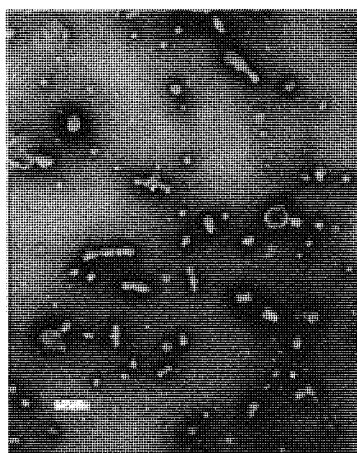


Fig.6.5 Negative stain (2% phosphotungstic acid) electron micrograph of DOPC/PEAA (1:1 mixture) at pH 6.1. Bar = 100 nm. The picture indicates micellar structure, which sometimes aggregates in stacks. (Reproduced from [43].)

As mentioned earlier, a change in the lipid molecular shape is considered the main driving force behind the bilayer-micelle transformation. This shape is usually represented by the critical packing parameter (P_c) defined as follows;

$$P_c = \frac{V}{l_c a_o}$$

where a_o is the polar head group area, V the volume of the hydrophobic tail(s) and l_c is the length of the hydrophobic chain(s) of the phospholipid [69], see Fig.6.6.

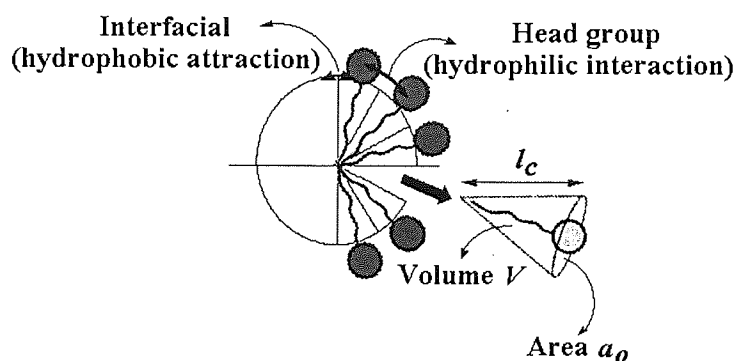


Fig.6.6 Schematic illustration of the parameters defining the critical packing parameter (P_c). (Redraw from [69].)

There is a direct correlation between the P_c value and the type of aggregate. For example, for a lamellar phase the phospholipid molecules occupy a cylindrical space and $V_c / l_c a_o = P_c = 1$. The more the phospholipid aggregates curve toward oil (e.g., the progression from lamellar \rightarrow hexagonal \rightarrow micellar) the smaller the value of P_c will be, which means that the headgroup area will be larger in relation to the surfactant volume. For reversed structures, the P_c increases in the order lamellar \rightarrow reversed hexagonal \rightarrow reversed micellar, see Fig.6.7.

The packing of the surfactant molecules (e.g., phospholipids) and also the type of surfactant aggregate formed should therefore depend on the values of a_o , V and l_c . Changing these parameters should influence the structure of surfactant aggregates formed and these parameters may practically be altered in a number of ways. Addition of a second surfactant (called cosurfactant) is one of the ways to alter these parameters and so control the structure of mixed aggregates.

Illustration removed for copyright restrictions

Fig.6.7 Schematic illustration of association structures formed in surfactant systems and the packing of surfactant molecules in different association structures. (Available online at <http://www.nonequilibrium.com/complexfluids.htm>.)

A survey of the literature revealed that in water, dilauroylphosphatidylcholine (DLPC), a lecithin homologue of two C_{12} acyl chains, self assembles into lipid bilayer arrangement, resembling a flat sheet [65]. Recalling the concept of the packing parameter mentioned earlier, this type of lecithin molecule should naturally adopt a cylindrical form ($P_c \sim 1$). As revealed by ^{31}P -NMR (see Fig.6.2a-d), adding PSMA under acidic conditions may alter the molecular shape of the phospholipid to a coned-shape form ($P_c < 1$) with the polar head group being larger than the hydrophobic tail. This phenomenon is believed to drive the lipid phase transformation from a bilayer phase to a hexagonal phase and eventually to a micellar phase. Decreasing the P_c value possibly correlates with an effective decrease in the hydrophobic volume as a result of the hypercoiled PSMA being incorporated within the interior of lipid aggregates. The incorporation of the collapsed PSMA chains is believed to strengthen the hydrophobic association between the lipid molecules, leading to a decrease in the hydrophobic volume and so a lowering of the P_c value. The changes of these packing parameters would probably lead to bilayer structural changes as well as lipid phase transitions, such as in the sequence bilayer \rightarrow hexagonal \rightarrow micellar.

6.5 CONCLUSIONS

The ability of high resolution ^{31}P -NMR to obtain the NMR spectra of hydrolyzed PSMA incorporated in phospholipid (DLPC) membranes was demonstrated in this study. It was shown that ^{31}P -NMR can be very useful in elucidating the different phases of phospholipid in the presence of PSMA copolymer under various conditions. More specifically, it was found that the strong interactions between PSMA and DLPC result in the disappearance of the bilayer structure and the formation of the isotropic phases (e.g., sonicated vesicles, cubic, rhombic, inverted micellar and micellar structures), which give rise to isotropic peaks in the ^{31}P -NMR spectra.

Changes in lipid molecular shape are considered the main driving force behind the bilayer-nonbilayer phase transformation. They are correlated with changes in the packing parameters (P_c , V , l_c and a_o). Incorporating the hypercoiled PSMA chains may strengthen hydrophobic association between the lipid molecules, leading to a decrease in hydrophobic volume (V) and so a lowering of the P_c value. This alteration should lead to a bilayer structural change as well as a lipid phase transition, for example as in the sequence bilayer \rightarrow hexagonal \rightarrow micellar.

The results obtained from this study also lead to a keen comprehension of important molecular phenomena. The PSMA has been shown to alter the phospholipid assembly in response to changes in pH, preferentially under acidic conditions. The pH-dependent membrane disruptive ability is believed to be associated with the conformational transition of the polymer from an expanded conformation to a relatively hydrophobic globular coil. The collapsed polymer chain may provide an increased number of hydrophobic sites for enhanced polymer adsorption to the phospholipid. Many questions still need to be addressed, e.g. how the phase behaviour of pure DLPC depends on pH and how increased polymer molecular weight affects the pH-dependent membrane disruptive ability of the PSMA. Additional ^{31}P -NMR data will be required in order to settle these matters.

CHAPTER 7
FABRICATION AND CHARACTERIZATION
OF A NOVEL DRUG DELIVERY
CONTACT LENS

7.1 INTRODUCTION

Topical delivery through eye drops, which accounts for approximately 90% of all ophthalmic formulations, is very inefficient and in some instances leads to serious side effects [70-72]. This is perhaps because the absorption of drugs in the eye is severely limited by some protective mechanisms that ensure the proper functioning of the eye and by other concomitant factors, for example drainage of the instilled solutions, lachrymation and tear turnover, metabolism, tear evaporation, nonproductive absorption/adsorption, limited corneal area and binding by the lachrymal proteins [70]. All of these factors may result in transcorneal absorption of 1% or less of the drug applied topically as a solution. The various pathways and factors involved in this ocular disposition, as discussed above, are schematically summarized in Fig.7.1.

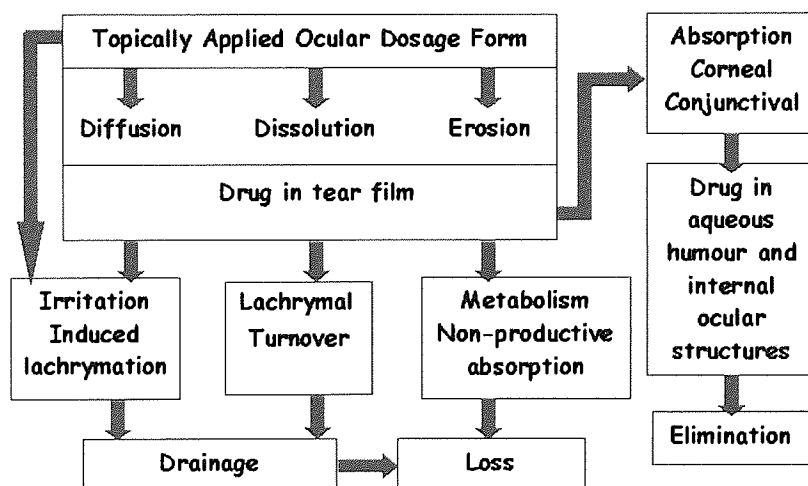


Fig.7.1 Schematic representation of the ocular disposition of topically applied formulations. (Modified from [70].)

With respect to above crisis, the new ophthalmic drug delivery systems that can increase the residence time of the drug in the eye, thereby reducing wastage and eliminating side effects would need to be developed. The contact lens that can release the controlled amount of drugs has emerged as a promising option in this regard. The concept of drug delivery system (DDS) contact lens was initially introduced by Waltman and Kaufman [73]. Since then many studies have investigated the ability of contact lenses to improve the corneal penetration and bioavailability of topically applied pharmaceutical agents.

Most of the previous attempts at using contact lenses for ophthalmic drug delivery have focused on soaking the contact lens in a drug solution to load the drug [71, 74, 75]. One of the recent studies focused on soaking the lens in eye drop solutions for 1 hour followed by insertion of the lens into the eye [75]. Researchers studied five different drugs and they concluded that the amounts of drug released by the lenses are lower or of the same order of magnitude as the amount of drug released by eye drops. In another recent study, researchers studied delivery of timolol maleate and brimonidine tartrate by absorbing it in the contact lens from a dilute solution of the drugs for approximately 3 months [71]. They then applied the soaked lenses in patients' eyes twice daily for periods of 30 minutes each. The contact lenses released most of the drug in this short time.

Although, soaked contact lenses are perhaps more efficient drug delivery systems than eye drops, they have a number of limitations [71]. First, the amount of drug that can be incorporated into the lens matrix by soaking is limited by the equilibrium solubility of the drug in the lens matrix, which is small for most hydrophobic drugs. Second, if the drug is incorporated into the matrix by soaking, the entire drug diffuses in a few hours. Gulsen et al. [71] concluded that soaked contact lenses can not provide slow and extended drug release. Also, it takes a few hours to load the lens with the drug from the aqueous solution, and the large fraction of the drug that is left in the solution is wasted.

Thus, there is a need for a novel drug delivery system that provides improved bioavailability, site-specific delivery and continuous drug release. The particle-laden contact lens has been proposed by many researchers as a promising candidate [71]. Recently, Graziacascione and coworkers published a study on encapsulating lipophilic drugs inside nanoparticles and entrapping the particles in hydrogels. They used poly(vinyl alcohol) (PVA) hydrogels as hydrophilic matrices for the release of lipophilic drugs loaded in poly(lactic acid-*co*-glycolic acid) (PLGA) particles. They compared the drug release rates from the hydrogels loaded with the particles with the delivery rates directly from the PLGA particles and found comparable results, which implies that the particles controlled the drug release rates. Derya and Anuj [71] also developed the particle-laden hydrogels both for therapeutic drug delivery to eyes and for the supervision of lubricants to alleviate eye problems prevalent in

extended lens wear. The poly(hydroxyethyl methacrylate) (PHEMA) hydrogel was chosen to be used as a secondary drug carrier and was synthesized by free radical polymerization in the presence of drug-laden microemulsion. The drug was entrapped in the microemulsions of hexadecane in water prior to polymerization with hydrogel-forming monomer. The results revealed that the contact lenses made with particle-loaded hydrogels released therapeutic levels of drug for a few days.

In this Chapter, the feasibility of using polymer-lipid nanostructures (PSMA-DLPC complexes) used in conjunction with soft contact lens as a new vehicle for ophthalmic drug delivery was demonstrated. The principle was studied by examining the encapsulation of model drugs (Rhodamine B and Oil red O dyes) as well as ophthalmic drug (Pirenzepine hydrochloride) in a new type of nanoparticle. The loaded particles were then encapsulated in a hydrogel matrix of the type used in soft contact lenses. It was assumed that if the nanoparticle size and loading are sufficiently low, the obtained particle-laden lens would remain transparent.

7.2 AIMS

The aim of this study was to develop a soft contact lens as a novel vehicle for ophthalmic drug delivery. The essential idea was to encapsulate the ophthalmic drug formulations in nanoparticle and disperse these drug-laden particles in the lens material (Fig.7.2). When this particle-laden contact lens is placed on the eye, the drug is expected to diffuse from the particles, travel through the lens matrix, and enter the post-lens tear film. Due to the slow diffusion of the drug molecules through the particles and the lens matrix, the particle-laden contact lens should provide continuous drug release for extended period of time.

In this work, the poly(2-hydroxyethyl methacrylate-*co*-methacrylic acid); poly(HEMA-*co*-MAA) and poly(vinyl alcohol) (PVA) were chosen to use as hydrogel matrix. The poly(HEMA-*co*-MAA) hydrogel was synthesized by free-radical thermal-polymerization of HEMA and MAA monomers in the presence of laden PSMA-DLPC complexes and a cross-linker such as ethyleneglycol dimethacrylate (EGDMA). The PVA hydrogel was prepared by free-radical photopolymerization of modified PVA macromers in the presence of laden PSMA-DLPC complexes, using patented 'Light-streamTM Technology' created by Ciba Vision. Model compounds, Rhodamine B and Oil red O dyes, as well as Pirenzepine drug were loaded into the PSMA-DLPC complexes then the laden complexes were incorporated physically into the hydrogel matrices. The advantage of using model compounds of the type employed is that its incorporation and release can be readily studied by colorimetry. The scanning electron microscopy (SEM) was used to observe the interior morphology of dye-laden complexes. The release studies were carried out by using UV-Vis spectroscopy.

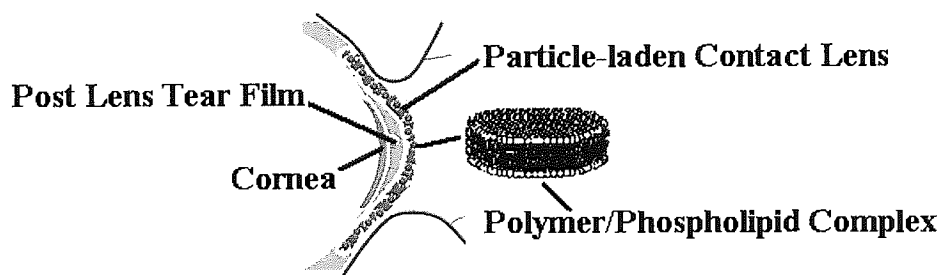


Fig.7.2 Schematic illustration of the vesicle-laden lens inserted in the eye. (Modified from [71].)

7.3 EXPERIMENTAL

7.3.1 Materials

Chemicals used in this study were obtained from commercial sources listed in Table 7.1.

Table 7.1 Chemicals used in this study.

Chemicals	Molecular Formula	MW	Suppliers
1. Poly(styrene- <i>alt</i> -maleic-anhydride) (PSMA)	$-(C_{12}H_{10}O_3)_n-$	1,600.0 (M_n)	Scientific-polymer product
2. 2-Dilauryl- <i>sn</i> -glycero-3-phosphocholine (DLPC)	$C_{32}H_{64}NO_8P$	621.8	Genzyme
3. Rhodamine B	$C_{28}H_{31}ClN_2O_3$	479.0	Sigma-Aldrich
4. Oil red O	$C_{26}H_{24}N_4O$	408.5	Sigma-Aldrich
5. Pirenzepine dihydrochloride	$C_{19}H_{21}N_5O_2 \cdot 2HCl$	424.3	Sigma-Aldrich
6. 2-Hydroxyethyl methacrylate (HEMA)	$C_6H_{10}O_3$	130.1	Cornelius
7. Methacrylic acid (MAA)	$C_4H_6O_2$	86.1	Acros Organics
8. Ethylene glycol dimethacrylate (EGDMA)	$C_{10}H_{14}O_4$	198.2	Acros Organics
9. Azobisisobutyronitrile (AIBN)	$C_8H_{12}N_4$	164.2	Aldrich
10. Modified PVA macromers	N/a	N/a	Ciba Vision

7.3.2 Synthesis Methods

7.3.2.1 Synthesis of PSMA-DLPC Complexes

The preparation method for PSMA-DLPC complex was described earlier in Chapter 2. Briefly, appropriate amounts of hydrogenated DLPC (1.50% w/v) and aqueous solution of PSMA (5% w/v) were mixed together. The polymer-lipid complexes were obtained by slowly lowering the pH of the resultant cloudy mixture to pH 4. The formation of these prefabricated complexes could be observed by an increase in the viscosity and transparency of the mixture. After the optically clear viscous solution was obtained, the pH of the mixture was gradually increased to pH 7.

7.3.2.2 Encapsulation of Active Compounds into PSMA-DLPC Complexes

The physical entrapment of the model drugs (Rhodamine B and Oil red O) and drug (Pirenzepine dihydrochloride) into PSMA-DLPC complexes was carried out in a similar way to that of the preparation of pure PSMA-DLPC complexes (detail in Chapter 2) except that appropriate amount of active compound was added together with DLPC and PSMA before lowering the pH of the solution to pH 4. The final concentrations of Rhodamine B, Oil red O and Pirenzepine drug in PSMA-DLPC complex were 0.5, 0.1 and 0.5% w/v, respectively. Chemical structures and some characteristics of the three active compounds are presented in Fig.2.1 and Table 2.1, respectively.

7.3.2.3 Freeze-drying of Loaded PSMA-DLPC Complexes

In this work, freshly prepared encapsulated PSMA-DLPC complexes, as obtained from Section 7.3.2.2, was freeze-dried without a cryoprotectant. Firstly, sample was dispensed in glass vials and frozen at -40°C for 20 min. After that the frozen sample was immediately placed on the freeze-dryer plate of temperature -60°C . Sublimation lasted 48 hours at a vacuum pressure of 10-13 Pa and without heating, being maintained at the condenser surface temperature of -60°C . Finally, the glass vial

was sealed under anhydrous conditions and stored at 4°C until being re-hydrated by using the same initial volume of deionized water.

7.3.2.4 Synthesis of Vesicle-Loaded Hydrogel Membranes

(a) Poly(HEMA-*co*-MAA) Hydrogel

To synthesize the vesicle-loaded hydrogel membrane, a freeze-dried powder of PSMA-DLPC complexes containing active compound, prepared in Section 7.3.2.3, was re-hydrated first with deionized water. After that, appropriate amount of this solution was mixed with the hydrogel-forming monomers, HEMA and MAA, prior to polymerization. Hydrogel membrane was prepared by free-radical polymerization using EGDMA and AIBN as crosslinking agent and initiator, respectively. The monomer mixture was degassed for 25 min prior to injection into the mould, shown in Fig.2.3. The injected mould was left for three days in the oven, being maintained at 60°C and then was post-cured at 90°C for three hours in order to complete a reaction. The composition of all constituents used to synthesize vesicle-loaded hydrogel membrane was shown in Table 7.2. Theoretical loading concentrations of dye and drug in poly(HEMA-*co*-MAA) hydrogels were expected to be ~0.14 mg/g of hydrogel.

Table 7.2 Feed compositions of smart hydrogel membrane.

Chemicals	Weight (g)	Roles
1.HEMA	3.88	Monomer
2.MAA	0.12	Monomer
3.EGDMA	0.02	Crosslinking agent
4.AIBN	0.02	Initiator
5.Water	0.20	Solvent

(b) Poly(vinyl alcohol) Hydrogel Membrane (PVA Hydrogel)

To synthesize the loaded hydrogel membrane, a freeze-dried powder of PSMA-DLPC complexes containing active compound, prepared in Section 7.3.2.3, was re-hydrated first with deionized water. Then, appropriate amount of aqueous dispersion of PSMA-DLPC complexes was thoroughly mixed with 5.0 g of the functionalized PVA macromer prior to photopolymerization. The obtained mixture was then poured onto the glass sheet mould, shown in Fig.2.3, and exposed to the long wavelength UV light (365 nm, 10 mW/cm²) for 20 min. Theoretical loading concentrations of dye/or drug in PVA hydrogels were expected to be ~0.14 mg/g of hydrogel.

In this study, aqueous solution of functionalized PVA macromer was a present from Ciba Vision. The photoinitiator 'Irgacure® 2959' was already added to the macromer solution as received. Macromer was a water soluble polymer of poly(vinyl alcohol) modified by the addition of *N*-acryloylaminoacetaldehyde-dimethylacetal [34]. The acrylic side chain is photocrosslinked to form a stable hydrogel. The network is formed by photocrosslinking using Lightstream Technology™ process. This fast, light-curing process has been extensively documented in both the patent and scientific literature [34, 35]. The resultant material characteristics are listed once again in Table 7.3.

Table 7.3 Characteristics of resultant PVA hydrogels synthesized by photopolymerization of functionalized PVA macromer using Lightstream Technology™ process [34].

Parameter	Measured value
Light transmission	≥99% (380-780 nm)
Refractive index	1.38 @ 589.3 nm
Water content	69 ± 2%; determined gravimetrically
Oxygen permeability (Dk)	26 barriers @ 35°C
Elastic modulus (Young's)	0.91 MPa

7.3.2.5 Loading of Dye or Drug into the Hydrogels

To understand the interaction of drug (or dye) with the hydrogel matrices and to see if polymerization reactions (e.g., thermal and photopolymerization) affect the stability of active compounds, the dye (or drug)-loading experiments were performed with both poly(HEMA-*co*-MAA) and PVA hydrogel membranes. The dye (or drug)-loading experiments were carried out in a similar way to that of the preparation of the vesicle-loaded membranes (described in Section 7.3.2.4-a,b) except instead of adding aqueous dispersion of loaded PSMA-DLPC complexes, appropriate amounts of active compound powders were added to the hydrogel-forming materials prior to polymerization. Theoretical loading concentrations of active compounds in each of hydrogel were expected to be ~0.42 mg/g of hydrogel.

7.3.3 Shape and Morphology Study of PSMA-DLPC Complexes

The shape of PSMA-DLPC complexes was studied through optical microscopy using a Leitz Dialux® 20 Microscope equipped with a MPS Wild camera. Sample was prepared by mixing 3 mL of PSMA solution (5% w/v) with 2 mL of aqueous mixture of dye and DLPC. After that, the pH of resultant mixture, containing PSMA, dye and phospholipid, was slowly adjusted to 4. This mixture was allowed to stand for 48 hours and then a few drops of sample were taken and placed on a glass slide. Micrographs of the sample were taken using the MPS 51 photomicrography unit. The final concentration of DLPC was 0.5% w/v while that of Rhodamine B dye was 0.5% and was 0.1% w/v for Oil red O.

The interior morphology of the encapsulated PSMA-DLPC complexes was carried out on the freeze-dried sample, prepared from Section 7.3.2.3. The sample was fractured carefully and its morphology was studied by using scanning electron microscopy (Stereoscan 90, Cambridge Instruments). Before SEM observation, specimens of the freeze-dried sample were fixed on aluminium stubs and coated with gold.

7.3.4 Hydrogel Characterization Studies

The transparency of the hydrogels with and without PSMA-DLPC complexes incorporated was measured by light transmittance study in UV-Vis spectrophotometer at a visible wavelength of 600 nm. The optical microscopy study was performed to determine the microstructure of the hydrogel membranes and to directly observe the vesicles entrapped inside the hydrogel matrix. A Leitz Dialux® 20 Microscope equipped with a MPS Wild camera was used to obtain micrographs of samples. Small piece of freshly synthesized vesicles-loaded hydrogel membrane, as prepared in Section 7.3.2.4, was soaked in deionized water for 10 min and then was placed on a glass slide. Micrographs of the sample were taken using the MPS 51 photomicrography unit.

7.3.5 *In Vitro* Release Studies

After synthesis of the hydrogels, release experiments were performed to establish that the trapped dye (or drug) can diffuse out of the hydrogels. Encapsulated hydrogel membranes, as derived from Section 7.3.2.4 and Section 7.3.2.5, were cut to give a uniform disk by using a cork borer No.6. Each disk was placed in glass vial filled with 5 mL of phosphate buffered saline (PBS) solution of pH 7.4 with gentle agitation at 125 rpm at room temperature. At a predetermined period of time, the sample disk was taken out from solution and placed into a new vial containing 5 mL fresh PBS solution. The concentration of Rhodamine dye and Pirenzepine drug, delivered from either dye (or drug)-loaded or vesicle-loaded hydrogels, was determined spectrophotometrically using UV-Vis spectrophotometer at 550 and 280 nm, respectively. All experiments were run in triplicate.

7.4 RESULTS AND DISCUSSION

7.4.1 Shape and Morphology Study of PSMA-DLPC Complexes

The solubilization of lipid bilayers by cosurfactants (e.g. detergent, bile salt, Triton X-100 and PEAA) is known to be accompanied by morphological changes of the bilayer and the emergence of mixed micelles containing both polar lipid and cosurfactants [76, 77]. The equilibrium and transient structures encountered in lipid-cosurfactant mixture, and the kinetics of the dissolution and of the closure to vesicles are important issues [76], and these have attracted considerable interest. In this study, the morphologies of the DLPC bilayer and the mixed PSMA-DLPC complexes during the solubilization process were studied for the first time through optical microscopy.

The transformation between the large multilamellar DLPC assemblies and mixed PSMA-DLPC complexes is believed to take place according to a three-stage model. This model has been elucidated by a wide variety of experimental techniques, for example turbidimetry, fluorescence energy transfer, magnetic resonance spectroscopy, quasi electric light scattering, centrifugation and electron microscopy [76-79]. The transformation process occurs in a typical three-stage sequence. First stage is the incorporation of PSMA polymeric micelles in the lipid assemblies. This incorporation is believed to progress up until the point where lipid assemblies become saturated with PSMA micelles. The second stage begins when the saturation point is reached. During this stage, the mixed PSMA-DLPC complexes start to form in aqueous solution. The final stage is characterized by the disintegration of saturated lipid assemblies and the sequential formation of very small mixed complexes. The destabilization and eventual disintegration of the ordinary lipid assemblies is caused by an excessive number of small mixed complexes inside the larger structure.

Similar vesicle solubilization has been previously observed by López and coworkers [78]. The dynamic light scattering and freeze-fracture electron microscopy results led them to draw the conclusion that the Triton X-100 is capable of dissolving phospholipid vesicles into small mixed micelles. Representative cartoons, corresponding to the structure proposed for the sequential states of the Triton X-100/PC system during the vesicle to micelle transformation suggested by López et al, are presented in Fig.7.3a-e. The cartoons shown in Fig.7.3a-e were redrawn in accordance with their five Triton X-100/phosphatidylcholine (PC) systems differing in surfactant concentrations ranges from 0 to 40 mM Triton X-100. Micrographs of the systems, described by (a)-(e), are shown in Fig.7.3 next to the cartoons.

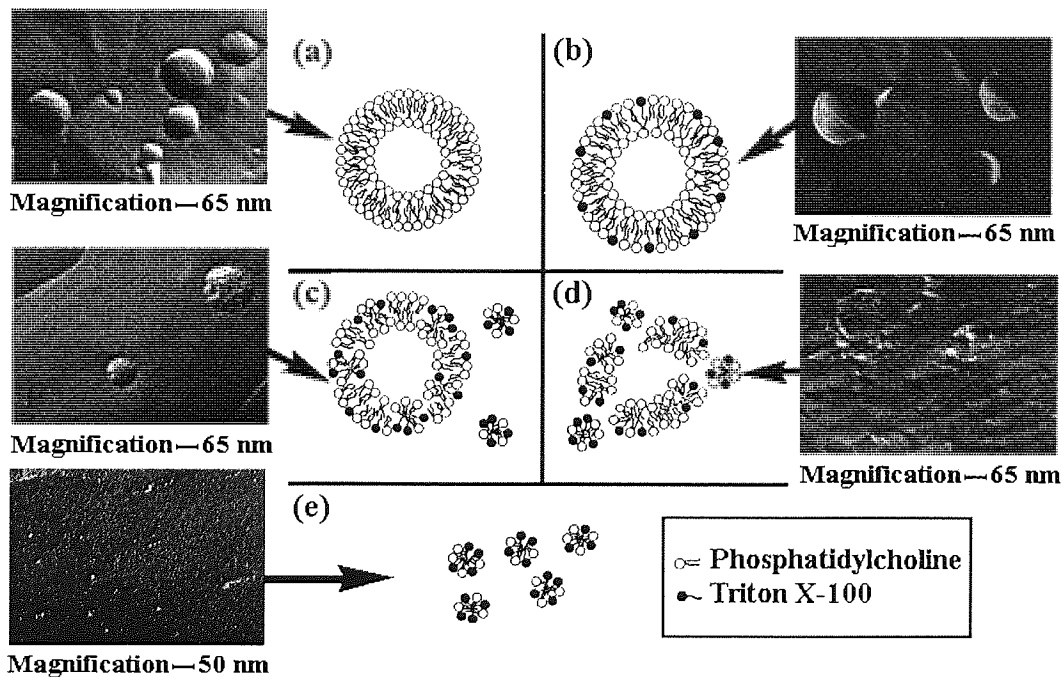


Fig.7.3 Representative cartoons corresponding to the structures proposed for the sequential states of lipid-surfactant interaction during vesicle to micelle transformation. (a) Pure liposome. (b) Enlargement of liposome. (c) Vesicle with clear sign of local disintegration and formation of mixed micelles. (d) Coexistence of mixed micelles and vesicle fragments without intermediate aggregates. (e) Only mixed micelles present. The PC concentration was fixed at 3.5 mM while the Triton X-100 concentrations were (a) 0, (b) 2.2, (c) 3.3, (d) 8.6 and (e) 40 mM. Micrographs of the systems described by (a)-(e) are shown next to the cartoons. (Picture modified from [78].)

López and coworkers [78] postulated that the vesicle solubilization is mainly governed by a local disintegration of the vesicle ('in situ' bilayer perforation). The formation of mixed micelles within the bilayer and the subsequent separation of these micelles from the liposome surface would lead to the formation of surfactant-stabilized holes on the vesicle surface. This process ends with the complete solubilization of liposomes without the formation of complex intermediate structures [78]. It seems that the liposome solubilization process, as proposed by López and coworkers [78], may be used to explain the mechanism by which PSMA solubilizes DLPC assemblies.

The optical micrographs of aqueous dispersions of PSMA-DLPC complexes, containing Rhodamine B and Oil red O, are presented in Fig.7.4 and Fig.7.5, respectively. The micrographs obtained provide direct evidence that this type of polymer-lipid assembly possesses ability to solubilize a wide variety of active compounds ranging from very hydrophobic ones, such as Oil red O, to amphipathic ones, such as Rhodamine B. The Rhodamine and Oil red O-loaded complexes are found to be spherical in shape with a wide size distribution, see Fig.7.4 and Fig.7.5. These visible loaded complexes range in size between 1 and 20 μm . The fact that the resultant dispersion of PSMA-DLPC complexes loaded with Oil red O appears transparent, see Fig.7.6, considerably proves the concept of using this new vesicle to render oil soluble active agents in a clear aqueous formulation that is most acceptable for ophthalmic drug delivery.

An important feature of the long term stability of mixed PSMA-DLPC complexes containing 0.5% Rhodamine dye was revealed using optical microscopy. If an aqueous dispersion of mixed complexes is not stable on its own, then one would expect to see some sort of vesicle aggregation over a long time scale. Fig.7.7 shows an optical micrograph of aggregates observed in aqueous solution of PSMA-DLPC complexes at pH 4 after 1 week of incubation. The micrograph illustrates that most of the spherical mixed complexes (indicated by arrow heads in Fig.7.7) were successfully dispersed in water, however, some of them spontaneously incorporated into domains of macroscopic dimension (indicated by arrow in Fig.7.7). The presence of macroscopic aggregates containing large numbers of small mixed complexes suggests that complexes

of PSMA and DLPC may not be stable over time. This phenomenon occurring over a long period of time should eventually lead to a macroscopic phase separation.

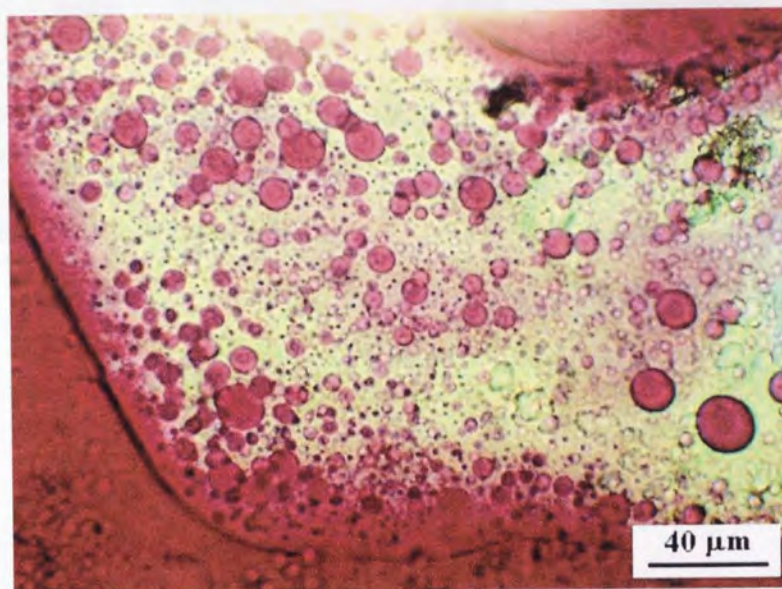


Fig.7.4 Optical micrograph at pH 4 of PSMA-DLPC complexes loaded with Rhodamine B dye at 40x magnification. Concentration of PSMA, DLPC and dye used were 3.0, 0.5 and 0.5% w/v, respectively.

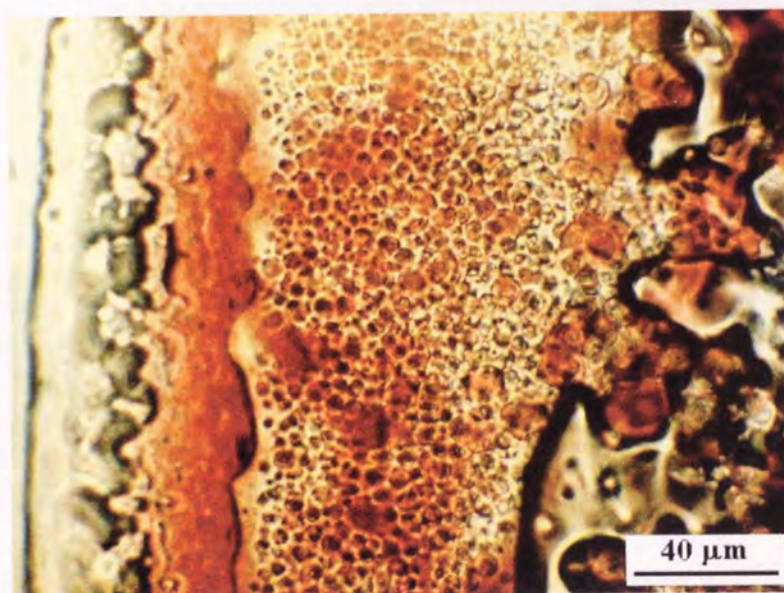


Fig.7.5 Optical micrograph at pH 4 of PSMA-DLPC complexes loaded with Oil red O dye at 40x magnification. Concentration of PSMA, DLPC and dye used were 3.0, 0.5 and 0.1% w/v, respectively.



Fig.7.6 Photograph showing optical transparencies of PSMA-DLPC samples; (A) before lowering of pH sample to 4; (B) at pH 4; (C) 30 min after addition of Oil red O, at pH 4 and (D) 3 days after addition of Oil red O, at pH 4. The concentrations of PSMA, DLPC and Oil red O were 3.0, 0.5 and 0.1% w/v, respectively.

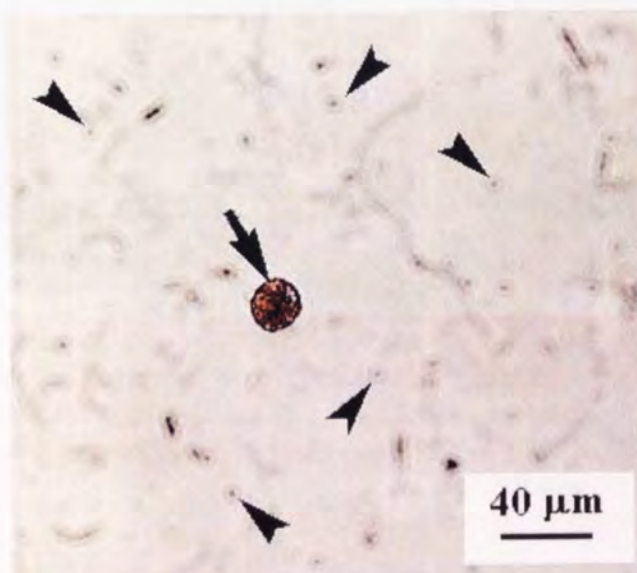


Fig.7.7 Optical micrograph of particles observed in aqueous dispersion of PSMA-DLPC complexes after 4 days of incubation. Arrow heads show small mixed complexes. Arrow shows macroscopic aggregates containing small mixed complexes. Small complexes are randomly aggregated within larger assemblies giving a non-periodic inner structure. Concentrations of DLPC, PSMA and Rhodamine were 0.5, 3.0 and 0.5% w/v, respectively. (Magnification x40.)

The SEM micrographs showing the interior morphology of Rhodamine-loaded PSMA-DLPC complexes are presented in Fig.7.8a-b. As seen in Fig.7.8b, mixed complexes (indicated by black arrows), containing 0.5% dye, are spherical in shape with a wide size distribution. The visible complexes in Fig.7.8b range in size between 1 and 10 μm , in consistent with optical micrograph results shown in Fig.7.4.

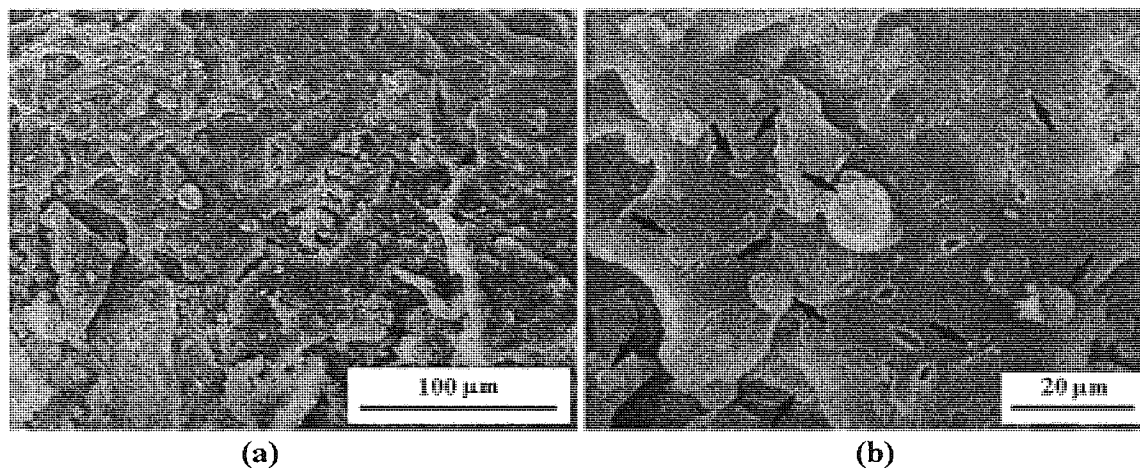


Fig.7.8 SEM micrographs showing interior morphology of Rhodamine-loaded PSMA-DLPC mixed complexes at magnification of (a) 320x and (b) 1030x. The concentrations of DLPC, PSMA and Rhodamine B were 0.5, 3.0 and 0.5% w/v, respectively. Arrows point mixed PSMA-DLPC complexes.

7.4.2 Hydrogel Characterization Studies

7.4.2.1 Transparency of Loaded Hydrogel Membranes

When the loaded PSMA-DLPC complexes were added to the polymerization mixture of either PVA or poly(HEMA-*co*-MAA), the obtained mixture was transparent with no sign of visible aggregates. This observation suggests that little or no interaction occurred between the vesicle constituents and the polymerization mixtures. The hydrogels, formed by polymerization of this clear mixture, were also clear and had the transmittance values of more than 98%. The results revealed that the PVA and poly(HEMA-*co*-MAA) hydrogels with vesicles incorporated had transmittance values as high as their pure ones, see Table 7.4. The fact that the incorporation of PSMA-DLPC vesicles does not significantly change the transparency of hydrogel indicates that the vesicle size remained small after polymerization.

Table 7.4 Transmittance values of the PVA and poly(HEMA-*co*-MAA) hydrogels with and without dye (or drug) loaded-PSMA/DLPC vesicle incorporation.

Hydrogel type	Transmittance (%)
PVA (with Rhodamine loaded-vesicles)	99.5
PVA (with Rhodamine, no vesicle)	99.8
PVA (with drug loaded-vesicles)	100.0
PVA (with drug, no vesicle)	100.0
PVA (no Rhodamine, no drug, no vesicle)	99.9
Poly(HEMA- <i>co</i> -MAA) (with Rhodamine loaded-vesicles)	98.9
Poly(HEMA- <i>co</i> -MAA) (with Rhodamine, no vesicle)	97.6
Poly(HEMA- <i>co</i> -MAA) (with drug loaded-vesicles)	100.0
Poly(HEMA- <i>co</i> -MAA) (with drug, no vesicle)	100.0
Poly(HEMA- <i>co</i> -MAA) (no Rhodamine, no drug, no vesicle)	99.2

Transmittance values were obtained at 600 nm for gels with a 1 mm thickness.

7.4.2.2 Microstructure of Vesicle-Loaded Hydrogels

The optical microscopy study was performed to determine the microstructure of hydrogel membranes and to directly observe the vesicles entrapped inside the hydrogel matrices. The optical micrographs of PVA hydrogel loaded with Rhodamine dye at 10x and 40x magnification are shown in Fig.7.9a and Fig.7.9b, respectively. In the micrograph in Fig.7.9a, the dye-loaded PVA hydrogel appears smooth and non-porous. However, the micrograph of this hydrogel taken at higher magnification shows aggregates whose size is between 5 and 10 μm (indicated by arrow in Fig.7.9b). The micrograph also indicates that these microspheres are capable of encapsulating Rhodamine dye within their microstructures. An attempt has been made to explain the formation of these aggregates. One of many explanations is correlated with the unincorporated PVA. This fraction of PVA macromer was suggested by Winterton et al. [34] to be the small amount of PVA macromer that did not participate in the cross-linking reaction to form the hydrogel. This unincorporated PVA is believed to self-aggregate to form microspheres, as observed in Fig.7.9b and Fig.7.9d.

Optical micrographs of PVA hydrogel containing loaded PSMA-DLPC vesicles are also shown in Fig.7.9c-d. Both micrographs were taken at 40x magnification. The micrograph in Fig.7.9c provides evidence that mixed vesicles were successfully entrapped in the PVA network. The trapped vesicles are spherical in shape with a wide size distribution. The vesicle size ranges from 6 to 14 μm , which is comparable to that of vesicles in solution. This finding indicates that the PSMA-DLPC vesicles were stable after photopolymerization.

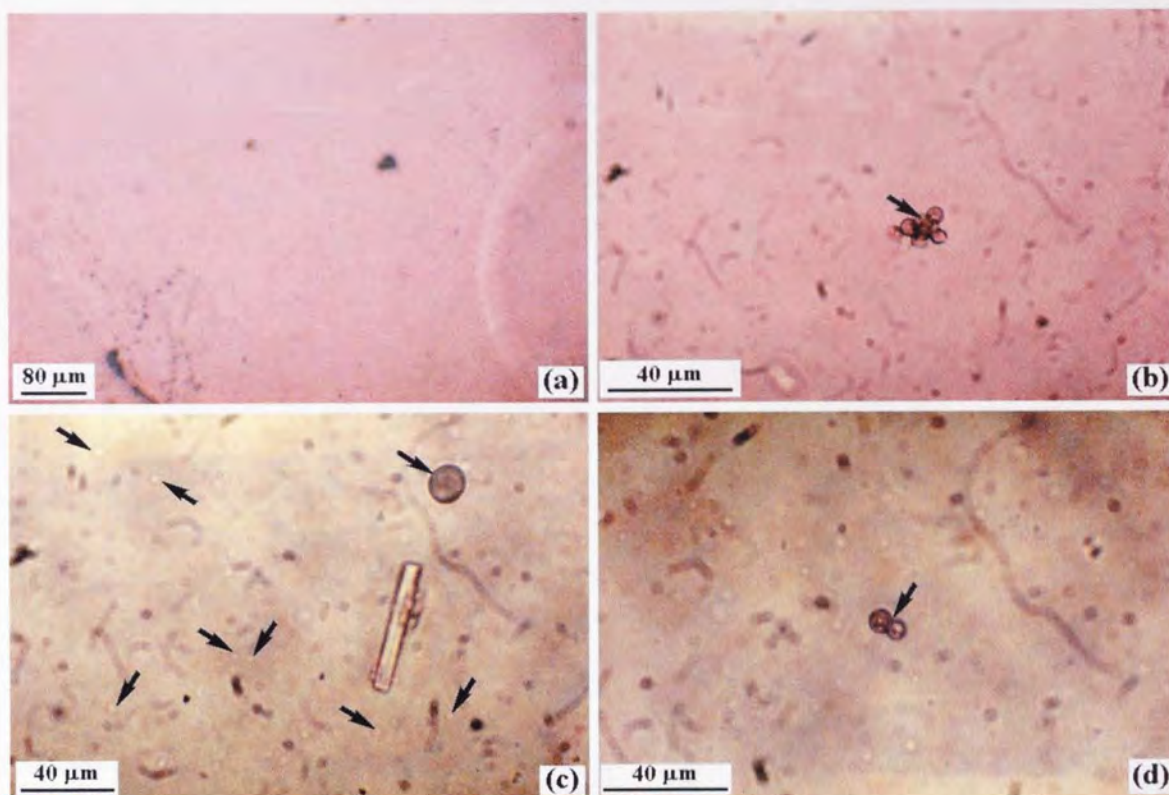


Fig.7.9 Optical micrographs of Rhodamine-loaded PVA hydrogel at (a) 10x and (b) 40x magnifications. The optical micrographs of PVA hydrogel containing Rhodamine-loaded DLPC-PSMA vesicles at magnification of 40x are also shown in (c)-(d). Arrows in (b) and (d) indicate possible self-aggregation of PVA. Arrows in (c) indicate mixed PSMA-DLPC vesicles entrapped in PVA network.

The optical micrographs of poly(HEMA-*co*-MAA) hydrogels in the absence and presence of loaded DLPC-PSMA vesicles are shown in Fig.7.10a and Fig.7.10b-f, respectively. As seen in Fig.7.10a, the Rhodamine-loaded poly(HEMA-*co*-MAA) hydrogel appears smooth with no visible particular aggregation. The successful incorporation of the DLPC-PSMA vesicles into HEMA-based hydrogel is demonstrated in Fig.7.10b-f. Most of the visible vesicles, observed in Fig.7.10b, appear to be spherical in shape with size ranging from 4 to 65 μm . The size of vesicles entrapped in hydrogel is found to be about 3 times the size of a single vesicle dispersed in aqueous solution (see Fig.7.4). This implies that the vesicles, as seen in Fig.7.10b-f, must be a cluster or bigger microparticles formed by coalescence.

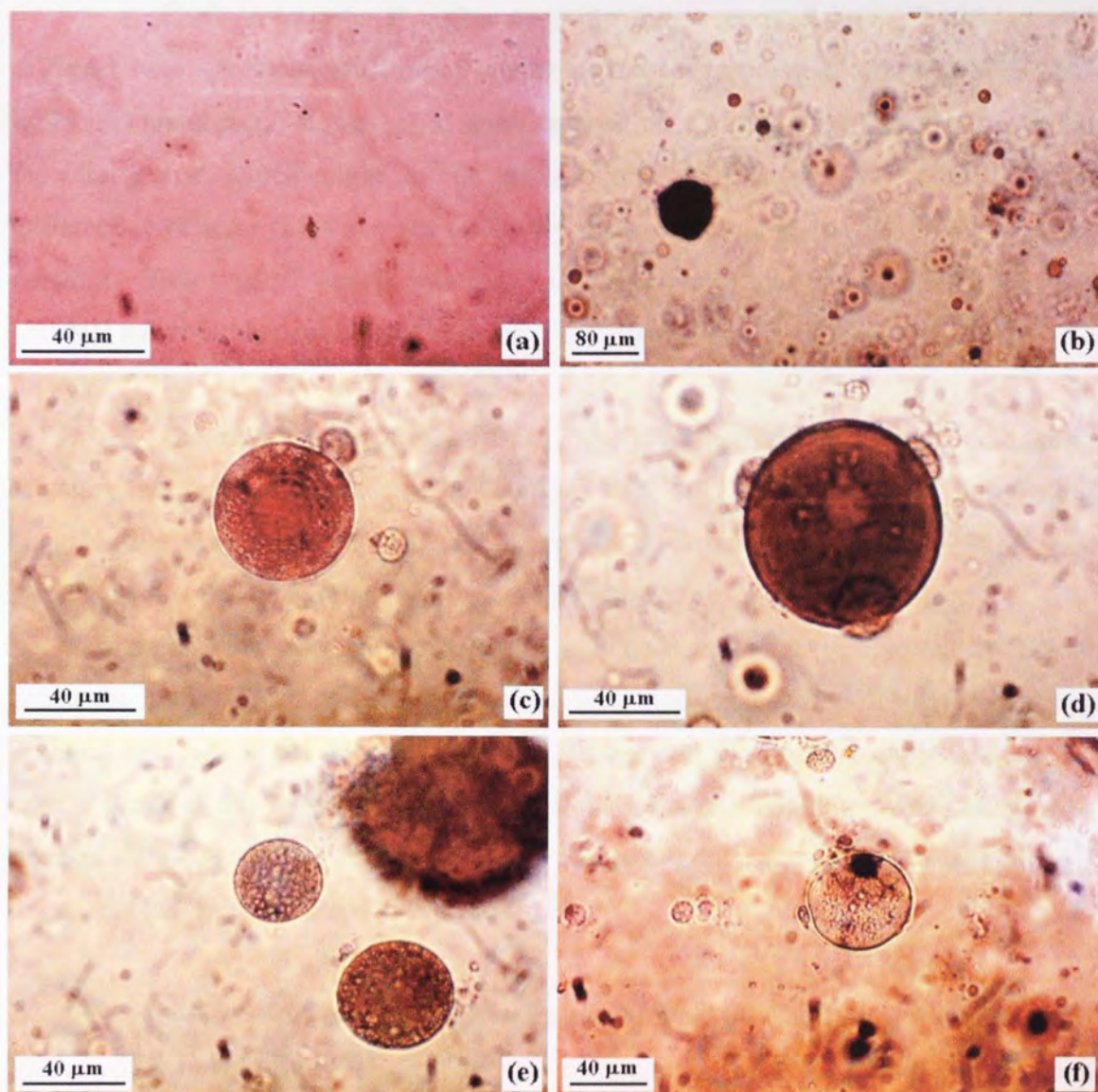


Fig.7.10 Optical micrographs of (a) Rhodamine-loaded poly(HEMA-*co*-MAA) hydrogel membrane and poly(HEMA-*co*-MAA) membranes loaded with DLPC-PSMA vesicles. Panels (b)-(f) showing variation of morphology and size of loaded vesicles dispersed in HEMA-based hydrogels. Micrograph (b) was taken at 10x magnification while the rest were taken at 40x magnification.

The micrographs at higher magnification, presented in Fig.7.10c-f, reveal different vesicular microstructure of loaded vesicles incorporated within poly(HEMA-co-MAA) membrane. However, no small unilamellar vesicles (SUVs) were observed in the micrograph, which might be due to the equipment's physical limitations. Large unilamellar vesicles (LUVs) were uniformly distributed within poly(HEMA-co-MAA) network. This type of vesicle was found to coexist with giant multilamellar vesicles (MLVs) and the spherical bilayer vesicles (Fig.7.10c-f).

The microparticles, shown in Fig.7.10c-f, possess a non-periodic inner structure that is possibly made of small mixed PSMA-DLPC complexes. This finding suggests that a dispersion of small mixed complexes may not be stable in HEMA-based hydrogel due to the relatively high hydrophobicity of the gel matrix. The polymerization condition should be taken into account in the vesicle accumulation. Since the poly(HEMA-co-MAA) hydrogel was synthesized at 60°C by chemically initiated free radical polymerization, it is potential that the mixed complexes may not remain stable at this temperature. As a consequence of this condition, small complexes perhaps join together in domains of macroscopic dimension giving supramolecular microstructure as is observed in Fig.7.10c-f.

The same phenomenon was also observed by Chauhan and Gulsen, who published a novel drug delivery system comprising a HEMA-based contact lens materials having dispersed dimyristoyl phosphatidylcholine (DMPC) liposome [80]. Their SEM image and confocal microscopy results demonstrated that the mean diameter of liposome entrapped in the poly(HEMA) gel is about a few micrometers, which is significantly larger than that for the liposome solution (~20 nm). They hypothesized that liposome aggregation may occur during the polymerization.

7.4.3 *In Vitro* Release Studies

7.4.3.1 Dye Loading and Release Studies

A model compound, Rhodamine B was used to examine the controlled release in the novel smart drug delivery hydrogel containing PSMA-DLPC vesicles.

Before continuing the discussion further, it is worth to mention some important characteristics of Rhodamine B. Rhodamine B is a kind of xanthene dye, whose optical properties depend on many factors, such as solvent, concentration and pH value [81, 82]. The carboxyl group participates in a typical acid-base equilibrium. The acid and basic forms of Rhodamine B are strongly coloured and luminescent, however, the lactone form is colourless and shows no emission because the π -electron system of the dye chromophore is interrupted [81]. Fig.7.11 presents the different forms of the Rhodamine B dye.

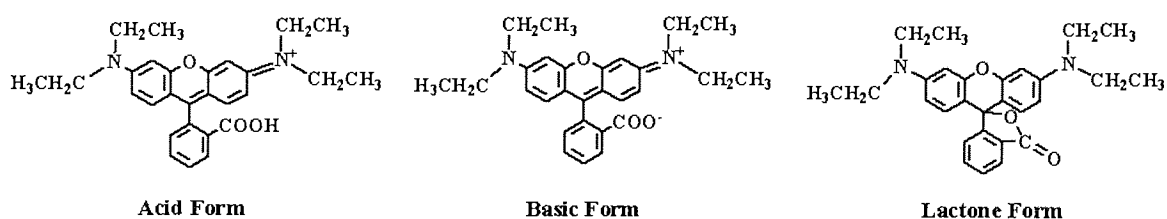


Fig.7.11 Molecular (ionic) structures of Rhodamine B equilibrium species [81].

The system of double bonds can be redistributed with the charge placed on the other nitrogen and thus, due to resonance between the two forms, the positive charge is shared between the two nitrogen atoms [82]. The pK_a for the aromatic carboxylic acid group is about 4.2 [82]. The solubility of Rhodamine B is very low at pH values below the pK_a and therefore at pH 4, the pH at which the dye encapsulation occurs, the Rhodamine dye (exist in acid form, see Fig.7.11) may be incorporated within PSMA-DLPC vesicle through hydrogen bonding as well as hydrophobic interaction. It should be pointed out that the electrostatic interaction between the dye molecule and polar head group of DLPC can possibly be involved in the encapsulation process.

Binding of Rhodamine B to PSMA-DLPC mixed complexes is shown in Fig.7.12. It appears that the ionization state of the carboxyl group may affect the vesicle binding efficiency. At pH 7.4, the pH at which the release experiments are performed, the binding of Rhodamine (existing in basic zwitterionic form, see Fig.7.11) is presumably reduced by repulsion of the carboxylate group from the vesicle surface. This condition would result in increased dye solubility in water and hence dye diffusion out of mixed vesicle.

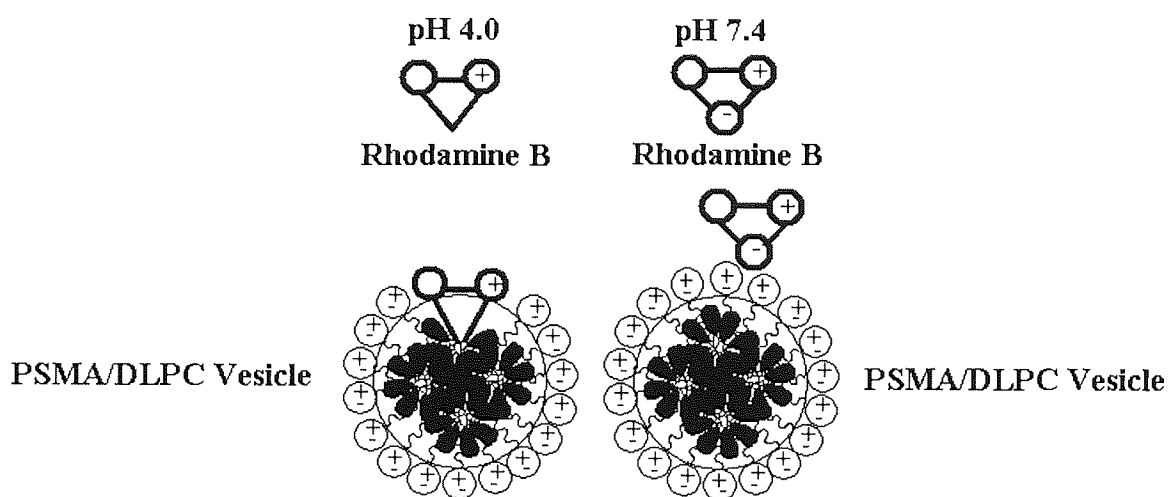


Fig.7.12 Binding of Rhodamine B to PSMA-DLPC vesicles.

(a) Dye Loading Study

As described in Section 7.3.2.4 and 7.3.2.5, the method to fabricate hydrogel containing active compounds (dye or drug on its own and in PSMA-DLPC vesicles) was to directly mix aqueous dispersions of such compounds with the polymerization mixture. It is possible that by using this method, the active compound may be involved in the polymerization reaction, undergo undesirable reactions or destabilize under polymerization conditions. For this reason, it is crucial to perform additional experiments in order to quantify the amount of active compounds that can actually be loaded within the hydrogel after polymerization. Table 7.5 presents actual dye loading (mg dye/g of hydrogel) and the percentage loading efficiencies of dye in hydrogels after polymerization.

Table 7.5 Comparison of percentage loading efficiencies of Rhodamine dye in PVA and poly(HEMA-co-MAA) hydrogels after polymerization.

Hydrogel	Initial loading (mg/g of gel)	Actual loading in hydrogel (mg/g of gel)	Loading efficiency (%)
PVA1	0.42	0.42	100.0
PVA2	0.12	0.11	91.7
pHEMA-MAA1	0.40	0.30	75.0
pHEMA-MAA2	0.13	0.08	61.5

PVA1 = Poly(vinyl alcohol) with Rhodamine dye incorporation

PVA2= Poly(vinyl alcohol) with Rhodamine-loaded PSMA-DLPC vesicle incorporation

pHEMA-MAA1 = Poly(HEMA-co-MAA) with Rhodamine dye incorporation

pHEMA-MAA2 = Poly(HEMA-co-MAA) with Rhodamine-loaded PSMA-DLPC vesicle incorporation

It is assumed that if Rhodamine dye becomes involved in the polymerization reaction or if dye fails to maintain its stability under polymerization conditions, then the actual dye loading in the obtained hydrogel would be less than the initial dye loading (or, in other words, loading efficiency is <100%). The data presented in Fig.7.13, shows that in PVA1 hydrogel, a high loading efficiency (100%) was achieved, confirming that Rhodamine dye can maintain its stability after photopolymerization of PVA macromer. In the case of PVA2 hydrogel, only 91.7% loading efficiency was reached (Table 7.5). It is possible that in this case, some of the dye molecules transformed from the fundamental state to the colourless leuco form (Fig.7.11-lactone form). This structural alteration can possibly be explained in terms of electron transfer process in the presence of electron-donor species. The resultant of this reaction would be dye deactivation and hence, less intense absorption. It is possible as well, that the dye may undergo undesirable reactions (e.g., H-abstraction) and then lose its functionality after polymerization. Also, the maximum absorbance wavelength of the dye can possibly be shifted from its original position. This shift, which may be caused by solubilization of the dye in hydrogel medium, possibly explains the loading efficiency of PVA2 not reaching 100%.

Only ~75% of the dye initially loaded was found to be successfully entrapped in pHEMA-MAA1 hydrogel, see Table 7.5. This suggests that the Rhodamine dye may not be sufficiently stable after thermal polymerization. It is feasible that dye becomes involved in free-radical polymerization reaction. Moreover, the dye may undergo competitive reactions, for example H-abstraction, electron transfer and aggregation, during thermal polymerization. Dye aggregation could affect the dye efficiency and photostability [83]. In general, the extent of aggregation depends on the temperature of the solution and is fully reversible. Dimerization is presumed to be the dominant form of aggregation in 10^{-6} to 10^{-3} M aqueous Rhodamine solutions. In restricted media (e.g. silica gel, protein, membrane, film and micelle) the kinetics and the extent of dye aggregation are affected by the embedding properties of host. Hydrogen bonding, hydrophobic forces and electrostatic interaction are all considered important for the dimerization [83]. In pHEMA-MAA2 hydrogel, the loading efficiency value was 61.5%, lesser than the value obtained in poly(HEMA-co-MAA) with dye incorporation. This reflects that the presence of PSMA-DLPC vesicles diminishes dye stability. The mechanism of vesicle induced-dye destruction is still a puzzle. Electron transfer process seems to be part of this mechanism.

(b) Release Study from PVA Hydrogels

The release profiles of Rhodamine dye from dye-loaded PVA (denoted as PVA1) and vesicle-loaded PVA (denoted as PVA2) hydrogels in phosphate buffered saline solution (pH 7.4) at room temperature are shown in Fig.7.13. Experimental results are expressed as percentages of fractional cumulative dye release versus time. A fractional cumulative release of dye (M_t/M_0) is defined as a ratio of cumulative amount of dye released in time t (M_t), to the total amount of dye incorporated into hydrogel (M_0). The actual dye loading concentrations in PVA1 and PVA2 hydrogels were 0.42 and 0.11 mg dye/g of hydrogel, respectively.

For PVA1 hydrogel, the initial release of dye (0-60 min) displays a sharp burst pattern. It accounts for most of the total dye release from the gel. This finding strongly suggests a weak interaction between Rhodamine B dye and the PVA matrix. The active agent, physically entrapped into the network, is usually released with a rate strictly related to the characteristics of the hydrogel. The complex

structural evolution of the network formed during polymerization of acrylate-modified PVA macromers (Acr-PVA) has been studied recently by Martens and Anseth [35]. They proposed that even though the Acr-PVA macromer provides advantages with respect to the rapid synthesis of crosslinked gels through photopolymerization without the addition of any small molecular weight crosslinker, the resulting network is more loosely crosslinked than networks formed with glutaraldehyde at comparable crosslinker concentrations. It is hypothesized that functionalized PVA macromer synthesized in this work may form a loose network that would in general be unable to retain the dye within its mesh. This condition may contribute to the PVA burst release as is observed in Fig.7.13.

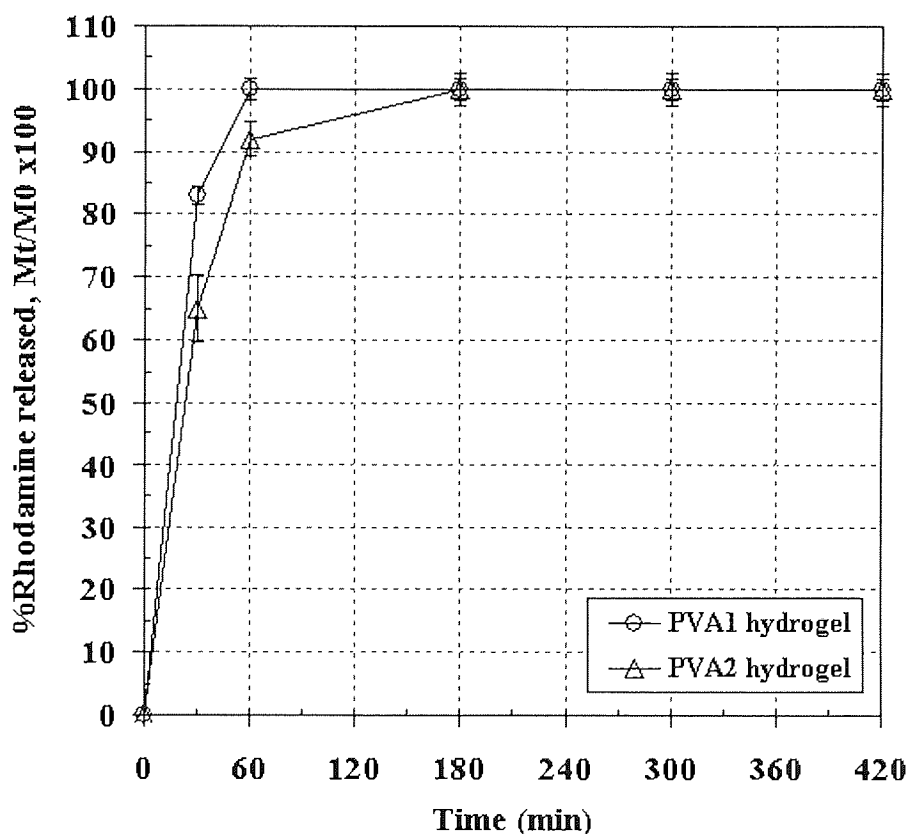


Fig.7.13 Rhodamine-release data from PVA hydrogels with dye (denoted as PVA1) and PSMA-DLPC vesicle (denoted as PVA2) incorporation. Actual dye loading in PVA1 and PVA2 hydrogels were 0.42 and 0.11 mg dye/g of hydrogel, respectively.

As seen in Fig.7.13, the initial burst release of dye is also observed for PVA2 hydrogel but lower than that of PVA1 hydrogel. Approximately 90% of the dye was released within 60 min, followed by a gradual release of another 10% after a further 120 min. The initial burst is perhaps due to the diffusion of the dye that was present in the PVA2 hydrogel but was outside the PSMA-DLPC vesicles, e.g., untrapped dye. It is possible that during the photopolymerization of PVA2, a fraction of dye came out of the vesicles either by diffusion or vesicles breaking up. This fraction of dye may diffuse out of the gel faster because the only resistance to the dye transport in this case is a simple diffusion through the hydrogel matrix. Dye molecules that were bound to the vesicle surface or entrapped within PSMA-DLPC vesicles may attribute to the gradual dye release between 60 and 180 min, as observed in Fig.7.13 in the PVA2 profile.

The overall results show that the PSMA-DLPC vesicles incorporated within the PVA hydrogel matrix only extend the initial burst release from the hydrogel by two hours. This situation may be described in terms of the PVA network being too large. If the network mesh size is too large, then it is possible that the gel network may fail to retain the very small dye-loaded vesicles. These vesicles as well as the free dye will thus rapidly diffuse out of the hydrogel during initial burst release. As a consequence of this, the obtained release profile of dye delivered from PVA hydrogel with vesicle encapsulation (PVA2) should look similar to the profile obtained from the dye-loaded PVA hydrogel (PVA1). However, more experiments need to be performed to conclusively determine the validity of this assumption.

(c) Release Study from Poly(HEMA-co-MAA) Hydrogels

The release experiments were also performed in phosphate buffered saline solution (pH 7.4) with Rhodamine B dye. The percentage of fractional cumulative dye release as a function of time for dye-loaded poly(HEMA-co-MAA) (denoted as pHEMA-MAA1) and vesicle-loaded poly(HEMA-co-MAA) (denoted as pHEMA-MAA2) hydrogels, are shown in Fig.7.14. The actual dye loading concentrations in pHEMA-MAA1 and pHEMA-MAA2 hydrogels were 0.30 and 0.08 mg dye/g of hydrogel, respectively.

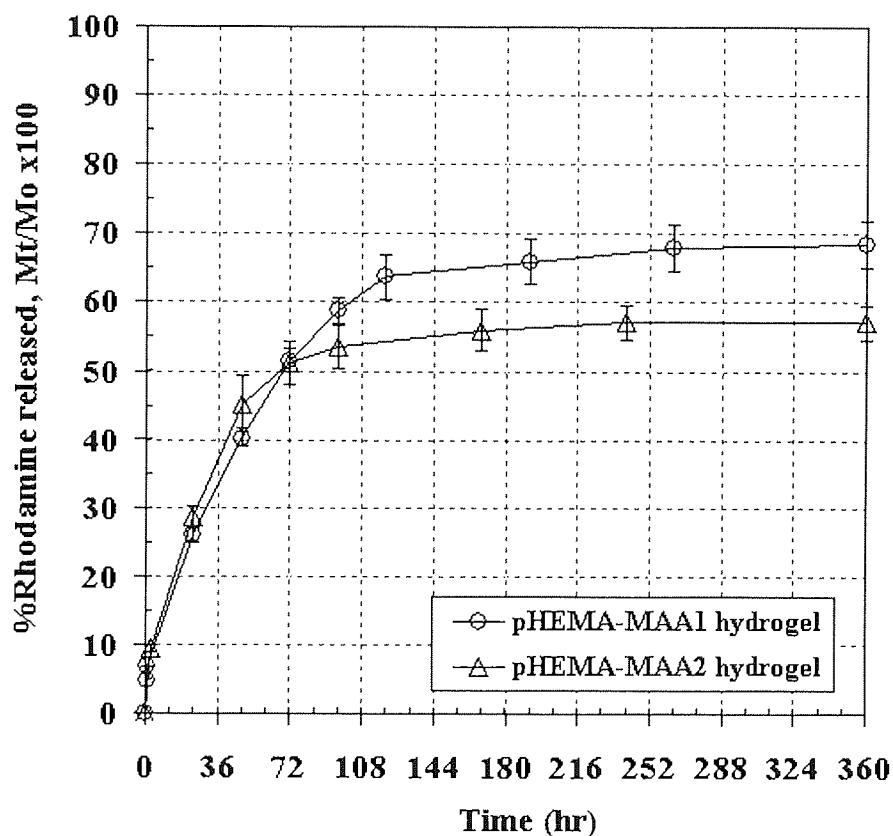


Fig.7.14 Rhodamine-release data from poly(HEMA-co-MAA) hydrogels with dye (denoted as pHEMA-MAA1) and PSMA-DLPC vesicle (denoted as pHEMA-MAA2) incorporation. Actual dye loading in pHEMA-MAA1 and pHEMA-MAA2 hydrogels were 0.30 and 0.08 mg dye/g of hydrogel.

The release profile of dye from pHEMA-MAA1 hydrogel, as illustrated in Fig.7.14, shows slow release with no significant lag time. This hydrogel releases approximately 67% of total dye loaded at the end of 10 days. The finding demonstrates that poly(HEMA-*co*-MAA) hydrogel by itself can provide a sustained release for Rhodamine B over 10 days. The delayed release may be associated with dye-hydrogel interaction. It is known that the hindrance caused by interactions between solute and the hydrogel network is an important factor in solute transport in and release from ionic hydrogels. Under physiological conditions, Rhodamine B existing in zwitterionic form, illustrated in Fig.7.12, is assumed to interact with anionic hydrogels through hydrogen bonding as well as electrostatic interactions. The strong interaction between the hydrogel network and dye molecules would result in a slow dye release, as is observed in the pHEMA-MAA1 profile in Fig.7.14. Interesting results are obtained by comparing dye release profiles from pHEMA-MAA1 (Fig.7.14) and PVA1 (Fig.7.13) hydrogels. The release rate of dye from the PVA hydrogel was much faster than that from pHEMA-MAA hydrogel, indicating that the hydrogel matrix of the latter can interact with dye more strongly than with the former one.

As seen in Fig.7.14, the pHEMA-MAA2 and pHEMA-MAA1 hydrogels exhibit similar *in vitro* release profiles. Both of them show a slow burst release followed by a sustained dye release over 10 days. The burst release was attributed to the dye located at the surface of PSMA-DLPC vesicles and possibly, the unencapsulated dye. It is possible that during thermal polymerization of hydrogel, a fraction of dye came out of the vesicles either by diffusion or vesicles aggregation. This may also cause the burst effect in the hydrogels.

Even though release profile of pHEMA-MAA1 looks similar to that of pHEMA-MAA2, however, the amounts of the cumulative release after 3 days were different. For instance, at the end of 10 days, the % cumulative dye releases were 67 and 57 for pHEMA-MAA1 and pHEMA-MAA2 hydrogels, respectively. The prolonged release from pHEMA-MAA2 hydrogel is perhaps due to the fact that dye incorporated within PSMA-DLPC vesicles encounters the extra resistance. The entrapped dye, which accounts for ~10% difference in cumulative dye release after 10 days between pHEMA-MAA1 and pHEMA-MAA2 profiles, as shown in Fig.7.14, would thus diffuse out of the gel on a longer time scale.

The question of whether the dye is released out from the pHEMA-MAA2 hydrogel as individual dye molecules or in complex with PSMA-DLPC vesicles needs more attention. This study postulates that both cases are likely to occur. In the case of dye alone, the diffusion rates of dye from vesicle to gel matrix and then to the release medium as well as the hydrogel mesh size, all dominate the release of the dye from the hydrogel. However, in the case of dye within vesicles, the release rate of dye should also depend on vesicle-hydrogel interaction and the vesicle surface/volume ratio. Smaller vesicles have higher surface/volume ratio, from which it follows that it will be easier for the encapsulated drug to release (via diffusion) from them [84]. It stands to reason that by adjusting the vesicle size, a controlled dye release from hydrogel may be accomplished. This postulation was previously proved by Ruel-Gariépy et al., who proposed the use of chitosan-based hydrogel containing liposomes in sustained delivery of hydrophilic molecules. Their release studies showed that an increase in liposome size from 100 to 280 nm drastically decreased the release kinetics as well as the initial burst release of carboxyfluorescein (CF) from hydrogel [85].

One should remember that although an increase vesicle size can possibly extend release of dye from pHEMA-MAA2 hydrogel, vesicles that are larger than the mesh size of the hydrogel will get permanently entrapped within the hydrogel. In this case, the dye would diffuse out of pHEMA-MAA2 hydrogel by diffusing from vesicle to gel matrix and then from gel matrix to release medium. A way to trigger the release of this portion of dye from vesicles is of interest. One such approach, postulated here for the first time, is to destabilize the vesicles by introducing destabilizing agent, for example lysozyme. Lysozyme, which is the most abundant protein in human tears, is believed to be one of many good candidates for this sort of reaction. The mechanism of which lysozyme destabilize PSMA-DLPC vesicles may be described in terms of the competitive complexation between PSMA-DLPC and PSMA-lysozyme. At physiological pH, it is likely that the positively charged lysozyme can associate with uncoiled PSMA through electrostatic attraction between the negative charges on the carboxyl groups of the polymer and the positive charges on lysozyme molecules. This association is hypothesized to destabilize the PSMA-DLPC vesicles and so enhance the leakage of active compound from the vesicles.

One may wonder if the negatively charged lysozyme can diffuse into the poly(HEMA-*co*-MAA) matrix under the physiological conditions. Theoretically, penetration of lysozyme into poly(HEMA-*co*-MAA) hydrogels containing 3% MAA is possible, because the molecular dimensions of lysozyme (30x30x45 Å) are less than the effective pore size of hydrogel (31.6 Å) [86]. Literature reviews revealed that lysozyme can actually penetrate into HEMA/MAA copolymer hydrogels within an hour [86, 87]. The rapid uptake of lysozyme protein by poly(HEMA-*co*-MAA) hydrogel is probably due to the favorable electrostatic interactions between the protein (net charge on the order of +7 at physiological pH) and the polymer gel. The study by Garrett et al. [87] revealed that the degree of penetration of lysozyme into the hydrogels increases with the increased MAA content in the poly(HEMA-*co*-MAA) hydrogels. Their finding suggested the role of charge, presenting in both hydrogels and protein, in controlling protein penetration as well as in increasing the porosity of the hydrogels.

7.4.3.2 Drug Loading and Release Studies

In this study, Pirenzepine was used to determine whether the use of PSMA-DLPC vesicles can prolong the release of hydrophilic drug from hydrogels.

Pirenzepine drug is a relatively selective anti-muscarinic agent which has attracted clinical interest for the control and management of myopia progression. Pirenzepine was proved to be able to reduce the axial elongation and myopia in visually impaired chick eye and currently, Pirenzepine ophthalmic gel is being under investigation for the treatment of myopia [88]. Pirenzepine is a large hydrophobic basic drug which has inherently low water solubility and is therefore used for conventional pharmaceutical formulations in the form of its water soluble hydrochloride salt. The active molecule has feature associated with its size, solubility profile and pH sensitivity which it shares with some of the candidate drugs for treatment of allergic eye disease. A chemical structure, ultraviolet spectrum and the quantification of Pirenzepine are shown in Fig.7.15 and Table 7.6.

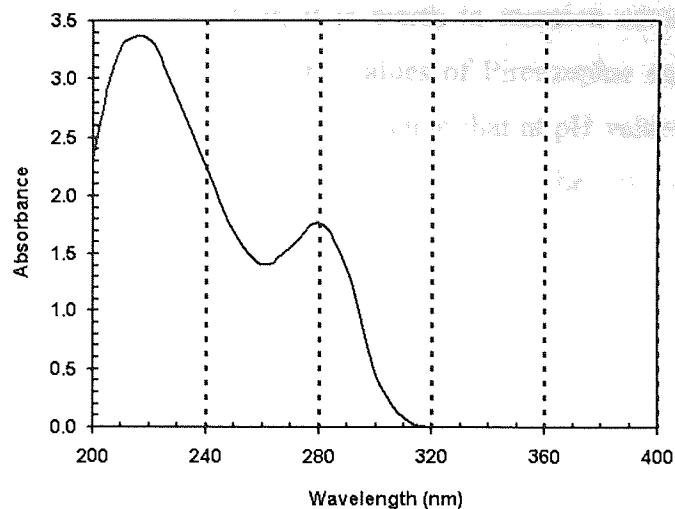
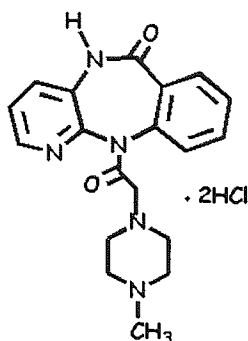


Fig.7.15 Chemical structure of Pirenzepine dihydrochloride drug (left) and ultraviolet spectrum of the drug in acidic solution (right).

Table 7.6 Some quantification of Pirenzepine drug [89].

Quantification	
High performance liquid chromatography	In plasma: limit of detection 2.5 $\mu\text{g/L}$
Radioimmunoassay	In plasma/urine: limit of detection 0.25 $\mu\text{g/L}$ in plasma and 4 $\mu\text{g/L}$ in urine
Therapeutic concentration	Following a single oral dose of 50 mg to 87 subjects, a mean peak plasma concentration of 0.05 mg/L was attained in 2 hours
Bioavailability	About 20-30%
Half-life	Plasma half-life about 11 hours
Clearance	Plasma clearance about 3.5 mL/min/kg
Protein-binding	In plasma about 10%
Dose	100-150 mg of drug daily

Before continuing the discussion further, it is worth to mention some important characteristics of the Pirenzepine drug. The pK_a values of Pirenzepine are about 2.1 and 8.1 [89]. Based on these pK_a values, one may assume that at pH values ranging from 2.1 to 8.1, Pirenzepine should exist in its ionized form and so, be able to dissolve in aqueous solution. However, at pH well above 8.1, the amino groups in the Pirenzepine's piperazine ring are deprotonated, and therefore the Pirenzepine molecule should be completely in its nonionized form. The solubility of the drug at such pH is thus expected to be very low. The pH at which drug encapsulation occurs (pH 4) and the pH at which the release experiments were performed (pH 7.4) both lie between the pK_a values. Therefore, at these pH values, it is less likely that Pirenzepine (existing in ionized form) will be adsorbed at surface of the PSMA-DLPC vesicles through electrostatic forces.

(a) Drug Loading Study

With regards to the methodology of fabrication of hydrogels containing active compounds (Pirenzepine on its own and in PSMA-DLPC vesicles), it is possible that the active compounds may be involved in the polymerization reaction, undergo undesirable reactions or destabilize under polymerization conditions. For this reason, it is important to perform additional experiment to quantify the amount of drug that can actually be incorporated within hydrogel after polymerization. Table 7.7 presents actual loading (mg drug/g hydrogel) and the percentage loading efficiency of drug in hydrogels after polymerization.

Table 7.7 Comparison of percentage loading efficiencies of Pirenzepine drug in PVA and poly(HEMA-*co*-MAA) hydrogels after polymerization.

Hydrogel	Initial loading (mg/g of gel)	Actual loading in hydrogel (mg/g of gel)	Loading efficiency (%)
PVA3	0.98	0.98	100.0
PVA4	0.76	0.70	92.1
pHEMA-MAA3	6.90	5.98	86.7
pHEMA-MAA4	1.54	2.07	100.0

PVA3= Poly(vinyl alcohol) with drug incorporation

PVA4= Poly(vinyl alcohol) with drug-loaded PSMA-DLPC vesicle incorporation

pHEMA-MAA3= Poly(HEMA-*co*-MAA) with drug incorporation

pHEMA-MAA4= Poly(HEMA-*co*-MAA) with drug-loaded PSMA-DLPC vesicle incorporation

It is assumed that if Pirenzepine becomes involved in the polymerization reaction or if the drug fails to maintain its stability under reaction conditions, then the actual drug loading in the obtained hydrogel would be less than the initial drug loading (or, in other words, loading efficiency is <100%). The data presented in Table 7.7 shows that in PVA3 hydrogel, a high loading efficiency (100%) was achieved, confirming that Pirenzepine drug can maintain its functionality after photopolymerization of PVA macromer. In the case of PVA4 hydrogel, only 92.1% loading efficiency was reached (Table 7.7). It is possible that in this case, some of the drug molecules undergo undesirable reactions (e.g., H-abstraction) or become involved in the polymerization reaction. These would destabilize and cause the drug to lose its functionality after polymerization.

Only 86.7% of the drug initially loaded was successfully incorporated in pHEMA-MAA3 hydrogel, see Table 7.7. This, once again, demonstrates that the drug may not be sufficiently stable after thermal polymerization at 60°C. In pHEMA-MAA4 hydrogel, the loading efficiency value was 100%, as high as that obtained in the case of poly(HEMA-*co*-MAA) with drug incorporation. This reflects that the presence of PSMA-DLPC vesicles may increase the stability of Pirenzepine during polymerization. The mechanism of vesicle-enhanced drug stabilization is still a mystery. More experiments will need to be performed in order to shed light on this issue.

(b) Release Study from PVA Hydrogels

The release experiments were performed in phosphate buffered saline solution (pH 7.4) with Pirenzepine drug. The percentage of fractional cumulative drug release as a function of time for drug-loaded PVA (denoted as PVA3) and vesicle loaded-PVA (denoted as PVA4) hydrogels, are shown in Fig.7.16. The actual drug loading concentrations in PVA3 and PVA4 hydrogels were 0.98 and 0.70 mg drug/g of hydrogel, respectively.

PVA3 and PVA4 show identical drug release profiles. The initial drug release of Pirenzepine from both PVA hydrogels (0-30 min) displays a sharp burst pattern. It accounts for the entire drug incorporated within hydrogel (or, in other words reaching 100% cumulative release). This finding suggests a weak interaction between the drug and the PVA matrix. It seems that at pH 7.4, there is a low affinity between Pirenzepine and the hydrogel.

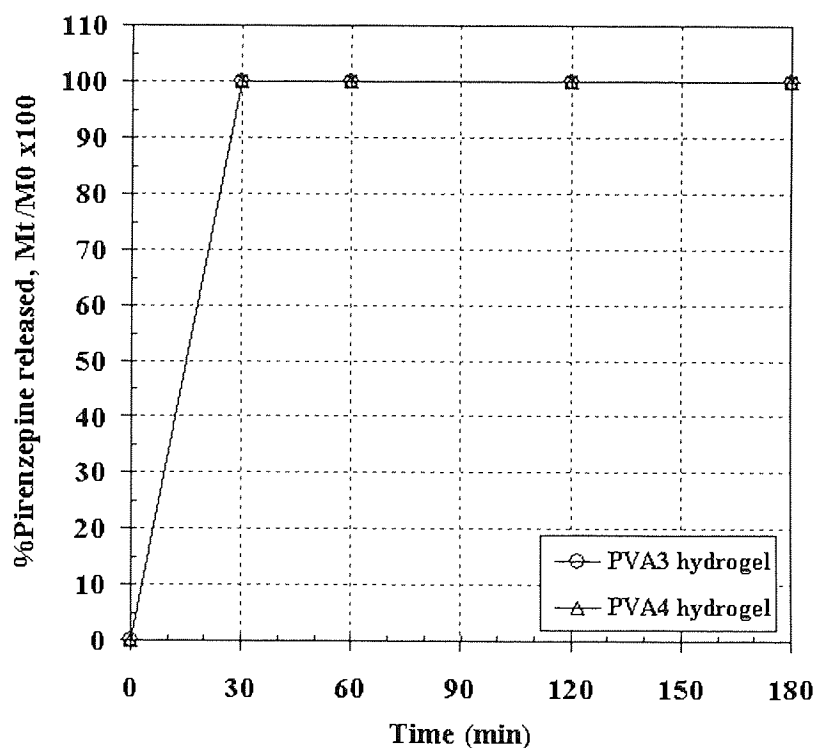


Fig.7.16 Pirenzepine-release data from PVA hydrogels with drug (denoted as PVA3) and PSMA-DLPC vesicle (denoted as PVA4) incorporation. Actual drug loading in PVA3 and PVA4 hydrogels were 0.98 and 0.70 mg drug/g hydrogel, respectively.

A possible explanation for the rapid release of Pirenzepine from vesicle containing-hydrogel (PVA4 hydrogel) can be given if, at physiological pH, Pirenzepine preferentially binds to vesicles at their outer surface and not within the inner core. The interaction between vesicle and drug would then not offer much resistance to the diffusion of the drug, and therefore the resulting release profile should resemble one obtained without vesicle encapsulation, thus explaining the similarity in the drug release profiles between PVA3 and PVA4 hydrogels. Destabilization of vesicles during photopolymerization of PVA macromer may also be a cause for the rapid release of Pirenzepine from PVA4 hydrogel.

By comparing release profiles of dye and drug incorporated within PVA hydrogel, as shown in Fig.7.13-PVA1 profile and the PVA3 profile in Fig.7.16, it is found that PVA hydrogel can maintain Rhodamine within its matrix longer than Pirenzepine. This is not surprising since Pirenzepine is more hydrophilic than Rhodamine B, and so it is less likely to remain in the hydrogel.

It seems likely that the use of PSMA-DLPC vesicles to delay the release from hydrogels will be more effective for more hydrophobic compounds. This is logical, because these compounds are more probable to incorporate within the vesicles. Such compounds, when incorporated within the vesicles, will experience the extra resistance presented by the inner core of PSMA-DLPC complexes and the compounds will thus diffuse out of the gel on a longer time scale.

(c) Release Study from poly(HEMA-co-MAA) Hydrogels

Release experiments were also performed in phosphate buffered saline solution (pH 7.4) with Pirenzepine drug. The percentage of fractional cumulative drug release as a function of time for drug-loaded poly(HEMA-co-MAA) (denoted as pHEMA-MAA3) and vesicle-loaded poly(HEMA-co-MAA) (denoted as pHEMA-MAA4) hydrogels, are shown in Fig.7.17. The actual drug loading concentrations in pHEMA-MAA3 and pHEMA-MAA4 hydrogels were 5.98 and 2.07 mg drug/g of hydrogel, respectively.

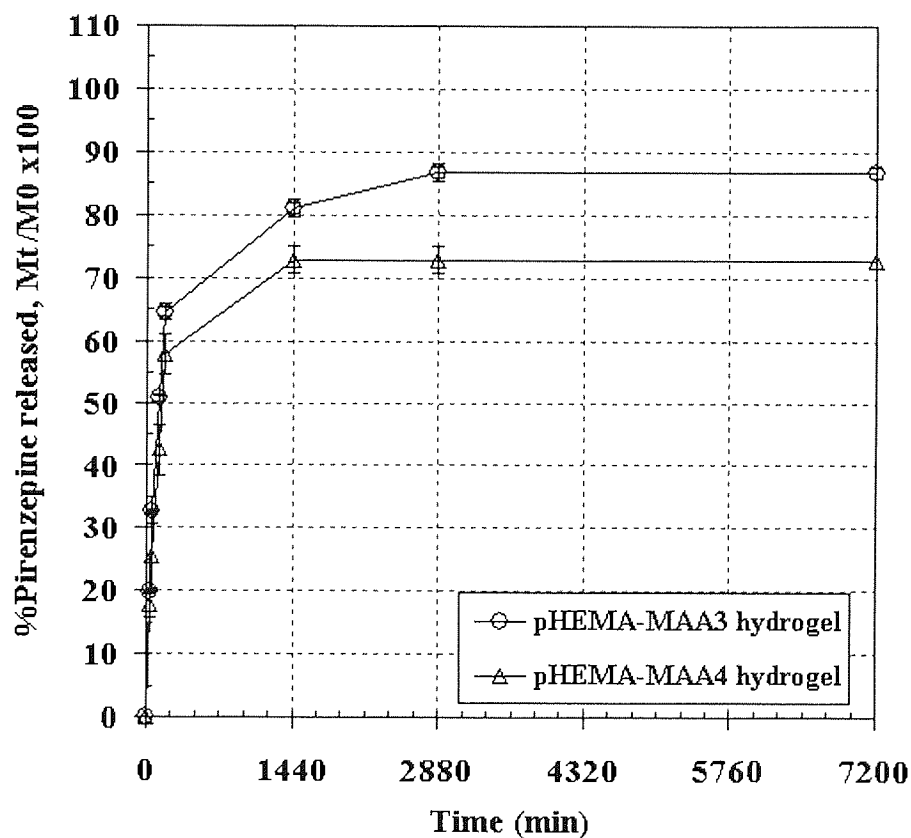


Fig.7.17 Pirenzepine-release data from poly(HEMA-co-MAA) hydrogels with drug (denoted as pHEMA-MAA3) and PSMA-DLPC vesicle (denoted as pHEMA-MAA4) incorporation. Actual drug loading in pHEMA-MAA3 and pHEMA-MAA4 hydrogels were 5.98 and 2.07 mg drug/g hydrogel, respectively.

As observed in Fig.7.17, both pHEMA-MAA3 and pHEMA-MAA4 hydrogels exhibit a burst release (between 0-180 min) followed by a slower release phase. For pHEMA-MAA3 hydrogel, the burst release of Pirenzepine accounted for around 65% of the total amount of drug present in the hydrogel. This fraction of drug was believed to locate at the surface of the hydrogel and subsequently release out of the hydrogel through simple diffusion. The slow release of the drug from pHEMA-MAA3 hydrogel occurred between 3 and 48 hours and accounted for another 20%. The delayed release may be associated with the drug-hydrogel interaction. Under physiological conditions, Pirenzepine existing in ionized form is assumed to interact with anionic charges of the hydrogel through hydrogen bonding as well as electrostatic attraction. The strong interaction between the hydrogel network and drug molecules should result in a slow dye release, as is observed in the pHEMA-MAA3 profile in Fig.7.17.

As seen in the pHEMA-MAA3 profile, shown in Fig.7.17, there was no significant further release of the drug from the hydrogel after 48 hours. The release study of Pirenzepine from pHEMA-MAA3 hydrogel showed that ~15% of entrapped drug still remained after 2 days. This fraction of the drug may experience extremely slow diffusion through the gel and so, release out over a very long period of time. It is also possible that this last fraction of Pirenzepine may become irreversibly trapped within the pHEMA-MAA3 hydrogel.

Interesting results were obtained by comparing drug release profiles from PVA3 (Fig.7.16) and pHEMA-MAA3 (Fig.7.17). The release rate of the drug from PVA hydrogel was found to be significantly faster than that from pHEMA-MAA hydrogel, indicating that the drug can interact with the hydrogel network of the latter more strongly than with the former one.

During the first 24 hours, the release rates of Pirenzepine from pHEMA-MAA3 and pHEMA-MAA4 hydrogels were similar (~20% per hour for the first 3 hours and ~0.7% per hour between hours 3 and 24). However, after 24 hours, the release rates for the two hydrogels were different. For pHEMA-MAA4 hydrogel, there was no further drug release after 1 day but for pHEMA-MAA3 (without vesicle encapsulation) the drug was progressively released at a rate of 0.2% per hour until the end of the second day. The slow release from pHEMA-MAA3 hydrogel occurred between 24 and

48 hours and accounted for another ~7%, which was attributed to the entrapped drug located within the bulk of hydrogel matrix.

As observed in the pHEMA-MAA4 profile (Fig.7.17), around 70% of Pirenzepine present in the hydrogel was released out to the release medium after 24 hours. The remaining drug was assumed to be bound either with the polymer network, or with the vesicles. Based on the fraction of unreleased drug (15%) remaining in the pHEMA-MAA3 hydrogel, the experimental results demonstrate that vesicle encapsulation can increase the drug retention of poly(HEMA-co-MAA) hydrogel by 15% of the total drug loading concentration.

The process of Pirenzepine diffusing out of the hydrogels was assumed to be complex due to the possibility of the drug adsorbing to the polymer matrix. This process was believed to be even more complicated in the presence of PSMA-DLPC vesicles. Following a publication by Gulsen et al. [90], two possible reasons for this complication are as follows. Firstly, the drug present inside carriers encounters the extra resistance offered by the inner core of vesicles. Secondly, on the addition of monomer to vesicles, some of the vesicular components may dissolve in the polymerization mixture and these components are expected to adsorb on the surface of the hydrogel matrix. If this situation occurs, the drug has to compete with the dissolved components for adsorption to the hydrogel matrix.

Gulsen et al. [90] developed a model of multi-component adsorption to the gel matrix for drug release from microemulsion-laden HEMA gels. This complex model can be considerably simplified by assuming that the surface of the HEMA matrix is saturated with the vesicular compartment (e.g. surfactant) and thus, the adsorption of the drug to the gel matrix can be neglected. If the adsorption of the drug is neglected, its transport through the gel can be modelled by the diffusion equation. The model proposed by Gulsen et al. also assumes that the time scales for release of the drug from the particles is much slower than the time scale for diffusion through the gel, and thus the drug released by the particles can be neglected while determining the flux of the drug trapped directly in the hydrogel.

Based on a model developed by Gulsen et al., the release of Pirenzepine from vesicle-laden hydrogels may be modeled in terms of exponential functions, through the following equation [90, 91];

$$C_1(1-e^{-t/\tau_1})+C_2(1-e^{-t/\tau_2})$$

where C_1 , C_2 , τ_1 and τ_2 are empirically determined constants.

The equation above implies the presence of two different time scales for drug release. The first term of the above equation explains the drug release at short time occurring at the beginning of experiments. At this stage, the diffusion resistance in the hydrogel controls the release rate of the drug located in the hydrogel, but outside the vesicles. The second term of the above equation describes the slower release rate of the fraction of drug encapsulated within vesicles. The equation also implies that the release of the drug may depend on many parameters including thickness of hydrogel, diffusion coefficient of the drug in hydrogel, number of vesicles in hydrogel, radius and the area/volume ratio of vesicles. More details concerning the above equation can be found in the works of Gulsen and co-workers [71, 80, 90, 91].

7.5 CONCLUSIONS

A method for the formation of polymer-lipid vesicles was described. It has been shown that these lipid-based structures can be loaded with hydrophobic compounds (e.g. Oil red O), which makes them a potentially valuable vehicle for drug delivery. A range of compounds (Oil red O, Rhodamine B and Pirenzepine dihydrochloride) differing in structure and hydrophobicity were used in order to characterize the factors that affect incorporation and release. The methodology allowed each of these compounds to be incorporated into the polymer-lipid vesicles prior to polymerization with hydrogel-forming monomers (e.g. HEMA, MAA and PVA macromer). The encapsulation of these loaded polymer-lipid vesicles within hydrogels gave optically clear hydrophilic polymer matrices.

Optical micrographs revealed that the loaded vesicles were successfully trapped in both PVA and poly(HEMA-*co*-MAA) hydrogels. However, in the case of poly(HEMA-*co*-MAA) hydrogel, the vesicles may associate to form supramolecular structures during thermal polymerization. The release characteristics of the hydrogels were found to be influenced by many factors, such as hydrophobicity of the incorporated compounds and morphology of the hydrogel networks. It is postulated here that vesicle size may affect the release characteristics of such compounds from the hydrogels. In all of the cases studied, it has been found that the hydrogel incorporated with the loaded vesicles can retain active compounds and deliver them at slow rate for a long period of time. By the use of other trigger mechanisms available in the eye, it appears that effective drug-releasing hydrogel contact lenses may be fabricated using this methodology.

CHAPTER 8
SUMMARY AND DISCUSSION:
SUGGESTIONS FOR FURTHER WORK

8.1 SUMMARY AND DISCUSSION

8.1.1 The Study of Polymer-Lipid Interaction

Hypercoiling polymers can be said to mimic the behaviour of some of the functions that account for the essential living processes, and therefore, be suited for application to living systems and in particular to biomedicine.

In aqueous media, at least over a particular pH range, the associating polymers such as poly(styrene-*alt*-maleic anhydride) (PSMA) will generally adopt a helical coil configuration with the hydrophobic side chain groups presented along one facet and the anionic hydrophilic groups presented along the opposite facet. This smart behaviour can mimic that of native apoproteins that arrange their hydrophobic and hydrophilic group at opposite facets of α -helical coil to form an amphipathic structure. When these hypercoiling polymers are combined with film-forming lipid such as dilauroylphosphatidylcholine (DLPC), they associate to produce lipid-polymer nanostructures analogous to lipoprotein assemblies such as HDL (high density lipoprotein) present in the blood plasma and responsible for transporting the fatty materials around the body. As such, they represent a new biomimetic delivery vehicle for fatty or water insoluble substances for both pharmaceutical and cosmetic industries.

One goal of this study was to develop a better understanding of polymer-lipid association, especially in the system of PSMA and DLPC. The details concerning this interaction may lead to the development of a more efficient drug delivery system for poorly water soluble drugs. Such details were previously described in Chapters 3-6. The ternary phase diagrams of the water-DLPC-PSMA system were constructed as a mean to represent the formation of polymer-lipid complexes and to examine the effects of various factors such as pH, temperature and counterions, on the association of lipid and this pseudo protein. Results showed that the DLPC-PSMA association was dependent on the molecular ratios between polymer and phospholipid, temperature, pH, and charge shielding effect obtained from the added salt and the presence of counterions. Moreover, the polymer architecture and the polymer molecular weight have also been found to play an important role for the formation of these complexes.

Other physical and spectroscopic techniques such as the Langmuir-Blodgett Trough, surface tension measurements and the ^{31}P -NMR were also used in this study to explore the association behaviour of PSMA both at the air-water interface and in solution, as well as its interaction with phospholipid membranes.

The Langmuir Trough technique was successfully proven to be useful to study the pH-dependent monolayer formation of PSMA. The ability of PSMA to form an insoluble monolayer at the interface was found to be related to the interaction between the polymer and the subphase. The water-polymer interaction was believed to be more pronounced when the PSMA molecules are mostly ionized. This ionization of PSMA leads the polymer molecules to dissolve into water subphase and not to maintain at the air-water interface. However, when the polymer-water interaction is less favorable, for example when the PSMA molecules are unionized (achieved by using phthalate buffer of pH 4 as a subphase), the polymer molecules may repel from the bulk of subphase, thus forming an insoluble monolayer at the interface. Results also suggest that the conformational configuration of PSMA at the interface, which results from inter- and intra molecular interactions, depends on various parameters including pH subphase, polymer molecular weight and polymer architecture.

Valuable details concerning the PSMA-induced membrane disruption were also obtained using Langmuir Trough technique. The ability of the PSMA to interact with the DLPC monolayer is found to be increased with decreasing the pH. Furthermore, the structural reorganization of the mixed monolayer is also found to be sensitive to the polymer molecular weight. The π -Area isotherms of DLPC monolayers in the presence of high molecular weight PSMA types (MW 120,000 and 350,000) show the LE-LC phase transition. This transition was proposed to be correlated to a phase transform of the PSMA monolayer from a horizontal to a more oriented vertical arrangement at the interface. The mixed monolayer, consisting of PSMA (MW 1,600), however, does not show a clear LE-LC phase transition. This implies that the lower molecular weight PSMA type is preferential oriented with lipid monolayer in a horizontal position over the whole range of compression. Interestingly, results also revealed that the penetration of polymer to the phospholipid monolayer is strongly related to the hydrophobic association and thus, more pronounced in high molecular weight PSMA types (MW 120,000 and 350,000).

The surface tension measurements were also used in this study to investigate, for the first time, the association and adsorption behaviour at the air-water interface of PSMA as well as its interaction with DLPC. Some aspects of the fundamental behaviour of the PSMA-DLPC complexes, such as surface adsorption and bulk behaviour were revealed from this study. It was found that all three PSMA types (MW 1,600, 120,000 and 350,000) show surface activity in aqueous pH 12, 6 and 4 solutions. The surface activity for all PSMA types increased with decreasing pH. At pH 4, the PSMA (MW 1,600) shows the strongest surface activity. It was postulated here that PSMA molecules preferentially aggregate in solution up to a certain concentration before adsorbing onto the surface. This behaviour differs from that of simple surfactants whose molecules first saturate the interface before forming micelles in solution. Equilibrium was believed to control the partition of PSMA molecules between the bulk solution and air-water interface.

The results from surface tension measurements also give additional information concerning the association of PSMA and DLPC. Apart from the number of hydrophobic moieties in the polymer backbone, the polymer chain architecture, chain flexibility and the polymer charge density are found to be all important factors influencing the hydrophobically PSMA-DLPC association.

It was shown that ^{31}P -NMR can be very useful in elucidating the different phases of phospholipid (DLPC) in the presence of PSMA copolymer under different conditions. More specifically, it was found that the strong interactions between the polymer and DLPC result in the disappearance of the bilayer structure and the formation of the isotropic phases which give rise to the isotropic peaks in the ^{31}P -NMR spectra.

Changes in lipid molecular shapes, which are considered as the driving force for the bilayer-nonbilayer phase transition of DLPC, were assumed to be correlated with the changes in the packing parameters. This alteration should lead to a bilayer structural change as well as a lipid phase transition. The interpretation of NMR spectra leads to a clear comprehension of important molecular phenomena. The PSMA alters the phospholipid assembly in response to changes in pH, preferentially under acidic conditions. The pH-dependent membrane disruptive activity was believed to be

associated with the conformational transition of the polymer from an extended conformation to a relatively hydrophobic globular coil. The collapsed polymer chain may provide an increased number of hydrophobic sites for enhanced polymer adsorption to the phospholipid.

8.1.2 The Polymer-Lipid End-State Complexes: A Stoichiometric Model

Experimental results, including ternary phase behaviour analysis and ^{31}P -NMR, suggest that homogeneity of the mixed PSMA-DLPC complexes depends, inter alia, on the three important factors;

1. Actual concentrations of PSMA and DLPC
2. Kinetic pathway during lipid transformation
3. Hydrophobicity and molecular weight of PSMA

Before further discussion, some terms need to be defined. The terms 'phospholipid assemblies', 'lipid assemblies' and 'DLPC assemblies' refer to the ordinary lipid structures obtained by suspending lipid in pure water. Furthermore, the terms 'polymer-lipid complexes', 'PSMA-DLPC complexes' and 'complexes' refer to any structures that will be obtained as a result of PSMA associating with lipid assemblies.

By analogy to natural systems, e.g. the bile salt-lipid system, the interaction of PSMA with DLPC assemblies is assumed to start with the adsorption of polymer onto the lipid assemblies followed by the formation of a number of polymer-lipid complexes, varying in size and configuration. The end-state complexes possibly possess a spherical mixed micellar structure with sizes ranging up to 400 nm.

Properties of the end-state complexes, such as size, configuration and lipid composition, are believed to depend on the concentrations of both DLPC and PSMA. These parameters govern the transitions that the complexes undergo before reaching a metastable state. The dependency of the transition steps on polymer concentration is explained as follows.

At very low polymer concentrations, the added PSMA possibly adsorbs onto the lipid assemblies, leading to an increase in size of the complexes. Under these conditions, the end-state complexes are expected to have a structure similar to that of the original lipid assemblies and possess a relatively narrow size distribution.

At higher polymer concentrations, the added polymer probably induces the formation of different types of polymer-lipid complexes (e.g. discs, cylindrical micelles and spherical micelles). These complexes, varying in size and shape, may start to form within the saturated lipid assemblies and then liberate out from the assemblies. The development of bridges between two mixed polymer-lipid complexes through hydrophobic association of PSMA can possibly occur under these conditions. This phenomenon will be even more pronounced if the type of polymer used has a very high hydrophobic content. In this case, the polymer-induced lipid solubilization will eventually end up in variety of complexes with wide vesicle size distributions.

A complete disintegration of lipid assemblies into very small polymer-lipid complexes can only be observed when the polymer concentration used is in large excess when compared to the lipid. The end of the process is the complete solubilization of lipid assemblies without the formation of further intermediates. In this case, the end-state mixed complexes, having a very narrow size distribution, might possibly be so small that their light scattering can not be observed.

With consideration to the results obtained from phase diagrams (for PSMA with MW 1,600) and the mechanisms mentioned above, it is assumed that a mass ratio of at least 2:1 (PSMA:DLPC) is required to complete the transformation of the DLPC assemblies into small mixed polymer-lipid complexes. Most of the end-state complexes obtained with mass ratios above 2:1 (PSMA:DLPC) are believed to be small spherical mixed micelles with a very narrow size distribution. Since the resultant

mixture was optically clear, it is logical to further assume that the end-state complexes form nanoscale-sized features. A single sharp isotropic peak ($\delta=0$ ppm), obtained when the pH of the PSMA-DLPC mixture was lowered to 4, also supports the presence of a monodisperse configuration of the end-state complexes (spherical mixed micelles).

Another important parameter concerning the homogeneity of end-state complexes is the hydrophobicity of the polymer used. It is likely that the increased hydrophobicity of PSMA, obtained by increases in the alternating sequence and the degrees of hydrophobic substitution, enhances its ability to disrupt the lipid assemblies and so, induce lipid transformation. However, from another point of view, such an increase might possibly broaden the end-state size distribution, which could be explained in terms of stronger intermolecular attraction (e.g. hydrophobic association) between the polymer chains. More complex polymer-lipid configurations, differing in shape and size, are likely to appear in this case. This complexity may partly be associated with the development of a hydrophobic bridge between the unincorporated parts of the polymer chains located at the outer surface of mixed complexes. The bridge thus links up the mixed complexes, resulting in a further transition into larger supramolecular structures.

The configuration of PSMA-DLPC complexes, perhaps, ranges from lipid bilayer vesicles, cylindrical micelles, spherical micelles, disk-like micelles and lamellae-based aggregates. Similar system reported that the cylindrical and disk-like mixed micelles appeared as kinetic intermediates. Moreover, the lamellar based structures were suggested to form as a consequence of the two parallel disk-like mixed micelles being stacked upon to each other [92]. The end-state complexes may represent either a true equilibrium state or non-equilibrium metastable state, whose structure is generally path dependent and possibly have a very long life time.

Based on phase behaviour analysis, it was found that the use of high molecular weight PSMA (MW 120,000) to induce transformation of DLPC assemblies into mixed complexes required a lesser (1:5) mass ratio of PSMA to DLPC when compared to the low molecular weight PSMA (MW 1,600). This suggests that PSMA (MW 120,000) has a greater affinity to bind with the DLPC assemblies, possibly due to its higher hydrophobic content. Long term stability results, however, show that mixed

complexes consisting of this high molecular weight PSMA and DLPC lost their optical transparency after 2 weeks, which was much faster than the formulation produced from PSMA (MW 1,600). This observation may be explained in terms of the bridging effect, possibly occurring more prevalently in systems where the PSMA has longer chain length and greater hydrophobic content. Bridging causes the complexes to aggregate and form micrometer scale aggregates that can scatter visible light, producing a turbid solution.

In order to theoretically quantify properties of the end-state PSMA-DLPC complexes, such as size and composition, a stoichiometric model of the end-state complexes will be proposed. Some definitions and simplifying assumptions will be made.

Assumptions

The following assumptions are made for the derivation of the stoichiometric model.

- A1. End-state mixed complexes appear as spherical mixed micelles with a narrow size distribution.
- A2. The phospholipid molecules are all located at the surface of the micelles with their polar head groups facing toward water and their apolar hydrocarbon tails oriented radially inward.
- A3. The phospholipid molecules in the micelles are oriented as a single monolayer.
- A4. The hypercoiled polymer chains are packed within the inner hydrophobic zone of the micelles.

Definitions

Fig 8.1 shows a schematic illustration of the structural model, indicating the parameters defined below.

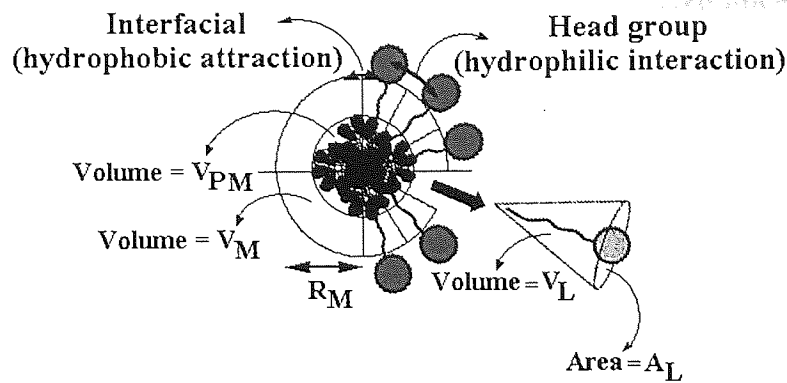


Fig.8.1 Schematic illustration for the parameters.

V_L is defined as the volume occupied by a single phospholipid molecule in a mixed micelle.

V_{PM} is defined as the total volume of hypercoiled polymer chains in a mixed micelle.

V_M is defined as the volume of a mixed micelle.

R_P is defined as the radius of a single hypercoiled polymer chain.

R_M is defined as the radius of a mixed micelle.

A_L is defined as the molecular area of a single phospholipid molecule.

A_M is defined as the surface area of a mixed micelle.

N_{LM} is defined as the number of phospholipid molecules present in a mixed micelle.

N_{LT} is defined as the number of phospholipid molecules present in the system.

N_M is defined as the total number of mixed micelles in the system.

N_{PM} is defined as the number of polymer chains present in a mixed micelle.

M_L is defined as the number of mole of phospholipid in the system.

M_P is defined as the number of mole of polymer in the system.

N_A is defined as Avogadro's number (6.02×10^{23}).

Calculation of the number of phospholipid molecules in a mixed micelle

The surface area, A_M , of a mixed micelle is given by:

$$A_M = 4\pi R_M^2$$

Since the area a lipid molecule occupies on the micelle surface is A_L , it follows that the number, N_{LM} , of phospholipid molecules in an end-state mixed micelle is:

$$N_{LM} = \frac{4\pi R_M^2}{A_L}$$

Calculation of the number of mixed micelles in the system

The number, N_{LT} , of phospholipid molecules in the system is the number of mole, M_L , of lipid multiplied by Avogadro's number:

$$N_{LT} = M_L N_A$$

Therefore, the number, N_M , of mixed micelles in the system is:

$$N_M = \frac{N_{LT}}{N_{LM}} = \frac{M_L N_A}{(4\pi R_M^2 / A_L)}$$

Calculation of the free volume for the polymer in a mixed micelle

The total volume, V_{LM} , occupied by phospholipid molecules in a mixed micelle is:

$$V_{LM} = V_L N_{LM}$$

The free volume, V_{PM} , for the polymer in a mixed micelle is estimated as the difference between the volume of the mixed micelle and the total volume of phospholipid in the mixed micelle:

$$V_{PM} = V_M - V_{LM}$$

Calculation of the number of polymer chains in a mixed micelle

The number, N_{PM} , of polymer chains in a mixed micelle is estimated as the ratio between the free volume for polymer in a mixed micelle and the volume of one hypercoiled polymer chain:

$$N_{PM} = \frac{V_{PM}}{V_P} = \frac{V_M - V_L N_{LM}}{\frac{4}{3} \pi R_P^3}$$

Application of the stoichiometric model to the PSMA-DLPC system

The above equations may be simplified using the following values obtained from the literature: $A_L = 0.7 \text{ nm}^2$ [93], $V_{LM} = 1 \text{ nm}^3$ [92, 94], $R_P = 1.5$ (for PSMA-MW 1,600) or 10.0 nm (for PSMA-MW 120,000) [48].

$$N_{PM} \approx \frac{R_M^2 (R_M - 4.29)}{R_P^3}$$
$$N_{LM} \approx 18 R_M^2$$
$$N_M \approx \frac{M_L 3.35 \times 10^{22}}{R_M^2}$$

If the moles of phospholipid and polymer are given, then some properties of the mixed micelles for varying size (radius of 25, 50 and 100 nm), such as the number of mixed micelles in the system, the numbers of phospholipid and polymer molecules present in a mixed micelle and the percentage of excess polymer, may be predicted.

Further attempts were made to connect the results of the calculations, using the equations previously derived, with the phase behaviour analysis in Fig.3.1-2 and the mechanism of polymer-induced lipid solubilization proposed earlier.

As previously proposed, the complete transformation of lipid assemblies into small monodisperse spherical PSMA-DLPC micelles with radius below 200 nm requires a certain minimum amount of polymer. This critical amount can be determined by varying the amount of polymer added into the formulation, while keeping the lipid concentration constant. The amount is then defined as the least amount of polymer required to convert a cloudy PSMA-DLPC suspension (two-phase) into a substantially clear formulation (single phase). Therefore, for a given lipid concentration, the corresponding critical value of the polymer falls on the phase boundary between the single and two phase in the ternary phase diagram.

In the stoichiometric model, the critical amount of polymer may be calculated for a given amount of lipid and a given radius of mixed micelle. This critical value is determined as the amount of polymer that gives zero percent of excess polymer. Analogously to the experimental method of determining the critical amount, it is possible to compute this amount using the stoichiometric model, by incrementally increasing the amount of polymer, while keeping the lipid amount and micelle radius constant.

At a constant DLPC concentration of 0.5% w/v (40.20 μ Mole), the critical amounts of PSMA (MW 1,600) obtained for the end-state mixed micelle radii of 25, 50 and 100 nm, were 0.50 (15.62 μ Mole), 1.00 (31.25 μ Mole) and 3.00% w/v (93.75 μ Mole), respectively, Table 8.1. The corresponding experimental results give a boundary point in the phase diagram for PSMA and DLPC concentrations of 1.0 and 0.5% w/v, respectively. Therefore, one may conclude that the radius of the end-state mixed micelles, consisting of PSMA (MW 1,600) and DLPC, should be approximately 50 nm.

Similarly, at a DLPC concentration of 0.5% w/v (40.20 μ Mole), the critical amounts of PSMA (MW 120,000) obtained for the resultant mixed micelle radii of 25, 50 and 100 nm, were 0.10 (0.04 μ Mole), 0.25 (0.10 μ Mole) and 0.50% w/v (0.21 μ Mole), respectively, Table 8.2. The corresponding experimental results give a boundary point in the phase diagram for PSMA and DLPC concentrations of 0.10 and 0.50% w/v, respectively. This suggests that the radius of the end-state mixed micelles, consisting of PSMA (MW 120,000) and DLPC, is likely to be ~25 nm which is half a size of that should obtain for PSMA (MW 1,600)-DLPC mixed micelles. The reduced size of the mixed micelles produced from PSMA (MW 120,000) indicates a stronger hydrophobic association between the polymer and the phospholipid.

Table 8.1 Evaluation of stoichiometric model by comparison with ternary phase diagram data of water-DLPC-PSMA (MW 1,600) system (see Fig.3.1a).

R_M (nm)	Lipid concentration (μ Mole)	Polymer concentration (μ Mole)	Percent of Excess PSMA *	Phase diagram location
25	20.10 (0.25%w/v)	7.81 (0.25% w/v)	0.00	Within two phase region
50	20.10 (0.25% w/v)	15.62 (0.50% w/v)	0.00	On boundary line
100	20.10 (0.25%w/v)	31.25 (1.00% w/v)	0.00	Within single phase region
25	40.20 (0.50% w/v)	15.62 (0.50% w/v)	0.00	Within two phase region
50	40.20 (0.50% w/v)	31.25 (1.00% w/v)	0.00	On boundary line
100	40.20 (0.50% w/v)	93.75 (3.00% w/v)	0.00	Within single phase region
25	80.40 (1.00% w/v)	28.12 (0.90%w/v)	0.00	Within two phase region
50	80.40 (1.00% w/v)	62.50 (2.0% w/v)	0.00	On boundary line
100	80.40 (1.00% w/v)	125.00 (4.00% w/v)	0.00	Within single phase region

* The % excess polymer is calculated as the difference between the number of polymer molecules initially present in the system and the number of polymer molecules used to form the mixed micelles.

Table 8.2 Evaluation of stoichiometric model by comparison with ternary phase diagram data of water-DLPC-PSMA (MW 120,000) system (see Fig.3.2a).

R_M (nm)	Lipid concentration (μ Mole)	Polymer concentration (μ Mole)	Percent of Excess PSMA*	Phase diagram location
25	20.10 (0.25% w/v)	0.02 (0.06% w/v)	0.00	On boundary line
50	20.10 (0.25% w/v)	0.05 (0.12% w/v)	0.00	Within single phase region
100	20.10 (0.25% w/v)	0.11 (0.26% w/v)	0.00	Within single phase region
25	40.20 (0.50% w/v)	0.04 (0.10% w/v)	0.00	On boundary line
50	40.20 (0.50% w/v)	0.10 (0.25% w/v)	0.00	Within single phase region
100	40.20 (0.50% w/v)	0.21 (0.50% w/v)	0.00	Within single phase region
25	80.40 (1.00% w/v)	0.08 (0.20% w/v)	0.00	On boundary line
50	80.40 (1.00% w/v)	0.20 (0.50% w/v)	0.00	Within single phase diagram
100	80.40 (1.00% w/v)	0.42 (1.00% w/v)	0.00	Within single phase region

* The % excess polymer is calculated as the difference between the number of polymer molecules initially present in the system and the number of polymer molecules used to form the mixed micelles.

The stoichiometric model proposed above successfully predicts the phase boundary for the PSMA-DLPC-water system as well as the size and composition of end-state complexes. Thus, it is likely that the end-state complexes have a shape similar to the model one (spherical mixed micelles with lipid located at the surface and polymer inside the hydrophobic zone). However, this proposed model is in all likelihood incomplete as it does not explain surface activity and bridging effects. This is because symmetrical structures, such as spherical micelles, normally do not give rise to surface activity of compounds. Moreover, the model assumes that all polymer molecules are located within the inner region of the micelles, while bridging effects are explained in terms of polymer interactions.

Therefore, the model needs to be extended to take into account the effects of polymer occupying area on the micelle surface. The proposed model is a first attempt to give a structure for the end-state complex. It is unlikely that the proposed extension will be sufficient to precisely predict all fundamental properties of interest. Clearly further work will be needed to validate and further develop this model.

8.1.3 Drug Delivery Application of Polymer-Lipid Complexes

The PSMA-DLPC complexes are believed to be ideally suited to transport and delivery of drug substances into the body, especially oily materials, by either topical (skin or eye) or systematic (via lung) routes or directly into the blood circulation. It is also possible to target specific cells and parts of cell within the body by incorporating targeting proteins or lectins into the structure. The polymer-lipid complexes may offer an entirely novel platform technology to treat disease processes that arise from deficiencies in lubrication, such as the degenerative joint diseases so apparent in osteoarthritis and the dry eye condition prevalent in rheumatic patients. The likely presence within the lung and the eye of natural nanostructures formed from interaction between apoproteins and lipids suggests that synthetic mimics would offer an effective means of rendering these bio-surfaces lubricious and wettable. The nanostructures formed may be act as powerful surfactants and these properties could be utilized to provide a surface coating of delicate tissues such as those of the lung, e.g. in the treatment of neonatal respiratory distress syndrome (RDS) [27].

For ocular applications, the nanostructure formulation offer both a vesicle for ocular drug delivery and a treatment for the common eye condition known as dry eye disease. This formulation has the great advantage over existing products in that it enable oil soluble active agents to be incorporated into a clear and colourless aqueous composition that is most acceptable to the eye and avoids the use of ointments and emulsion. The aqueous gel formulation of the nanostructure is perhaps the most acceptable and long lasting presentation for ophthalmic applications from the viewpoint of both patient and practitioner.

In this study, the potential of using the novel polymer-lipid complexes, consisting of anionic PSMA (hydrolyzed to styrene maleic acid) and hydrogenated DLPC, in conjunction with hydrogel as a new vehicle for ophthalmic drug delivery was determined. The principle was studied by examining the encapsulation of active compounds in a new type of nanoparticle. The incorporated nanoparticles were then encapsulated in a hydrogel matrix of the type used for soft contact lenses.

Results shown that the polymer-lipid complexes can be successfully loaded with hydrophobic compounds (e.g. Oil red O), confirming them a potentially valuable vehicle for drug delivery. A range of compounds (Oil red O, Rhodamine B and Pirenzepine dihydrochloride) differing in structure and hydrophobicity were used in order to characterize the factors that affect incorporation and release. The methodology allowed each of these compounds to be incorporated into the polymer-lipid complexes prior to polymerization with hydrogel-forming monomers (e.g. HEMA, MAA and PVA macromer). The encapsulation of these loaded polymer-lipid complexes within hydrogels gave optically clear hydrophilic polymer matrices.

Optical micrographs revealed that the loaded complexes were successfully trapped in both PVA and poly(HEMA-*co*-MAA) hydrogels. However, in the case of poly(HEMA-*co*-MAA) hydrogel, the complexes may associate to form supramolecular structures during thermal polymerization. The release characteristics of the hydrogels were found to be influenced by morphology of the hydrogel networks (e.g. mesh size, crosslinking density and ionicity) and the nature of the solute to be transported (e.g. hydrophobicity, solubility and size). It is postulated here that vesicle size may also play a vital role in the release characteristics of such compounds from the hydrogels.

The release kinetics of Pirenzepine from the vesicle containing poly(HEMA-*co*-MAA) hydrogels may be summarized as a three phase release (or in other words, three stage release);

1. The first phase is rapid release of approximately 60% of the solute (e.g. dye or drug) present within the hydrogel. This may account for the unencapsulated fraction of the solute located either at the surface of the vesicles or throughout the hydrogel matrix.
2. The second phase requires longer period of time and this is the release of a further ~10-15% of the entrapped solute. The solute released during this stage is believed to be the one which is entrapped within or adsorb at the interface of the vesicles.
3. The third phase can be described as a no-release phase. There was the retention of approximately 25-30% of the solute in the polymer matrix, which only release at an infinitestimally slow rate, but may partition over time into a more hydrophobic lipid-containing component such as tissue or plasma. This fraction of the solute may correspond to the solute that is strongly bound within the inner core of the vesicles.

By the use of other trigger mechanisms available in the eye, it appears that effective drug-releasing hydrogel contact lenses may be fabricated using this methodology.

8.2 SUGGESTIONS FOR FURTHER WORK

The work presented in this thesis is a preliminary investigation of the feasibility of using the PSMA-DLPC complexes in conjunction with hydrogels as a new vehicle for ophthalmic drug delivery. The pilot study suggests that by using this approach, the controlled release of active compounds, especially hydrophobic drugs, from hydrogels may be achieved. Some important properties of these polymer-lipid complexes, such as phase behaviour, association behaviour and drug encapsulation efficiency have been established through this work, however, other crucial information will obviously be needed in order to gain a better understanding and provide a better scientific foundation for future development. To obtain such details, additional experiments will need to be performed and these will be outlined in the subsequent sections.

8.2.1 Purification and Characterization of the Polymer-Lipid Complexes

In order to make effective use of PSMA-DLPC complexes (or PSMA-DLPC vesicles) for drug delivery applications, rapid and efficient methods are needed to separate the complexes from their unencapsulated contents. Size exclusion chromatography (SEC) is one of many techniques that may be used to separate the non-encapsulated drug from the loaded vesicles. This can be achieved by passing the prefabricated polymer-lipid formulation through a gel exclusion chromatography column (e.g. Sephadex G-50 sizing column).

A major advantage of this technique is that beyond separating the vesicles from the solute, it also fractionates heterogeneous suspensions into monodispersed sub-populations. The SEC technique can be scaled both on analytical and preparative scales. The applicability of conventional SEC is strongly improved by using a HPLC system associated to gel columns with a size selectivity range allowing vesicle characterization in addition to particle fractionation. Numerous examples of applications are found in literature reviews which concern polydispersity, size and

encapsulation stability, material release, permeability of bilayers, vesicle formation and reconstitution and interaction/insertion of amphiphilic molecules.

By passing the vesicle suspension through the SEC column, fractions of the sample differing in vesicle size are obtained and these can then be analyzed further using the following methodologies;

(a) *Vesicle size distribution*

The average size and size distribution of vesicles are very important parameters when the vesicles are intended for therapeutic use. A valid morphological characterization of vesicles can be obtained by freeze-fracture electron microscopy. This procedure is not suitable for stability monitoring because it is a laborious and is regarded as a time consuming method. A more suitable method to monitor the stability of vesicles is the dynamic light scattering technique which is sufficient capable of detecting changes in vesicles that are on stability. This technique has some limitations when used on polydisperse samples, however, the auto-correlation function, utilized in the calculation of vesicle size distribution determination, provides an accurate average size of vesicles [95].

(b) *Percent drug encapsulation*

The vesicle preparations are a mixture of encapsulated and unencapsulated drug fractions. The unencapsulated drug fraction is also referred to as 'free' drug. In a majority of procedures, the free and encapsulated drug fractions are separated to assess the free drug concentration as a first experimental step. Then the encapsulated fraction of the drug is treated with a detergent to lyse the vesicles and to completely discharge the drug from the vesicles into surrounding aqueous media. Thus, exposed drug is assayed by a suitable technique.

(c) *Quantification of phosphatidylcholine [96]*

The level of phosphatidylcholine (PC) is a key variable of liposome-based drug formulations for sustained release and/or targeting. To date, routine quantification of PC mainly employs quantitative thin layer chromatography and various forms of wet digestion methods whereby colorimetric or turbidimetry are being used. All these methods are quite time consuming. For the determination of choline-containing phospholipids in physiological substrates such as serum, high density lipoproteins, amniotic fluid, and bile, various enzymatic assays have been described. These assays are based on phospholipase-D cleaving off the choline moiety. Test kits containing the required enzymes and substrates are commercially available.

Apart from enzymatic assay technique, elemental analysis can also be used to quantify the PC contents in the vesicles [97]. Based on the fact that is no nitrogen atom in PSMA molecules, therefore the number of nitrogen atoms obtained must reflect the amount derived from the phospholipid

(d) *Vesicle zeta-potential*

The measurement of zeta potential facilitates the understanding of the dispersion and aggregation process and this has long been used for characterizing colloidal drug delivery systems. To determine the zeta potential of the vesicles, the vesicle dispersions may need to be diluted with deionized water and their electrophoretic mobility is thus measured by photon correlation spectroscopy. The mobilities are then converted into zeta potential values through Henry's equation [98].

(e) *Sterilization of vesicles* [95]

There are five different sterilization methods available from which one can choose. They include steam, dry heat, gas, ionization radiation and filtration. Each differs in mechanisms of microbial removal, parameters of operation, and applicability to any given product. However, they all share two common characteristics which are; providing sterility and requiring validation and monitoring to prove their effectiveness. The selection of sterilization process is dictated by the product itself. For the thermolabile liquid (such as the PSMA-DLPC formulation), the filtration through filter membrane (e.g. pore size 0.2 μ m) seems to be the only available sterilization technique since the lipid is likely to hydrolyze at high temperature of sterilization.

(f) *Stability of vesicles*

The stability of the vesicles is a major consideration in all steps of their preparation and administration. A stability study program should include a section for product characterization and the product stability during storage. One should also identify factors that may affect the stability of the product prior to starting a stability study program. For example, the liposomes prepared with distearoylphosphatidylcholine (DSPC) showed an optimal stability at pH 6.5 in aqueous solutions at 70°C. Influence of environmental factors such as temperature, light, oxygen and heavy metal ions may initiate chemical or physical reactions. These reactions may include changes in size distribution of vesicles and oxidation and hydrolysis of lipids [95]. The visual appearance, average size and size distribution are important parameters to examine. There are a number of methods to follow the physical stability of vesicles, for instance light scattering and electron microscopy.

In considering the micrograph results obtained, it has been postulated earlier that the polymerization reaction may affect the stability of the vesicles (i.e. induce vesicle aggregation). In order to prove this argument, a stability study program will thus need to be performed. One of many ways to investigate the vesicle stability is to measure the changes in the vesicle sizes as a function of time after polymerization. This can simply be assessed by the use of scanning electron microscopy.

(g) *In vitro* cytotoxicity of vesicles

Cytotoxicity studies of PSMA and DLPC have shown that these compounds are biologically safe [27, 97, 99]. However, it is also necessary to establish the non-toxicity of PSMA-DLPC complexes.

Cytotoxicity can be measured by the MTT assay, Trypan blue (TB) assay, Sulforhodamine B (SRB) assay, WST assay and clonogenic assay. A colorimetric assay using MTT was first introduced by Mossman as a quantitative measure of mammalian cell survival and proliferation. It is a laboratory test and a standard colorimetric assay for measuring cellular activity. MTT assay is used to determine cytotoxicity of potential medicinal agents and other toxic materials. MTT is a yellow tetrazolium salt which can be converted into a blue formazan by dehydrogenases of a live cell. The assay is based on the principle that the amount of formazan produced, which can be determined by a spectrophotometer, is directly proportional to the number of live cells [100].

8.2.2 Study of Drug Release from Polymer-Lipid Complexes

In order to determine if the drug can diffuse out of the polymer-lipid vesicles, additional drug release experiments will need to be performed. The most common methods used to study drug release from vesicles are sample and separate and dialysis methods [101].

The more conventional method is the sample and separate method, often referred to as the tube method, in which drug-loaded vesicles are placed within a sealed tube, vial or stoppered Erlenmeyer flask containing buffer, and the release study is conducted over a specific time. Isolation of the vesicles is achieved by filtration or by centrifugation. Advantages of this method are accurate measurement of the initial burst of drug from vesicles and the possibility for preservation of experimental conditions by replacement of the buffer. The disadvantages, however, are an inconvenient sampling technique and undesired withdrawal of vesicles from the release medium. To overcome these problems, sampling is often performed by using a filter attached to a

syringe. Another alternative is centrifugation, which facilitates the withdrawal of supernatant. However, upon centrifugation, vesicles must be re-suspended by shaking or vortexing. Re-suspension of the vesicles is typically difficult to achieve because of vesicle aggregation.

An alternative method is dialysis, in which the loaded vesicles are separated from the bulk medium by a dialysis membrane. The drug release into the bulk medium occurs through the membrane. At a predetermined period of time, a sample is withdrawn and the concentration of the drug present in the sample is then determined by spectrophotometry. Dialysis membranes with varying molecular weight exclusion cutoffs (MWCOCs) and compositions are widely used in a variety of fields. When using dialysis techniques, sampling and media replacement are convenient owing to a physical separation of the vesicles from the outer release medium. However, an initial preparation is required for the dialysis setup. In some cases, equilibration with the outer medium is achieved slowly because of the small membrane surface area available for drug passage [101]. Slow equilibration may limit the accuracy of the drug evaluation, especially in an initial burst release measurements. This disadvantage can be overcome by using a commercial dialyzer with a large surface area to facilitate drug transport.

An example of using commercial dialysis membranes to study drug release from microspheres is given by D'Souza and DeLuca [101]. The following diagram illustrates the dialysis setup for their *in vitro* release study using the Float-a-Lyzer.

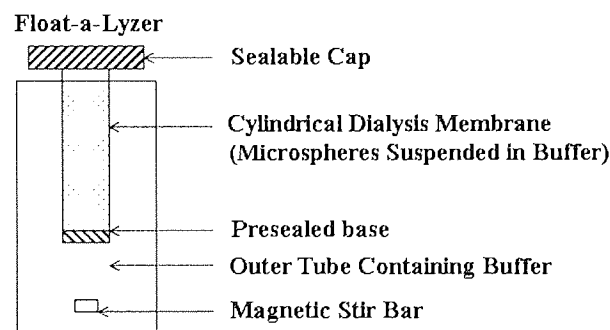


Fig.8.2 Illustration of setup for *in vitro* release from microspheres using the Float-a-Lyzer [101].

D'Souza and DeLuca showed that an in vitro release method using a regenerated cellulose membrane dialysis apparatus (Float-a-Lyzer) was suitable for studying in vitro release of peptide-loaded biodegradable microspheres even at elevated temperature. Moreover, the release results revealed a good reproducibility, implying that the commercially available Float-a-Lyzer is reliable and suitable for drug release testing. Furthermore, the technique is easily modified, by changing the release medium, yielding further details of the release study.

8.2.3 Study of Drug Release from Vesicle loaded-Hydrogels

The work in this thesis gives a preliminary feasibility study of using PSMA-DLPC vesicles in conjunction with hydrogels as a novel drug delivery vehicle. Data from this study shows that by using this approach, poly(HEMA-co-MAA) hydrogels can successfully retain the active compounds for longer period of time. However, this study should be extended further to obtain a better understanding of the dependence of release rate on a number of parameters, such as:

(a) *Vesicle size*

The size of vesicles may affect the release profile of drugs from the vesicle containing hydrogels. This has been proven in the case of chitosan-based hydrogel with liposome encapsulation [85]. Ruel-Gariépy et al. [85] demonstrated that the release rate of carboxyfluorescein (CF) can be controlled either by adjusting the liposome size and composition. An increase in liposome size from 100 to 280 nm drastically decreased the release kinetics as well as the initial burst release. With large multilamellar liposomes, the release was almost abolished with less than 6% CF release after 7 days. Their results suggested that only the very small vesicles will be released from the hydrogel, whereas the larger one will remain trapped within the gel matrix.

(b) *Release trigger mechanism*

The work in this thesis has shown that at the end of the release study, some of the loaded vesicles were still trapped within the poly(HEMA-co-MAA) hydrogel matrix. It would be good to know if this last fraction of drug can be released. A way of releasing the drug from the trapped vesicles is to de-stabilize them using a trigger mechanism. One such mechanism is to introduce a destabilizing agent, such as lysozyme. Lysozyme, which is the most abundant protein in human tears, is believed to be one of many good candidates for this sort of reaction. The mechanism of which lysozyme destabilize PSMA-DLPC vesicles may be described in terms of the competitive complexation between PSMA-DLPC and PSMA-lysozyme. At physiological pH, it is likely that the positively charged lysozyme can associate with uncoiled PSMA through electrostatic attraction. This association is expected to destabilize the vesicles and so enhance the leakage of the drug from the vesicle. Another possible trigger mechanism is to introduce phospholipase A₂ into the release medium. Phospholipase A₂ has been utilized by Ruel-Gariépy et al. [85] to degrade the liposomal bilayer and trigger the release of entrapped CF. Phospholipase A₂ is calcium-dependent enzymes that hydrolyze the *sn*-2-ester of glycerophospholipids to generate a free fatty acid and a lysophospholipid. The introduction of this enzyme has been shown to accelerate the release rate of CF by 5-9% per a day [85].

(c) *Solute diffusion*

Characteristics of hydrogels, vesicles as well as drugs greatly influence drug diffusion, which obviously affects the obtained drug release profiles. For hydrogels, several characteristics such as, ionization, swelling ratio and mesh size, have been reported to play important roles in drug diffusion [102]. The swelling ratio describes the amount of water that is contained within the hydrogel at equilibrium and is a function of the network structure, crosslinking ratio, hydrophilicity and ionization of the functional group. The mesh or pore size of hydrogels is also important as it defines the space available for drug transport [102]. The mesh size is dependent on the type of copolymer used and varies with the concentration of ionizable groups in the polymer.

The drug characteristics are as important as those of the gel. The size, shape and ionization of the drug affect its diffusion through membranes. In the case of ionization, if the gel and the drug are ionized, interactions may occur and these may either hinder or assist in the diffusion process, depending on the charges of the gel and drug. Drug size is another vital factor because the permeability coefficient of the drug decreases as its hydrodynamic radius approaches the size of the mesh size [102].

Future studies must be performed in order to examine some drug characteristics (e.g. permeability, partition and diffusion coefficients) as well as the effect of several factors, including mesh size and equilibrium swelling ratio of hydrogels, solute size and hydrophilicity of the gel and drug, on diffusion of the drug and its eventual release behaviour.

REFERENCES

- [1] M.A. Yessine, J.C. Leroux, Membrane-destabilizing Polyanions: Interactions with Lipid Bilayers and Endosomal Escape of Biomacromolecules. *Adv. Drug Deliv. Rev.* 56(7) (2004) 999-1021.
- [2] S.R. Tonge, B.J. Tighe, Responsive Hydrophobically Associating Polymers: A Review of Structure and Properties. *Adv. Drug Deliv. Rev.* 53 (2001) 109-122.
- [3] S.R. Tonge, Hypercoiling and Hydrophobically Associating Polymers: Interfacial Synthesis, Surface Properties and Pharmaceutical Applications. PhD Thesis, Aston University, Birmingham, 1994.
- [4] R.M. Fuoss, Polyelectrolyte II. Poly-4-vinylpyridonium chloride and Poly-4-vinyl-*N-n*-butylpyridonium bromide. *J. Polym. Sci.* 3(2) (1948) 246-263.
- [5] R.C. Sutton, L. Thai, J.M. Hewitt, C.L. Voycheckand, J.S. Tan, Microdomain Characterization of Styrene-Imidazole Copolymers. *Macromolecules* 21 (1988) 2432-2439.
- [6] S.P. Gasper, J.S. Tan, Conformational Studies of Poly(ethylacrylate-*co*-acrylic acid). *Polym. Sci. Technol.* 2 (1973) 387-400.
- [7] P. Dubin, U.P. Strauss, Hydrophobic Hypercoiling in Copolymers of Maleic acid and Alkyl Vinyl Ethers. *J. Phys. Chem.* 71(8) (1967) 2757-2758.
- [8] P.L. Dubin, U.P. Strauss, Hydrophobic Bonding in Alternating Copolymers of Maleic Acid and Alkyl Vinyl Ethers. *J. Phys. Chem.* 74(14) (1970).
- [9] W. Dannhauser, W.H. Glaze, R.L. Dueltgen, K. Ninomiya, Evidence from Intrinsic Viscosity and Sedimentation for Hypercoiled Configurations of Styrene-Maleic Acid Copolymer. *J. Phys. Chem.* 64 (1960) 954-955.
- [10] T. Okuda, N. Ohno, K. Nitta, S. Sugai, Conformational Transition of the Copolymer of Maleic Acid and Styrene in Aqueous Solution II. *J. Polym. Sci. Polym. Phys. Ed.* 15 (1977) 749-755.
- [11] H.E. Jorgensen, U.S. Strauss, Exploratory Studies on the Surface Activity of Polysoaps. *J. Phys. Chem.* 65 (1961).
- [12] G.S. Pop, S.V. Pakhovchishin, V.V. Mank, P.I. Kuprienko, N.M. Nazarchuk, T.P. Voloshchuk, Structure of Copolymers of Styrene and Maleic Acid as Their Ammonium Salts and the Colloid and Chemical Properties of the Aqueous Solutions. *Colloid J.* 43(4) (1981) 637-641.
- [13] V.P. Boiko, Surface Tension of Aqueous Solutions of a Copolymer of Styrene and Maleic Acid at the Interface with Water. *Colloid J.* 38(3) (1976) 486-489.
- [14] L.H. Layton, U.P. Strauss, A Comparison of the Solubilization of Several Paraffin Hydrocarbons by a Polysoap. *J. Colloid Sci.* 9 (1954) 149-156.
- [15] D.A. Tirrell, D.Y. Takigawa, K. Seki, pH-Sensitization of Phospholipids Vesicles via Complexation with Synthetic poly(carboxylic acid)s. *Ann. NY Acad. Sci.* 446 (1985) 237-248.
- [16] K. Seki, D.A. Tirrell, pH-dependent Complexation of Poly(acrylic acid) Derivatives with Phospholipid Vesicle Membranes. *Macromolecules* 17 (1984) 1692-1698.

- [17] K.A. Borden, K.M. Eum, K.H. Langley, D.A. Tirrell, On the Mechanism of Polyelectrolyte-Induced Structural Reorganization in Thin Molecular Films. *Macromolecules* 20 (1987) 454-456.
- [18] D.A. Tirrell, Environmentally Sensitive Vesicles for Controlled Drug Delivery In: Pulsed and Self-regulated Drug Delivery CRC Press, Inc., Florida, 1990, pp. 109-116.
- [19] M.-A. Yessine, M. Lafleur, H.-U. Petereit, C. Meier, J.-C. Leroux, Characterization of the Membrane Destabilizing Properties of Different pH-Sensitive Methacrylic Acid Copolymers. *Biophys. Biochim. Acta* 1613 (2003) 28-38.
- [20] N. Murthy, J. Robichaud, P.S. Stayton, O.W. Press, A.S. Hoffman, D.A. Tirrell, Design of Polymers to Increase the Efficiency of Endosomal Release of Drugs. *Proc. Int. Symp. Control. Release Bioact. Mater.* 25 (1998) 224-225.
- [21] G.A. Serrano, P.-G. Jesús, Protein-Lipid Interactions and Surface Activity in the Pulmonary Surfactant System. *Chem. Phys. Lipids Rev.* 141 (2006) 105-118.
- [22] M.J. LaDu, S.M. Gilligan, J.R. Lukens, V.G. Cabana, C. A. Reardon, L.J.V. Eldik, D.M. Holtzman, Nascent Astrocyte Particles Differ from Lipoproteins in CSF. *J. Neurochem.* 70(5) (1998).
- [23] M. Hammel, P. Laggner, R. Prassl, Structural Characterization of Nucleoside Loaded Low Density Lipoprotein as a Main Criterion for the Applicability as Drug Delivery System. *Chem. Phys. Lipids* 123 (2003) 193-207.
- [24] M. Krieger, L.C. Smith, R.G.W. Anderson, J.L. Goldstein, Y.J. Kao, H.J. Pownall, A.M. Gotto, M.S. Brown, Reconstituted Low Density Lipoprotein: A Vehicle for the Delivery of Hydrophobic Fluorescent Probes to Cells. *J. Supramol. Struct.* 10 (1979) 467-478.
- [25] R.A. Firestone, Low-Density Lipoprotein as a Vehicle for Targeting Antitumor Compounds to Cancer Cells. *Bioconjug. Chem.* (5) (1994) 105-113.
- [26] P.C.d. Smidt, A.J. Versluis, T.J.v. Berkel, Transport of Sulfonated Tetraphenylporphine by Lipoproteins in the Hamster. *Biochem. Pharmacol.* 43 (1992) 2567-2573.
- [27] B.J. Tighe, S. Tonge, Lipid-Containing Compositions and Uses Thereof, PC International Patent Application No. PCT/GB98/02546, 1998.
- [28] M. Wientzek, C.M. Kay, K. Oikawa, R.O. Ryan, Binding of Insect Apolipoprotein III to Dimyristoylphosphatidylcholine Vesicles. *J. Biological Chem.* 269 (1994) 4605-4612.
- [29] H. Maeda, SMANCS and Polymer-Conjugated Macromolecular Drugs: Advantages in Cancer Chemotherapy. *Adv. Drug Deliv. Rev.* 46 (2001) 169-185.
- [30] E.A. Rawlins, Bentley's Textbook of Pharmaceutics, 8th ed., Bailliere Tindall, 1977.
- [31] J.H. Ward, N.A. Pepas, Preparation of Controlled Release Systems by Free-radical UV Polymerizations in the Presence of a Drug. *J. Control Release* 71 (2001) 183-192.

- [32] R.H. Schmedlen, K.S. Masters, J.L. West, Photocrosslinkable Polyvinyl Alcohol Hydrogels that can be Modified with Cell Adhesion Peptides for use in Tissue Engineering. *Biomaterials* 23 (2002) 4325-4332.
- [33] N. Buhler, H.P. Haerri, M. Hofmann, C. Irrgang, A. Mühlebach, B. Müller, F. Stockinger, Nelfilcon A, A New Material for Contact Lenses. *Chimia* 53 (1999) 269-274.
- [34] L.C. Winterton, J.M. Lally, K.B. Sentell, L.L. Chapoy, The Elution of Poly(vinyl alcohol) from a Contact Lens: The Realization of a Time Release Moisturizing Agent/Artificial Tear. *Biomed. Mater. Res. Part B: Appl. Biomater.* (2006) 424-432.
- [35] P. Martens, K.S. Anseth, Characterization of Hydrogels Formed from Acrylate Modified Poly(vinyl alcohol) Macromers. *Polymer* 41 (2000) 7715-7722.
- [36] S. Sugai, Hydrophobic Domains of Maleic acid Copolymers, in: P. Dubin (Ed.), *Microdomains in Polymer Solution*, Polymer Science and Technology, Plenum, 1985.
- [37] K. Seki, D.A. Tirrell, Modification of Dipalmitoyl-phosphatidylcholine Bilayers by Poly(alpha-ethacrylic acid)s of Variable Microstructure. *Poly. Prepr. (Am. Chem. Soc. Div. Poly. Chem.)* 24(2) (1983) 26.
- [38] K.A. Borden, C.L. Voycheck, J.S. Tan, D.A. Tirrell, Polyelectrolyte Adsorption Induces a Vesicle-to-Micelle Transition in Aqueous Dispersions of Dipalmitoylphosphatidylcholine. *Polym. Prepr. (Am. Chem. Soc. Div. Poly. Chem.)* 28(1) (1987) 284-285.
- [39] T.O. Kyung, K.B. Tatiana, V.K. Alexander, Micellar Formulations for Drug Delivery Based on Mixtures of Hydrophobic and Hydrophilic Pluronic Block Copolymers. *J. Control. Rel.* 94 (2004) 411-422.
- [40] B. Deme, M. Dubois, T. Zemb, B. Cabane, Coexistence of Two Lyotropic Lamellar Phase Induced by a Polymer in a Phospholipid-water System. *Colloid and Surfaces A: Physicochemical and Engineering Aspects* 121 (1997) 135-143.
- [41] A. Polozova, F.M. Winnik, Contribution of Hydrogen Bonding to the Association of Liposomes and Anionic Hydrophobically Modified Poly(*N*-isopropylacrylamide). *Langmuir* 15 (1999) 4222-4229.
- [42] C. Ladavière, M. Toustou, T. Gulik-Krzywicki, C. Tribet, Slow Reorganization of Small Phosphatidylcholine Vesicles Upon Adsorption of Amphiphilic Polymers. *J. Colloid Interface Sci.* 241 (2001) 178-187.
- [43] J.L. Thomas, D.A. Tirrell, Polymer-induced Leakage of Cations from Dioleoylphosphatidylcholine and Phosphatidylglycerol Liposomes. *J. Control. Release* 67 (2000) 203-209.
- [44] M. Fujiwara, R.H. Grubbs, J.D. Baldeschwieler, Characterization of pH-Dependent Poly(acrylic acid) Complexation with Phospholipid Vesicles. *J. Colloid Interf. Sci.* 185 (1977) 210-216.
- [45] U.K.O. Schroeder, D.A. Tirrell, Structural Reorganization of Phosphatidylcholine Vesicle Membranes by Poly(2-ethylacrylic acid). Influence of the Molecular Weight of the Polymer. *Macromolecules* 22 (1989) 765-769.

- [46] A. Pinazo, M.R. Infante, S.Y. Park, E.I. Franses, Surface Tension Behavior of Aqueous Dilauroylphosphatidylcholine (DLPC). *Colloid and Surfaces B: Biointerfaces* 8 (1996) 1-11.
- [47] L. Zhao, S. Feng, Effects of Lipid Chain Length on Molecular Interactions Between Paclitaxel and Phospholipid within Model Biomembranes. *J. Colloid Interf. Sci.* (2003) 1-14.
- [48] G. Garnier, M. Duskova-Smrckova, R. Vyhnanekova, T.G.M.v.d. Ven, J.-F. Revol, Association in Solution and Adsorption at an Air-Water Interface of Alternating Copolymers of Maleic Anhydride and Styrene. *Langmuir* 16 (2000) 3757-3763.
- [49] L. Gargallo, B. Miranda, A. Leiva, D. Radic, M. Urzua, H. Rios, Surface Acitivity of Hydrophobically Modified Alternating Copolymers. *Polymer* 45 (2004) 5145-5150.
- [50] C. Kusonwiriawong, P. Wetering, J.A. Hubbell, H.P. Merkle, E. Walter, Evaluation of pH-Dependent Membrane-Disruptive Properties of Poly(acrylic acid) Derived Polymers. *Eur. J. Pharm. Biopharm.* (2003) 237-246.
- [51] P.A. Demchenko, V.P. Boiko, Investigation of Conformational Changes in Styrene-maleic acid Copolymer During Ionization in Aqueous Solutions. *Polymer Sci. U.S.S.R.* 15(10) (1972) 2626-2633.
- [52] D.J.F. Taylor, R.K. Thomas, J. Penfold, Polymer/Surfactant Interactions at the Air/Water Interface. *Adv. Colloid Interface Sci.* (2007), doi: 10.1016/j.cis.2007.1001.1002.
- [53] M. Treeby, G.C. Chitanu, K. Kogej, Association of Cationic Surfactants with Maleic Acid Copolymers: Depending of Binding on the Nature of the Neutral Comonomer Unit. *J. Colloid Interf. Sci.* 288 (2005) 280-289.
- [54] J. Penfold, R.K. Thomas, D.J.F. Taylor, Polyelectrolyte/Surfactant Mixture at the Air-Solution Interface. *Curr. Opin. Colloid Interface Sci.* (2006), doi: 10.1016/j.cocis.2006.1008.1003.
- [55] S.F. Santos, D. Zanette, H. Fischer, R. Itris, A Systematic Study of Bovine Serum Albumin (BSA) and Sodium Dodecylsulfate (SDS) Interactions by Surface Tension and Small Angle-X-Ray Scattering. *J. Colloid Interf. Sci.* 262 (2003) 400-408.
- [56] J. Peuvot, A. Schanck, M. Deleers, R. Brasseur, Piracetam-induced Changes to Membrane Physical Properties. *Biochem. Pharm.* 50 (1995) 1129-1134.
- [57] M.M. Pincelli, P.R. Levstein, C.A. Martín, G.D. Fidelio, Cholesterol-induced Stabilization of Lamellar Structures in Ganglioside-containing Lipid Aggregates. A ³¹P-NMR Study. *Chem. Phys. Lipids* 94 (1998) 109-118.
- [58] P.F. Knowles, D. Marsh, W.H. Evans, Magnetic Resonance of Membranes. In: *Biochemical Journal Reviews* 1991, Portland Press Ltd., London, 1992, pp. 625-641.
- [59] E. London, G.W. Feigenson, Phosphorous NMR Analysis of Phospholipids in Detergents. *J. Lipid Res.* 20 (1979) 408-412.
- [60] M. Auger, Membrane Structure and Dynamics as Viewed by Solid-state NMR Spectroscopy. *Biophys. Chem.* 68 (1997) 233-241.

- [61] Z. Huang, R.M. Epand, Study of the Phase Behaviour of Fully Hydrated Saturated Diacyl Phosphatidylserine/Fatty acid Mixtures with ^{31}P -NMR and Calorimetry. *Chem. Phys. Lipids* 86 (1997) 161-169.
- [62] C.M. Franzin, P.M. Macdonald, A. Polozova, F.M. Winnik, Destabilization of Cationic Lipid Vesicles by an Anionic Hydrophobically Modified Poly(*N*-isopropylacrylamide) Copolymer: A Solid-state ^{31}P -NMR and ^2H -NMR Study. *Biochim. Biophys. Acta* 1415 (1998).
- [63] B. Bechinger, Detergent-like Properties of Magainin Antibiotic Peptide: A ^{31}P Solid-state NMR Spectroscopy Study. *Biochim. Biophys. Acta* 1712 (2005) 101-108.
- [64] M.N. Triba, P.F. Devaux, D.E. Warschawski, Effects of Lipid Chain Length and Unsaturation on Bicelles Stability. A Phosphorous NMR Study. *Biophys. J.* 91 (2006) 1357-1367.
- [65] J.H. Kleinschmidt, L.K. Tamm, Structural Transitions in Short-chain Lipid Assemblies Studied by ^{31}P -NMR Spectroscopy. *Biophys. J.* 83 (2002) 994-1003.
- [66] R. Lipowsky, Vesicles and Biomembranes. *Encyclopedia of Applied Physics* 23 (1998) 200-222.
- [67] D. Chapman, Association of Membrane Constituents Using Nuclear Resonance Spectroscopy. In: *Molecular Association in Biological and Related Systems*, American Chemical Society, Washington D.C., 1968, pp. 88-98.
- [68] A. Maldonado, R. López-Esparza, R. Ober, T.Gulik-Krzywicki, W. Urbach, C.E. Williams, Effect of a Neutral Water-Soluble Polymer on the Lamellar Phase of a Zwitterionic Surfactant System. *J. Colloid Interf. Sci.* 296 (2006) 365-369.
- [69] M. Malmsten, *Surfactants and Polymers in Drug Delivery*, Marcel Dekker, Inc., 2002.
- [70] M.F. Saettone, Progress and Problems in Ophthalmic Drug Delivery. *Business Briefing: Pharmatech*. 2002, Available on line at: <http://www.touchbriefings.co.uk/pdf/17/pt031r28saettone.pdf>.
- [71] D. Gulsen, A. Chauhan, Ophthalmic Drug Delivery through Contact Lenses. *Invest. Ophthalm. Vis. Sci.* 45 (2004) 2342-2347.
- [72] J.C. Lang, Ocular Drug Delivery Conventional Ocular Formulations. *Adv. Drug Deliv. Rev.* 16 (1995) 39-43.
- [73] S.R. Waltman, H.E. Kaufman, Use of Hydrophilic Contact Lenses to Increase Ocular Penetration of Topical Drugs. *Invest. Ophthalmol.* 9 (1970) 250-255.
- [74] C.C.S. Karlgard, N.S. Wong, L.W. Jones, C. Moresoli, *In Vitro* Uptake and Release Studies of Ocular Pharmaceutical Agents by Silicone-containing and *p*-HEMA Hydrogel Contact Lens Materials. *Int. J. Pharm.* 257 (2003) 141-151.
- [75] E.M. Hehl, R. Beck, K. Luthard, R. Guthoff, Improved Penetration of Aminoglycosides and Fluoroquinolones into the Aqueous Humour of Patients by Means of Acuvue Contact Lenses. *Eur. J. Clin. Pharmacol.* 55 (1999) 317-323.
- [76] M. Almgren, Mixed Micelles and Other Structures in the Solubilization of Bilayer Lipid Membranes by Surfactants. *Biochim. Biophys. Acta* 1508 (2000) 146-163.

- [77] A.M. Seddon, P. Curnow, P.J. Booth, Membrane Proteins, Lipids and Detergents: Not Just a Soap Opera. *Biochim. Biophys. Acta* 1666 (2004) 105-117.
- [78] O. López, A.d.l. Maza, L. Coderch, C. López-Iglesias, E. Wehrli, J.L. Parra, Direct Formation of Mixed Micelles in the Solubilization of Phospholipid Liposomes by Triton X-100. *FEBS Letters* 426 (1998) 314-318.
- [79] E. Vivares, L. Ramos, Polyelectrolyte-induced Peeling of Charged Multilamellar Vesicles. *Langmuir* 21 (2005) 2185-2191.
- [80] D. Gulsen, C.-C. Li, A. Chauhan, Dispersion of DMPC Liposomes in Contact Lenses for Ophthalmic Drug Delivery. *Curr. Eye Res.* 30 (2005) 1071-1080.
- [81] A.A. Silveira, J. Flora, M.R. Davolos, Rhodamine B-containing Silica Films from TEOS Precursor: Substrate Surface Effects Detected by Photoluminescence *Surface Sci.* 601 (2007) 1118-1122.
- [82] B.O. Haglund, D.E. Wurster, L.-O. Sundelöf, S.M. Upadrashta, Effect of SDS Micelles on Rhodamine-B Diffusion in Hydrogels. *J. Chem. Education* 73 (1996).
- [83] P. Ilich, P.K. Mishra, S. Macura, T.P. Burghardt, Direct Observation of Rhodamine Dimer Structures in Water. *Spectrochimica Acta Part A* 52 (1996) 1323-1330.
- [84] Z. Zhanga, S.-S. Feng, The Drug Encapsulation Efficiency, *In Vitro* Drug Release, Cellular Uptake and Cytotoxicity of Paclitaxel-loaded Poly(lactide)-tocopheryl polyethylene glycol succinate Nanoparticles. *Biomaterials* 27 (2006) 4025-4033.
- [85] E. Ruel-Gariépy, G. Leclair, P. Hildgen, A. Gupta, J.-C. Leroux, Thermosensitive Chitosan-based Hydrogel Containing Liposomes for the Delivery of Hydrophilic Molecules. *J. Control Release* 82 (2002) 373-383.
- [86] A.P. Sassi, S.-H. Lee, Y.H. Park, H.W. Blanch, J.M. Prausnitz, Sorption of Lysozyme by HEMA Copolymer Hydrogels. *J. Appl. Polym. Sci.* 60 (1996) 225-234.
- [87] Q. Garrett, B. Laycock, R.W. Garrett, Hydrogel Lens Monomer Constituents Modulate Protein Sorption. *Invest. Ophthalm. Vis. Sci.* 41 (2000) 1687-1695.
- [88] J. Tu, P. Li, X. Yang, H. Pang, HPLC Determination of Pirenzepine Hydrochloride in Rabbit Aqueous Humor. *J. Chromatogr. B.* 822 (2005) 300-303.
- [89] A.C. Moffat, *Clarke's Analysis of Drugs and Poisons in Pharmaceuticals Body Fluids and Postmortem Material*, Pharmaceutical Press, 2004.
- [90] D. Gulsen, A. Chauhan, Dispersion of Microemulsion Drops in HEMA Hydrogel: A Potential Ophthalmic Drug Delivery Vehicle. *Int. J. Pharm.* 292(1-2) (2005) 95-117.
- [91] A. Chauhan, D. Gulsen, Ophthalmic Drug Delivery System, United States Patent Application Publication No.US 2004/0241207 A1, 2004.
- [92] J. Leng, S.U. Egelhaaf, M.E. Cates, Kinetics of the Micelle-to-Vesicle Transition: Aqueous Lecithin-Bile Salt Mixtures. *Biophysical J.* 85 (2003) 1624-1646.

- [93] J.G. Linhardt, D.A. Tirrell, pH-Induced Fusion and Lysis of Phosphatidylcholine Vesicles by the Hydrophobic Polyelectrolyte Poly(2-ethylacrylic acid). *Langmuir* 16 (2000) 122-127.
- [94] O. Edholm, J.F. Nagle, Areas of Molecules in Membranes Consisting of Mixtures. *Biophysical J.* 89 (2005) 1827-1832.
- [95] V. Vemuri, C.T. Rhodes, Preparation and Characterization of Liposomes as Therapeutic Delivery Systems: A Review. *Pharmaceutica Acta Helvetiae* 70 (1995) 95-111.
- [96] L. Ingebrigtsen, M. Brandl, Determination of the Size Distribution of Liposomes by SEC Fractionation, and PCS Analysis and Enzymatic Assay of Lipid Content. *AAPS Pharm. Sci. Tech.* (2002), Available on line at:<http://www.aapspharmscitech.org>.
- [97] A.K. Iyer, K. Greish, J. Fang, R. Murakami, H. Maeda, High-loading Nanosized Micelles of Copoly(styrene-maleic acid)-zinc protoporphyrin for Targeted Delivery of a Potent Heme Oxygenase Inhibitor. *Biomaterials* 28 (2007) 1871-18881.
- [98] L.R.-Guilatt, P. Couvreur, G. Lambert, D. Goldstein, S. Benita, C. Dubernet, Extensive Surface Studies Help to Analyse Zeta Potential Data: the Case of Cationic Emulsions. *Chem. Phys. Lipids* 131 (2004) 1-13.
- [99] H. Maeda, SMANCS and Polymer-conjugated Macromolecular Drugs: Advantages in Cancer Chemotherapy. *Adv. Drug Deliv. Rev.* 46 (2001) 169-185.
- [100] D. WoldeMeskel, G. Abate, M. Lakew, S.Goshu, A. Selassie, H. Miorner, A. Aseffa, Evaluation of a Direct Colorimetric Assay for Rapid Detection of Rifampicin Resistant Mycobacterium Tuberculosis. *Ethiop. J. Health Dev.* 1 (2005) 51-55.
- [101] S.S. D'Souza, P.P. DeLuca, Development of a Dialysis *In Vitro* Release Method for Biodegradable Microspheres. *AAPS Pharm. Sci. Tech.* 2 (2005), Available on line at:<http://www.aapspharmscitech.org>.
- [102] N.A. Peppas, S.L. Wright, Drug Diffusion and Binding in Ionizable Interpenetrating Networks from Poly(vinyl alcohol) and Poly(acrylic acid). *Eur. J. Pharm. Biopharm.* 46 (1998) 15-29.